ON

The Brr2 RNA helicase

and its Protein and RNA interactions

Daniela Hahn

A Thesis presented for the degree of

Doctor of Philosophy

The University of Edinburgh

2011

For Alexander

Declaration

I hereby declare that I am the sole author of this thesis and the work presented is my own. Results obtained through the collaboration with other individuals or institutions are appropriately indicated. All sources of information have been acknowledged by means of referencing.

Daniela Hahn

Edinburgh, October 2011

Acknowledgements

Firstly, I would like to thank the Darwin Trust of Edinburgh, for funding my PhD studies.

Jean, thank you for providing me with the opportunity to work in your lab and for guiding me through my PhD. You introduced me to, and allowed me to explore the world of science. Working in your lab has been challenging, rewarding and educating in many ways. Thank you.

I thank all members of the Beggs lab, past and present, for contributing to my PhD. Thank you for providing discussion, much laughter and cheerfulness and for being great colleagues. Special thanks go to Olivier Cordin for recognising my potential and for collaborating.

A further thank you goes to David Tollervey my second supervisor. Thank you for your scientific interest and enthusiasm. Thank you for providing discussion, opinions and having an open door.

Also, many thanks to all members of the Tollervey lab, especially Claudia, Agata and Wiebke for supplying scientific scrutiny and keeping me weekend lab-company. I thank Sander Granneman, who encouraged me to pursue my own scientific ideas and who helped me implement them. The occasional late-night pep talk was much appreciated! A special thank you goes to Greg Kudla, without whose help my work would not have been the same. I enjoyed collaborating with you.

I would like to thank Cosmin Saveanu and Alain Jacquier for fruitful collaboration. I thank Ray O'Keefe and Scott Stevens for kindly sharing yeast strains and plasmids.

Ich danke meiner Familie, meinen Eltern und Geschwistern für bedingungslose Liebe. Danke, dass Ihr immer an mich glaubt, für mich da seid mich ermutigt und mich auf vielfälitge Arten und Weisen unterstützt habt.

To my love Alexander, I thank you for being the voice of reason, for always seeing the positive side of things, even if I don't. Thank you for being my best friend, my confident and companion, my harshest critic and my biggest supporter. I thank you for loving me. I love you.

Danke.

Common Abbreviations

ATP	adenosine triphosphate
aa	amino acid
Amp	ampicillin
ARS	autonomous replication sequence
bp	base pair
H2	Brr2 C-terminal helicase domain
Sec63-2	Brr2 C-terminal Sec63 domain
H1	Brr2 N-terminal helicase domain
Sec63-1	Brr2 N-terminal Sec63 domain
CEN	centromere element
cDNA	complementary DNA
°C	degree Celsius
DNA	deoxyribonucleic acid
dNTP	deoxyribonucleotide triphosphate
DMSO	dimethylsulfoxide
E. coli	*Escherichia coli*
EtOH	ethanol
EtBr	ethidium bromide
Fig.	figure
HRP	horse radish peroxidise
MAT	mating type
T_m	melting temperature
mRNA	messenger RNA
µg	microgram
µl	microliter
mM	millimolar
min	minute
M	molar
nm	nanomter
nt	nucleotide

ORF	open reading frame
OD_{600}	optical density at 600 nm
PCR	polymerase chain reaction
rpm	revolutions per minute
RNase	ribonuclease
RNA	ribonucleic acid
RNP	ribonucleoprotein particle
rNTP	ribonucleoside triphosphate
rRNA	ribosomal RNA
RT	room temperature
S. cerevisiae	*Saccharomyces cerevisiae*
SGD	Saccharomyces genome database
sec	second
SDM	site-directed mutagenesis
snRNA	small nuclear RNA
SDS	sodium dodecyl sulphate
xg	times g-force
tRNA	transfer RNA
UV	ultra violet
U	unit
V	Volt
vol.	volume
v/v	volume/volume
W	Watt
w/v	weight/volume
WT	wild type
WH	winged helix domain
YMM	yeast minimal medium
Y2H	yeast two-hybrid

Abstract

The dynamic rearrangements of RNA and protein complexes and the fidelity of pre-mRNA splicing are governed by DExD/H-box ATPases. One of the spliceosomal ATPases, Brr2, is believed to facilitate conformational rearrangements during spliceosome activation and disassembly. It features an unusual architecture, with two consecutive helicase-cassettes, each comprising a helicase and a Sec63 domain. Only the N-terminal cassette exhibits catalytic activity. By contrast, the C-terminal half of Brr2 engages in protein interactions. Amongst interacting proteins are the Prp2 and Prp16 helicases. The work presented in this thesis aimed at studying and assigning functional relevance to the bipartite architecture of Brr2 and addressed the following questions: (1) What role does the catalytically inert C-terminal half play in Brr2 function, and why does it interact with other RNA helicases? (2) Which RNAs interact with the different parts of Brr2?

(1) In a yeast two-hybrid screen novel *brr2* mutant alleles were identified by virtue of abnormal protein interactions with Prp2 and Prp16. Phenotypic characterization showed that *brr2* C-terminus mutants exhibit a splicing defect, demonstrating that an intact C-terminus is required for Brr2 function. ATPase/helicase deficient *prp16* mutants suppress the interaction defect of *brr2* alleles, possibly indicating an involvement of the Brr2 C-terminus in the regulation of interacting helicases.

(2) Brr2-RNA interactions were identified by the CRAC approach (*in vivo* Cross-linking and analysis of cDNA). Physical separation of the N-terminal and C-terminal portions and their individual analyses indicate that only the N-terminus of Brr2 interacts with RNA. Brr2 cross-links in the U4 and U6 snRNAs suggest a step-wise dissociation of the U4/U6 duplex during catalytic activation of the spliceosome. Newly identified Brr2 cross-links in the U5 snRNA and in pre-mRNAs close to 3' splice sites are supported by genetic analyses. A reduction of second step efficiency upon combining *brr2* and U5 mutations suggests an involvement of Brr2 in the second step of splicing.

An approach now described as CLASH (Cross-linking, Ligation and Sequencing of Hybrids) identified Brr2 associated chimeric sequencing reads. The inspection of chimeric U2-U2 sequences suggests a revised secondary structure for the U2 snRNA, which was confirmed by phylogenentic and mutational analyses.

Taken together these findings underscore the functional distinction of the N- and C-terminal portions of Brr2 and add mechanistic relevance to its bipartite architecture. The catalytically active N-terminal helicase-cassette is required to establish RNA interactions and to provide helicase activity. Conversely, the C-terminal helicase-cassette functions solely as protein interaction domain, possibly exerting regulation on the activities of interacting helicases and Brr2 itself.

Table of contents

Chapter 1 – General introduction

1.1 Pre-mRNA splicing

Pre-mRNA splicing is an essential process required for the expression of many genes in eukaryotes. It takes place in the nucleus concomitant with or after transcription, but before mRNA export to the cytoplasm and translation. Pre-mRNA splicing involves the removal of non coding regions (introns) from within the body (usually) coding, region of the primary transcript and the joining of coding regions (exons) to give rise to translatable mRNA.

Genes of higher eukaryotes mostly contain more than one intron; in fact introns can often make up the majority of the primary transcript. The presence of multiple introns allows the joining of different combinations of exons, a phenomenon termed alternative splicing [1]. The widespread existence of alternative splice patterns in genes of higher eukaryotes is a major factor in enhancing the relative diversity of eukaryotic proteomes compared to the corresponding genomes [2].

In the lower eukaryote *Saccharomyces cerevisiae* (*S. cerevisiae* or yeast) introns are found only in approximately 4% of all genes. In most cases these genes will contain a single intron of moderate size (less than 600 nt). Furthermore, introns are generally located near the 5′ end of the gene, resulting in small 5′ exons. *S. cerevisiae* nevertheless makes an ideal model organism for the study of pre-mRNA splicing. It possesses a constitutive splicing machinery that is highly evolutionarily conserved. Strikingly, 85% of yeast splicing factors have a clear evolutionarily conserved counterpart in humans [3]. Since the yeast system is accessible to genetic manipulation and mutational studies, it has much aided our current understanding of pre-mRNA splicing.

1.2 The mechanism of pre-mRNA splicing

Central to the process of splicing are two consecutive transesterification reactions (Fig. 1.1). In the first reaction the 2′ hydroxyl group of a particular adenosine residue - the branch point adenosine – becomes nucleophilic and attacks the 5′ most phosphodiester moiety of the intron, the 5′ splice site (5′ ss) (Fig. 1.1 top).

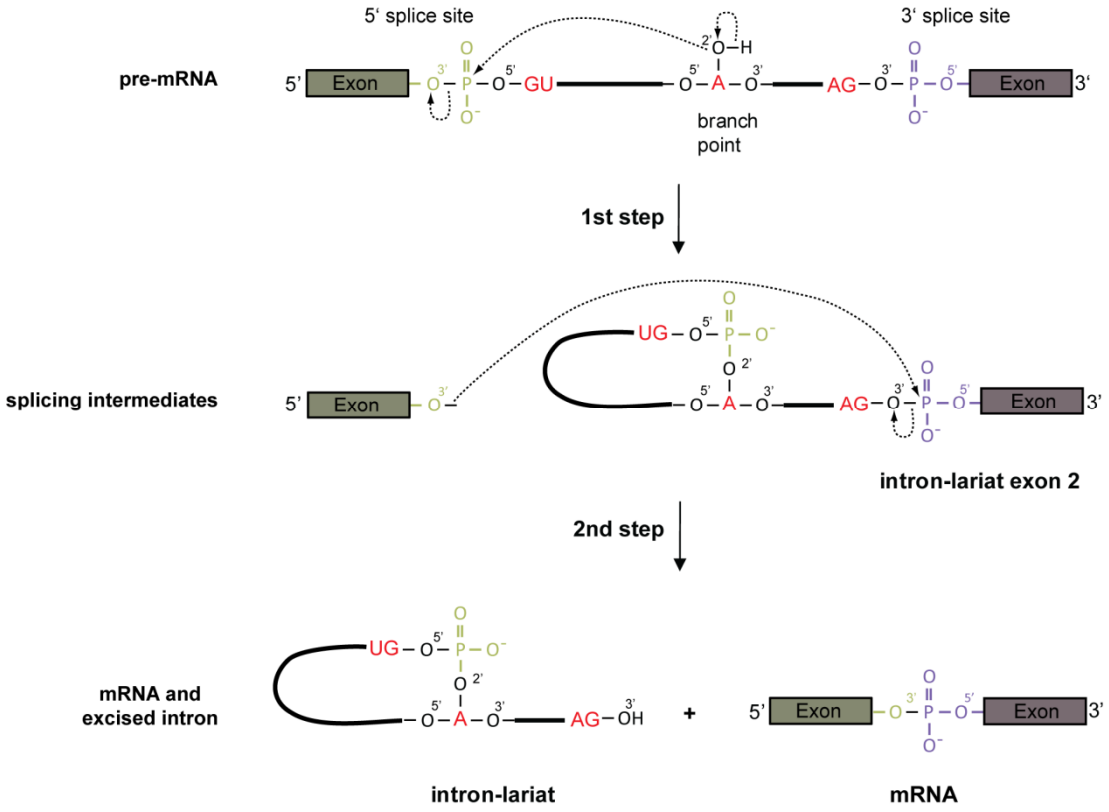

Figure 1.1 Schematic representation of the chemical reactions occurring during the two step process of pre-mRNA splicing. Depicted is a pre-mRNA containing a single intron **(top)**. During the first chemical step of splicing the 2' hydroxyl of a specific adenosine base at the branch site becomes nucleophilic and implies a nucleophilic attack on the phosphodiester moiety at the 5' splice site (marked in green). This results in the formation of two intermediates: the 5' exon in a free from and in the branched intron-lariat 3' exon **(centre)**. In the second transesterification reaction the free 3' hydroxyl anion of the 5' exon attacks the phosphodiester moiety at the 3' splice site (marked in purple) to yield the joined exons as well as the excised intron-lariat **(bottom)**.

This leads to the formation of two intermediates: a free 5′ exon and the 3′ exon-intron in a branched lariat structure, in which the 5′ end of the intron is covalently linked to the branch point adenosine via a 2′-5′ phosphodiester bond

(Fig. 1.1 centre). In the second transesterification reaction the free 3′ hydroxyl group of the 5′ exon attacks the 3′ most phosphodiester moiety of the intron, the 3′ splice site (3′ ss). The second reaction results in the joining of the 5′ and 3′ exons; simultaneously the intron-lariat is excised (Fig. 1.1 bottom). These reactions must occur with single nucleotide precision and are tightly controlled and catalyzed by a multi ribonucleoprotein (RNP) complex, the spliceosome.

1.3 Spliceosome mediated splicing

The main building blocks of the spliceosome are preformed RNA-protein complexes, so called snRNPs (for small nuclear ribonucleoprotein complexes). Each snRNP contains one of five small nuclear RNAs (snRNA), namely U1, U2, U4, U5 or U6. A set of common Sm proteins, or in the case of U6 Lsm proteins, are associated with the snRNAs. In addition each snRNP contains several specific proteins [4]. In addition various non-snRNP splicing factors are required (see below) and the snRNPs undergo extensive remodelling throughout the splicing reaction [5].

In order for the splicing reaction to occur, widely accepted models predict that the spliceosome assembles in a stepwise manner on each pre-mRNA substrate (Fig. 1.2) [6]. U1 and U2 snRNPs initially bind to the 5′ splice site and the branch point, respectively. Subsequently U4/U6 and U5 snRNPs join and interact with the pre-mRNA as a pre-assembled U4/U6·U5 tri-snRNP complex. This results in the formation of the pre-catalytic spliceosome, or complex B.

In yeast an alternative spliceosome assembly pathway was suggested based on the isolation (under low-salt conditions) of a complex consisting of all five spliceosomal snRNPs, which was termed the penta-snRNP [7]. This has lead to the suggestion that the spliceosome may exist in a more extensively pre-assembled form which allows concomitant recruitment of all snRNPs to the pre-mRNA [8].

Although all snRNPs are present in complex B it is still catalytically inactive (Fig. 1.2). Extensive conformational and compositional rearrangements (catalytic

activation) are required in order to render the spliceosome competent to carry out the first transesterification reaction.

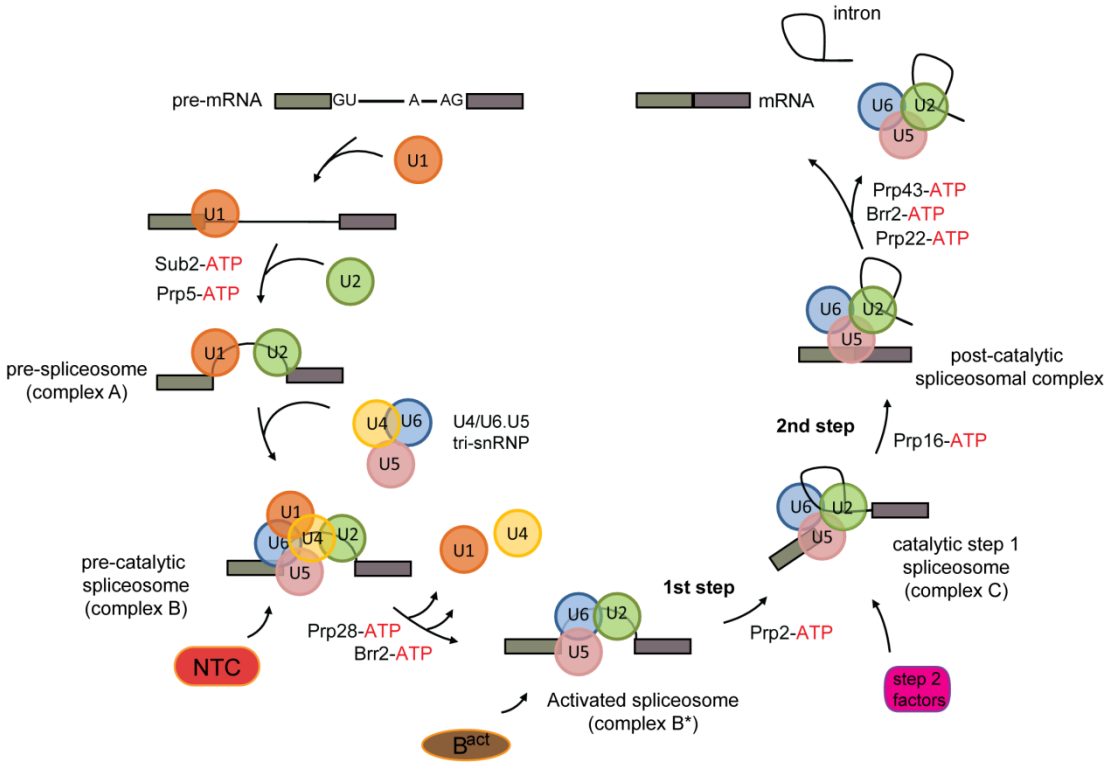

Figure 1.2 Schematic representation of the spliceosome assembly and disassembly pathway in yeast. The stepwise interaction of spliceosomal snRNPs (U1, U2, U4, U5 and U6, coloured circles) with the pre-mRNA substrate, splicing intermediates and products is depicted. Consecutive joining, remodelling and dissociation of snRNPs and recruitment of non-snRNP proteins or protein complexes (NTC, B^{act} and step 2 factors, depicted as red brown and pink symbols) result in the formation of complex A, B, B*, C and finally the post-catalytic spliceosomal complex. Evolutionarily conserved DExD/H-box ATPases/helicases act at specific steps of the splicing reaction to catalyse RNA-RNA rearrangements and RNP remodelling (ATP-dependent steps are indicated by red ATP).

A number of RNA-RNA rearrangements must occur. Base-pairing interactions between U4 and U6 snRNAs must be disrupted and mutually exclusive interactions between U2 and U6 must be established. Also, the U1 snRNA interaction with the 5′ ss is exchanged for interactions with U6 and U5 snRNAs (reviewed in [9]). Formation of these alternative RNA interactions is supported by association of the heteromeric Prp19 complex (NTC) (Fig. 1.2 red) [10, 11]. Once completed, these transitions give rise to the catalytically activated spliceosome (complex B*) in which

the first step of splicing takes place. Subsequent to step 1, complex C is formed. The spliceosomal complex and the remaining snRNPs undergo further structural and compositional transitions before step 2 catalysis occurs [12]. The second catalytic step leads to formation of the post-catalytic spliceosomal complex. This complex is actively disassembled, once again requiring several RNA-RNA rearrangements. Interactions between U5 snRNA and the spliced mRNA are disrupted allowing release of the mRNA and its export to the cytoplasm. Also, the snRNP-bound lariat intron must be dismantled (Fig. 1.2). This requires disruption of base-pairing interactions between the U6 snRNA and the 5′ ss as well as disruption of base-pairing between the U2 snRNA and the branch point. The intron-lariat is debranched through the activity of Dbr1 and subsequently degraded. The snRNPs are recycled; therefore the mutually exclusive base-pairing interactions involving U2, U6 and U4 must be restored to their original configurations, generating a free U2 snRNP and the U4/U6 di-snRNP and out of this the U4/U6·U5 tri-snRNP.

1.4 Changes in the spliceosomal protein composition

The spliceosome is a particularly protein-rich RNP and proteins make up the majority of its molecular mass [5]. To date ~ 90 distinct proteins are known to be involved in pre-mRNA splicing in *S. cerevisiae* ([3] and references therein). The more elaborate human spliceosome is thought to encompass a total of ~ 170 factors ([5] and references therein).

Studies on purified yeast spliceosomes, in particular on intermediate spliceosomal complexes (in yeast of complexes B, B^{act} and C), have revealed a remarkable exchange of proteins from one stage of the splicing process to the next [3]. Spliceosomal proteins of different groups and functions are required to join and leave the spliceosome in a highly ordered fashion (Fig. 1.3).

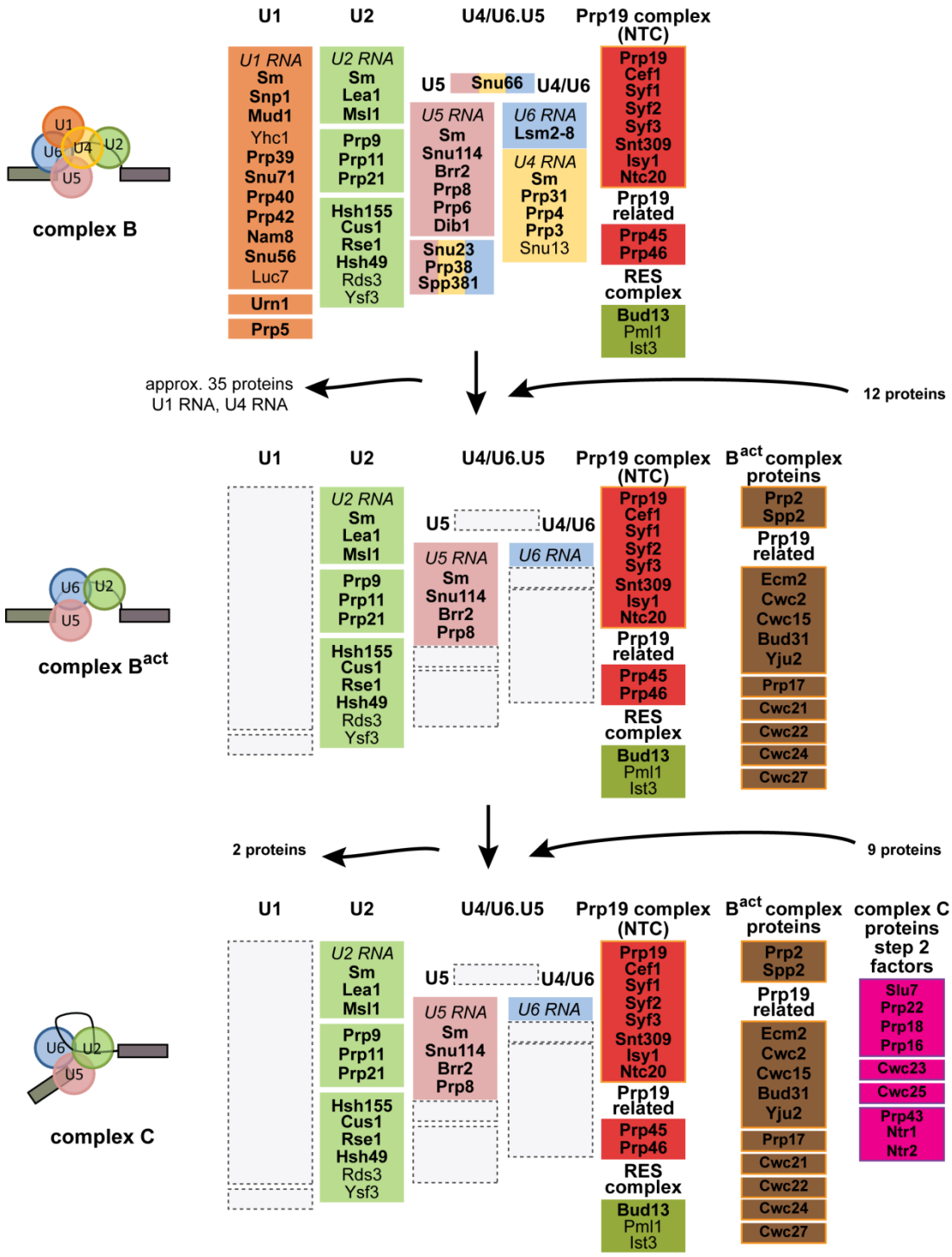

Figure 1.3 Compositional dynamics of spliceosomal complexes in *S. cerevisiae* according to [3]. Fabrizio *et al.* (2009) determined the protein composition of spliceosomal complexes B, B^{act} and C by Mass spectrometry. Proteins are grouped according to snRNP association, function and their presence in a stable heteromeric complex (coloured boxes). Furthermore, proteins are grouped according to their association with a particular spliceosomal complex (complex B, top; B^{act}, centre; and C, bottom). Figure adapted from [3].

During the transition from complex B to B^{act} (the B^{act} complex is an intermediate complex which precedes the catalytically activated B* complex [3]), along with the U4 and U1 snRNAs, approximately 35 proteins dissociate from the spliceosome (Fig. 1.3 top, centre). Many of these are snRNP or snRNP stabilising proteins. However, 12 additional non-snRNP proteins are recruited at this stage. A part of these proteins were termed B^{act} proteins, as they are absent in the pre-catalytic complex B but are recruited upon activation. A further set of proteins is termed Prp19 related, based on their interactions with the Prp19 complex [10]. These proteins most likely substitute for snRNP proteins and serve to induce and maintain a catalytically competent conformation of the spliceosome. During the subsequent transition to the catalytic first step spliceosome (complex C) most of the so-called second step factors are recruited. These are proteins known to function just prior to or during the second step of splicing [13]. Also the factors required for disassembly of the spliceosome associate at this stage.

The majority of the identified proteins have known roles during the splicing process; however the function of some remains elusive. Quite possibly, a number of these proteins function in coupling the splicing machinery with other RNA processing machineries, such as the transcription, 3′ end processing and quality control machineries [14].

1.5 Identifying features of introns

The spliceosome must discriminate exons and introns and must locate exon-intron borders with high precision to ensure splicing fidelity. However, introns lack sequence conservation, apart from minimal regions flanking the 5′ and 3′ splice sites and the branch point. Comparative sequence analysis and mutational studies determined consensus sequences that define the intron and contribute to the splicing reaction [15].

1.5.1 The 5’ splice site of U2-type introns

In yeast the 5’ ss consensus sequence is defined by (near) perfect complementary to a region of the U1 snRNA, allowing initial recognition of the 5’ ss via base-pairing with the U1 snRNA. This interaction is then stabilised by binding of proteins, such as U1-C. In yeast the consensus sequence of the 5’ ss is R/GUAAGU (the cleavage site is denoted by /). The metazoan consensus sequence is more degenerate (AG/GURAGU). In higher eukaryotes efficient usage of a 5’ ss can be facilitated by stabilising snRNA-pre-mRNA interactions through binding of additional proteins like the U1-70K protein as well as SR proteins (reviewed in [16]). The first two nucleotides of the intron (G^1U^2) are invariant and mutation of these positions and the adjacent conserved sequence of the 5’ ss can affect splicing. Often the first transesterification reaction can be carried out, but the subsequent second step does not occur, indicating that cleavage at the 3' ss is sensitive to the sequence of the first step intermediate(s) [17, 18]. Some human genetic diseases such as cystic fibrosis, ovarian and breast cancer could be linked to mutations in 5’ ss (as well as 3’ ss) that lead to inappropriate or cryptic ss usage, provoking exon-skipping, nucleotide polymorphisms or the emergence of premature termination codons [1].

1.5.2 The branch point

The branch point sequence is recognised by base-pairing interactions with a cognate region of the U2 snRNA, and again establishment and maintenance of this interaction is assisted and regulated by protein factors [19]. In yeast the branch point sequence is highly conserved (UACUAAC) and is usually located 20-60 nucleotides upstream of the 3’ ss. The 3’ most adenosine of this sequence is invariant (underlined in Fig. 1.4). It does not base pair with U2; instead it is bulged out from the intermolecular duplex. It provides the nucleophile required for the first transesterification reaction and is the site at which the branch of the lariat forms (see Fig. 1.1) [20]. Metazoan introns contain a similar, although not as strictly

conserved consensus, YNYURAY. Mutational analysis of mammalian introns revealed a greater flexibility with respect to selection and activation of a nucleophile [21].

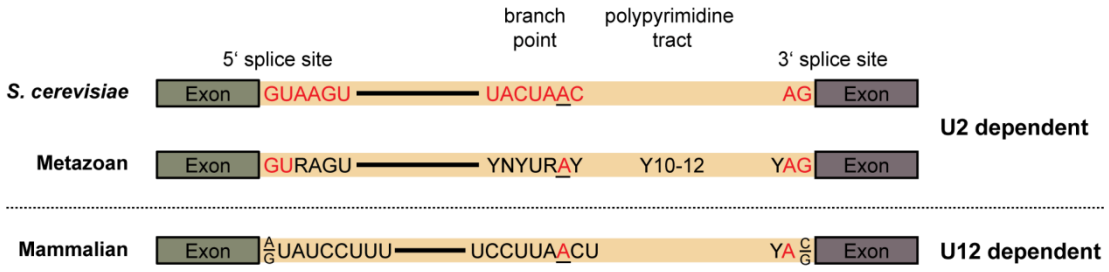

Figure 1.4 Conserved sequence elements of U2 and U12-type introns. The exons (grey) contain the coding information and are separated by the intron (peach). The consensus sequences found in U2 and U12-type introns differ. Consensus sequences found in *S. cerevisiae* and metazoan U2-type and in mammalian U12-type introns at the 5' splice site, branch point (underlined nt) and 3' splice site are indicated [5, 22]. Red colour indicates highly conserved nucleotides. N is any nucleotide, R is a purine and Y is a pyrimidine. The polypyrimidine tract is a pyrimidine-rich region between branch point and 3' splice site. Figure adapted from [5].

1.5.3 The 3' splice site of U2-type introns

Recognition and definition of the 3' ss is less well understood compared to recognition of the 5' ss and BP. Here identification of the splice site is not initiated by base-pairing interactions with a complementary snRNA, but relies more heavily on protein factors [16].

Yeast as well as metazoan introns end in an AG dinucleotide. Apart from the terminal AG the sequence environment of the 3' ss shows little conservation, except that in many cases the 3' ss is preceded by pyrimidines. As opposed to yeast introns, metazoan U2-type introns contain a more extensive pyrimidine-rich region upstream of the 3' ss, the polypyrimidine tract (py-tract) (Fig. 1.4).

Mutation of the py-tract of mammalian introns blocks the early steps of spliceosome assembly. In the presence of short py-tracts also the 3' ss AG

dinucleotide is required for efficient first step chemistry, however long py-tracts can bypass the requirement for the 3′ ss AG [23]. In mammals the py-tract serves as a protein recognition and interaction region that allows cooperative recognition of the BP and 3′ ss [5].

In yeast recognition of the BP is realised by the conserved BP/U2 sequences and does not rely on the presence of a pyrimidine-rich region near the 3′ ss. In experimental settings the 3′ ss can be truncated or mutated without abrogating spliceosome assembly and first step catalysis [24, 25]. However, in an experimental setting that allows the choice between alternative 3′ ss the presence of a U-rich region upstream of a particular 3′ ss can greatly enhance the usage of this splice site [26].

Therefore, yeast and mammalian systems differ in their requirements for BP, py-tract and 3′ ss sequences, however the functions of all three sequence elements near the 3′ end of the intron seems to be conserved.

1.5.4 U12-type introns and the minor spliceosome

In metazoan and plant genes a rare class of distinct introns was identified [27, 28]. Initially termed AT-AC introns they are now referred to as minor-class or U12-type introns [29]. The frequency of this deviant type of introns in the genome is comparably low (found in about 1/300 genes in mammals [30]), compatible with the low abundance of the splicing machinery that removes these introns (about 1% relative to components of the U2-dependent spliceosome [30]). What distinguishes U12-type introns are longer and distinct consensus sequences at the 5′ end of the intron and the branch site as well as the absence of a polypyrimidine tract upstream of the 3′ ss (Fig. 1.4 bottom). In the minor spliceosome U11 replaces U1, for the recognition of the 5′ ss and U12 replaces U2 and establishes base-pairing interactions with the BP. Furthermore, U4atac and U6atac replace U4 and U6 [31]. Although the sequences of these snRNAs differ considerably between minor and

major spliceosomes, the secondary structures and base-pairing interactions established in both classes of spliceosomes reveal striking commonality, such that activation and action of the minor spliceosome parallels that of the major spliceosome [32, 33]. Interestingly, the U5 snRNP is shared between both classes of spliceosomes. Moreover, proteomic studies revealed many overlaps with the U2-dependent spliceosome; especially the protein composition of the U4/U6·U5 and U4atac/U6atac·U5 tri-snRNP particles exhibit striking similarity [22, 34]. The remarkable parallels in protein composition, snRNA structures and RNA-RNA interactions between the U2- and U12-dependent spliceosomes strongly reinforce our notion of the architecture of the spliceosome and how its design and composition facilitates intron removal.

1.6 The active site of the spliceosome

Due to the extensive interplay of protein and RNA components during assembly and catalytic activation, the spliceosome was referred to as an RNP enzyme [5]. However, it remains unclear whether the cooperation between protein and RNA extends to the chemical catalysis of splicing. The chemical reaction carried out by the spliceosome recapitulates the self-splicing that is catalysed by group II introns [35]. Furthermore, short sequences of some snRNAs resemble catalytic portions of group II introns [36]. Phosphorthioate-suppression experiments demonstrated that a portion of the U6 snRNA, the U6 intramolecular stem loop (U6 ISL), mediates positioning of a structurally or possibly catalytically important metal ion [37], a function also recognised for a U6-like structure of a group II intron [36]. In addition, synthetic RNAs, consisting only of portions of U2, U6 and the pre-mRNA are sufficient to carry out a reaction that resembles the first step of splicing [38]. At present it remains unclear to what extent this reduced system parallels the situation in the protein-rich spliceosome. Nevertheless, these observations provide compelling evidence that the snRNAs and the pre-mRNA form essential parts of the

active site in spliceosome. Yet, it remains unclear whether group II introns and the spliceosome share the same chemical catalytic principles.

Elaborate biochemical and genetic experiments place the Prp8 protein at or near the catalytic centre of the spliceosome. Prp8 is a 280 kDa U5-specific protein, which can be cross-linked to the 5′ ss, the BP, and the 3′ ss. Based on these findings Prp8 was suggested to function as a scaffold for protein and RNA at the active site (reviewed in [39]). Recently crystal structures of a Prp8 fragment known to interact with the 5′ ss were resolved. Intriguingly, they identified an RNase H-like domain with a truncated catalytic centre [40-42]. In conjunction with mutational analyses, targeting the predicted active site of the RNase H-like domain and the surrounding region, these findings were interpreted to suggest that Prp8 might directly participate in the chemical catalysis of splicing [40-42]. This would make the active site of the spliceosome a true collaboration between protein and RNA [43].

1.7 Driving forces of spliceosome dynamics

Key to the splicing reaction is the establishment of a dynamic network of RNA-RNA interactions including base-pairing between pre-mRNA and snRNA, as well as base-pairing of different snRNAs. Thus, it is essential that formation of distinctive structures is enabled or disabled while other structures need to be actively disrupted throughout the splicing reaction.

The two transesterification reactions occurring during splicing are essentially isoenergetic [44]. Spliceosome-mediated splicing however is an ATP-dependent process and at several distinctive steps of the splicing cycle the energy released by ATP hydrolysis is required. Intriguingly, at least one member of the DExH/D box family of putative RNA helicases seems to be involved at each of these energy-dependent steps (Fig. 1.2) [45].

1.7.1 DExD/H-box RNA helicases

RNA helicases (as DNA helicases) possess an enzymatic activity that allows converting the energy released by NTP hydrolysis into mechanical movement, to promote nucleic acid strand separation and/or protein displacement [46]. While DNA helicases often work processively, RNA helicases are generally thought to lack processivity. Often their targets appear to be short stretches of RNA. Characteristic for helicases is the occurrence of certain signature motifs in their primary sequence, based on which they can be grouped into superfamilies and families [47, 48]. Superfamily 2 (SF2) comprises a subgroup of helicases referred to as DExD/H box proteins. These helicases are closely related and their overall structural organisation is similar [49]. In DExD/H box helicases up to nine conserved motifs can be recognised (Q motif, motif I, Ia, Ib, II, III, IV, V and VI) [50]. Although they are closely related, the conserved sequence motifs show significant differences. In some DExD/H box helicases motifs Ia and Ib cannot be identified as discrete motifs. The eponymous one letter amino acid sequence of motif II allows to name and differentiate between the DEAD, DEAH, DExD and DExH (also Ski2-like) helicase families (x can be any amino acid) [51, 52].

Although DExD/H box helicases were grouped into different families, they all show structural similarity to the DNA-binding protein RecA and feature two RecA-like domains [49]. Motifs I-VI are central components of the enzymatic core, which forms two discrete domains connected by a flexible linker. In between these domains a groove or cleft is formed which can accommodate a nucleotide for hydrolysis. The RNA substrate interacts with the bottom of the RecA-like domains. The conserved motifs are largely facing into this cleft and contribute to ATP binding, ATP hydrolysis as well as helicase activity (mechanical movement) [51].

RNA helicases considerably vary in size; some possess amino- or carboxy-terminal extensions of more than 500 residues, while others are practically devoid of any extensions beyond the helicase core. The eukaryotic translation initiation factor eIF4A for instance contains all basic enzymatic activities, but is flanked by only

about 70 amino acids upstream and downstream of the conserved helicase motifs [53]. N- and/or C-terminal extensions have been shown to convey additional functional features. Terminal extensions can facilitate tightened RNA-binding, increase processivity, or provide a binding region for interacting proteins ([49, 54, 55] and references therein).

Strikingly, most RNA helicases show very little to no substrate specificity when analysed *in vitro*. Yet, most biological processes depend upon highly selective and substrate specific unwinding or dissociation functions. It is likely that specificity is conferred by the interactions of flanking sequences and sequences on the external surfaces of the enzymatic core. It is feasible that the flanking regions can form independent interactions with the substrate, either directly or through interactions with additional factors. Protein specific carboxy- and/or amino-terminal extensions are therefore thought to support determination of substrate specificity and to control protein activity [56, 57].

1.7.2 Spliceosomal RNA helicases

Among the multitude of different proteins contributing to splicing, eight were recognised as members of the DExD/H box protein family of RNA helicases (table 1.1). The fact that as many as eight different RNA helicases appear to be involved in pre-mRNA splicing underscores the importance of transitions in RNA structure and RNP composition during the splicing reaction [6].

RNA helicases involved in pre-mRNA splicing have been studied genetically and biochemically. Their involvement at different stages of the splicing cycle is reflected by the different functional roles that have been proposed. Functions as RNA chaperones, “unwindases”, protein-binding or base-pairing “facilitators”, “maturases” and RNPases have been suggested.

Table 1.1 RNA helicases involved in pre-mRNA splicing in *S. cerevisiae*

RNA helicase	signature motif	duration of interaction	stage in splicing	proposed substrate(s)
Sub2	DEAD	***transient*** recruited to pre-spliceosome, release after assembly	pre-spliceosome assembly	branch point /BBP/Mud2
Prp5	DEAD	***transient*** recruited to pre-spliceosome, release in dispute	pre-spliceosome assembly	U2/Cus2
Prp28	DEAD	in dispute	spliceosome activation, release of the U1	U1/5' ss/U1-C
Brr2	DEIH and DDAH	***permanent*** stable U5 component	spliceosome activation release of U4 and spliceosome disassembly	U4/U6 and U2/U6
Prp2	DEAH	***transient*** recruited to complex B^{act}, exits before step 2	activation of step 1, release of SF3a/b proteins	?
Prp16	DEAH	***transient*** recruited to complex C, point of release unknown	step 2 activation	U2/U6; 3' ss ?
Prp22	DEAH	***transient*** recruited to complex C, released with mRNA	mRNA release	U5/3'exon
Prp43	DEAH	***transient*** recruited to complex C, present until spliceosome disassembly	intron release and spliceosome disassembly	U6 ?

Helicases can act on RNA-protein or RNA-RNA interactions; in all cases ATP-hydrolysis elicits conformational changes within the spliceosome. DExD/H box helicases with RNPase activity seem to function in the removal of proteins that stabilize or facilitate the formation of structures crucial to spliceosome function, e.g. positioning of splice sites and conformations of snRNAs. Alternatively, DExD/H box helicases can act on RNA-RNA interactions by directly targeting snRNA/snRNA or snRNA/pre-mRNA base-pairing interactions. While some spliceosomal DExD/H box proteins have been studied in great detail, for many of them neither the actual biological substrate nor the mechanism regulating their activity is fully understood. Nevertheless, their activities could be linked to certain remodelling events (see Fig. 1.2, Table 1.1):

Prp5 is required for formation of the pre-spliceosome. It is believed to remove Cus2 from the U2 snRNP and to remodel the structure of the U2 snRNA in

an ATP-dependent manner [58]. During catalytic activation of the spliceosome Prp28 has been suggested to function as an RNPase triggering the release of the U1 snRNP presumably by destabilizing the U1-C protein [59, 60]. At the same time Brr2 is involved in the release of the U4 snRNP. It is suggested to disrupt base pairing between the U4 and U6 snRNAs [61]. Prp2 triggers a conformational rearrangement prior to the first catalytic step which presumably involves the destabilisation of SF3a/b [62-64] proteins. Prp16 activity brings about changes to the spliceosomal conformation after the first, but prior to the second catalytic step [65]. Recent findings suggest that the ATPase activity of Prp16 removes Cwc25 and Yju2 from the spliceosome resulting in a step 2 competent conformation [66]. Prp16 also directly interacts with the 3′ ss and was implicated in 3′ ss selection [67]. ATP-hydrolysis by Prp22 is required subsequent to the second step. It disrupts base pairing interactions between the U5 snRNA and the spliced mRNA, a process required to release the spliced mRNA from the post catalytic complex [68]. Subsequently, the activities of Prp43 and Brr2 trigger spliceosome disassembly [69-71].

1.8 Brr2

1.8.1 Brr2 identification

Brr2 has been identified as an essential splicing factor in four labs concurrently; notably by using four different approaches. In a screen for cold-sensitive mutants that exhibit splicing defects Noble & Guthrie (1996) identified the mutant allele *brr2-1* and cloned the corresponding gene *BRR2* (for bad response to refrigeration). Xu *et al.* [72] identified the same splicing factor by screening for mutations that caused synthetic lethality when combined with the U2 *snr20-G21C* mutation. The identified transacting factor was denoted Slt22, for synthetic lethal with U2 (*slt22-1* is the corresponding mutant allele). Lauber *et al.* [73] purified a component of the human U5 snRNP termed U5-200K, and in parallel identified and

cloned its yeast homologue Snu246. Finally, Lin & Rossi [74] identified the mutant allele *rss1-1* as a suppressor of an experimentally induced 3′ ss block. The corresponding protein Rss1 turned out to be identical to the factors mentioned above. In a later publication the same gene/protein was also referred to as *PRP44*/Prp44 [75]. Throughout this work, the common name Brr2 will be used.

1.8.2 Brr2 domain architecture

The primary sequence of Brr2 reveals the presence of five distinct domains (Fig. 1.5 top). At its N-terminus Brr2 contains a region of 450 amino acids which is not conserved among species and a functional role has not yet been proposed. Brr2 is a member of the DExH box (or Ski2-like) helicase family and shows sequence homology to the antiviral yeast protein Ski2 as well as the DNA helicase Mer3/Hfm1 [76].

Brr2 features an unusual architecture (Fig. 1.5 top). It comprises two helicase domains (Fig. 1.5, H1 and H2). Both contain the conserved motifs characteristic of DExH box RNA helicases. The amino acid sequences within the conserved motifs of H2 are more degenerate than those of H1, and in H2 motif V cannot be clearly identified. Mutations that were predicted to be functionally deleterious were tolerated with little consequence [75]. The predicted structural organisation of H1 and H2, however, appears to be highly conserved, as judged by the succession and spacing of secondary structural motifs. Although an ATPase activity could only be demonstrated for H1 [75], the structure of H2 gives reason to speculate that it might retain the ability to bind a nucleotide.

Brr2 comprises another well conserved domain in two copies, the Sec63 domain (Fig. 1.5, Sec63-1 and Sec63-2). This domain is alternatively referred to as Brl domain, for Brr2-like domain. Extensive homology search and BLAST analysis have revealed that Sec63 domains are conserved in Brr2 and its homologues [77]. Sec63

domains can also be found in other yeast proteins; they apparently appear in a limited number of domain combinations (Fig. 1.5 bottom).

In the eponymous ER translocon-associated protein Sec63 protein the Sec63 domain is located downstream of a DnaJ chaperone domain. Often, Sec63 domains are found in combination with helicase domains. These can occur either as a single repeat of helicase and Sec63 domain (e.g. in Mer3/Hfm1) or as a tandem repeat of the two domains (e.g. in Brr2 and Slh1). Thus, Brr2 is not the only helicase featuring this unusual domain composition [77].

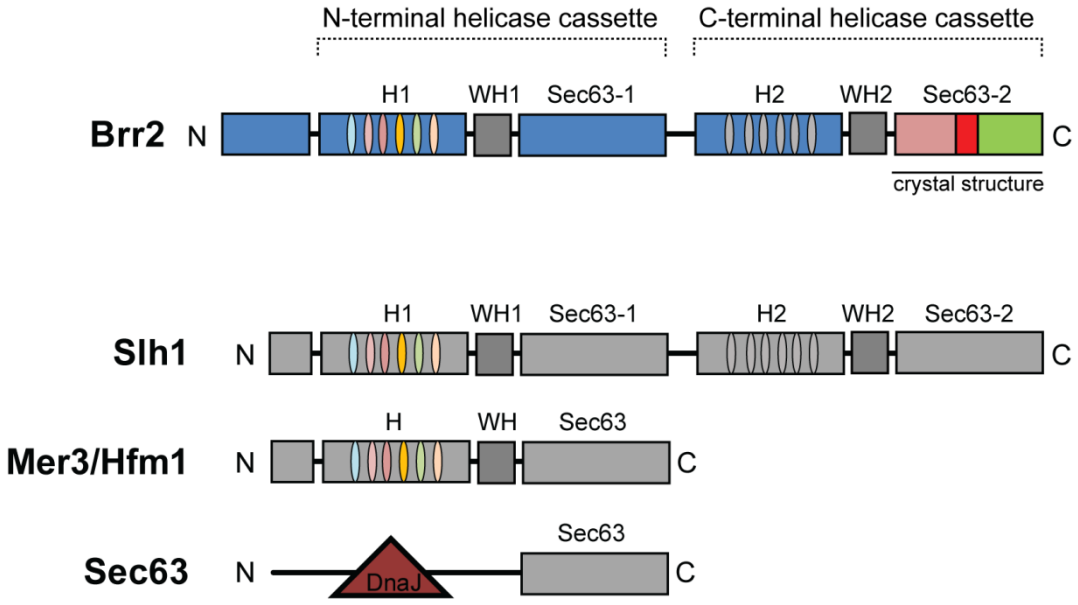

Figure 1.5 Domain organisation of *S. cerevisiae* Brr2 and of other proteins harbouring Sec63 domains. (Top) Brr2 comprises an N-terminal domain of unknown function, two DExD/H-box helicase domains (H1 and H2) as well as two Sec63 domains (Sec63-1 and Sec63-2). The structure of Sec63-2 has been solved recently [77, 78]. Helicase and Sec63 domains are connected by a winged helix domain (WH) and are believed to form helicase cassettes (dashed brackets) [77, 78]. **(Bottom)** Sec63 domains can be found in combination with helicase domains in other yeast helicases like Slh1 and Mer3/Hfm1. In addition, a Sec63 domain was found in combination with another domain in the yeast ER translocon protein Sec63, which harbours a DnaJ and a Sec63 domain.

Recently, two reports have presented crystal structures of the C-terminal Sec63 domain of *S. cerevisiae* Brr2 [78, 79]. The Sec63 domain consists of three interconnected structural domains that are arranged in a triangular fashion. The helical bundle domain is composed of compactly ordered alpha helices. The second, much smaller helical domain adopts a helix-loop-helix fold. And the third domain consists of β-strands only and forms an immunoglobulin-like β-sandwich.

Despite the absence of obvious sequence similarity, structural similarities have been recognised between the C-terminal Sec63 domain of Brr2 and domains 4 and 5 of the DNA helicase Hel308 [78-81]. Based on elaborate structural modelling it was concluded that structural similarity to Hel308 extends to the helicase domain [78, 79]. Pena *et al.* (2009) observed a further similarity to the Hel308 structure and pointed out that a winged helix (WH) domain functions as a connector to link and position the helicase and Sec63 domains (Fig. 1.5). Based on these observations a structural model was generated in which Brr2's C-terminal helicase, WH, and Sec63-like domains form a functional unit, or helicase cassette, resembling Hel308 (Fig. 1.5, dashed bracket). Due to high sequence conservation the N-terminal helicase, WH, and Sec63 domains of Brr2 were also predicted to form a helicase cassette, concluding that Brr2 likely consists of a unique N-terminal domain plus two consecutive helicase cassettes (Fig. 1.5) [78, 79]. The two helicase cassettes are predicted to have a similar overall structure and organisation, in which the Sec63 domain is positioned opposite to the helicase domain, forming a central channel through which a single stranded nucleic acid molecule can be threaded.

Mutational studies suggested that catalytic activity resides in the N-terminal helicase module [79]. Due to the apparent absence of ATPase activity in H2 the C-terminal helicase cassette, it was suggested to function as a protein interaction platform rather than as a catalytically active domain. Indeed, several essential splicing factors have been found to interact with the C-terminal helicase and Sec63 domains of Brr2 [82, 83].

1.8.3 Proposed Brr2 functions

Many lines of evidence indicate that Brr2 is the factor responsible for separation of the U4/U6 snRNA duplex during catalytic activation of the spliceosome [61, 75, 84]. Brr2 purified from yeast and U5-200K (the human Brr2 homologue, hereafter referred to as hBrr2) purified from HeLa were shown to be capable of unwinding the U4/U6 duplex *in vitro* [84, 85]. However, like other RNA helicases, Brr2/hBrr2 does not show substrate specificity when analysed *in vitro*. Raghunathan & Guthrie (1998) demonstrated that release of U4 from the U4/U6·U5 tri-snRNP requires both functional Brr2 and ATP. It was suggested, that particularly the activity of the first helicase domain is needed for unwinding of U4/U6 [75].

Different mutant phenotypes implicate Brr2 functions at additional other stages of the splicing cycle. Aberrant snRNP profiles, e.g. the formation of high molecular weight complexes of unusual compositions or exceptionally low tri-snRNP levels have been observed in several Brr2 mutants [70, 72, 75, 76].

While most of the mutants exhibit a splicing defect before or at the first catalytic step, the *brr2*-R1107A mutant additionally showed accumulation of excised intron-lariats. Hence, Brr2 was suggested to function after the second catalytic step in spliceosome disassembly and intron release [70]. Brr2 possesses RNA stimulated ATPase activity *in vitro* (Brr2 purified from yeast). Because it was most strongly stimulated by the U2/U6 snRNA duplex [72] and because U2/U6 base-pairing is still intact in the post-catalytic spliceosomal complex, Brr2 was proposed to disrupt U2/U6 base-pairing interactions in order to release the lariat-intron [70]. Previous genetic studies, which identified synthetic lethal interactions between a *brr2* allele and U2 mutations that disrupt U2/U6 base-pairing, were interpreted to suggest that Brr2 acts as a "proof-reader" for U2/U6 base-pairing interactions during spliceosome assembly and activation [86].

The addition of antibodies specific for hBrr2 to *in vitro* splicing reactions caused an accumulation of intron-lariat exon 2 intermediate, suggesting a functional involvement of hBrr2 in the second step of splicing. However, the experimental design did not allow discrimination between direct or indirect inhibitory effects [73].

1.8.4 Regulation of Brr2 activity

If Brr2 activity is required at several stages of the splicing reaction intermittent stimulation and repression of its activity must be assured. To date mainly two proteins, Prp8 and Snu114, are implicated in regulation of Brr2 activity. Like Brr2 and Prp8, Snu114 is a component of the U5 snRNP; together these proteins form a salt-stable complex [87].

Snu114 is the only GTPase identified in the spliceosome to date. It shows homology to elongation factor G and is predicted to undergo substantial conformational rearrangements upon GTP hydrolysis [88]. Elegant studies in which a mutation switched the nucleotide specificity from GTP to XTP demonstrated that stalled spliceosomes would only show U4/U6 unwinding, when supplied with hydrolysable XTP [89], suggesting that Snu114 most probably functions in controlling Brr2 activity. A more recent study suggests that Snu114 controls Brr2 activity, depending on its nucleotide state. In its GTP-bound state Snu114 promotes Brr2 activity, but when bound to GDP it represses Brr2 activity [70]. It remains unknown whether Snu114 elicits control over Brr2 activity directly or via interactions to Prp8.

Prp8 is suggested to be a key regulator of spliceosome activation [90-92]. Different regions of Brr2 and Prp8 were found to interact. The N-terminus of Prp8 was found to interact with the C-terminus of Brr2, while a C-terminal Prp8 fragment showed an interaction with full length Brr2 or fragments lacking only a short N-terminal region [82]. According to Liu *et al.* (2006) the N- and C-termini of human Prp8 interact with helicase domain 2 of hBrr2.

Genetic interactions first indicated Prp8 as a regulator of Brr2 activity. *prp8* mutants interact genetically with *snu114* and *brr2* alleles. A mutation in Prp8 can suppress the spliceosome activation defect of a *brr2* allele [88, 91]. A recent study suggested that Prp8 can regulate Brr2 driven processes dependent on its ubiquitination status [93]. Furthermore, the presence of a C-terminal fragment of Prp8 (referred to as Prp8-CTF) stimulates Brr2 helicase activity *in vitro*, although it suppresses Brr2 ATPase activity [85]. Currently, the mechanism of regulation remains unknown and it remains unclear how regulation can be realised *in vivo*.

1.8.5 Brr2 and Retinitis Pigmentosa

Autosomal dominant retinitis pigmentosa (adRP) is a heritable eye disease that leads to progressive retinal degeneration, ultimately resulting in blindness. Surprisingly, RP related alleles were found in genes encoding pre-mRNA splicing factors. Initially mutations in the human genes *PRPF31*, *PRPF3*, *PAP-1* as well as *PRPF8* were identified (reviewed in ref. [94]). However it remains poorly understood how mutations in splicing factors, whose functions are required ubiquitously, lead to retina specific degenerations. In order to understand the disease mechanism, the effects of adRP mutations on the splicing machinery were studied. Because the loci of adRP mutations are often conserved from yeast to human, yeast frequently served as a model system.

hBrr2 was suggested to play indirect as well as direct roles in relation to the molecular mechanism underlying adRP. adRP mutations in *PRPF8*, the human ortholog of *S. cerevisiae PRP8*, alter amino acids at the extreme C-terminus of the protein and interfere with the interactions between Brr2 and Prp8 [82, 83, 85, 95, 96]. However, different mechanisms were suggested for how this interaction defect might induce adRP. One suggested molecular mechanism is a U5 snRNP maturation defect. Impaired protein interactions between Brr2 and Prp8 lead to the formation of an alternative U5 snRNP precursor particle, reducing the level of

functional tri-snRNPs, and thus reducing splicing efficiency [95]. Based on *in vitro* experiments that tested the effects of the *PRP8* adRP mutations on the Brr2-Prp8-CTF interaction, a complementary or alternative disease mechanism was suggested. If Prp8-CTF carries adRP alleles, the normally observed enhancement of Brr2 mediated U4/U6 unwinding is lost (see above). This lack of stimulation was observed even when mutant Prp8-CTF was present in molar excess, thus it is unlikely to be simply due to a weakened Brr2-Prp8 interaction [85]. It is difficult to fully separate the Brr2 unwinding defect from the Prp8-Brr2 interaction defect, still the rational was that adRP may result from deregulated activation of spliceosomes, causing reduced splicing efficiency [85].

An immediate connection between hBrr2 and adRP comes from two recent reports that added hBrr2, encoded by *SNRNP200* (also known as *ASCC3L1*), to the list of splicing factors that can carry adRP provoking alleles [97, 98]. The identified mutations cause substitutions p.S1087L and p.R1090L in hBrr2, which in yeast Brr2 correspond to N1104L and R1107L. Interestingly, both mutations locate to the N-terminal Sec63-like domain of hBrr2/Brr2. Functional characterisation of the mutations in yeast Brr2 established that neither N1104L nor R1107L shows tri-snRNP assembly defects, precluding a U5 snRNP maturation defect as a likely cause of this form of adRP. Instead both mutations lead to defective U4/U6 unwinding in native tri-snRNPs [97]. These observations suggest a U4/U6 unwinding defect as a molecular basis for adRP; concluding that adRP associated with splicing factors might stem from insufficient activation/regulation of hBrr2 helicase activity during spliceosome activation [85, 97].

There is much to be learned about the mechanism(s) underlying adRP. Further investigation will be required to address if the hBrr2 adRP mutations compromise the protein's helicase activity directly, or if they interfere with regulation of its helicase activity instead. Do mutations in the N-terminal Sec63 domain interfere with Prp8 and Snu114 interaction? Also, given that a similar mutation of the same residue in Sec63-1 (*brr2* R1107A) affects both U4/U6

dissociation and spliceosome disassembly [70], it is conceivable that *brr2* R1107L might also affect both processes. Hence, it remains to be determined if a defect in spliceosome disassembly plays a role in adRP. (This paragraph was reproduced from [99])

1.9 Research aims of this thesis

Brr2 plays an essential role in pre-mRNA splicing and over the past years it has become the focus of an increasing number of studies. The recent discovery that mutations within hBrr2 can be linked to adRP emphasised the significance of hBrr2/Brr2 function further. However, the unusual domain organisation and bipartite architecture of Brr2 still leave many question unanswered. These regard not only the regulation of its enzymatic activity, but also the functional contribution of each of its domains. The key questions addressed in this thesis are:

1. What role does the catalytically inert C-terminal half play in Brr2 function, and why does it interact with other RNA helicases?

Yeast two-hybrid analyses revealed that the C-terminal helicase cassette of Brr2 engages in protein interactions. The region most important for protein binding comprises parts of helicase domain 2 and Sec63 domain 2 [82, 83]. Because Brr2 is thought to have several different functions throughout the splicing reaction, it is plausible that multiple interactions will contribute to its functions. Interactions with different binding partners, such as Snu114 and Prp8 seem to regulate Brr2 activity (see above, 1.8.3). On the other hand, it is conceivable that Brr2 affects, possibly controls the activity of some of its binding partners [82]. Interestingly, the C-terminal domains of Brr2 interact with at least two other spliceosomal RNA helicases, Prp2 and Prp16 [82]. Therefore, this project aimed at characterising determinants within the C-terminus of Brr2, and the Sec63-2 domain in particular, that contribute to these interactions. In addition the project aimed at providing

initial evidence for a mutual regulatory relationship between the C-terminus of Brr2 other interacting helicases.

2. Which RNAs interact with the different parts of Brr2?

Despite the fact that Brr2 is an essential splicing factor, its precise RNA substrates are not known. The U4/U6 duplex is one substrate clearly indicated by genetic experiments, but direct interactions of Brr2 with the U4 and U6 snRNAs have never been shown. More importantly, the mechanism by which dissociation of the U4/U6 duplex is achieved is not fully understood. Further insight into this process will contribute to a more comprehensive understanding of the complex sequence of rearrangements underlying spliceosome activation. The domain architecture of Brr2, comprising two structurally very similar helicase cassettes, poses another question: Which parts of Brr2 interact with RNA? Is the catalytically inactive C-terminal cassette of Brr2 involved in RNA interactions at all? Therefore, another aim of my PhD project was to identify and functionally characterise Brr2-RNA interactions that are established during the different stages of splicing.

1.10 References

1. Caceres, J.F. and Kornblihtt, A.R. (2002) Alternative Splicing: multiple control mechanisms and involvement in human disease. Trends in Genetics. **18**, 186-193.

2. Nielsen, T.W. and Graveley, B.R. (2010) Expansion of the eukaryotic proteome by alternative splicing. Nature. **463**, 457-463.

3. Fabrizio, P., Dannenberg, J., Dube, P., Kastner, B., Stark, H., Urlaub, H. and Lührmann, R. (2009) The Evolutionarily Conserved Core Design of the Catalytic Activation Step of the Yeast Spliceosome. Molecular Cell. **36**, 593-608.

4. Jurica, M.S. and Moore, M.J. (2003) Pre-mRNA Splicing: Awash in a Sea of Proteins. Cell. **12**, 5-14.

5. Wahl, M.C., Will, C.L. and Lührmann, R. (2009) The Spliceosome: Design Principles of a Dynamic RNP Machine. Cell. **136**, 701-718.

6. Brow, D.A. (2002) Allosteric cascade of spliceosome activation. Annual Review of Genetics. **36**, 333-360.

7. Stevens, S.W., Ryan, D.E., Ge, H.Y., Moore, R.E., Lee, T.D. and Abelson, J. (2002) Composition and Functional Characterisation of the Yeast Spliceosomal Penta-snRNP. Molecular Cell. **9**, 31-44.

8. Malca, H., Shomron, N. and Ast, G. (2002) The U1 snRNP base pairs with the 5' splice site within a penta-snRNP. Molecular and Cellular Biology. **23**, 3442-3455.

9. Nilsen, T.W. (1998) RNA-RNA interactions in nuclear pre-mRNA splicing. In RNA structure and function, R.W. Simons and M. Grunberg-Manago, eds. Cold Spring Harbor Laboratory Press, Cold Spring Harbor, New York, pp. 279-308.

10. Chan, S.-P., Kao, D.-I., Tsai, W.-Y. and Cheng, S.-C. (2003) The Prp19-Associated Complex in Spliceosome Activation. Science. **302**, 279-282.

11. Chan, S.-P. and Cheng, S.-C. (2005) The Prp19-associated Complex Is Required for Specifying Interactions of U5 and U6 with Pre-mRNA during Spliceosome Activation. Journal of Biological Chemistry. **280**, 31190-31199.

12. Konarska, M.M., Vilardell, J. and Query, C.C. (2006) Repositioning of the Reaction Intermediate within the Catalytic Center of the Spliceosome. Molecular Cell. **21**, 543-553.

13. Umen, J.G. and Guthrie, C. (1995) The second catalytic step of pre-mRNA splicing. RNA. **1**, 869-885.

14. Maniatis, T. and Reed, R. (2002) An extensive network of coupling among gene expression machines. Nature. **416**, 499-506.

15. Mount, S.M. (1982) A catalogue of splice junction sequences. Nucleic Acids Research. **10**, 459-472.

16. Will, C.L. and Lührmann, R. (1997) Protein functions in pre-mRNA splicing. Curent Opinion in Cell Biology. **9**, 320-328.

17. Newman, A.J. (1985) Molecular consequences of specific mutations on yeast mRNA splicing *in vivo* and *in vitro*. Cell. **42**, 335-344.

18. Parker, R. and Guthrie, C. (1985) A point mutation in the conserved hexanucleotide at a yeast 5' splice junction uncouples recognition, cleavage, and ligation. Cell. **41**(1), 107-118.

19. Reed, R. (1996) Initial splice site recognition and pairing during pre-mRNA splicing. Opin. Genet. Dev. **6**, 215-220.

20. Smith, J.D., Konarska, M.M. and Query, C.C. (2009) Insights into Branch Nucleophile Positioning and Activation from an Orthogonal Pre-mRNA Splicing System in Yeast. Molecular Cell. **34**, 333-343.

21. Qeury, C.C., Moore, M.J. and Sharp, P.A. (1994) Branch nucleophile selection in pre-mRNA splicing: evidence for the bulged duplex model. Genes & Development. **8**, 587-597.

22. Will, C.L. and Lührmann, R. (2005) Splicing of a rare class of introns by the U12-dependent spliceosome. Journal of Biological Chemistry. **386**, 713-724.

23. Reed, R. (1989) The organisation of 3' slice site sequences in mammalian introns. Genes & Development. **3**, 2113-2123.

24. Rymond, B.C. and Rosbash, M. (1985) Cleavage of 5' splice site and lariat formation are independent of 3' splice site in yeast mRNA splicing. Nature. **317**, 735-737.

25. Vijayraghavan, U., Parker, R., Tamm, J., Iimura, Y., Rossi, J. and Abelson, J. (1986) Mutations in conserved intron sequences affect multiple steps in the yeast splicing pathway, particularly assembly of the spliceosome. EMBO. **5**, 1683-1695.

26. Patterson, B. and Guthrie, C. (1991) A U-rich tract enhances usage of an alternative 3' splice site in yeast. Cell. **64**, 181-187.

27. Hall, S.L. and Padgett, R.A. (1994) Conserved sequences in a class of rare eukaryotic nuclear introns with non-consensus splice sites. Journal of Molecular Biology. **239**, 357-365.

28. Jackson, I.J. (1991) A reappraisal of non-consensus mRNA splice sites. Nucleic Acids Research. **19**, 3795-3798.

29. Sharp, P.A. and Burge, C.B. (1997) Classification of introns: U2-type or U12-type. Cell. **91**, 875-879.

30. Levine, A. and Durbin, R. (2001) A computational scan for U12-dependent introns in the human genome sequence. Nucleic Acids Research. **29**, 4006-4013.

31. Tarn, W.Y. and Steitz, J.A. (1997) Pre-mRNA splicing: the discovery of a new spliceosome doubles the challenge. Trends in Biochemical Sciences. **22**, 132-137.

32. Frilander, M.J. and Steitz, J.A. (2001) Dynamic Exchanges of RNA interactions Leading to Catalytic Core Formation in the U12-dependent Spliceosome. Molecular Cell. **7**, 217-226.

33. Patel, A.A. and Steitz, J.A. (2003) Splicing double: Insights from the second spliceosome. Nat. Rev. Mol. Cell Biol. **4**, 960-970.

34. Schneider, C., Will, C.L., Makarova, O.V., Makarov, E.M. and Luhrmann, R. (2002) Human U4/U6·U5 and U4atac/U6atac·U5 tri-snRNPs exhibit similar protein compositions. Molecular and Cellular Biology. **22**, 3219-3229.

35. Toor, N., Keating, K.S. and Pyle, A.M. (2009) Structural insight to RNA splicing. Current Opinion in Structural Biology. **19**(3), 260-266.

36. Toor, N., Keating, K.S., Taylor, S.D. and Pyle, A.M. (2008) Crystal structure of a self-spliced group II intron. Science. **320**, 77-82.

37. Yean, S.L., Wuenschell, G., Termini, J. and Lin, R.J. (2000) Metal-ion coordination by U6 small nuclear RNA contributes to catalysis in the spliceosome. Nature. **408**, 881-884.

38. Valdakhan, S. and Manley, J.L. (2001) Splicing-related catalysis by protein-free snRNAs. Nature. **413**, 701-707.

39. Grainger, R.J. and Beggs, J.D. (2005) Prp8 protein: At the heart of the spliceosome. RNA. **11**, 533-557.

40. Yang, K., Zhang, L., Xu, T., Heroux, A. and Zhao, R. (2008) Crystal Structure of the ß-finger domains of Prp8 reveals analogy to ribosomal proteins. PNAS. **105**(37), 13817-13822.

41. Pena, V., Rozov, A., Lührmann, R. and Wahl, M.C. (2008) Structure and Function of an RNase H domain at the heart of the spliceosome. EMBO. **27**, 2929-2940.

42. Ritchie, D.B., Schellenberg, M.J., Gesner, E.M., Raithatha, S.A., Stuart, D.T. and Macmillan, A.M. (2008) Structure elucidation of a PRP8 core domain from the heart of the spliceosome. Nature Structural & Molecular Biology. **15**, 1199-1205.

43. Abelson, J. (2008) Is the spliceosome a ribonucleoprotein enzyme? Nature Structural & Molecular Biology. **15**, 1235-1237.

44. Moore, M.J., Query, C.C. and Sharp, P.A. (1993) Splicing of precursors to mRNA by the splicosome. In The RNA World, R.F. Gesteland and J.F. Atkins, eds. (Cold Spring Harbour, NY: Cold Spring Harbour Laboratory Press), 303-357.

45. Staley, J.P. and Guthrie, C. (1998) Mechanical Devices of the Splicosome: Motors, Clocks, Springs and Things. Cell. **92**, 315-326.

46. Jankowsky, E. and Bowers, H. (2006) Remodeling of ribonucleoprotein complexes with DExH/D RNA helicases. Nucleic Acids Research. **34**(15), 4181-4188.

47. Gorbalenya, A.E. and Koonin, E.V. (1993) Helicases: amino acid sequence comparisons and structure-function relationships. Curent Opinion in Strucural Biology. **3**, 419-429.

48. Fairman-Williams, M.E., Guenther, U.P. and Jankowsky, E. (2010) SF1 and SF2 helicases: family matters. Current Opinion in Structural Biology. **20**(3), 313-324.

49. Cordin, O., Banroques, J., Tanner, K.N. and Linder, P. (2005) The DEAD-box protein family of RNA helicases. Gene. **367**, 17-37.

50. Linder, P. (2006) Dead-box proteins: a family affair--active and passive players in RNP-remodeling. Nucleic Acids Research. **34**(15), 4168-4180.

51. Rocak, S. and Linder, P. (2004) DEAD-box Proteins: The driving forces behind RNA metabolism. Nature Reviews. **5**, 232-241.

52. Bleichert, F. and Baserga, S.J. (2007) The long unwinding road of RNA helicases. Molecular Cell. **27**(3), 339-352.

53. Caruthers, J.M. and McKay, D.B. (2002) Helicase structure and mechanism. Curent Opinion in Strucural Biology. **12**, 123-133.

54. de la Cruz, J., Kressler, D. and Linder, P. (1999) Unwinding RNA in Saccharomyces cerevisiae: DEAD-box proteins and related families. TIBS. **24**, 192-198.

55. Linder, P., Gasteiger, E. and Bairoch, A. (2000) A comprehensive web resource on RNA helicases from the baker's yeast Saccharomyces cerevisiae. Yeast. **16**, 507-509.

56. Wang, Y. and Guthrie, C. (1998) PRP16, a DEAH-box RNA helicase, is recruited to the splicosome primarily via its nonconserved N-terminal domain. RNA. **4**, 1216-1229.

57. Schneider, S. and Schwer, B. (2001) Functional domains of the yeast splicing factor Prp22p. Journal of Biological Chemistry. **276**, 21184-21191.

58. Perriman, R.J. and Ares, M. (2007) Rearrangement of competing U2 RNA helices within the spliceosome promotes multiple steps in splicing. Genes & Development. **21**(7), 811-820.

59. Staley, J.P. and Guthrie, C. (1999) An RNA Switch at the 5' Splice Site Requires ATP and the DEAD Box Protein Prp28p. Molecular Cell. **3**, 55-64.

60. Chen, J.Y.-F., Stands, L., Staley, J.P., Jackups, R.R., Latus, L.J. and Chang, T.-H. (2001) Spcific Alterations of U1-C Protein or U1 Small Nuclear RNA Can Eliminate the Requirement of Prp28p, an essential DEAD Box Splicing Factor. Molecular Cell. **7**, 227-232.

61. Raghunathan, P.L. and Guthrie, C. (1998) RNA unwinding in U4/U6 snRNPs requires ATP hydrolysis and the DEIH-box splicing factor Brr2. Current Biology. **8**, 847-855.

62. Warkocki, Z., Odenwälder, P., Schmitzová, J., Platzmann, F., Stark, H., Urlaub, H., Ficner, R., Fabrizio, P. and Lührmann, R. (2009) Reconstitution of both steps of Saccharomyces cerevisiae splicing with purified spliceosomal components. Nature Structural & Molecular Biology. **16**(12), 1237-1243.

63. Teigelkamp, S., McGarvey, M., Plumpton, M. and Beggs, J.D. (1994) The splicing factor PRP2, a putative RNA helicase, interacts directly with pre-mRNA. EMBO. **13**(4), 888-897.

64. Lardelli, R.M., Thompson, J.X., Yates, J.R.r. and Stevens, S.W. (2010) Release of SF3 from the intron branchpoint activates the first step of pre-mRNA splicing. RNA. **16**(3), 516-528.

65. Schwer, B. and Guthrie, C. (1992) A conformational rearrangement in the splicosome is dependent on PRP16 and ATP hydrolysis. EMBO. **11**(13), 5033-5039.

66. Tseng, C.K., Liu, H.L. and Cheng, S.-C. (2010) DEAH-box ATPase Prp16 has dual roles in remodeling of the spliceosome in catalytic steps. RNA. **17**(1), 145-154.

67. McPheeters, D.S. and Muhlenkamp, P. (2003) Spatial Organization of Protein-RNA Interactions in the Branch Site-3' Splice Site Region during pre-mRNA Splicing in Yeast. Molecular and Cellular Biology. **23**(12), 4174–4186.

68. Schwer, B. (2008) A Conformational Rearrangement in the Spliceosome Sets the Stage for Prp22-Dependent mRNA Release. Molecular Cell. **30**, 743-754.

69. Martin, A., Schneider, S. and Schwer, B. (2002) Prp43 is an essential RNA-dependent ATPase required for release of lariat-intron from the spliceosome. Journal of Biological Chemistry. **277**(20), 17743-17750.

70. Small, E.C., Leggett, S.R., Winans, A.A. and Staley, J.P. (2006) The EF-G-like GTPase Snu114p Regulates Spliceosome Dynamics Mediated by Brr2p, a DExD/H Box ATPase. Molecular Cell. **23**, 389-399.

71. Arenas, J.E. and Abelson, J. (1997) Prp43: An RNA helicase-like factor involved in spliceosome disassembly. PNAS. **94**(22), 11798-11802.

72. Xu, D.M., Nouraini, S., Field, D., Tang, S.J. and Friesen, J.D. (1996) An RNA-dependent ATPase associated with U2/U6 snRNAs in pre-mRNA splicing. Nature. **381**, 709-713.

73. Lauber, J., Fabrizio, P., Teigelkamp, S., Lane, W.S., Hartmann, E. and Lührmann, R. (1996) The HeLa 200 kDa U5 snRNP-specific protein and its homologue in *Saccharomyces cerevisiae* are members of the DEXH-box protein family of putative RNA helicases. EMBO. **15**(15), 4001-4015.

74. Lin, J. and Rossi, J. (1996) Identification and characterization of yeast mutants that overcome an experimentally introduced block to splicing at the 3' splice site. RNA. **2**, 835-848.

75. Kim, H.-D. and Rossi, J. (1999) The first ATPase domain of the yeast 246-kDa protein is required for *in vivo* unwinding of the U4/U6 duplex. RNA. **5**, 959-971.

76. Noble, S.M. and Guthrie, C. (1996) Identification of Novel Genes Required for Yeast Pre-mRNA Splicing by Means of Cold-Sensitive Mutations. Genetics. **143**, 67-80.

77. Ponting, C.P. (2000) Proteins of the endoplasmic-reticulum-associated degradation pathway: domain detection and function prediction. Biochemical Journal. **351**, 527-535.

78. Pena, V., Mozaffari Jovin, S., Fabrizio, P., Orlowski, J., Bujnicki, J.M., Lührmann, R. and Wahl, M.C. (2009) Common Design Principles in the Spliceosomal RNA Helicase Brr2 and in the Hel308 DNA Helicase. Molecular Cell. **35**, 454-466.

79. Zhang, L., Xu, T., Maeder, C., Bud, L.-O., Shanks, J., Nix, J., Guthrie, C., Pleiss, J.A. and Zhao, R. (2009) Structural evidence for consecutive Hel308-like modules in the spliceosomal ATPase Brr2. Nature Structural & Molecular Biology. **16**, 731-739.

80. Buttner, K., Nehring, S. and Hopfner, K. (2007) Structural basis for DNA duplex separation by a superfamily-2 helicase. Nature Structural & Molecular Biology. **14**, 647-652.

81. Richards, J., Johnson, K., Liu, H., McRobbie, A., McMahon, S., Oke, M., Carter, L., Naismith, J. and White, M. (2008) Structure of the DNA repair helicase hel308 reveals DNA binding and autoinhibitory domains. Journal of Biological Chemistry. **283**, 5118-5126.

82. van Nues, R. and Beggs, J.D. (2001) Functional Contacts With a Range of Splicing Proteins Suggest a Central Role for Brr2p in the Dynamic Control of the Order of Events in Spliceosomes of *Saccharomyces cerevisiae*. Genetics. **157**, 1457-1467.

83. Liu, S., Rauhut, R., Vornlocher, H.-P. and Lührmann, R. (2006) The network of protein-protein interactions within the human U4/U6.U5 tri-snRNP. RNA. **12**, 1418-1430.

84. Laggerbauer, B., Achsel, T. and Luhrmann, R. (1998) The human U5-2OOkD DEXH-box protein unwinds U4/U6 RNA duplices *in vitro*. PNAS. **95**(8), 4188-4192.

85. Maeder, C., Kutach, A.K. and Guthrie, C. (2008) ATP-dependent unwinding of U4/U6 snRNAs by the Brr2 helicase requires the C terminus of Prp8. Nature Structural & Molecular Biology. **16**(1), 42-48.

86. Xu, D. and Friesen, J.D. (2000) Splicing Factor Slt11p and Its Involvement in Formation of U2/U6 Helix II in Activation of the Yeast Spliceosome. Molecular and Cellular Biology. **21**(4), 1011-1023.

87. Achsel, T., Ahrens, K., Brahms, H., Teigelkamp, S. and Lührmann, R. (1998) The Human U5-220kD Protein (hPrp8) Forms a Stable RNA-Free Complex with Several U5-Specific Proteins, Including an RNA Unwindase, a Homologue of Ribosomal Elongation factor EF-2, and a Novel WD-40 Protein. Molecular and Cellular Biology. **18**(11), 6756-6766.

88. Brenner, T.J. and Guthrie, C. (2005) Genetic Analysis Reveals a Role for the C Terminus of the Saccharomyces cerevisiae GTPase Snu114 During Splicosome Activation. Genetics. **170**, 1063-1080.

89. Bartels, C., Urlaub, H., Luhrmann, R. and Fabrizio, P. (2003) Mutagenesis suggests several roles of Snu114p in pre- mRNA splicing. Journal of Biological Chemistry. **278**(30), 28324-28334.

90. Kuhn, A. and Brow, D.A. (2000) Suppressors of a Cold-Sensitive Mutation in Yeast U4 RNA Define Five Domains in the Splicing Factor Prp8 That influence Splicosome Activation. Genetics. **155**, 1667-1682.

91. Kuhn, A.N., Reichl, E.M. and Brow, D.A. (2002) Distinct domains of splicing factor Prp8 mediate different aspects of spliceosome activation. PNAS. **99**(14), 9145-9149.

92. Kuhn, A.N., Li, Z.R. and Brow, D.A. (1999) Splicing factor Prp8 governs U4/U6 RNA unwinding during activation of the spliceosome. Molecular Cell. **3**(1), 65-75.

93. Bellare, P., Small, E.C., Huang, X., Wohlschlegel, J.A., Staley, J.P. and Sontheimer, E.J. (2008) A role for ubiquitin in the spliceosome assembly pathway. Nature Structural & Molecular Biology. **15**(5), 444-451.

94. Hartong, D.T., Breson, E.L. and Dryja, T. (2006) Retinitis Pigmentosa. Lancet. **368**, 1795-1809.

95. Boon, K.-L., Grainger, R.J., Ehsani, P., Barras, D., Auchynnikava, T., Inglehearn, C.F. and Beggs, J.D. (2007) *prp8* mutations that cause human retinitis pigmentosa lead to a U5 snRNP maturation defect in yeast. Nature Structural & Molecular Biology. **14**(11), 1077-1083.

96. Pena, V., Liu, S., Bujnicki, J.M., Lührmann, R. and Wahl, M.C. (2007) Structure of a multipartite protein-protein interaction domain in splicing factor Prp8 and its link to Retinitis pigmentosa. Molecular Cell. **25**(4), 615-624.

97. Zhao, C., Bellur, D., Lu, S., Zhao, F., Grassi, M.A., Bowne, S.J., Sullivan, L.S., Daiger, S.P., Chen, L.J., Pang, C.P., Zhao, K., Staley, J.P. and Larsson, C. (2009) Autosomal-Dominant Retinitis Pigmentosa Caused by a Mutation in *SNRNP200*, a Gene Required for Unwinding of U4/U6 snRNAs. The American Journal of Human Genetics. **85**, 617-627.

98. Li, N., Mei, H., MacDonald, I.M., Jiao, X. and Fielding Hejtmancik, J. (2009) Mutations in ASCC3L1 on chromosome 2q11.2 are associated with autosomal dominant retinitis pigmentosa in a Chinese Family. Invest. Ophtalmol. Vis. Sci. **09-3725**.

99. Hahn, D. and Beggs, J.D. (2010) Brr2p RNA helicase with a split personality: Insights into structure and function. Biochemical Society Transactions. **38**, 1105-1109.

Chapter 2 – Materials and Methods

2.1 Sources of Reagents

2.1.1 Chemicals

Unless otherwise stated chemicals were purchased from the following sources: Sigma or Fluka (both Sigma-Aldrich Company Ltd.), Fisher Chemicals, BDH Laboratory Supplies (AnalaR, VWR), Scotlab and Amersham Biosciences (GE Healthcare).

2.1.2 Enzymes

Restriction enzymes, DNA and RNA Polymerases as well as other enzymes were purchased from the following sources unless stated otherwise: New England Biolabs (NEB), Invitrogen, Roche, Promega, Finnzymes (Takara Bio Europe), Epicentre Biotechnologies and Qiagen.

2.1.3 Reagents for Growth Media

Reagents for growth media were purchased from the following sources: Formedium, Gibco BLR, Sigma, Fisher Scientific, Difco Laboratories and BD Biosciences.

2.1.4 Antibiotics

Ampicillin was purchased from Essential Generics (Engham, Surrey, UK), kanamycin (Geneticin) from Gibco, tetracycline from Duchefa. Hygromycin B was purchased from Calbiochem (EDM Biosciences, Inc. La Jolla, USA). Nourseothricin was purchased from HKI, Werner BioAgents (Jena, Germany) under the name clonNAT.

2.2 Growth media

2.2.1 Preparation and Storage

All media were autoclaved (10 min at 121°C) or filter sterilised (Nalgene Nunc or Millipore 0.22 μm). For solid media 2% (w/v) agar (Formedium) was added prior to autoclaving. Liquid media were stored at room temperature and warmed or cooled to the appropriate temperature as required. Plates were stored at 4°C and warmed in a drying oven before use.

2.2.2 Yeast Media

Table 2.1 Yeast Media

Medium	Composition
YPDA	1% (w/v) Yeast extract, 2% (w/v) Bacto-Peptone, 2% (w/v) Glucose, 0.003% (w/v) Adenine sulphate
YPGal	As YPDA, but 2% (w/v) Galactose instead of Glucose
YMM	0.67% (w/v) Yeast nitrogen base without amino acids, 2% (w/v) Glucose or 2% (w/v) Galactose
SD- or SD Gal-	YMM with 2 g/l of Drop out powder (Kaiser mix, Formedium)
5-FOA	0,67% (w/v) Yeast nitrogen base without amino acids, 2% (w/v) Glucose or Galactose, 0.2% (w/v) -Ura Drop out powder (Kaiser mix, Formedium) 0.005% (w/v) Uracil, 0.1% (w/v) 5-Fluorotic acid (Formedium)
Pre-sporulation medium	0.3% (w/v) Peptone, 0.8% (w/v) Yeast extract, 2% (w/v) Potassium acetate
Sporulation medium (liquid)	0.3% (w/v) Potassium acetate, pH to 7.0 with acetic acid, 0.02% (w/v) Raffinose
Sporulation medium (plates)	2% (w/v) Potassium acetate, 0.1% (w/v) Yeast extract, 2% (w/v) agar

2.2.3 Bacterial Media

Table 2.2 Bacterial Media

Medium	Composition
LB	1% (w/v) bacto-tryptone, 0.5% (w/v) Yeast extract and 0.5% (w/v) NaCl, pH adjusted to 7.2 with sodium hydroxide
SOC	2% (w/v) bacto-tryptone, 0.5% (w/v) yeast extract, 0.06% (w/v) NaCl, 0.02% (w/v) KCl, 0.1% (w/v) $MgCl_2$, 0.12% (w/v) $MgSO_4$ and 0.4% (w/v) Glucose
M9-L	0.1% (w/v) Drop out powder -Leu (Kaiser mix, Formedium), 2 mM $MgSO_4$, 0.2 mM $CaCl_2$, pH adjusted to 6.5 with sodium hydroxide, 0.2% (w/v) Glucose, M9 salts: 6 µg/ml Na_2HPO_4, 3 µg/ml KH_2PO_4, 0.5 µg/ml NaCl, 1 µg/ml NH_4Cl

2.2.4 Antibiotics

Antibiotics were added to liquid media immediately before use. Solid media were autoclaved then cooled to approximately 55°C before antibiotics were added. Ampicillin, tetracyclin and nourseothrycin stock solutions were prepared at 1000-fold higher than the final concentration required and were stored at -20°C. Geneticin (kanamycin) and hygromycin B solutions were purchased readymade and stored at 4°C.

Table 2.3 Antibiotics

Antibioticum	Abbreviation	Solvent	Final concentration (µg/ml)
Ampicillin	Amp	H_2O	100
Hygromycin B	Hyg	PBS	300
Kanamycin (Geneticin)	Kan	H_2O	200
Nourseothrycin	Nat	H_2O	100
Tetracycline	Tet	EtOH	5

2.3 Commonly used buffers

All buffers listed in Table 2.4 were prepared using deionised water and were either autoclaved or filter sterilised (0.22 µm, Nalgene Nunc) prior to use.

Table 2.4 Commonly used buffers

Buffer	Composition
50xTAE	2 M Tris-base, 5.71% (v/v) acetic acid, 50 mM EDTA
10x TE	100 mM Tris-HCl, 10 mM EDTA pH 8.0
10xTBE	0.89 M Tris-base, 0.89 M boric acid, 20 mM EDTA
20x MOPS SDS-Page running buffer	1 M MOPS, 1 M Tris-base, 20% (w/v) SDS, 20 mM EDTA
10x Western Transfer buffer	200 mM Tris-base, 1.5 M Glycine
20x SSC	3 M NaCl, 0.3 M Sodium Citrate (pH adjusted to 7.4 with NaOH)
1x PBS	140 mM NaCl, 3 mM KCl, 8 mM Na_2HPO_4, 1.4 mM H_2PO_4, 20 mM $MgCl_2$

2.4 *Escherichia coli* strains

The *Escherichia coli* (*E. coli*) strains used in this study are listed in Table 2.5. TOP10 and XL10 gold cells were used for cloning and propagation of plasmids. MC1066 cells were used for plasmid rescue of *LEU2* marked plasmids from yeast (2.11.2).

Table 2.5 *E. coli* strains used in this study

Strain	Genotype	Source
TOP 10	F– *mcr*A Δ(*mrr-hsd*RMS-*mcr*BC) Φ80*lac*ZΔM15 Δ*lac*X74 *rec*A1 *ara*D139 Δ(*ara leu*) 7697 *gal*U *gal*K *rps*L (StrR) *end*A1 *nup*G	Invitrogen
MC1066	*gal*U *gal*K *str*A^R *hsd*R$^-$ (Δ*lac-IPOZYA*)*X74 trpC9830 leuB6 pyr74*::Tn5 (Km^R)	Casaban M. *et al.,* 1983
XL10 gold	*end*A1 *gln*V44 *rec*A1 *thi*-1 *gyr*A96 *rel*A1 lac Hte Δ(*mcr*A)183 Δ(*mcr*CB-*hsd*SMR-*mrr*)173 tet^R F'[*pro*AB *lac*I^{q}ZΔM15 Tn10(Tet^R Amy Cm^R)]	Stratagene

2.5 *Saccharomyces cerevisiae* strains

All *Saccharomyces cerevisiae* (*S. cerevisiae* or yeast) strains used throughout and created for this study are listed in the table 2.6.

Table 2.6 *S. cerevisiae* strains used in this study

Strain	Genotype
L40ΔG	*MAT***a** *his3Δ200 trp1-901 leu2-3,112 ade2 LYS2*::(4lexAop-*HIS3*) *URA3*::(8lexAop-lacZ) Δgal4::*KAN* ((Kan^R))
W303 2n	*MAT***a**/*MAT*α {*leu2-3,112 trp1-1 can1-100 ura3-1 ade2-1 his3-11,15}* [*phi*+]
W303α	*MAT*α *leu2-3,112 trp1-1 can1-100 ura3-1 ade2-1 his3-11,15* [*phi*+]
BY4741	*MAT***a** *his3Δ1 leu2Δ0 LYS2 met15Δ0 ura3Δ0*
BY4742	*MAT*α *his3Δ1 leu2Δ0 lys2Δ0 MET15 ura3Δ0*
W303 brr2Δ	*MAT***a** *leu2-3,112 trp1-1 can1-100 ura3-1 ade2-1 his3-11,15* [*phi*+] *KANMx6*::brr2Δ [pRS316-BRR2]
W303 brr2Δ/prp16Δ	*MAT*α *leu2-3,112 trp1-1 can1-100 ura3-1 ade2-1 his3-11,15* [*phi*+] *KANMx6*::brr2Δ *NatNT2::prp16*Δ [pRS316-BRR2/PRP16]
W303 brr2Δ/isy1Δ	*MAT***a** *leu2-3,112 trp1-1 can1-100 ura3-1 ade2-1 his3-11,15* [*phi*+] *KANMx6*::brr2Δ *NatNT2::isy1*Δ [pRS316-BRR2]
W303 brr2Δ/U5Δ	*MAT*α *leu2-3,112 trp1-1 can1-100 ura3-1 ade2-1 his3-11,15* [*phi*+] *KANMx6*::brr2Δ *HphNT1::snR7*Δ [pRS316-BRR2/U5]
W303 brr2Δ/U4Δ	*MAT***a** *leu2-3,112 trp1-1 can1-100 ura3-1 ade2-1 his3-11,15* [*phi*+] *KANMx6*::brr2Δ *HphNT1::snR14*Δ [pRS316-BRR2/U4]
W303 brr2Δ/U2Δ	*MAT*α *leu2-3,112 trp1-1 can1-100 ura3-1 ade2-1 his3-11,15* [*phi*+] *KANMx6*::brr2Δ *HphNT1::snR20*Δ [pRS316-BRR2/U2]
W303 U2Δ	*MAT*α *leu2-3,112 trp1-1 can1-100 ura3-1 ade2-; his3-11,15* [*phi*+] *KANMX6::snRN20*Δ [pRS416-U2]
W303 U4Δ	*MAT*α *leu2-3,112 trp1-1 can1-100 ura3-1 ade2-; his3-11,15* [*phi*+] *HphNT1::snRN14*Δ [pRS416-U4]
W303 brr2Δ *GalS::3HA-prp18*	*MAT***a** *leu2-3,112 trp1-1 can1-100 ura3-1 ade2-1 his3-11,15* [*phi*+] *KANMx6*::brr2Δ *Nat-GalS::3HA-prp18* [pRS316-BRR2]
W303 brr2Δ *GalS::3HA-slu7*	*MAT***a** *leu2-3,112 trp1-1 can1-100 ura3-1 ade2-1 his3-11,15* [*phi*+] *KANMx6*::brr2Δ *Nat-GalS::3HA-slu7* [pRS316-BRR2]
U5KO	*MAT***a** *leu2Δ1 his3Δ200 trp1Δ63 ura3-52 KanMX4::snR7* [pRS416-U5]
U5KO *GalS::3HA-brr2*	*MAT***a** *leu2Δ1 his3Δ200 trp1Δ63 ura3-52 KanMX4::snR7 Nat-GalS::3HA-brr2* [pRS416-U5]
tetON RIBO1	*MAT***a** *leu2-3,112 trp1-1 can1-100 ura3-1 ade2-; his3-11,15* [*phi*+] *leu2::*P_{adh1}*-tetR-SSN6-LEU2* [p414 *(*P_{ADH1}*-t-tA')*]
tetON RIBO1 *GalS::brr2*	*MAT***a** *leu2-3,112 trp1-1 can1-100 ura3-1 ade2-; his3-11,15* [*phi*+] *leu2::*P_{adh1}*-tetR-SSN6-LEU2, HIS3-GalS::brr2* [p414 *(*P_{ADH1}*-t-tA')*]
BY4742 prMFα BRR2	*MAT*α *his3Δ1 leu2Δ0 lys2Δ0 MET15 ura3Δ0 prMFα2Nat*^{R}*::BRR2*
BY4742 prMFα brr2 L1951P	*MAT*α *his3Δ1 leu2Δ0 lys2Δ0 MET15 ura3Δ0 prMFα2Nat*^{R}*::brr2 L1951P*
BY4742 prMFα brr2 L1930P	*MAT*α *his3Δ1 leu2Δ0 lys2Δ0 MET15 ura3Δ0 prMFα2Nat*^{R}*::brr2 L1930P*

2.6 Plasmids

All plasmids used throughout this study and created for this study are listed in tables 2.7-2.11. All plasmids created for this study were constructed by using standard cloning techniques (2.11.9). Mutant derivatives of plasmids were created by SDM (2.11.10.3) or Megaprimer PCR (2.11.10. 4).

Table 2.7 Plasmid backbones

Plasmid	Description	Reference
pACTII stop	*2 µ*, *TRP1*, expresses Gal4AD	[1]
pBTM116	*2 µ*, *LEU2*, expresses LexA	[2]
pRS313	*HIS3, ARS, CEN*	[3]
pRS314	*TRP1, ARS CEN*	[3]
pRS315	*LEU2, ARS CEN*	[2]
pRS316	*URA3, ARS, CEN*	[2]
pRS413	*TRP1, ARS, CEN,* P*MET*25	M. Reins
pRS415-HTP	*LEU2, ARS, CEN,* p*MET*25*,* encodes HTP-tag	S. Granneman
pGID3	Amp^R cloning vector, encodes *MATα* driven *NAT* marker gene	[4]

Table 2.8 Plasmids used as PCR templates for making yeast strains

Plasmid	Description	Reference
pFA6a-kanMX6	used as PCR template for the amplification of Kan deletion cassette	[5]
pFA6a-natNT2	used as PCR template for the amplification of Nat deletion cassette	[6]
pFA6a-hphNT1	used as PCR template for the amplification of Hph deletion cassette	[2]
pYM-N32	used as PCR template for the amplification of a *GalS* promoter and N-terminal 3-HA epitope tag	[2]
pYM-N30	used as PCR template for the amplification of a *GalS* promoter	[2]

Table 2.9 Yeast Two-hybrid plasmids created for this study

Plasmid	Description
pBTM116-PRP2	*PRP2* ORF cloned *EcoR*I/*Pst*I in-frame with LexA
pBTM116-PRP16	*PRP16* ORF cloned *EcoR*I/*Pst*I in-frame with LexA
pBTM116-prp16 L335F	derivative of pBTM116-PRP16, created by SDM
pBTM116-prp16 K379R	derivative of pBTM116-PRP16, created by SDM
pBTM116-prp16 D473E	derivative of pBTM116-PRP16, created by SDM

Plasmid	Description
pBTM116-prp16 H476D	derivative of pBTM116-PRP16, created by SDM
pBTM116-prp16 T507A	derivative of pBTM116-PRP16, created by SDM
pBTM116-prp16 Q685H	derivative of pBTM116-PRP16, created by SDM
pBTM116-prp16 R686Q	derivative of pBTM116-PRP16, created by SDM
pBTM116-prp16 R686I	derivative of pBTM116-PRP16, created by SDM
pBTM116-prp16-302	derivative of pBTM116-PRP16, created by SDM
pBTM116-prp16-201	derivative of pBTM116-PRP16, created by SDM
pBTM116-prp16-202	derivative of pBTM116-PRP16, created by SDM
pBTM116-prp16-203	derivative of pBTM116-PRP16, created by SDM
pACTIIstop-brr2 H2-Sec63-2	Gal4AD in-frame fusion with a Brr2 fragment encoding aa 1-97 + 1294-2163
pACTIIstop-brr2 H2-Sec63-2 V1922A	derivative of pACTIIstop-brr2 H2-Sec63-2, created by SDM
pACTIIstop-brr2 H2-Sec63-2 Q1931R	derivative of pACTIIstop-brr2 H2-Sec63-2, created by SDM
pACTIIstop-brr2 H2-Sec63-2 S1935P	derivative of pACTIIstop-brr2 H2-Sec63-2, created by SDM
pACTIIstop-brr2 H2-Sec63-2 E1952G	derivative of pACTIIstop-brr2 H2-Sec63-2, created by SDM
pACTIIstop-brr2 H2-Sec63-2 S1966D	derivative of pACTIIstop-brr2 H2-Sec63-2, created by SDM
pACTIIstop-brr2 H2-Sec63-2 N1972D	derivative of pACTIIstop-brr2 H2-Sec63-2, created by SDM
pACTIIstop-brr2 H2-Sec63-2 V2045D	derivative of pACTIIstop-brr2 H2-Sec63-2, created by SDM
pACTIIstop-brr2 H2-Sec63-2 L2096D	derivative of pACTIIstop-brr2 H2-Sec63-2, created by SDM
pACTIIstop-brr2 H2-Sec63-2 W2099R	derivative of pACTIIstop-brr2 H2-Sec63-2, created by SDM

Table 2.10 Shuffle plasmids created for this study

Plasmid	Description
pRS316-BRR2	*URA3*, *ARS*, *CEN*, *BRR2* ORF with -279nt upstream and +292nt downstream sequence, cloned *Sac*I/*Kpn*I
pRS316 BRR2/PRP16	derivative of pRS316-BRR2, PRP16 ORF with -310nt upstream and +179nt downstream sequence, cloned into *Kpn*I site
pRS316-BRR2/U4	derivative of pRS316-BRR2, snR14 gene (U4) with -402nt upstream and +398nt downstream sequence, in-Fusion cloning to *Kpn*I site
pRS316-BRR2/U5	derivative of pRS316-BRR2, snR7 gene encoding U5 with -402nt and +480nt downstream sequence, in-Fusion cloning to *Kpn*I site
pRS316-BRR2/U6	derivative of pRS316-BRR2, snR6 gene encoding U6 with -500nt upstream and +500nt downstream sequence, cloned in *Kpn*I site
RS316-BRR2/U2	derivative of pRS316-BRR2, snR20 gene encoding U2 with -400nt upstream and +400nt downstream sequence cloned in *Kpn*I site
pRS315-BRR2	*LEU2*, *ARS*, *CEN*, *BRR2* ORF with -279nt upstream and +292nt downstream sequence cloned *Sac*I/*Xma*I
pRS315-brr2 *rss1-1*	derivative of pRS315-BRR2, created by SDM, encodes amino acid substitution G858R in *BRR2* ORF
pRS315-brr2 Sec63-2Δ	derivative of pRS315-BRR2, created by SDM, encodes a stop codon after amino acid E1852 in *BRR2* ORF
pRS315-brr2 R1107P	derivative of pRS315-BRR2, created by SDM
pRS315-brr2 R1899G	derivative of pRS315-BRR2, created by SDM
pRS315-brr2 K1925R	derivative of pRS315-BRR2, created by SDM
pRS315-brr2 C1769R	derivative of pRS315-BRR2, created by SDM

Plasmid	Description
pRS315-brr2 I1763M	derivative of pRS315-BRR2, created by SDM
pRS315-brr2 W1772A	derivative of pRS315-BRR2, created by SDM
pRS315-brr2 Y1779A	derivative of pRS315-BRR2, created by SDM
pRS315-brr2 R1781P	derivative of pRS315-BRR2, created by SDM
pRS315-brr2 D1793G	derivative of pRS315-BRR2, created by SDM
pRS315-brr2 S1795P	derivative of pRS315-BRR2, created by SDM
pRS315-brr2 L1814I	derivative of pRS315-BRR2, created by SDM
pRS315-brr2 L1814S	derivative of pRS315-BRR2, created by SDM
pRS315-brr2 V1815I	derivative of pRS315-BRR2, created by SDM
pRS315-brr2 D1823G	derivative of pRS315-BRR2, created by SDM
pRS315-brr2 N1849A	derivative of pRS315-BRR2, created by SDM
pRS315-brr2 S1854A	derivative of pRS315-BRR2, created by SDM
pRS315-brr2 G1857A	derivative of pRS315-BRR2, created by SDM
pRS315-brr2 T1862P	derivative of pRS315-BRR2, created by SDM
pRS315-brr2 L1883P	derivative of pRS315-BRR2, created by SDM
pRS315-brr2 L1930P	derivative of pRS315-BRR2, created by SDM
pRS315-brr2 A1932P	derivative of pRS315-BRR2, created by SDM
pRS315-brr2 L1951P	derivative of pRS315-BRR2, created by SDM
pRS315-brr2 I2071T	derivative of pRS315-BRR2, created by SDM
pRS315-brr2 I2073N	derivative of pRS315-BRR2, created by SDM
pRS315-brr2 S2148P	derivative of pRS315-BRR2, created by SDM
pRS315-brr2 Y1775C+N1972D	derivative of pRS315-BRR2, created by SDM
pRS315-brr2 L1814I+Q1931R	derivative of pRS315-BRR2, created by SDM
pRS315-brr2 S1795P+S1966D	derivative of pRS315-BRR2, created by SDM
pRS315-brr2 D1823G+W2099R	derivative of pRS315-BRR2, created by SDM
pRS315-brr2 R1781C+V2045D	derivative of pRS315-BRR2, created by SDM
pRS315-brr2 L1814S+L2075S	derivative of pRS315-BRR2, created by SDM
pRS315-brr2 T1862P+D2027G	derivative of pRS315-BRR2, created by SDM
pRS315-brr2 V1815I+S2148P	derivative of pRS315-BRR2, created by SDM
pRS315-brr2 I1763M+V1922A	derivative of pRS315-BRR2, created by SDM
pRS315-brr2 D1793G+T2132A	derivative of pRS315-BRR2, created by SDM
pRS315-brr2 R1781P+S2098C	derivative of pRS315-BRR2, created by SDM
pRS315-brr2 V1922A	derivative of pRS315-BRR2, created by SDM
pRS315-brr2 Q1931R	derivative of pRS315-BRR2, created by SDM
pRS315-brr2 S1935P	derivative of pRS315-BRR2, created by SDM
pRS315-brr2 E1952G	derivative of pRS315-BRR2, created by SDM
pRS315-brr2 V2045D	derivative of pRS315-BRR2, created by SDM
pRS315-brr2 W2099R	derivative of pRS315-BRR2, created by SDM
pRS315-brr2 I1763M	derivative of pRS315-BRR2, created by SDM
pRS315-brr2 W1772A	derivative of pRS315-BRR2, created by SDM
pRS315-brr2 Y1779A	derivative of pRS315-BRR2, created by SDM
pRS315-brr2 R1793G	derivative of pRS315-BRR2, created by SDM
pRS315-brr2 S1795P	derivative of pRS315-BRR2, created by SDM
pRS315-brr2 L1814S	derivative of pRS315-BRR2, created by SDM

Plasmid	Description
pRS315-brr2 D1823G	derivative of pRS315-BRR2, created by SDM
pRS315-brr2 N1849A	derivative of pRS315-BRR2, created by SDM
pRS315-brr2 I1854A	derivative of pRS315-BRR2, created by SDM
pRS315-brr2 G1857A	derivative of pRS315-BRR2, created by SDM
pRS315-brr2 T1862P	derivative of pRS315-BRR2, created by SDM
pRS315-BRR2-HTP	derivative of pRS315-BRR2, created by Megaprimer PCR, C-terminal in-frame fusion of HTP-tag
pRS313-BRR2	*HIS3*, *ARS*, *CEN*, *BRR2* ORF with -279nt upstream and +292nt downstream sequence cloned *Sac*I/*Xma*I
pRS313-brr2 *rss1-1*	derivative of pRS313-BRR2, created by SDM
pRS313-brr2 R1107P	derivative of pRS313-BRR2, created by SDM
pRS313-brr2 L1951P	derivative of pRS313-BRR2, created by SDM
pRS313-brr2 Sec63-2Δ	derivative of pRS313-BRR2, created by SDM
pRS415-brr2 N-HTP	*LEU*, *ARS*, *CEN*, pMet25, Brr2 fragment aa 1-1314 in-frame with C-terminal HTP-tag, cloned *BamH*I/*Xba*I
pRS415-brr2 C-HTP	*LEU*, *ARS*, *CEN*, pMet25, Brr2 fragment aa 1+1313-2163 in-frame with C-terminal HTP-tag, cloned *BamH*I/*Xba*I
pRS413-brr2 N	*HIS3*, *ARS*, *CEN*, pMet25, Brr2 fragment aa 1-1314, cloned *Xma*I/*Cla*I
pRS3413-brr2 C	*HIS3*, *ARS*, *CEN*, pMet25, Brr2 fragment aa 1+1313-2163, cloned *Xma*I/*Cla*I
pRS415-brr2 N R1107P-HTP	derivative of pRS415-brr2 N-HTP, created by SDM
pRS415-brr2 C L1930P-HTP	derivative of pRS415-brr2 C-HTP, created by SDM
pRS415-brr2 C L1951P-HTP	derivative of pRS415-brr2 C-HTP, created by SDM
pRS415-brr2 C R1899G-HTP	derivative of pRS415-brr2 C-HTP, created by SDM
pRS415-brr2 C K1915R-HTP	derivative of pRS415-brr2 C-HTP, created by SDM
pRS314-PRP16	*TRP1*, *ARS*, *CEN*, *PRP16* ORF with -304nt upstream and +170nt downstream sequence, cloned into *Xma*I site
pRS314-prp16 L335F	derivative of pRS314-PRP16, created by SDM
pRS314-prp16 K379R	derivative of pRS314-PRP16, created by SDM
pRS314-prp16 D473E	derivative of pRS314-PRP16, created by SDM
pRS314-prp16 H476D	derivative of pRS314-PRP16, created by SDM
pRS314-prp16 T507A	derivative of pRS314-PRP16, created by SDM
pRS314-prp16 Q685H	derivative of pRS314-PRP16, created by SDM
pRS314-prp16 R686Q	derivative of pRS314-PRP16, created by SDM
pRS314-prp16 R686I	derivative of pRS314-PRP16, created by SDM
pRS314-prp16-302	derivative of pRS314-PRP16, created by SDM
pRS314-prp16-201	derivative of pRS314-PRP16, created by Megaprimer PCR
pRS314-prp16-202	derivative of pRS314-PRP16, created by Megaprimer PCR
pRS314-prp16-203	derivative of pRS314-PRP16, created by Megaprimer PCR
pRS314-U2	*TRP1*, *ARS*, *CEN*, snR20 gene encoding U2 with -402nt upstream and +402 nt downstream flanking sequence, cloned in *Kpn*I site
pRS314-U2 G1139A	derivative of pRS314-U2, carries substitution G1139A
pRS314-U2 C1141U	derivative of pRS314-U2, carries substitution C1141U
pRS314-U2 G1139, C1141U	derivative of pRS314-U2, carries substitutions G1139, C1141U
pRS314-U2 G1139A, U1152C	derivative of pRS314-U2, carries substitutions G1139A, U1152C

Plasmid	Description
pRS314-U2 G1139A, C1141U, U1152C	derivative of pRS314-U2, carries substitutions G1139A, C1141U, U1152C
pRS314-U2 G143A, G145A	derivative of pRS314-U2, carries substitutions G143A, G145A
pRS314-U2 Δ 5' stem V	derivative of pRS314-U2, deletion of nt 139-150
pRS314-U2 mut 5' stem V	derivative of pRS314-U2, nt 138-151 exchanged for 5'GGUAACGCAGAUUC
pRS314-U2 mut 5' stem V + stem IV	derivative of pRS314-U2, substitutions G1139A, C1141U, U1152C + nt 138-151 exchanged for 5'GGUAACGCAGAUUC
pRS314-U2 mut 3' stem V	derivative of pRS314-U2, nt 1156-1170 exchanged for 5'GAGAUCUGCGUUACU
pRS314-U2 mut 5' stem V + mut 3' stem V	derivative of pRS314-U2, nt 138-151 exchanged for 5'GGUAACGCAGAUUC + nt 1156-1170 exchanged for 5'GAGAUCUGCGUUACU
pRS314-U2 U23G	derivative of pRS314-U2, carries substitution U23G
pRS314-U2 U23G + Δ 5' stem V	derivative of pRS314-U2, carries substitution U23G + deletion of nt 139-150
pRS314-U2 U23G + mut 5' stem V	derivative of pRS314-U2, carries substitution U23G + nt 138-151 exchanged for 5'GGUAACGCAGAUUC
pRS314-U2 U23G + mut 5' stem V + mut stem IV	derivative of pRS314-U2, carries substitutions U23G + G1139A, C1141U, U1152C + nt 138-151 exchanged for 5'GGUAACGCAGAUUC
pRS413-U4 Δ3'SL	derivative of pRS413-U4, carries deletion of nt 93-141
pRS314-U4 Δtop 3'SL	derivative of pRS413-U4, deletion of nt 94-100 + nt 132-140
pRS314-U4 Δ138	derivative of pRS413-U4, deletion of nt 138
pRS314-U4 Δ136-139	derivative of pRS413-U4, deletion of nt 136-139
pRS314-U4 Δ139-141	derivative of pRS413-U4, deletion of nt 139-141
pRS314-U4 Δ131-133	derivative of pRS413-U4, deletion of nt 131-133
pRS314-U4 Ins 3U U138	derivative of pRS413-U4, insertion of 3U nt at position 138

Table 2.11 Plasmids kindly donated by others

Plasmid	Description	Source
pGDP-BRR2-TAP	high copy plasmid expressing TAP-tagged Brr2	Scot Stevens
pRS314-U5	shuffle plasmid expressing U5 snRNA	Ray O'Keefe
pRS314-U5-1	shuffle plasmid expressing U5-1 mutant	Ray O'Keefe
pRS314-U5-2	shuffle plasmid expressing U5-2 mutant	Ray O'Keefe
pRS314-U5-3	shuffle plasmid expressing U5-3 mutant	Ray O'Keefe
pRS314-U5 Δ96/97	shuffle plasmid expressing U5 Δ96,97 mutant	Ray O'Keefe
pRS314-U5 Δ93	shuffle plasmid expressing U5 Δ93 mutant	Ray O'Keefe
pRS314-U5 ΔC112,G113	shuffle plasmid expressing U5 Δ112,113 mutant	Ray O'Keefe
pRS314-U5 Ins 1U G93/C94	shuffle plasmid expressing U5 Ins 1U G93/C94 mutant	Ray O'Keefe
pRS314-U5 Ins 1U C94/C95	shuffle plasmid expressing U5 Ins 1U C94/C95 mutant	Ray O'Keefe
pRS314-U5 Ins 1U U97/U98	shuffle plasmid expressing U5 Ins 1U U97/U98 mutant	Ray O'Keefe
pRS413-U4	shuffle plasmid expressing U4 snRNA	Ray O'Keefe
pRS413-U4-cs1	shuffle plasmid expressing U4 cs-1 mutant	Ray O'Keefe
pRS413-U4 G58A	shuffle plasmid expressing U4 G58A mutant	Ray O'Keefe

Plasmid	Description	Source
pRS413-U4 U64C,G65A	shuffle plasmid expressing U4 U64C,G65A mutant	Ray O'Keefe
pRS416-U2	*ARS, CEN, URA3*, helper plasmid expressing U2 snRNA	Ray O'Keefe
p283	modified pGEM1 used as template for *in vitro* transcription of *ACT1* splicing substrate	Ray O'Keefe

2.7 Oligonucleotides

All oligonucleotides used throughout this study are listed in tables 2.12-2.17. Oligonucleotides used for PCR amplification, cloning, sequencing, as Northern probes or labelled probes for Primer extensions were synthesised by Invitrogen. Oligonucleotides used for CRAC experiments were obtained from IDT (Integrated DNA Technologies).

Table 2.12 Oligonucleotides used for cloning, sequencing and colony PCR

Oligo Name	Alias	Sequence	Description
U4 160 R	379	5' aaaggtattccaaaaattccc	U4 IVT
U4 160 short R	405	5' aaaggtattccaaaaattc	U4 IVT
T7 U6 1 F	401	5' GGATCCTAATACGACTCACTATAGGGAGAGGgttcgcgaagtaacccttcg	U6 IVT
T7 U6 112 R	402	5' aaaacgaaataaatctctttg	U6 IVT
Act T7 F	242	5' attaatacgactcactataggg	IVT splicing substrate
Act tetra loop R	243	5' ATGGTCCCGAAGGACCATccccctcatcaccaacgtag	
pBTM116-Prp16 F	240	5' gggctggcggttggggttattcgcaacggcgactggctggaattcATGGGTCAT TCGGGGCGTGAGG	gap repair, pBTM116-Prp16
pBTM116-Prp16 R	241	5' atcataaatcataagaaattcgcccggaattagcttggctgcagCTAAAAAAAA GGCTTCCTTCTTTTG	
SEQ int PRP16-F	36	5' gaggtagtaagctggttg	SEQ *PRP16*
SEQ int PRP16-R	37	5' gtttgttacaccaatgcg	SEQ *PRP16*
SEQ intPRP16-F2	42	5' cacttgtcagggcaagag	SEQ *PRP16*
SEQ intPRP16-R2	41	5' gcaaatcttttggttgctc	SEQ *PRP16*
SEQ prp16 5' R	290	5' caggcgttagttcttttgac	SEQ *PRP16*
SEQ prp16 3' F	291	5' cgaaaaagcaaaatatactg	SEQ *PRP16*
SEQ prp16 R3	296	5' ctgttattttggctgcttgatg	SEQ *PRP16*
Col PCR prp16 -103 F	292	5' ctattttctcaaataataaaagcgg	Col PCR *PRP16*
Col PCR Prp16 +115	227	5' ctcaatgtaagcactccacg	Col PCR *PRP16*

Oligo Name	Alias	Sequence	Description
PRP16mut subclone F	293	5’ caccactgttttgaacactgccatgggggaagtactaggc	subcloining *PRP16*
PRP16mut subclone R	294	5’ gttcatagtgttcaccaaagaggcctgtagttgtggcctcctg	
PRP16 in pRS316-BRR2 F	319	5’ cactaaagggaacaaaagctgggtacccccttatagttagatgcgctc	cloning *PRP16* in pRS316-BRR2
PRP16 in pRS316-BRR2 R	320	5’ gttgtgccattgttctcaagggtaccgattgtagcagtatgggtaac	
EcoRI-PRP2-F	1	5‘ gGAATTCatgtcaagtattacatctgaaacc	cloning, pBTM116-Prp2
PstI-PRP2-R	2	5‘ aaCTGCAGaacaatgcattggtacacctgtcaaaaaaccttcacc	
SEQ intPRP2-R2	40	5’ gatactgggcttatccatc	SEQ *PRP2*
SEQ-intPRP2-F	19	5’ gatgagctactacaagag	SEQ *PRP2*
F-Seq-Gal4AD		5’ CTATTCGATGATGAAGATACCCC	
ABS1	96	5’ gcgtttggaatcactacagg	SEQ Y2H plasmids
ABS2	97	5’ cacgatgcacagttgaagtg	
EP Megaprimer Sec2-F	83	5’ ctctgaacaacgagatagcaaattc	error prone PCR
EP Megaprimer Sec2-R	84	5’ ctacgattcatagatctctcgagcg	
inFusion brr2 pGID F	249	5’ GCAGGTCGACGGATCCCTCTGAACAACGAGATAGCAAATTC	cloning of pGID3 brr2
inFusion brr2 pGID R	250	5’ ATTAACCCGGGGATCCGATTTTATTTCACATTTATTTCAAAGG	
pGID3 NAT R	246	5’ gaatgttatatattgaaatccattcgattatccaggactaaacaatgattttacatcgat gaattcgagctcgttttcg	
Brr2 -276 pRS F	141	5’ gccagtgaattgtaatacgactcactatagggcgaattggagctc*cattcagacaggaacaaacttg*	gap repair pRS316/5-Brr2
Brr2+292 pRS R	142	5’ gctcggaattaaccctcactaaagggaacaaaagctgggtacc*cttgagaacaatggcacaacc*	pRS316-Brr2
Brr2+292pRS XmaI R	144	5’ gtcgacggtatcgataagcttgatatcgaattcctgcagcccggg*cttgagaacaatggcacaacc*	pRS315-Brr2
Brr2 +97 R	117	5’ gctataaactgtatatatcac	SEQ *BRR2*
pRS31 universal R	143	5’ gttgtgtggaattgtgagc	pRS SEQ
SEQ-delta4-R4	78	5’ CAAGCTGTGAATCAGTAAG	SEQ *BRR2*
SEQ brr2 60 R	220	5’ caacaccttattggacatctc	SEQ *BRR2*
SEQ delta4-F0	87	5’ caataacattaataaaggac	SEQ *BRR2*
SEQ delta4-F1	55	5’ ctgtttggcaaatgctcgtg	SEQ *BRR2*
SEQ delta4-F2	56	5’ atgatggtgcagagcataaatatatg	SEQ *BRR2*
SEQ delta4-F3	57	5’ cactatggcgtatcatttttactatt	SEQ *BRR2*
SEQ-delta4 F3.5	101	5’ ccatggatttggcgcagatg	SEQ *BRR2*
SEQ delta-F4	58	5’ ccttgaggatgaagagaggga	SEQ *BRR2*
SEQ-delta4-R1	77	5’ GCATATATTTATGCTCTGC	SEQ *BRR2*
SEQ-delta4 R3	100	5’ gaccgtctcgacgttaatttc	SEQ *BRR2*
seq brr2 Sec63 1-R	289	5’ cctgttttccatattttc	SEQ *BRR2*
check Brr2 100R	446	5’ gaggattttggctggtattc	Col PCR *BRR2*
check Brr2 -100F	447	5’ gctactaaagctatgtc	Col PCR *BRR2*

Oligo Name	Alias	Sequence	Description
1-1314 pRS415 F	206	5’ gtcagatacatagatacaattctattacccccatccatactctagaatgactgagcatgaaacgaagg	cloning brr2 N-HTP
1-1314 pRS415 R	207	5’ gttggaatatcataatcatggtgatggtgatggtgctccatggatccccggaagtttaaatccattgaag	
1-1314 p413 XmaI F	211	5’ aattctattacccccatccatacatctagaactagtggatccccccgggATGactgagcatgaa acgaagg	cloning brr2 N
1-1314 p413 ClaI R	212	5’ agcgtgacataactaattacatgactcgaggtcgacggtatcgatTTAcggaagtttaaatcc attgaagg	
1+1313-2163 p413 XmaI F	213	5’ ctattacccccatccatacatctagaactagtggatccccccgggATGccgaaaaaatttc ctcctcctac	cloning brr2 C
1+1313-2163 p413 ClaI R	214	5’ aagcgtgacataactaattacatgactcgaggtcgacggtatcgatTTAtttcacattta tttcaaaggac	
1+1313-2163 p415 F	215	5’ gtcagatacatagatacaattctattacccccatccatactctagaATGcttc cgaaaaaatttcctcctc	cloning brr2 C-HTP
1313-2163 pRS415 F	209	5’ gttggaatatcataatcatggtgatggtgatggtgctccatggatcctttcacatttatttcaaaggac	
megaprimer cHTP R	247	5’ gaatgttatatattgaaatccattcgattatccaggactaaacaatgattTCAggttgacttccccgcgg	cloning Brr2-HTP
IF sub BRR2 in pRS313 F	*358*	5’ ATATCAAGCTTATCGATCATTCAGACAGGAACAAACTTG	subcloning of *BRR2*
IF sub BRR2 in pRS313 R	*359*	5’ AGGTCGACGGTATCGATCTTGAGAACAATGGCACAAC	
col PCR U4 -89 F	386	5’ cagaatattagttagcttc	Col PCR U4
col PCR U4 +87 R	*387*	5’ cagtccggtatccctaacc	
U4 in pRS316-BRR2 F	382	5’ CCATTGTTCTCAAGGGTACCccaccaagaaaatgccataaac	in-Fusion cloning U4 in pRS316-BRR2
U4 in pRS316-BRR2 R	383	5’ GGGAACAAAAGCTGGGTACCgagtaaggtaactatgaatttag	
U5 in pRS316-BRR2 F	303	5’ gggttgtgccattgttctcaagggtaccgtagtgactaaacatggacgc	cloning of U5 in pRS316-BRR2
U5 in pRS316-BRR2 R	304	5‘ cactaaagggaacaaaagctgggtaccggtttcttttcctgcaactgc	
U5 col PCR new F	321	5’ gtgctcagtataaaaagcgcatag	Col PCR U5
U5 col PCR new R	322	5’ ggataaaagcaaatgcttcaatgg	
IF U5 in pRS314 F	344	5’ TCGAGGGGGGGCCCGGTACCGTAGTGACTAAACATGGACGC	in-Fusion cloning U5 in pRS314
IF U5 in pRS314 R	345	5’ GGGAACAAAAGCTGGGTACCGGTTTCTTTTCCTGCAACTGC	
SEQ U5 (-64) F	360	5’ gcgcatagtaagacttttg	SEQ U5
prp18 +100 R	*465*	5’ gtctatgtttgcggattc	Col PCR *SLU7*, *PRP18*
slu7 +100 R	*466*	5’ cttatagtaccatggttgatttc	
U2 in pRS314 F	338	5‘cgacctcgaggggggcccggtaccgaacagaggagagaacgagaaagc	in-Fusion pRS314-U2
U2 in pRS314 R	339	5‘cactaaagggaacaaaagctgggtacccgggtctgcagaggacgag	
SEQ U2 +300 R	348	5’ ccagttatggtgtgtggcg	SEQ U2
SEQ U2 5’ F	332	5’ cgaatctctttgccttttggc	SEQ U2
SEQ U2 3’ UTR +58 R	331	5’ cgaatctctttgccttttggc	SEQ U2

Table 2.13 Oligonucleotides used for site directed mutagenesis

Oligo Name	Alias	Sequence
V2045D 3-P8 F	103	5’ gcgcaggtcgccgcgtttgAtaacaattacccc
V2045D 3-P8 R	104	5’ ggggtaattgttaTcaaacgcggcgacctgcgc
N1972D 7-N13 F	105	5’ ctttcagcaaacgggtatttgGatgctactaccgcc
N1972D 7-N13 R	106	5’ ggcggtagtagcatCcaaatacccgtttgctgaaag
Q1931R 6-N4 F	107	5’ gagctttaaagttttcttattgttacGagcatatttttcacgtcttg
Q1931R 6-N4 R	108	5’ caagacgtgaaaaatatgctCgtaacaataagaaaactttaaagctc
S1966P 6-F17 F	109	5’ gtagtggttgatatccttCcagcaaacgggtatttgaatg
S1966P 6-F17 R	110	5’ cattcaaatacccgtttgctgGaaggatatcaaccactac
W2099R 4-D9 F	111	5’ gtttgataagctagaaagtCggtggttggttttaggtgaag
W2099R 4-D9 R	112	5’ cttcacctaaaaccaaccaccGactttctagcttatcaaac
T2132A 1-24L F	113	5’ gcaatatgaattggaatttgacGctccgacatctggtaaac
T2132A 1-24L R	114	5’ gtttaccagatgtcggagCgtcaaattccaattcatattgc
V1922A 1-19E F	115	5’ cacacctcttctggttcggCgagctttaaagttttcttattg
V1922A 1-19E R	116	5’ caataagaaaactttaaagctcGccgaaccagaagaggtgtg
E1842stop F	118	5’ gagatgatgaagcaactgaaTAATAAatcatttctaccttgagcaac
E1842stop R	119	5’ gttgctcaaggtagaaatgatTTATTAttcagttgcttcatcatctc
L1930P Brr2 F	120	5’ cggtgagctttaaagttttcttattgCCAcaagcatatttttcacgtcttgaattacc
L1930P Brr2 R	121	5’ ggtaattcaagacgtgaaaaatatgcttgTGGcaataagaaaactttaaagctcaccg
A1932P Brr2 F	122	5’ gctttaaagttttcttattgttacaaCcatatttttcacgtcttgaattacctg
A1932P Brr2 R	123	5’ caggtaattcaagacgtgaaaaatatgGttgtaacaataagaaaactttaaagc
S1935P Brr2 F	124	5’ gttttcttattgttacaagcatattttCcacgtcttgaattacctgtcgac
S1935P Brr2 R	125	5’ gtcgacaggtaattcaagacgtgGaaaatatgcttgtaacaataagaaaac
E1952G Brr2 F	126	5’ caaaatgatttaaaagacattctagGaaaggttgttccactaattaacgtag
E1952G Brr2 R	127	5’ ctacgttaattagtggaacaacctttCctagaatgtcttttaaatcattttg
L2096P Brr2 F	128	5’ ctgaaaagtatccgtttgataagcCagaaagttggtggttggttttag
L2096P Brr2 R	129	5‘ctaaaaccaaccaccaactttctGgcttatcaaacggatacttttcag
QC S2148P Brr2 F	138	5’ caatttggtgtgtctgtgatCcatatcttgacgcagataaagagttg
QC S2148P Brr2 R	139	5’ caactctttatctgcgtcaagatatgGatcacagacacaccaaattg
QC Brr2 K1925R F	145	5’ ctcttctggttcggtgagctttaGagttttcttattgttacaagc
QC Brr2 K1925R R	146	5’ gcttgtaacaataagaaaactCtaaagctcaccgaaccagaagag
QC Brr2 R1899G F	147	5’ gttccactcagaaaaggagacGgagcattacttgtcaaattaag
QC Brr2 R1899G R	148	5’ cttaatttgacaagtaatgctcCgtctccttttctgagtggaac
QC Brr2 L1883P F	149	5’ caacgctcaaaaacatgctgtatgttcCttcaacagcagtagaattc
QC Brr2 L1883P R	150	5’ gaattctactgctgttgaaGgaacatacagcatgtttttgagcgttg
QC Brr2 L1951P F	151	5’ aatgatttaaaagacattcCagaaaaggttgttccactaattaacgtag
QC Brr2 L1951P R	152	5’ ctacgttaattagtggaacaacctttttctGgaatgtcttttaaatcatt
QC Brr2 V2045D F	163	5’ cacagcttgcgcaggtcgccgcgtttgAtaacaattacccc
QC Brr2 V2045D R	164	5’ cgaataagtaagttcaacgttggggtaattgttaTcaaacgc
QC Brr2 W2099R F	165	5’ gtatccgtttgataagctagaaagtCggtggttggttttaggtgaagtatc
QC Brr2 W2099R R	166	5’ gatacttcacctaaaaccaaccaccGactttctagcttatcaaacggatac
QC Brr2 S2148P F	167	5’ cttaacaatttggtgtgtctgtgatCcatatcttgacgcagataaagagttg
QC Brr2 S2148P R	168	5’ caactctttatctgcgtcaagatatgGatcacagacacaccaaattgttaag
QC Brr2 I1763M F	171	5’ caacgagatagcaaattctattatGcaaagcaaacaagattgtgttgac

Oligo Name	Alias	Sequence
QC Brr2 I1763M R	172	5’ gtcaacacaatcttgtttgctttgCataatagaatttgctatctcgttg
QC Brr2 W1772A F	173	5’ caaagcaaacaagattgtgttgacGCgtttacatattcgtatttctatcg
QC Brr2 W1772A R	174	5’ cgatagaaatacgaatatgtaaacGCgtcaacacaatcttgtttgctttg
QC Brr2 Y1779A F	175	5’ gactggtttacatattcgtatttcGCtcgtcgtatccatgtgaatccaag
QC Brr2 Y1779A R	176	5’ cttggattcacatggatacgacgaGCgaaatacgaatatgtaaaccagtc
QC Brr2 R1781P F	177	5’ catattcgtatttctatcgtcCtatccatgtgaatccaagctattatg
QC Brr2 R1781P R	178	5’ cataatagcttggattcacatggataGgacgatagaaatacgaatatg
QC Brr2 D1793G F	179	5’ caagctattatggcgtaagggGtacgtctccacatggaatttcag
QC Brr2 D1793G R	180	5’ ctgaaattccatgtggagacgtaCcccttacgccataatagcttg
QC Brr2 S1795P F	181	5’ ctattatggcgtaagggatacgCctccacatggaatttcagttttttg
QC Brr2 S1795P R	182	5’ caaaaaaactgaaattccatgtggagGcgtatcccttacgccataatag
QC Brr2 L1814S F	183	5’ gttgaaacttgtttgaatgactCagttgaatcatccttcattg
QC Brr2 L1814S R	184	5’ caatgaaggatgattcaactGagtcattcaaacaagtttcaac
QC Brr2 L1814I F	185	5’ ttagttgaaacttgtttgaatgacAtagttgaatcatccttcattg
QC Brr2 L1814I R	186	5’ caatgaaggatgattcaactaTgtcattcaaacaagtttcaactaa
QC Brr2 V1815I F	187	5’ gaaacttgtttgaatgacttaAttgaatcatccttcattgaaattgacg
QC Brr2 V1815I R	188	5’ cgtcaatttcaatgaaggatgattcaaTtaagtcattcaaacaagtttc
QC Brr2 D1823G F	189	5’ gaatcatccttcattgaaattgGcgatacagaagctgaagtaacc
QC Brr2 D1823G R	190	5’ ggttacttcagcttctgtatcgCcaatttcaatgaaggatgattc
QC Brr2 N1849A F	191	5’ ctgaaatcatttctaccttgagcGCcgggctaattgcttctcactatg
QC Brr2 N1849A R	192	5’ catagtgagaagcaattagcccgGCgctcaaggtagaaatgatttcag
QC Brr2 I1852A F	193	5’ catttctaccttgagcaacgggctaGCtgcttctcactatggcgtatc
QC Brr2 I1852A R	194	5’ gatacgccatagtgagaagcaGCtagcccgttgctcaaggtagaaatg
QC Brr2 G1857A F	195	5’ cgggctaattgcttctcactatgCcgtatcatttttactattcag
QC Brr2 G1857A R	196	5’ ctgaatagtaaaaaatgatacgGcatagtgagaagcaattagcccg
QC Brr2 T1862P F	197	5’ ctcactatggcgtatcatttttttCctattcagtcattcgtttcttc
QC Brr2 T1862P R	198	5‘ gaagaaacgaatgactgaatagGaaaaaatgatacgccatagtgag
QC Prp16 L335F F	228	5’ gatttgcgacgatacagctTttttcacgccatcaaaagatgac
QC Prp16 L335F R	229	5’ gtcatcttttgatggcgtgaaaaAagctgtatcgtcgcaaatc
QC Prp16 K379R F	230	5’ gtgaaacgggctcaggtaGaaccacgcaacttgcacag
QC Prp16 K379R R	231	5’ ctgtgcaagttgcgtggttCtacctgagcccgtttcac
QC Prp16 H476D F	232	5’ cgtgtgttattattgatgaagctGatgaaaggtcattaaatacagac
QC Prp16 H476D R	233	5’ gtctgtatttaatgacctttcatCagcttcatcaataataacacacg
QC Prp16 T507A F	234	5’ ctcataatcacttcagcaGcaatgaatgcgaagaagttctc
QC Prp16 T507A R	235	5’ gagaacttcttcgcattcattgCtgctgaagtgattatgag
QC Prp16 R686Q F	236	5’ catatcaaaagctaacgccgaccaaCAatccggaagagcggg
QC Prp16 R686Q R	237	5’ cccgctcttccggatTGttggtcggcgttagcttttgatatg
QC PRP16 R686I F	264	5’ catatcaaaagctaacgccgaccaaaTatccggaagagcgggaag
QC PRP16 R686I R	265	5’ cttcccgctcttccggatAtttggtcggcgttagcttttgatatg
QC PRP16 Q685H F	266	5’ catatcaaaagctaacgccgaccaTagatccggaagagcgggaag
QC PRP16 Q685H R	267	5’ cttcccgctcttccggatctAtggtcggcgttagcttttgatatg
QC PRP16 D473E F	268	5’ gataaatattcgtgtgttattattgaAgaagctcatgaaaggtc
QC PRP16 D473E R	269	5’ gacctttcatgagcttcTtcaataataacacacgaatatttatc
QC PRP16 Y386D F	323	5’ ggtaaaaccacgcaacttgcacagGatttatatgaagaaggatatgcc

Oligo Name	Alias	Sequence
QC PRP16 Y386D R	324	5’ ggcatatccttcttcatataaatCctgtgcaagttgcgtggttttacc
QC brr2 G858R F	315	5‘ gatgtctattcacctgaaaagAggtcctgggaacaactttctccacaag
QC brr2 G858R R	316	5‘ cttgtggagaaagttgttcccaggaccTcttttcaggtgaatagacatc
QC brr2 E909K F	313	5’ ctctcggttttaaatcaacaattaccaataAaatcgcaatttgtttcaaaattag
QC brr2 E909K R	314	5‘ ctaattttgaaacaaattgcgattTtattggtaattgttgatttaaaaccgagag
QC brr2 R1107P F2	286	5’ gatatagtgtttattcaccaaaatgctggtCCgttattgcgtgctatgtttgaaatatg
QC brr2 R1107P R2	287	5’ catatttcaaacatagcacgcaataacGGaccagcattttggtgaataaacactatatc
QC U4 D top 3’ SL F	424	5’ gttgaaatttaattataaaccagaccgtctccaattcggtgttcgcttttgaatacttcaagggaatttttggaataccttt
QC U4 D top 3’ SL R	425	5’ aaaggtattccaaaaattcccttgaagtattcaaaagcgaacaccgaattggagacggtctggtttataattaaatttcaac
QC U4 138 ins 3U F	414	5‘ cttttgaatacttcaagactatgTTTTagggaatttttggaataccttt
QC U4 138 ins 3U R	415	5‘ aaaggtattccaaaaattccctAAAAcatagtcttgaagtattcaaaag
QC U4 D136-139 F	412	5’ cttttgaatacttcaagactagggaatttttggaataccttt
QC U4 D136-139 R	413	5’ aaaggtattccaaaaattccctagtcttgaagtattcaaaag
QC U4D 139-141 F	410	5’ cttttgaatacttcaagactatgtgaatttttggaataccttt
QC U4D 139-141 R	411	5’ aaaggtattccaaaaattcacatagtcttgaagtattcaaaag
QC U4 delta 3’SL F	403	5’ gaaatttaattataaaccagaccgtctgaatttttggaataccttt
QC U4 delta 3’SL R	404	5’ aaaggtattccaaaaattcagacggtctggtttataattaaatttc
QC U4 delta 131-133 F	395	5’ cggtgttcgcttttgaatacttcaatatgtagggaatttttggaataccttt
QC U4 delta 131-133 R	396	5’ aaaggtattccaaaaattccctacatattgaagtattcaaaagcgaacaccg
QC U4 delta U138 F	380	5’ gcttttgaatacttcaagactatgagggaatttttggaataccttt
QC U4 delta U138 R	381	5’ aaaggtattccaaaaattccctcatagtcttgaagtattcaaaagc
U2 del 5’ side LR F	351	5’ catttttggcacccaaaataataaaatacttttaagcaagttgttttccgctaatg
U2 del 5’ side LR R	352	5’ cattagcggaaaacaacttgcttaaaaagtattttattattttgggtgccaaaaaatg
mut U2 5’ side stem F	325	5’ gacgcctgtttttaaagttAGRGACGUCGCRAYCctcgcacttgtggagtcgttc
mut U2 5’ side stem R	326	5’ gaacgactccacaagtgcgagGRTYGCGACGTCYCTaactttaaaaacaggcgtc
mut U2 3’ side stem F	327	5’ cgttcttgacttttactttGRTYGCTTGATGTTYCTctcgtcttcccgttcgctc
mut U2 3’ side stem R	328	5’ gagcgaacgggaagacgagAGRAACATCAAGCRAYCaaagtaaaagtcaagaacg
mut LR U2 5’ stem F	329	5’ cacccaaaataataaaaTGGACaGaAAGAgacttttaagcaagttg
mut LR U2 5’ stem F	330	5’ caacttgcttaaaaagtcTCTTtCtGTCCAttttattattttgggtg
mut 5’ stem U2 F	340	5’ tgacgcctgtttttaaagttagRgacgtcgcRaYcctcgcacttgtggagtcgtt
mut 5’ stem U2 R	341	5’ aacgactccacaagtgcgaggRtYgcgacgtcYctaactttaaaaacaggcgtca
mut LR U2 3’ stem F	346	5’ ctttggtcgcttgatgtttctctcgtcttTcTgttcgctcttttattttttattttttttttccttgacttcgc
mut LR U2 3’ stem R	347	5’ gcgaagtcaaaggaaaaaaaaaaataaaaaaataaaagagcgaacAgAaagacgagagaaacatcaagc gaccaaag
U2 del 5’ side LR F	351	5’ catttttggcacccaaaataataaaatacttttaagcaagttgttttccgctaatg
U2 del 5’ side LR R	352	5’ cattagcggaaaacaacttgcttaaaaagtattttattattttgggtgccaaaaaatg
QC U2 comp 3 LR F	363	5’ cttttacttggtcgcttgatgtttctcGAGATCTGCGTTACTctcttttattttttattttttttttccttttgac
QC U2 comp 3 LR R	364	5’ gtcaaaggaaaaaaaaaataaaaaaataaaagagAGTAACGCAGATCTCgagaaacatcaagcg accaaagtaaaag
QC U2 scramble 5 LR F	361	5’ acatttttggcacccaaaataataaaaGGTAACGCAGATTCctttttaagcaagttgttttccgctaatg
QC U2 scramble 5 LR R	362	5’ cattagcggaaaacaacttgcttaaaaagGAATCTGCGTTACCttttattattttgggtgccaaaaaatgtg
QC U2 U23G F	417	5’ acgaatctctttgccttttggcGtagatcaagtgtagtatctgttc
QC U2 U23G R	418	5’ gaacagatactacacttgatctaCgccaaaaggcaaagagattcgt

Capital letters indicate mutated nucleotides.

Table 2.14 Oligonucleotides used for yeast genomic deletion/insertion

Oligo Name	Alias	Sequence	Description
del ISY1 NAT F	*349*	5' caccgttatatcgcaaggcgcaccacatcagtaatcagatacctgtgcattccgtac gctgcaggtcgac	making of W303 brr2Δ/ *isy1*Δ
del ISY1 NAT R	*350*	5' gtgatggtcattcgaaatagtgcctcttctaaatgtttgaataattttccatagatcgat gaattcgagctcg	
brr2 pGALS NAT F	449	5' taaatataagtaattgctttggaagatttaccgtgagccttcgttattaaaaatgCG TACGCTGCAGGTCGAC	construction of RIBO1 *GalS::brr2*
brr2 pGALS NAT R	450	5' cataacgataaatttctctaatttttttggccttatccttcgtttcatgctcagtCATCG ATGAATTCTCTGTCG	
prp18 pGALS F	461	5' caatggaaagaacttcaatgtttttcctctacaagtaataagagcataaaatgCG TACGCTGCAGGTCGAC	construction of W303 brr2Δ *GalS::3HA-prp18*
prp18 pGALS R	462	5' ctttcttcttctagaaatttcacctttaagatactggctagatctaggtcCATCG ATGAATTCTCTGTCG	
slu7 pGALS F	463	5' cacttctgaaaaagataccagttacactgaaatacaacgatcggattacataatgCG TACGCTGCAGGTCGAC	construction of W303 brr2Δ *GalS::3HA-slu7*
slu7 pGALS R	*464*	5' cttttatttctgttaatagtgcttcgattttcgttgtttctgctgttattattCATCG ATGAATTCTCTGTCG	
del Hph U5 F	*301*	5' aagcagctttacagatcaatggcggagggaggtcaacatcaagaactgtgcgtac gctgcaggtcgac	construction of *W303* brr2Δ/U5Δ
del Hph U5 R	*302*	5' acgccctccttactcattgagaaaaagggcagaaaagttccaaaaaatatggatcg atgaattcgagctcg	
del Hph PRP16 -51 F	*280*	5' gactgcagatgataaaacacaagaaggcccaaagacaatacaaatacctctcgta cgctgcaggtcgac	construction of W303 brr2Δ/prp16Δ
del Hph PRP16 +53 R	*281*	5' ctatataataacatatatgaatattttgcctattagcacgctcttcccataaaatcga tgaattcgagctcg	
del Hph U4 F	*384*	5' atccttatgcacgggaaatacgcatatcagtgaggattcgtccgagattgtgcgtacg ctgcaggtcgac	construction of W303 brr2Δ/U4Δ
del Hph U4 R	385	5' aaaggtattccaaaaattccctacatagtcttgaagtattcaaaagcgaacatcg atgaattcgagctcg	
del Hph U2 F	299	5' cttgttatcagatttattcattttgtttctacttgttttttttttaaatcccccgtac gctgcaggtcgac	construction of U2Δ
del Hph U2 R	300	5' catatattttatatacttacatatttggttgcgtggtatatagaatctctcctttcatc gatgaattcgagctcg	

Table 2.15 Oligonucleotides used as Northern probes, for primer extensions and for 3' RACE-PCR

Oligo Name	Sequence	Description
U3 A B Exon2	5' ccaagttggattcagtggctc	^{32}P end-labelled, for primer extension [7]
ACT1/Cup1	5' ggcactcatgaccttc	^{32}P end-labelled, for primer extension [8]
U2	5' ctacacttgatctaagccaaaag	^{32}P end-labelled, for Northern hybridization, complementary to nt 15-37 of yeast U2 snRNA
U2 2-20F	5' gaatctctttgccttttg	sense oligo used for 3' RACE-PCR

Table 2.16 Oligonucleotides used for CRAC experiments

Oligo Name	Sequence	Reference
Solexa 5' linker	5' invddT-GTTCArGrArGrUrUrCrUrArCrArGrUrCrCrGrArCrGrArUrC	[9]
mirCAT33^{TM} linker	5' rAppTGGAATTCTCGGGTGCCAAGG/ddC	IDT
mirCAT33^{TM} RT	5' CCTTGGCACCCGAGAATT	IDT
Solexa 5' PCR	5'AATGATACTGCGACCACCGACAGGTTCAGAGTTCTACAGTCCGA	[9]
mirCAT Solexa PCR	5' CAAGCAGAAGACGGCATACGACCTTGGCACCCGAGAATTCC	[9]
L5a	5' invddT-ACACrGrArCrGrCrUrCrUrUrCrCrGrArUrCrUrArC	S. Granneman
L5c	5' invddT-ACACrGrArCrGrCrUrCrUrUrCrCrGrArUrCrUrGrA	S. Granneman
L5d	5' invddT-ACACrGrArCrGrCrUrCrUrUrCrCrGrArUrCrUrArCrArArGrC	S. Granneman
L5e	5' invddT-ACACrGrArCrGrCrUrCrUrUrCrCrGrArUrCrUrCrArCrArGrC	S. Granneman
L5f	5' invddT-ACACrGrArCrGrCrUrCrUrUrCrCrGrArUrCrGrCrCrGrArGrC	S. Granneman
M13 R	5' AACAGCTATGACCATG	Invitrogen
T7_seq	5' GTAAAACGACGGCCAGT	Invitrogen

Table 2.17 Oligonucleotides used for RT and RT-qPCR of RIBO1 reporter transcript

Oligo Name	Sequence	Reference
Ribo1_E1_R*	5' CCCGCATAGTCAGGAACATCG	[10]
Ribo1_3'_F	5' CGATTGCTTCATTCTTTTTGTTGC	[10]
Ribo1_3'_R*	5' CCTGGCAATTCCTTACCTTCCA	[10]
Ribo1_p2_F	5' AATTCGGGGGATCGACGGTA	[10]
Ribo1_p2_R	5' GGTGCAAGCGCTAGAACATACCA	[10]
Ribo1_m2_F	5' TTCGGGGGATCGACGGTAT	[10]
Ribo1_m2_R*	5' CCAAAGAAGCACCACCACCA	[10]

*oligos that were used for reverse transcription

2.8 Antibodies

The antisera, monoclonal or polyclonal antibodies used throughout this study are listed below in table 2.18.

Table 2.18 Antisera

Antibody	Description	Source
anti-LexA (2-12)	mouse monoclonal antibody used at 1:2000 for Western Blotting	Santa Cruz
anti-HA (F-7)	mouse monoclonal antibody used at 1:1000 for Western blotting	Santa Cruz
anti C-term Brr2 (C)	primary rabbit serum raised against C-terminal Brr2 peptide serum, used 1:5000 for Western blotting	O. Cordin
anti-Brr2 (N)	rat anti N-terminal Brr2 peptide purified antibody used 1:2000 for Western blotting	O. Cordin
anti-TAP	polyclonal rabbit antibody used at 1:5000 for Western blotting	Open Biosystems
PAP-HRP (anti peroxidase)	rabbit antibody, used at 1:10,000 for Western blotting	Sigma
anti-Rabbit IgG-HRP	used at 1:20,000 for Western blotting	Amersham Biosciences
anti-Rat IgG-HRP	used at 1:20,000 for Western blotting	Amersham Biosciences
anti-Mtr4	rabbit antibody used at 1:10,000 for Western blotting	Tollervey lab

2.9 Microbiological Methods

Genetically modified *S. cerevisiae* and *E. coli* are containment level 1 organisms and the relevant procedures for their handling and disposal were followed at all times. Established sterile technique was used at all times.

2.9.1 Cultivation of strains

2.9.1.1 Cultivation of Bacteria

E. coli transformed with a plasmid were cultivated in/on LB medium at 37°C, unless stated otherwise. To maintain selection pressure for the introduced plasmid the growth medium was supplemented with the appropriate antibiotic (Table 2.3).

2.9.1.2 Cultivation of Yeast

Yeast was grown at 25°C or 30°C, unless stated otherwise in/on the appropriate medium (Table 2.1). In order to maintain selection pressure for plasmids carrying auxotrophic markers, cells were cultivated in/on YMM medium supplemented with the appropriate Drop out powder i.e. synthetic defined (SD) medium (Table 2.1). Strains with antibiotic resistance genes integrated to the genome were grown in the presence of the appropriate antibiotic(s) (Table 2.3).

2.9.2 Preservation of strains

Both *S. cerevisiae* and *E. coli* strains were stored for short periods (up to eight weeks) on solid medium at 4°C. For long term storage stationary phase cultures of yeast or *E. coli* were mixed with sterile Glycerol to a final concentration of 15% (w/v), transferred to Cryo-S screw cap tubes (Greiner) and stored at -70°C.

2.9.3 Preparation of competent *E. coli*

Chemically-competent *E. coli* cells were "home-made". A 5 ml overnight culture was grown in LB^{Tet} medium supplemented with 20 mM $MgSO_4$. 2ml of the overnight culture were used to inoculate 250ml of LB with 20 mM $MgSO_4$. This culture was incubated at 23°C shaking at 200-280 rpm until OD_{600} = 0.4-0.6 was

reached. The culture was transferred to a centrifuge tube, cooled on ice for 10-15 minutes and then centrifuged (10 min, 3000 rpm, 4°C, Beckman 10,500 rotor). In the meantime, a sufficient number of 1.5 ml Eppendorf tubes was labelled and pre-chilled at -20°C. The pellet was gently resuspended in ice-cold TB buffer (10 mM Pipes-HCl pH 6.7, 15 mM $CaCl_2$, 0.25 M KCl, 55 mM $MnCl_2$) and incubated on ice for 10 minutes. Centrifugation was repeated and the cell pellet was gently resuspended in 20 ml of TB buffer supplemented with 1.5 ml of DMSO. After resting the cells on ice for 10 minutes, 200 µl-400 µl aliquots were dispensed into the pre-cooled tubes, snap-frozen in liquid nitrogen and stored at -70°C until required.

2.9.4 Transformation of *E. coli*

An aliquot of competent *E. coli* was thawed on ice and up to 10µl of plasmid DNA (2.11.1), SDM PCR (2.11.10.3) or Megaprimer PCR reaction (2.11.10.4) were added. DNA and cells were mixed gently and incubated on ice for 30 minutes followed by a 45-second heat shock at 42°C. The cells were cooled on ice for 2 minutes and 800µl of SOC medium were added. Cells were incubated for 1 hour at 37°C with shaking. Thereafter they were centrifuged briefly, resuspended in 100µl of SOC medium and plated on pre-warmed LB agar plates supplemented with the appropriate antibiotic (Table 2.3). Incubation at 37°C over night should then result in visible colonies.

Transformation of commercially available *E. coli* XL10 gold (Stratagene (Table 2.5)) was performed according to the manufacturer's instructions.

2.9.5 Transformation of *S. cerevisiae*

Yeast transformations were performed using the lithium acetate method [11] and variations thereof depending on whether plasmid DNA or linear DNA for genomic integration was introduced. For Plasmid transformations usually 200-800

ng of DNA (about 0.5 -1 µl of a plasmid Mini Prep (2.11.1)) were used. For genomic integration 1-5 µg of PCR amplified DNA was used. The PCR oligonucleotides used for the amplification were designed to provide 45 nucleotides complementary to the genomic integration site.

A 50 ml yeast culture was inoculated to an OD of 0.1-0.2 and grown to log-phase (OD 0.5-1.0). Cells were sedimented and washed with 10 ml H_2O. Thereafter the cells were resuspended in 1 ml of 100 mM Lithium acetate transferred to an Eppendorf tube and centrifuged in a table top centrifuge (3000xg, 1 min, RT). Cells were resuspended in 500 µl of 100 mM Lithium acetate. In a fresh tube 50 µl of this cell suspension was then combined with transformation mixture containing 240 µl 50% (w/v) PEG_{3350}, 36 µl 1 M Lithium acetate, 100 µg heat-denatured salmon sperm DNA (Roche), DNA (plasmid or PCR product) and H_2O to a total volume of 360 µl. The cells were resuspended by vortexing, incubated at room temperature with agitation for 30 minutes and then heat shocked for 20-40 minutes at 42°C. Finally, cells were centrifuged, resuspended in 100 µl sterile H_2O and spread on agar plates containing the required selectable medium. Plates were incubated for 2-3 days at 25°C-30°C. For selection with an antibiotic resistance marker cells were replica-plated onto selective media after 24 hours of incubation.

2.9.6 Yeast sporulation and tetrad dissection

A single colony of a diploid strain was used to inoculate 25 ml of pre-sporulation medium (Table 2.1) which was incubated at 30°C with 250 rpm for 24 hours. The cells were washed with H_2O and then spread on sporulation plates or used to inoculate 25 ml liquid sporulation medium. Typically, after 2-7 days incubation at 30°C (liquid cultures were incubated shaking at > 250 rpm) tetrads could be observed under the light microscope.

A small amount of cells was taken from the sporulation plate or culture, transferred to an Eppendorf tube and centrifuged briefly. Cells were resuspended in

18 µl of 1 M Sorbitol with 20 µg of Zymolyase (2 µl of 10 mg/ml stock, Boehringer Mannheim). To digest the cell walls this mixture was incubated at room temperature for 8 to 10 minutes. Digestion was stopped by adding 400 µl of ice cold H_2O. 10 µl of the cell suspension were dropped onto a YPDA plate; the drop was run down the plate to spread the cells in a straight line down the middle of the plate. A Singer MSM series micromanipulator was used to identify sufficiently digested tetrads and to separate their spores. Incubation of the plate allowed the individual spores to grow up to colonies, which could subsequently be tested for the desired markers or phenotypes.

2.9.7 Mating type testing

To test the mating type of haploid progeny following tetrad dissection, cells were streaked in a straight line on plates. A pair of *MAT***a** and *MATα* tester-strains was simultaneously streaked in parallel lines on a YPDA plate (usually BY4741 and BY4742). The plates were incubated over night or until plenty of growth was visible. Thereafter the strains were replica-plated to a double selectable medium with the lines of the strain in question perpendicular to those of the tester-strains. The medium was chosen to have a combination of selection markers allowing only those cells to grow that had undergone mating. Growth occurs at the intersection point of the lines with one of the tester-strains, thereby indicating the mating type of the strain in question.

2.9.7 Spot assay

Spot assays were used to compare the growth of different strains under various conditions. The OD_{600} of a liquid culture was determined and serial dilutions corresponding to OD_{600} readings of 0.2, 0.02 and 0.002 were made. These cell suspensions were transferred to flat-bottom 96-well plates (Sterilin or Greiner). A sterilised multi-pin "hedgehog" device was used to spot uniform amounts of cells

onto plates of the desired medium. Cells could be spotted to various different media, or plates could be incubated at different temperatures allowing comparison of growth under these conditions.

2.9.8 Plasmid shuffle assay

Addition of 5-Fluorotic acid (5-FOA) allows counter selection of *URA3* marked plasmids, which forms the basis for the plasmid shuffle assay [12]. A *URA3* marked plasmid provides the sole copy of a given gene, while a second copy of the gene (either a wild type or mutant version) can be expressed from a "shuffle" plasmid carrying another auxotrophic marker. Loss of the *URA3* marked plasmid can be induced by cultivating cells on 5-FOA containing plates (Table 2.1) so that cell growth depends on the copy of the gene expressed from the shuffle plasmid.

In double-shuffle strains two genes are deleted from the genome and are substituted from one *URA3* marked plasmid. Two individual shuffle vectors can be introduced, each encoding a wild type or mutant version of one of the genes deleted. Cultivation on medium containing 5-FOA cures the *URA3* marked plasmid, and thus allows testing of combinations of different mutant versions of the two genes in question.

2.9.9 Yeast two-hybrid assay

To test protein-protein interactions *in vivo* the yeast two-hybrid (Y2H) assay was used. Underlying principal: The proteins (or protein-fragments) of interest are fused to the two separate halves of an artificially divided transcription factor. Physical interaction between the proteins of interest reconstitutes the transcription factor, resulting in the expression of a reporter gene.

2.9.9.1 Standard yeast two-hybrid assay

The two-hybrid system used in this study combined a LexA-DNA binding domain (LexA-DB) with a Gal4-activation domain (Gal4-AD) to control the expression of a LexAop-*HIS3* reporter gene. The N-terminal LexA-DB fusions were expressed from the pBTM116 vector (*TRP1* marked) and N-terminal Gal4-AD fusions from the pACTII-stop vector (*LEU2* marked) (Table 2.7). The yeast strain used throughout this study was L40ΔG (Table 2.6). Protein interaction was assessed by monitoring growth on SD medium lacking histidine (-LWH) (Table 2.1). A competitive inhibitor of histidine biosynthesis, 3-amino-1,2,4-triazole (3-AT), was used to measure protein interaction strength. 3-AT counteracts expression of the *HIS3* reporter gene, thus growth is supported only if the interaction of the Y2H constructs leads to sufficient expression levels of the *HIS3* reporter.

2.9.9.2 Yeast two-hybrid screen used to identify protein interaction mutants

The procedure, used to identify mutants displaying aberrant protein-interactions was based on the classical two-hybrid assay (2.9.9.1), but was semi-automated to allow a higher throughput of clones. L40ΔG cells were sequentially transformed with a pBTM116 LexA-DB fusion construct and the library containing randomly mutated pACTII-stop Gal4-AD plasmids (2.11.11). Single colonies were picked and liquid cultures were inoculated in 150 µl SD -LW medium (Table 2.1) in 96-well plates (Sterilin). After 16 hours of incubation at 30°C each culture was homogenised by pipetting. A Singer ROTOR yeast handling robot was used to spot these cultures on SD -LW agar plates (50 ml rectangular plates, Singer). Cultures of four 96-well plates were combined on one agar plate to accommodate 384 clones. After 24 hour incubation at 30°C replica plating to SD -LWH medium, supplemented with different concentrations of 3-AT, followed. Plates were incubated at 30°C, 33°C or 14°C in a closed (but not airtight) box with moist tissue,

to prevent the agar from drying and breaking. Depending on temperature and culture medium, plates were incubated 2-14 days. Colony size of wild type and mutants were compared to identify clones of interest.

2.9.11 Genetic interaction mapping (GIM)

GIM with two query strains expressing *brr2* mutant alleles was carried out in collaboration with Dr. Cosmin Saveanu (Institut Pasteur, Centre National de la Recherche Scientifique, Paris, France). Strain preparation, data collection and analysis were performed as described [4].

2.10 Protein methods

2.10.1 SDS polyacrylamide gel electrophoresis

Proteins were separated on Tris-glycine NuPAGE 4-12% gradient gels (Invitrogen) in 1x MOPS buffer (Invitrogen). Before loading, protein samples were denatured by heating to 98°C for 5 minutes and collected by brief centrifugation. Gels were run according to the manufacturer's recommendations.

2.10.2 Western Blotting

Following SDS polyacrylamide gel electrophoresis (2.10.1), proteins were transferred to nitrocellulose membrane (Hybond C Extra, 0.45 μm pore size, Amersham Biosciences) or PVDF membrane (Immobilon-P 0.45μm pore size, Millipore) in a wet blot apparatus (Bio-Rad). The gel was assembled on the membrane and sandwiched between two sheets of Whatmann 3MM paper, soaked in 1x Western transfer buffer (Table 2.4) or 1x NuPAGE Transfer Buffer supplemented with 15% methanol (Invitrogen). Wet transfer was performed for 1.5

hours at 100 V. After transfer the membrane was blocked with 5% (w/v) fat-free dried milk in TBS (10 mM Tris-HCl pH 8.0, 250 mM NaCl) 0.1% Tween 20 for 1 hour at RT or overnight at 4°C.

Antibodies directed against the protein of interest or against an epitope tag fused to the protein of interest were used to detect the protein on the Western blot. All antibodies (see Table 2.3 for details) were diluted in 5% fat-free milk PBS 0.1% Tween 20. Primary antibodies were incubated with the membrane over night at 4°C. Secondary horseradish peroxidase coupled (HRP) antibodies were incubated for 1 hour at RT. Primary antibodies that were directly HRP coupled were incubated for 1 hour at RT. All incubation steps with antibodies were followed by three washes with TBS 0.1% Tween 20 for 10 minutes at RT. Proteins were detected using the HRP substrate, enhanced chemiluminescence RapidStep™ ECL reagent (Calbiochem), following the manufacturer's instructions.

2.10.3 Whole-cell protein extract preparation

Yeast cells (3-10 OD_{600}) were harvested and washed with ice-cold H_2O. The cell pellet was resuspended in 100 µl of ice-cold H_2O and 100 µl of Zirconia/Silica beads (0.5 mm, Thistle Scientific) and 20 µl of 100% TCA were added. To disrupt the cells, 6 minutes vortexing at 4°C followed. 1 ml of cold 5% TCA solution was added and the lysate was vortexed for 30 seconds at RT. To collect the protein-precipitate the samples were centrifuged (20,000xg, 15 min, 4°C, tabletop microfuge). The supernatant was removed and the protein pellet was resuspended in 30 µl of Dissociation buffer (100 mM Tris-HCl pH 6.8, 4 mM EDTA pH 8.0, 4% SDS, 20% Glycerol, 2% β-mercaptoethanol, 0.1% bromphenol blue). To neutralise the pH 20 µl of 1 M Tris pH 8.8 were added. The sample was vortexed for 2 minutes, and incubated at 95°C for 5 minutes to denature the protein. All liquids were collected by brief centrifugation and 15-20 µl of the sample were analysed by SDS PAGE and Western blotting (2.10.1, 2.10.2).

2.10.4 Preparation of splicing extract

Six litres of yeast culture was grown to an OD_{600} of 0.8 and harvested by centrifugation (3,000xg, 10 min, 4°C). The cell pellet was resuspended in 50 ml of ice-cold AGK buffer (10 mM Hepes-KOH (pH 7.9), 1.5mM $MgCl_2$, 200 mM KOH, 10% (v/v) Glycerol, complete protease inhibitors (Roche)) and centrifuged as before. This step was repeated with 30 ml AGK buffer. The supernatant was discarded and the cell pellet was weight. Subsequently 0.4 volumes of cold AGK buffer containing 2 mM DTT were then combined with the cell pellet into a viscous cell suspension. Pipetting small drops of cell suspension into liquid nitrogen resulted in snap freezing. The cell pellet could be stored at -70°C until required.

The frozen cell pellet was ground to fine powder in a mortar. Liquid nitrogen was used to pre-cool the mortar and was added during grinding to prevent thawing. The frozen powder was transferred to a chilled polycarbonate centrifuge tube, thawed on ice and spun (17,000 rpm, 30 min, 4°C) in a JA25.50 rotor (Beckman Avanti). Taking care to avoid the lipid-layer at the top, the supernatant was transferred to a chilled polycarbonate tube and centrifuged (40,000 rpm, 60 min, 4°C) in a Ti 70.1 rotor (Beckman XL-100). The supernatant was then transferred to SnakeSkin dialysis membrane (Pierce, MWCO 3.5 kDa) and was dialysed against 3 l of cold dialysis buffer (20 mM Hepes-KOH (pH 7.9), 50 mM KCl, 0.4 mM DTT) for 3 hours at 4°C. Finally the extract was aliquoted into pre-chilled microfuge tubes, snap-frozen in liquid nitrogen and stored at -70°C until used.

2.10.5 Pulldown assay of HTP-tagged proteins

From an exponentially growing cell culture 120 OD_{600} worth of cells were harvested by centrifugation (3000xg, 10 min, 4°C), washed in ice-cold PBS and transferred to a 50 ml Falcon tube (Greiner). After repeated centrifugation the cell pellet was snap-frozen by placing the tube into liquid nitrogen. The pellet was thawed on ice and resuspended in 900 µl of Lysis buffer (50 mM Hepes pH 7.5, 150

mM NaCl, 1 mM $MgCl_2$, 0.3% (v/v) Triton X-100, 1 mM DTT, complete protease inhibitors (Roche, 1 tablet in 50 ml)). 900 µl of Zirconia/Silica beads (0.5 mm, Thistle Scientific) were added and cells were lysed by five cycles of vortexing 1 min and cooling on ice for 1 min. Centrifugation (4,600 rpm, 5 min, 4°C, Sorvall Ledgend) cleared the lysate. Avoiding the lipid layer, 1 ml of supernatant was transferred to an Eppendorf tube and spun (20,000xg, 15 min, 4°C, tabletop centrifuge). The supernatant was added to 15 µl packed IgG Sepharose beads (GE healthcare), which were pre-equilibrated in Lysis buffer. Two hours of precipitation with end-over-end rotation at 4°C followed. Subsequently the supernatant was removed. The beads were washed 4 times with 1 ml of Lysis buffer, changing tubes during the last wash step. 30µl of Dissociation buffer (100 mM Tris-HCl pH 6.8, 4 mM EDTA pH 8.0, 4% SDS, 20% Glycerol, 2% β-mercaptoethanol, 0.1% bromphenol blue) was added and the sample was boiled for 5 min. Each sample was vortexed and centrifuged before 10-20µl were subjected to SDS page and Western blotting (2.10.1, 2.10.2).

2.10.6 Large scale affinity purification of protein from yeast

W303 was transformed with pGDP-BRR2-TAP, a high copy plasmid expressing TAP-tagged Brr2. Eight 2 litre yeast cultures were grown to an OD_{600} of 2-3, cells were harvested by centrifugation (3000xg, 10 min, 4°C) washed in PBS and resuspended in 0.4 vol. of TMN 150 buffer (50 mM Tris-HCl pH 7.8, 150 mM NaCl, 1.5 mM $MgCl_2$, 5 mM ß-Me, complete protease inhibitors (Roche, 1 tablet to 50 ml of buffer)). The cell suspension was dropped into liquid nitrogen, producing small granules of frozen yeast. In total 80 g of yeast pellet were gathered and used for the subsequent purification. Mechanical disruption of yeast cells was performed using a Retsch PM 100 planetary ball mill. The 200 ml grinding jar and 9 steel balls were cooled in liquid nitrogen before use. Approximately 50 ml of frozen yeast were ground at a time. Eight grinding cycles were performed at 400 rpm, 3 min forward

rotation, 1 min reverse rotation. In between cycles the grinding jar was removed from the mill and cooled in a bath of liquid nitrogen. Equal amounts of the resulting cell powder were distributed to 4 polycarbonate tubes; 10 ml of TMN 150 were added to each tube and thawed on ice. Centrifugation (17,000xg, 45 min, 4°C, Beckmann JA 25.50) cleared the lysate. Supernatants were transferred to 4 tubes and spun again (40,000xg, 1 h, 4°C, Beckman 70.1 Ti). The supernatants were distributed to two times 2 ml IgG Sepharose slurry (GE healthcare) and incubated 2 hours at 4°C with agitation. Beads were pelleted by brief centrifugation and 5 wash steps with 20 ml TMN buffer followed. TMN buffers containing 1000, 500, 250, 150 and 100 mM NaCl followed. The beads were transferred to a 15 ml Falcon tube and resuspended in 2.5 ml TMN 100 without proteinase inhibitors. 40 µl of GST-TEV protease were added and TEV-cleavage was carried out overnight at 4°C nutating. Beads were removed from the eluate with the help of mobicol columns (Bio-Rad). Eluates were pooled (5.5 ml) and concentrated by spinning (3000xg, 4°C) through a concentration column (Satorius) until the volume was 10 times reduced. An equal amount of glycerol was added; protein aliquots were snap frozen and stored at -80°C. Presence of Brr2 and purity of purification was determined by SDS-PAGE (2.10.1) and GelCode Blue staining (Pierce). The concentration of purified proteins was determined by Bradford assay using the Bio-Rad Protein assay as instructed by the manufacturer.

2.11 DNA methods

2.11.1 Extraction of plasmid DNA from *E. coli*

Plasmid minipreps were performed using either the QIAprep® Spin MiniPrep kit (Qiagen) or the GeneJET Plasmid Miniprep kit (Fermentas) according to manufacturer's instructions. For larger scale plasmid preparations the HiSpeed Plasmid Maxi kit (Qiagen) was used, again following the manufacturer's

instructions. DNA was generally eluted from the spin column in 10 mM Tris-HCl or H_2O and stored at -20°C.

2.11.2 Plasmid rescue from yeast

To recover plasmids from yeast the Zymoprep Yeast Plamid Miniprep II kit (Zymo Research) was used according to the manufacturer's instructions. Low copy yeast plasmids were eluted in 10 µl TE buffer, while high copy yeast plasmids (*2 µ*) were eluted in 20 µl TE buffer. 1-5 µl of eluate was used to transform *E. coli* (2.9.4).

2.11.3 Plasmid rescue of yeast two-hybrid prey plasmids

To selectively recover the prey-plasmid from a yeast two-hybrid clone, whilst omitting bait-plasmid the MC1066 *E. coli* strain was used (Table 2.5). Plasmid was isolated from yeast as described (2.11.2). MC1066 *E. coli* cells were transformed with the recovered plasmid and plated on M9-L medium (Table 2.2). Because MC1066 cells carry the *leuB6* allele, they are unable to synthesise leucine and thus can only grow on M9-L medium when transformed with a plasmid harbouring the *LEU2* gene that encodes the analogous leucine biosynthesis enzyme from yeast. The yeast two-hybrid prey plasmid pACTII-stop is *LEU2* marked. Transformation of MC1066 cells was performed as described (2.9.4, 2.11.2) and plasmid was isolated with the QIAprep Spin MiniPrep kit (Qiagen), performing all additional wash steps suggested for *end*A^+ bacteria. The recovered plasmid was analysed by restriction digest and could be used for sequencing or yeast transformation.

2.11.4 Restriction digestion of plasmid DNA

Restriction digests were performed according to the manufacturer's instructions for the enzymes used. Restriction enzymes were purchased from New England Biolabs (NEB). DNA agarose gel electrophoresis was performed as described in Sambrook & Russel [13], using 1 kb plus DNA ladder (Invitrogen) or 50 bp ladder (NEB) as size standards. Addition of Ethidium bromide to the gels allowed visualising DNA fragments under UV light.

2.11.5 DNA extraction from agarose gels

DNA fragments were excised from agarose gels, transferred to Eppendorf tubes and weighed. DNA was then purified with one of the following gel extraction kits according to the manufacturer's manual: Wizard® SV PCR and Gel Clean-up System (Promega) or QIAquick® Gel Extraction Kit (Qiagen). DNA was eluted in H_2O.

2.11.6 DNA purification from enzymatic reactions

To facilitate downstream applications, enzymes and unwanted buffer components were removed from PCR and other enzymatic reactions using one of the following purification kits according to manufacturer's instructions: Wizard® SV PCR and Gel Clean-up System (Promega), DNA Clean & Concentrator™-5 kit (Zymo Research), QIAquick PCR Purification kit (Qiagen). If high DNA concentrations were required, Qiagen kits could be used with MinElute spin columns which allow eluting DNA in small volumes (10-20 μl).

2.11.7 Ethanol precipitation of DNA

1/10 vol. 3 M sodium acetate (pH 5.3) was added to the DNA/RNA solution in a microfuge tube. Two volumes of chilled EtOH (96%) were added and the DNA/RNA precipitated for 30 minutes at -20°C. Subsequently the mix was centrifuged (20,000xg, 30 min, 4°C) and the supernatant removed. The DNA/RNA pellet was washed in 1 ml of 70% EtOH and centrifuged (20,000xg, 5 min, 4°C). After discarding the supernatant the pellet was air dried then dissolved in H_2O.

2.11.8 Quantification of DNA

Quantity of DNA and RNA samples, including recovered plasmid DNA, PCR products, DNA fragments after gel purification, or RNA and cDNA, were measured using the NanoDrop ND-1000 spectrophotometer.

2.11.9 DNA cloning strategies

2.11.9.1 Ligation of DNA fragments

DNA fragments for ligation were prepared by restriction digest, separated by agarose gel electrophoresis and gel extracted (2.11.5). To prevent re-ligation of the vector, linearised plasmid DNA was dephosphorylated using Antarctic phosphatase (NEB) which was then removed by EtOH precipitation (2.11.7). DNA was ligated using Fast link™ ligase (Epicentre Biotechnologies). The ligation mixture (5 µl) was used to transform *E. coli* (2.9.4). *E. coli* transformants were analysed by miniprep plasmid DNA extraction (2.11.1) and restriction digestion (2.11.4) and Sanger sequencing (2.11.12).

2.11.9.2 In-Fusion™ cloning

As an alternative to restriction/ligation-based cloning approaches the In-Fusion™ Advantage PCR Cloning Kit (Clontech Laboatories) could be used. It facilitates an *in vitro* recombination reaction to integrate an insert into a linearised vector fragment, mediated by 15 bp homologous sequence overlaps. The manufacturer's protocol was followed (http://www.clontech.com).

2.11.9.3 Cloning by yeast gap repair

A further alternative to restriction/ligation-based cloning is yeast gap repair. Here the ligation step is replaced by a homologous recombination event, which is carried out in living yeast cells. The vector backbone was digested and purified as described (2.11.5). The insert was PCR amplified with oligos providing 45 nt complementary sequence to the 3′ and 5′ ends of the linearised vector. After PCR amplification the insert was purified (2.11.5, 2.11.6). A log-phase yeast culture was co-transformed with purified vector (150 ng) and insert (500 ng) according to the lithium acetate yeast transformation protocol (2.9.5). Yeast cells were plated on selective medium appropriate for the marker harboured in the vector; successful recombination and gap repair resulted in yeast colonies. The plasmid was rescued from yeast, transformed into *E. coli* and analysed as described (2.11.2, 2.9.4, 2.11.4).

2.11.10 Polymerase chain-reaction (PCR)

PCR was used to amplify specific DNA sequences from plasmid DNA and genomic DNA for various molecular cloning purposes. PCRs were generally performed using one of the following DNA polymerases: Phusion® High-Fidelity polymerase (Finnzymes), LA Taq™ (Takara Bio Europe), Taq PCR Core kit (Qiagen) or *Pfu* polymerase (Promega).

2.11.10.1 Basic PCR

A basic 50 µl PCR reaction contained 1x reaction buffer, 2.5 µl primer (sense and antisense 10 pmol/µl each), 1 µl dNTP mix (10 mM each), 0.02 U polymerase and varying amounts of template DNA. Sterile H_2O was added to 50 µl. A basic profile for thermal cycling is shown below:

Step 1	98°C	30 sec	
Step 2	98°C	10 sec	
Step 3	50°C	30 sec	
Step 4	72°C	30 sec/kb	return to Step 2 for 34 cycles
Step 5	4°C	∞	

2.11.10.2 Yeast Colony PCR

To verify the presence of a deletion-cassette or tag at a specific genomic location, yeast colony PCR was performed using the *Taq* PCR Core kit (Qiagen). A small amount of yeast was added to 3 µl of 10 mM NaOH in a 0.5 ml thin wall PCR tube. To break open the yeast cells, this was incubated for 10 minutes in a PCR block at 99°C. The samples were cooled on ice and 22µl of the following PCR reaction mixture was added: 1 µl forward and reverse oligo (10 pmol/µl each), 1 µl dNTPs (10 mM each), 5 µl 5x Q-solution, 2.5 µl 10x reaction buffer with CoralLoad dye, 0.25 µl *Taq* Polymerase (5 U/µl) and H_2O to a final volume of 25 µl. Thermal cycling was performed as recommended by the manufacturer's protocol and the whole PCR reaction was directly loaded to an agarose gel and PCR products analysed.

2.11.10.3 Site-directed mutagenesis (SDM)

SDM was carried out based on the QuickChange method (Stratagene). In a PCR reaction the entire plasmid served as template. Mutagenic primers were used to amplify the full-length plasmid whilst introducing the desired mutation(s) into

the PCR product. Mutagenic oligos were designed according to the following guidelines: 25-40 nt length, mismatch in the middle of the oligo, 50-60% GC content, ideally no GC at the 3′ end and a melting temperature of T_m > 80°C, which was calculated using the following equation:

$$T_m = 81.5°C + 0.41 \times \%GC - (675/nt_{total}) - \%mismatch$$

with $\%mismatch = 100\% \times (nt_{mismatch} / nt_{total})$

Primers, dNTPs, 50 ng of template DNA, polymerase buffer and *Pfu* DNA polymerase (Promega) were combined with H_2O in a 50 µl reaction. Thermal cycling conditions were adapted as recommended for *Pfu* Polymerase. To digest the non-mutated plasmid template, 20 U of *Dpn*I (NEB) were added to the PCR reaction and incubated at 37°C for 2-3 hours or overnight. 5-8 µl of the *Dpn*I treated PCR reaction was used to transform 200 µl of competent *E. coli* (2.9.4). Plasmid from resulting colonies was sequenced to confirm the presence of the desired substitution(s) (2.11.12).

2.11.10.4 Megaprimer PCR

Megaprimer PCR is a two-step method that allows the introduction of small (single or a few nt) and larger changes (deletion or insertion of several 100 nt) to a target region of a plasmid without the need of restriction digestion and ligation. In a first PCR reaction the Megaprimer is amplified. It is 100-400 nt long and must contain the desired sequence changes, whilst being complementary to the target vector in its 5′ and 3′ ends. To ensure that no unwanted changes are introduced in the Megaprimer a proof-reading Polymerase (e.g. Phusion®, Finnzymes) was used for the first PCR. If a plasmid served as template, the PCR product was *Dpn*I treated before gel purification (2.11.5). In a second PCR reaction 400 ng of the purified fragment derived from the first reaction served as primer (i.e. Megaprimer). The

vector backbone of the target vector served as template. The PCR conditions for the second PCR were similar to those used for SDM (2.11.10.3). *Dpn*I treatment removed the non-mutated template. The digested PCR-reaction was transformed into *E. coli* (2.9.4); the presence of the desired changes was confirmed by sequencing (2.11.12).

2.11.10.5 Error prone PCR

To introduce random mutations into a target region of a plasmid error prone PCR was used. Reaction conditions were chosen to increase the naturally occurring error rate of the LA Taq™ polymerase (Takara Bio Europe) during the PCR amplification of a defined fragment. The addition of 0.75 mM $MnCl_2$ to the PCR buffer resulted in a more frequent incorporation of non-complementary nucleotides to the PCR product and an increased number of cycles or nested PCRs increased the error rate further, as determined by sequencing (2.11.12).

2.11.11 Generation of a randomly mutated plasmid library

To generate a library of randomly mutated fragments, integrated to a vector of interest, error prone PCR (2.11.10.5) was combined with Megaprimer PCR (2.11.10.4). The target fragment was amplified under error prone PCR conditions and then incorporated into the parental plasmid during a second round of PCR. To obtain a large number of transformants, commercially available ultra-competent *E. coli* XL10 Gold (Stratagene, Table 2.5) were used. To generate a library, colonies obtained from several PCR and transformation reactions were collected and pooled. Large scale plasmid preparations were performed to isolate plasmid DNA composing the library.

2.11.12 DNA Sanger sequencing

DNA sequencing reactions were performed using the BigDye® Terminator v3.1 Cycle Sequencing kit (Applied Biosystems), and were analysed by The GenePool Sequencing Service, Ashworth Laboratories, University of Edinburgh. Sequence analysis was performed using Sequencher 4.7 Demo software (Gene Codes Corporation).

2.12 RNA methods

2.12.1 Isolation of RNA from yeast

2.12.1.1 GTC-Phenol method

Approximately $2x10^7$ exponentially growing cells (OD_{600} of 0.2-0.8) were harvested by centrifugation (3000xg, 5 min, RT), washed with cold sterile water and pelleted as before. Cell pellets were frozen in liquid nitrogen and stored at -80°C until needed. All steps were performed on ice or at 4°C unless stated otherwise. Cell pellets were resuspended in 100 µl GTC-phenol mix (4 M guanidine thiocyanate, 0.05 M Tris-HCl pH 8.0, 0.01 M EDTA pH 8.0, 2% sarkosyl, 1% β-mercaptoethanol, 50% phenol), 100 µl of zirconia/silica beads (Thistle scientific) were added and vortexed for 5 minutes. Then an additional 600 µl GTC-phenol mix was added, the mixture was vortexed briefly and incubated for 10 minutes at 65°C. Samples were incubated on ice for 10 minutes and 160 µl NaOAc Mix (100 mM NaOAc, 1 mM EDTA, 10 mM Tris-HCl pH 8.0) as well as 300 µl chloroform were added. To achieve optimal phase separation the mixture was centrifuged (20,000xg, 20 min, 4°C). The aqueous phase was extracted with an equal volume of phenol/chloroform/isoamylalcohol (P/C/I, 25:24:1), then with chloroform and finally precipitated with 2.5 volumes EtOH (10 minutes incubation on ice). Centrifugation

(20,000xg, 10 min, 4°C) compacted the precipitate to a pellet. The pellet was washed with 70% EtOH, air-dried and resuspended in H_2O.

2.12.1.2 Hot Phenol method

Exponentially growing yeast cells (25 ml) were harvested at an OD_{600} of 0.5 by centrifugation (850xg, 5 min, RT, accuSpin™ 1 Fischer) and were washed once with H_2O. Cell pellets were resuspended in 400 µl AE (50 mM NaOAc pH 5.3, 10 mM EDTA; adjusted to pH 5.3 with acetic acid) and 0.9% SDS. An equal volume of Tris-buffered phenol (440 µl) (pH 8; Sigma) was added and vortexed to mix. The mixture was incubated for 45 minutes at 65°C in a shaking heating block at 1000 rpm, cooled to RT on ice and then spun for in a table top microfuge (20,000xg, 5 min, RT). The aqueous phase (400 µl) was extracted with an equal volume of phenol/chloroform (5:1, pH 4.5, Ambion), vortexed and left at room temperature for 5 minutes before centrifuging as before (20,000xg, 5 min, RT). The aqueous phase was extracted with an equal volume of chloroform as before and RNA was precipitated with 2.5 volumes of EtOH, collected by centrifugation and washed as in (2.12.1.1).

2.12.2 Purification of RNA by P/C/I extraction

To exchange buffer and remove proteins from RNA samples P/C/I (24:25:1) extraction was used. The reaction volume was increased to 250 µl with TE buffer. An equal volume of P/C/I and 1/10th volume of 3 M NaOAc pH 5.3 were added and the RNA extracted by vortexing for 20 sec. For phase separation the sample was spun (14,000xg, 5 min, RT). The aqueous phase was transferred to a fresh tube, 2 vol. of absolute EtOH were added and the RNA was precipitated for 30 min at -80°C. After centrifugation (14,000xg, 20 min, 4°C) the RNA was washed with 70% EtOH, air dried and resuspended in the desired amount of H_2O.

2.12.3 Preparation of end-labelled oligo probes

Oligonucleotides were 5′ end-labelled in order to use them as probes for Northern blotting or Primer extension. A 10 µl reaction containing 1x PNK reaction buffer, 10 mM DTT, 2-3 µl (20-30 µCi) [γ^{32}P]ATP and 10 U T4 polynucleotide kinase (PNK) (NEB) at 37°C for 1 hour. Thereafter, the PNK was heat inactivated at 65°C for 5 minutes. End-labelled oligos were purified from unincorporated nucleotides and enzyme using illustra™ ProbeQuant™ G-50 Micro purification columns (GE Healthcare) according to the manufacturer's instructions. Labelled oligonucleotides were eluted in 50 µl in H_2O.

2.12.4 *In vitro* transcription of RNA

2.12.4.1 Riboprobes

RNA transcripts were generated from transcription template generated by PCR. The template must contain the T7 promoter sequence (GGATCCTAATACGACTCACTATAGGGAGAGGA-forward primer) 5′ to the sequence to be transcribed. A 25 µl reaction also contained 0.6 µl 100 µM UTP, 1 µl 10 mM CTP/GTP/ATP mix, 2 µl 100 mM DTT, 0.2 µl 10 mg/ml BSA, 1x RNA polymerase reaction buffer, 5 µl (50 µCi) [α^{32}P]UTP and 1 µl T7 RNA polymerase (80 U/µl, NEB). The reaction mixture was incubated for 1 hour at 37°C. Unincorporated nucleotides were removed by spinning the probe through illustra™ ProbeQuant™ G-50 Micro purification columns (GE Healthcare) according to the manufacturer's instructions.

2.12.4.2 *In vitro* transcription of snRNAs

Larger amounts of snRNA transcripts were produced using the MEGAshortscript™ T7 kit (Ambion) according to the manufacturer's recommendations. Before terminating the reaction 1 U of CIAP Alkaline phosphatase (Promega) was added and incubated for 30 minutes at 37°C to dephosphorylate the 5′ ends of the transcript. The template DNA was hydrolysed by adding 2 U of TURBO DNase (Ambion) and incubation at 37°C for 15 minutes.

2.12.4.3 *In vitro* transcription of splicing substrate

RNA transcripts used as substrates for *in vitro* splicing reactions were capped with a m^7GpppG cap analogue. *In vitro* transcription was carried out in a 20 µl reaction: 2 µg DNA template, 2 µl rNTP mix (5 mM UTP, CTP, GTP and 0.2 mM ATP), 1 µl m^7GpppG cap analogue (10 mM, NEB), 2 µl 10x T7 Polymerase Buffer, 2 µl (20 µCi) [α^{32}P]ATP, 1 µl T7 RNA Polymerase. Transcription was carried out at 37°C for 30 minutes.

2.12.4.4 Purification of *in vitro* transcribed RNA

Transcripts used for *in vitro* splicing reactions or electrophoresis mobility shift assays (2.12.10 and 2.12.8) were purified by Polyacrylamide gel-extraction. The transcription reaction was stopped by placing it on ice. The reaction volume was increased by adding 10 mM Tris-HCl to a final volume of 400 µl. The RNA was P/C/I extracted and ethanol precipitated (2.12.2). The pellet was resuspended in 5 µl H_2O and an equal volume of FA (47% formamide, 10 mM EDTA, 0.025% bromphenol blue and 0.025% xylene cyanol) loading buffer. The whole sample was separated on a 6% 7 M urea PAA gel (2.12.5). For non-radioactive RNAs the gel was submerged in a staining bath (150 ml 1x TBE and 10 µl SYBR safe stain (Invitrogen)) stained for 10 minutes, thereafter de-stained for 10 minutes in 1x TBE. RNA was

visualised at 532 nm UV light. For radio-labelled RNAs the area of the gel containing the full-length transcript was visualised by autoradiography. RNA-bands were excised and the RNA was eluted from the gel by diffusion. For that the gel piece was incubated 2 times in 250 µl TNES buffer (20 mM Tris-HCl pH 8.0, 300 mM NaCl, 5 mM EDTA pH 8.0, 0.1% SDS) for 1 hour at 37°C. Thereafter the supernatants were pooled and the RNA was P/C/I extracted, Ethanol precipitated and resuspended in H_2O.

2.12.4.5 Renaturing and duplex formation of *in vitro* transcribed RNAs

Renaturing of RNA or annealing of two different RNAs was carried out in 20 µl reactions in 1x Buffer A (50 mM Tris pH 7.5, 150 mM NaCl, 1 mM EDTA). To anneal snRNA duplexes equimolar amounts of snRNAs (typically 100 pmol each) were added to the reaction. To convert the weight (weight concentration) of an RNA in the molar quantity (molar concentration) and vice versa a web based tool was used (http://molbiol.ru/eng/scripts/01_07.html).

RNA was denatured by heating to 80°C for 3 minutes, the reaction was then transferred to a rack at room temperature and left to cool for 40 minutes, before placing on ice. The efficiency of duplex formation was verified by running an aliquot of the annealed RNA on a native PAA gel (2.12.7).

2.12.5 Denaturing Polyacrylamide gel electrophoresis

Polyacrylamide (PAA) gel electrophoresis (PAGE) was performed according to standard protocols (e.g. Maniatis *et al.*, 1982). Prior to electrophoresis RNA samples were diluted with an equal volume of FA loading buffer (47% formamide, 10 mM EDTA, 0.025% bromphenol blue and 0.025% xylene cyanol) denatured for 3 minutes at 95°C, then snap-chilled on ice.

Sequencing gels contained 12% acrylamide-bis-acrylamide (18:1), 7 M urea and 1x TBE. They were 40 cm long and 0.1 mm thick. Low molecular weight RNAs were separated on 6, 7, 8 or 10% PAA 1x TBE 8 M urea gels (15 cm long and 0.3, 1 or 1.5 mm thick).

Following electrophoresis gels for primer extensions (2.12.9) and *in vitro* splicing reactions (2.12.10), typically 0.1-0.3 mm thick, were transferred to Whatman 3MM paper and dried for 30 minutes at 80°C before exposure to a phosphorimager screen.

2.12.6 Northern blotting

For Northern blotting, subsequent to electrophoresis, RNAs were transferred to nylon membrane (Hybond N or N+, GE Healthcare) by electro-blotting in a wet transfer tank. Transfer was carried out in 0.5x TBE either at 15 V overnight at 4°C, or for 1 hour at 60 V using a water cooled Trans Blot Cell (Bio-Rad). RNA was crosslinked to the membrane by UV light ("auto-crosslink" setting, 120 mJ/cm^2) in a UV Stratalinker® 1800 (Stratagene).

Membranes were pre-hybridised in 50 ml of Oligo-Hyb buffer (7% SDS, 170 mM Na_2HPO_4, 80 mM NaH_2PO_4, 0.5 mM EDTA) for 1 hour at 37°C. End-labelled oligoprobes (2.12.3) were added directly to the Oligo-Hyb buffer and were hybridised with the membrane over night at 37°C. Subsequently, membranes were rinsed once with 100 ml of 6x SCC, washed once with 100 ml 6x SCC at RT for 10 minutes and washed once under higher stringency with 100 ml of pre-warmed 2x SSC, 0.2% SDS for 10 minutes at 37°C. Membranes were dried with tissue paper, wrapped in saran wrap and exposed to an autoradiography film or to a phosphorimager screen. A Fujifilm FLA-5100 phosphorimager was used to scan images; where appropriate image quantification was carried out using the AIDA software (Raytest Isotopenmeßgeräte GmbH).

Riboprobes (2.12.4.1) were hybridised over night at 65°C in ULTRAhyb™ ultrasensitive hybridisation buffer (Ambion). Pre-hybridisation of the membrane in ULTRAhyb™ buffer was carried out while the oven was heating to 65°C and once warmed up was continued for 30 minutes at 65°C prior to addition of the purified probe. After hybridisation membranes were rinsed twice with 6x SSC and washed once with 6x SSC at RT for 15 minutes. Two high stringency washes were carried out with pre-warmed 0.2x SSC with 0.2% SDS at 65°C for 15 minutes. Membranes were dried and exposed as described before.

Membranes could be stripped from probes by washing the membranes twice in boiling 0.1x SSC with 0.1% SDS, allowing further hybridisations with different probes.

2.12.7 Native PAA gel electrophoresis

Native PAA gels were used to separate protein-RNA complexes (2.12.8). 0.5x TBE 6% acrylamide-bis-acrylamide (20:1) gels were 1 mm thick and 16 cm high. They were prepared by combining 23.6 ml of water with 6 ml Acrylamide 40% (w/v) (Bio-Rad) and 6 ml Bis 2% (w/v) (Bio-Rad) as well as 4 ml 5x TBE, 0.4 ml 10% APS and 40 µl TEMED. After polymerisation the gel was pre-run in cooled 0.5x TBE for 1 hour at 10 W, 4°C.

Here RNA samples were not mixed with loading buffer that contained dyes; to follow the migration front an empty lane was loaded with FA loading buffer containing bromphenol blue and xylene cyanol blue. Depending on the size of RNA of interest and the desired separation the gel was run for 5-6 hours at 10 W constant, 4°C. The gel could be transferred to 3MM Whatman paper and dried, if the RNA was radio-labelled. Alternatively, it could be transferred to a nylon membrane and the RNA was detected by Northern hybridisation as described (2.12.6).

2.12.8 Electrophoresis mobility shift assay (EMSA)

For EMSAs, varying amounts of purified protein (2.10.5) were incubated with *in vitro* transcribed, renatured RNA (12.4.2 and 12.4.5) to observe the formation of protein/RNA complexes. A constant amount of RNA (typically 10 nM) was combined with increasing amounts of protein (0-500 nM). In a 20 µl reaction protein and RNA were combined in 1x RNA binding buffer (10 mM Hepes pH 7.5, 1 mM $MgCl_2$, 100 mM NaCl, 5% Glycerol) and incubated on ice for 30 minutes. 2 µl of 10% Ficoll 400 were added and the sample was separated on a 6% native gel (2.12.7).

2.12.9 Primer extension

Primer extensions were performed on 2-8 µg total RNA (2.12.1) with 5′ end-labelled oligonucleotides (2.12.3). Oligo sequences were designed to give a melting temperature of 50°C, 50% GC/AT content, no single-nucleotide tracks, and a length of 19-21 nt.

0.1 pmol of end-labelled oligo and 2-8 µg of total RNA/sample were heat denatured 80°C for 3 minutes, then snap-chilled on ice. A reaction mixture containing 1x first strand buffer, 1 µl (40 U/µl rRNasin, Promega), 5 mM DTT and 2 mM dNTPs was prepared and added to the denatured RNA-oligo mix. After three minutes at 50°C 1 µl Super Script III reverse transcriptase (5 U/µl, Invitrogen) was added and reverse transcription was carried out for 30 minutes to 1 hour at 50°C. To stop the reaction, an equal volume of FA loading buffer was added and the sample was incubated for 3 minutes at 95°C. The reaction products were analysed on a 7-8% PAA gel or 12% PAA sequencing gel depending on the size of the expected products and the separation required. Primer extension products were compared to a radioactively labelled size marker or to an RNA sequencing reaction (see below).

Sequencing reactions were performed in parallel to primer extension reactions in order to know the length and sequence of extension products. Four sequencing reactions were carried out in parallel, one for each ddNTP. For each

reaction 2-8 µg of total RNA were mixed with 0.075 pmol end-labelled oligo and H_2O in a 6 µl reaction. Incubation at 80°C for 3 minutes and snap-chilling on ice allowed primer annealing. A master mix containing 1x first strand buffer, 1.5 µl (40 U/µl rRNasin, Promega), 5 mM DTT, 1.5 µl Super Script III reverse transcriptase (5 U/µl, Invitrogen) was prepared. For each of the nucleotides ddNTP/dNTPs mixtures were prepared, such that the final concentrations were 5 mM ddNTP and 2 mM dNTPs, respectively. Each RNA-primer mix was then combined with 4 µl of the reaction mixture and with 1 µl of ddNTP/dNTPs mixture (final concentrations 2.5 mM ddNTP and 1 mM dNTPs). The reaction was incubated for 50 minutes at 50°C, subsequently stopped by addition of an equal volume of FA loading buffer. Samples were heat denatured for 3 minutes at 95°C, snap-chilled on ice and separated on a 12% PAA gel (2.12.5).

2.12.10 *In vitro* splicing reaction

In vitro splicing reactions were carried out in a 10 µl reaction volume. Each reaction contained 1 µl 0.6 M KPO_4 pH 7.0, 1 µl 25 mM $MgCl_2$, 1 µl 20 mM ATP, 1 µl 30% PEG_{8000}, 4 µl splicing extract, 2 µl radio-labelled transcript (~100-1000 cps). The reaction was incubated at 25°C-37°C depending on experimental requirements, and terminated by placing on ice. Then 3 µl of Proteinase K solution (1 mg/ml Proteinase K, 50 mM EDTA, 1% (w/v) SDS) were added and the reaction was incubated at 37°C for 45 minutes. Thereafter 200 µl of splicing cocktail (50 mM NaOAc pH 5.3, 1 mM EDTA, 0.1% (w/v) SDS, 2 mg/ml Glycogen) and 450 µl P/C/I were added. RNA was extracted and EtOH precipitated (-70°C, 30 min). After centrifugation (20,000xg, 20 min, 4°C) RNA pellets were washed with 70% EtOH, air-dried and resuspended in 5 µl of H_2O. An equal amount of FA loading buffer was added and the RNA was separated on a 7% PAA gel. The gel was transferred to 3MM Whatman paper and dried. Autoradiography visualised RNA species.

2.12.11 Crosslinking of RNA and analysis of cDNA (CRAC)

2.12.11.1 UV cross-linking, cell lysis, IgG affinity-purification

Yeast strains expressing HTP-tagged proteins were grown in SD drop out medium to OD_{600} 0.5. The living cell culture (2.7 l) was poured into a custom-built *in vivo* cross-linking apparatus, the "Megatron", and the cell culture was irradiated with UV light (wavelength 254 nm) for 150 seconds. The cell suspension was transferred to chilled centrifuge bottles and the cells were pelleted by centrifugation (3,000xg, 10 min, 4°C, Beckman Avanti). Cell pellets were resuspended in ice-cold PBS, transferred to chilled Falcon tube and centrifuged again (3000xg, 5 min, 4°C, Sorvall Legend RT). The pellets were snap-frozen in liquid nitrogen and stored at -70°C.

All following steps were carried out on ice unless stated otherwise. For extract preparation the pellets were rapidly thawed in the palm of the hand, then resuspended in 1 volume TMN150 (50 mM Tris-HCl pH 7.8, 150 mM NaCl, 1.5 mM $MgCl_2$, 0.1% NP40) containing 5 mM β-mercaptoethanol (β-ME) and complete EDTA-free protease inhibitors (PIs, 1 tablet per 50 ml, Roche). Cell-lysis was achieved by vortexing in the presence of 2.5 volumes Zirconia beads (0.5 mm Zirconia/Silica beads, Thistle Scientific). Cells were vortexed for 1 minute then chilled on ice 1 min, this was repeated 4 times. A further 3 volumes of TMN150, 5 mM ß-ME and PIs were added and the lysate was cleared from Zirconia beads and cell debris by centrifugation (4,600xg, 20 min, 4°C, Sorvall Legend RT). The supernatant was transferred to chilled 10 ml Polycarbonate tubes and the lysate was cleared from chromatin, insoluble membrane components and Polysome fractions by centrifugation at 40,000xg, 1 hour, 4°C (Ti 70.1 rotor, Beckman XL-100). The cleared lysate was added to 1/10 V packed IgG sepharose beads (GE Healthcare) equilibrated in TMN150; these were incubated at 4°C for 2 hours with agitation.

Subsequently, the beads were washed twice with 10 ml TMN1000 (50 mM Tris-HCl pH 7.8, 1 M NaCl, 1.5 mM $MgCl_2$, 0.1% NP40) and 3x with 10 ml TMN150 (50 mM Tris-HCl pH 7.8, 150 mM NaCl, 1.5 mM $MgCl_2$, 0.1% NP40). After the last wash, the beads were resuspended in 600 µl TMN150 with 5 mM β-ME and 2 µl GST-TEV protease (here no protease inhibitors added) (TEV protease was generously supplied by Dr. Sander Granneman). To elute the protein from the beads TEV cleavage was performed in a shaking incubator at 18°C for 2 hours.

2.12.11.2 Partial RNase digestion, Ni affinity-purification

In order to trim the crosslinked RNA to manageable sizes the RNA contained in the TEV eluate was partially digested with an RNase A and T1 cocktail (RNace it 10 U/µl, Stratagene; here 1 U/rxn) for 5 minutes at 37°C. To fully inactivate the RNase, 0.4 g guanidinium hydrochloride (final concentration 6 M) was added to the mixture at the end of the incubation period. NaCl and imidazole were added to the reaction to final concentrations of 300 mM and 10 mM, respectively. The digested TEV eluate was then added to 50 µl Ni-NTA agarose (Qiagen) equilibrated in wash buffer 1 (WB 1, 50 mM Tris-HCl pH 7.8, 300 mM NaCl, 10 mM imidazole, 6 M guanidine-HCl, 0.1% NP40, 5 mM β-ME) and incubated overnight at 4°C on a shaking platform. After nickel binding, the beads were washed 2x with WB 1 and 3x with 1x PNK buffer (250 mM Tris-HCl pH 7.8, 50 mM $MgCl_2$, 5 mM β-ME).

At this stage the samples could be eluted and analysed by western blotting as described below. However, to generate a sequencing compatible library several enzymatic reactions needed to be performed before elution as described in section (2.12.11.3-.4). The Ni-NTA beads were washed 3x with wash buffer 2 (WB 2, 50 mM Tris-HCl pH 7.8, 50 mM NaCl, 10 mM imidazole, 0.1% NP40, 5 mM β-ME) and RNPs were eluted twice with 200 µl elution buffer (10 mM Tris-HCl pH 7.8, 50 mM NaCl, 150 mM imidazole, 0.1% NP40, 5 mM β-ME) for 5 minutes at RT. For further

analysis proteins were precipitated with 1/10 volume 100% TCA and 20 µg Glycogen (Roche), washed with acetone, resuspended in 1x NuPAGE loading buffer. SDS PAGE on 4-12% NuPAGE Bis-Tris gradient gels (Invitrogen) and Western blotting followed (2.10.1 and 2.10.2).

2.12.11.3 Dephosphorylation of RNA 5' ends, radio-labelling, linker ligation

If crosslinked RNAs were analysed further, several enzymatic reactions were performed while the crosslinked RNA-protein complexes remained immobilised on the Ni-NTA agarose. In order to remove the 3' phosphate left after the RNase digestion, alkaline phosphatase treatment followed. Therefore the Ni-NTA agarose was transferred to micro spin columns (Pierce) and resuspended in a 80 µl reaction mixture containing, 8 µl TSAP (thermostable alkaline phosphatase, Promega 1 U/µl), 2 µl RNasin (placental, Promega 40 U/µl) and 16 µl 5x PNK buffer (250 mM Tris-HCl pH 7.8, 50 mM $MgCl_2$, 5 mM β-ME). Phosphatase treatment was carried out for 30 minutes at 37°C. To inactivate the TSAP, the beads were washed 3x with WB 1 and 3x with 1x PNK.

Next, a linker was ligated to the 3' end of the RNA. The beads were resuspended in a 80 µl reaction containing 8 µl mirCAT33™ 3' linker (10 µM), 2 µl RNasin, 2 µl T4 RNA ligase (NEB, 10 U/µl) and 16 µl 5x PNK. The linker (Table 2.16) has a blocked 3' end and pre-activated adenosine at its 5' end, such that ligation can be carried out in the absence of ATP and formation of concatenated linkers is avoided. Linker ligation was carried out for 6 hours at 25°C. RNA ligase was inactivated by washes as described above.

To visualise RNPs the 5' end of the RNA was radioactively labelled. The reaction was carried out in a 80 µl reaction volume containing 4 µl (40 µCi) [γ^{32}P]ATP, 4 µl T4 PNK (from phage infected *E. coli*, 5 U/µl, Sigma or Invitrogen) and 16 µl 5x PNK buffer for 40 minutes at 37°C. To ensure phosphorylation of all 5'-

ends, 1 µl 100 mM ATP (Roche) was added and the reaction proceeded for a further 20 minutes. The enzyme was inactivated and the beads re-equilibrated for the next reaction by washing in WB 2 as described before.

Lastly, an RNA linker was ligated to the 5′ end of the RNA. A 80 µl reaction contained 2 µl Solexa 5′ linker or barcoded L5a, L5c, L5d, L5e or Lf (100 µM) (Table 2.16), 8 µl ATP (10 mM), 4 µl RNA ligase (NEB, 10 U/µl), 2 µl RNasin and 16 µl 5x PNK buffer. Ligations were carried out overnight at 16°C.

2.12.11.4 SDS PAGE, Western transfer, RNA elution

Following linker ligation the radio-labelled RNA-protein complexes were eluted from the nickel beads as described in (2.12.11.2), transferred to nitrocellulose membrane (Amersham) and detected by autoradiography. With the help of the autoradiogram, regions containing the labelled RNP were excised from the membrane and the RNA was recovered by Proteinase K digestion. Therefore, the membrane was incubated for 2 hours at 55°C in 400 µl WB 2 supplemented with 1% SDS, 5 mM EDTA (pH 8.0) and 100 µg Proteinase K (Roche). RNA was extracted with P/C/I (25:25:1) and precipitated with 2.5 volumes EtOH in the presence of 20 µg glycogen (Roche).

2.12.11.5 Reverse transcription, gel purification, cloning and sequencing

To synthesise cDNA the precipitated RNA was resuspended in a 10 µl reaction mix containing 1 µl miRCAT33™ RT oligo (10 µM) (Table 2.16) and 2 µl dNTPs (5 mM). This mixture was denatured for 3 min at 80°C and snap-chilled on wet ice. For first strand synthesis 4 µl 5x reaction buffer, 1 µl DTT (100 mM) and 1 µl rRNasin (40 U/µl, Promega) were added. Primer annealing was carried out at 50°C for 3 min. Reverse transcription was started by addition of 1 µl Super Script III (200

U/μl, Invitrogen) and incubated for 1 hour at 50°C. The enzyme was heat inactivated for 15 minutes at 65°C and the template RNA was digested for 30 minutes at 37°C with 2 μl RNase H (5 U/μl, NEB).

In order to obtain libraries compatible with sequencing, PCR reactions were carried out, containing the following mix: 5 μl 10x LA taq buffer, 0.5 μl LA Taq™ (5 U/μl Takara Bio Europe), 1 μl Solexa PCR oligos forward and reverse (10 μM), 2.5 μl dNTPs (5 mM each) and 1 μl of the reverse transcription reaction. The following conditions were used for thermal cycling:

Step 1	95°C	2 min	
Step 2	98°C	20 sec	
Step 3	52°C	20 sec	
Step 4	68°C	20 sec	return to Step 2 for 24 cycles
Step 5	72°C	5 min	
Step 6	4°C	∞	

For all cross-linking experiments 5 of the above PCR reactions were performed per sample, pooled, precipitated with EtOH or column purified using the DNA Clean & Concentrator™-5 kit (Zymo Research). The sample was gel-purified on a TBE 3% MetaPhor® agarose gel (Lonza). DNA ranging in size from 80 to 120 nt was excised from the gel and recovered using the MinElute Gel Purification Kit (Qiagen) according to the manufacturer's instructions. DNA was eluted in 20 μl H_2O. 2 μl of the library were TA-cloned into the pCR®2.1 TOPO® vector (Invitrogen) following the manufacturer's protocol. Transformation to competent *E. coli* TOP10 (Invitrogen) followed (2.9.4). Overnight cultures of single bacterial clones were grown. Colony PCRs were performed with T7_SEQ and M13R oligos (Table 2.16); sequencing was performed with the M13R oligo by The GenePool Sequencing Service, Ashworth Laboratories, University of Edinburgh. The remaining library was Solexa sequenced with single-end 50 base reads by The GenePool Sequencing Service.

2.12.11.6 CRAC bioinformatics

Bioinformatics analyses of the Sanger and Solexa sequencing data was performed in collaboration with Dr. Grzegorz Kudla and was previously described in [14].

2.12.12 Reverse transcription-quantitative PCR

Reverse transcription-quantitative PCR (RT-qPCR) was used to measure the abundance of RNA species such as mRNA pre-mRNA and splicing intermediates as described in [10]. Total RNA was extracted from yeast (2.12.1.1). Prior to cDNA synthesis 10 μg of RNA were treated with DNAse1 (0.9 U RQ1, Promega) according to the manufacturers' protocol to remove traces of genomic DNA that co-purify with the RNA. For cDNA synthesis a 10 μl reaction containing 5 μg DNAse treated RNA, 5x First strand synthesis buffer, 10 U RNAse inhibitor (Invitrogen), 10 mM dNTP mix, gene specific reverse primers 250 nm each and 7.5 U Transcriptor reverse transcriptase (Roche) was prepared. Reverse transcription was carried out at 55°C for 2 hours. After cDNA synthesis the remaining RNA was hydrolysed by the addition of 10 μl of RNaseA solution (0.1 mg/ml) and incubation at 37°C for 1 hour. Finally, the cDNA was diluted 1/20.

q-PCRs were performed in technical triplicate using SYBR green Jumpstart Taq ready mix (Sigma) in a Stratagene MX3005P real-time PCR machine. The reaction volume was 10 μl: 5 μl SYBR green q-PCR mix with 1/1000th volume ROX reference dye, forward and reverse primer (300 nm each) and 4 μl cDNA template. PCR cycling was carried out as follows:

Step 1	94°C	2 min	
Step 2	94°C	10 sec	
Step 3	63°C	10 sec	
Step 4	72°C	20 sec	return to Step 2 for 50 cycles

The obtained parameter were analysed using the MXPro Software (Stratagene) as described in [15].

2.12.13 Mapping 3' ends of RNA fragments

To identify the exact 3' end of an RNA or RNA-fragment a variation of a 3' RACE-PCR (**r**apid **a**mplification of **c**DNA-ends with **p**olymerase **c**hain **r**eaction) was used. In a 20 µl reaction 1 µl miRCAT33™ [16] cloning linker (10 µM) (Table 2.16) was ligated to 3' ends contained in 4 µg of total yeast RNA, using 2 µl T4 RNA ligase (NEB, 10 U/µl), 0.5 µl Rnasin (40 U/µl, Promega) and 4 µl 5x PNK buffer (250 mM Tris-HCl pH 7.8, 50 mM $MgCl_2$, 5 mM β-ME). Linker ligation was carried out for 2 hours at 25°C. The nucleic acids were ethanol precipitated (2.12.2). Reverse transcription was performed using an oligonucleotide complementary to the linker sequence (miRCAT33™ RT oligo, Table 2.16) followed by RnaseH digestion. PCR amplification with oligonucleotides complementary to the cloning linker and the target region upstream of the expected 3' end (here the 5' end of U2 snRNA (Table 2.15)) was carried out. The PCR products from 3 reactions were pooled, purified and separated on a TBE 3% MetaPhor® agarose gel. The PCR products of the desired length were excised from the gel, purified (2.11.5) and TA-cloned (TOPO® TA pCR®2.1 kit, Invitrogen). Plasmid prepared from individual *E. coli* colonies was sequenced and revealed the sequence of the cloned cDNA fragment, corresponding to the 3' end of RNA in question.

2.13 References

1. Fromont-Racine, M., Rain, J.-C. and Legrain, P. (1997) Toward a functional analysis of the yeast genome through exhaustive two-hybrid screens. Nature Genetics. **16**, 277-282.

2. Longtine, M.S., McKenzie, A.R., Demarini, D.J., Shah, N.G., Wach, A., Brachat, A., Philippsen, P., Pringle, J.R. and Jul, Y. (1998) Additional modules for versatile and economical PCR-based gene deletion and modification in *Saccharomyces cerevisiae*. Yeast. **14**(10), 953-961.

3. Sikorski, R. and Hieter, P. (1989) A system of shuttle vectors and yeast host strains designed for efficient manipulation of DNA in *Saccharomyces cerevisiae*. Genetics. **122**, 19-27.

4. Decourty, L., Saveanu, C., Zemam, K., Hantraye, F., Frachon, E., Rousselle, J.-C., Fromont-Racine, M. and Jacquier, A. (2008) Linking functionally related genes by sensitive and quantitative 85haracterization of genetic interaction profiles. PNAS. **105**(15), 5821-5826.

5. Longtine, M.S., McKenzie, A.r., Demarini, D.J., Shah, N.G., Wach, A., Brachat, A., Philippsen, P. and Pringle, J.R. (1998) Additional modules for versatile and economical PCR-based gene deletion and modification in *Saccharomyces cerevisiae*. Yeast. **14**(10), 953-961.

6. Janke, C., Magiera, M.M., Rathfelder, N., Taxis, C., Reber, S., Maekawa, H., Moreno-Borchart, A., Doenges, G., Schwob, E., Schiebel, E. and Knop, M. (2004) A versatile toolbox for PCR-based tagging of yeast genes: new fluorescent proteins, more markers and promoter substitution cassettes. Yeast. **21**(11), 947-962.

7. Fabrizio, P., Laggerbauer, B., Lauber, J., Lane, W.S. and Lührmann, R. (1997) An evolutionarily conserved U5 snRNP-specific protein is a GTP-binding factor closely related to the ribosomal translocase EF-2. EMBO. **16**(13), 4092-4106.

8. Liu, L., Query, C.C. and Konarska, M.M. (2007) Opposing classes of prp8 alleles modulate the transition between the catalytic steps of pre-mRNA splicing. Nature Structural & Molecular Biology **14**(6).

9. Wlotzka, W., Kudla, G., Granneman, S. and Tollervey, D. (2011) The nuclear RNA polymerase II surveillance system targets polymerase III transcripts. EMBO. **30**(9), 1790-1803.

10. Alexander, R., Barras, D., Dichtel, B., Kos, M., Obtulowicz, T., Koper, M., Karkusiewicz, I., Marikinti, L., Tollervey, D., Dichtel, B., Kufel, J., Bertrand, E. and Beggs, J.D. (2010) RiboSys, a high-resolution, quantitative approach to measure the *in vivo* kinetics of pre-mRNA splicing and 3'-end processing in *Saccharomyces cerevisiae*. RNA. **16**(12), 2570-2580.

11. Gietz, D.R. and Schiestl, R.H. (2007) High-efficiency yeast transformation using the LiAc/SS carrier DNA/PEG method. Nature protocols. **2**(1), 31-34.

12. Boeke, J., LaCroute, F. and Fink, G. (1984) A positive selection for mutants lacking orotidine-5'-phosphate decarboxylase activity in yeast: 5-fluoro-orotic acid resistance. Molecular and general Genetics. **197**(2), 345-346.

13. Sambrook, J. and Russel, D.W. (2001) Molecular Cloning: A laboratory manual. Cold Spring Harbor Laboratory Press, Cold Spring Harbor, New York. **3 ed**.

14. Granneman, S., Kudla, G., Petfalski, E. and Tollervey, D. (2009) Identification of protein binding sites on U3 snoRNA and pre-rRNA by UV cross-linking and high-throughput analysis of cDNAs. PNAS. **106**(24), 9613-9618.

15. Alexander, R., Innocente, S.A., Barras, D. and Beggs, J.D. (2010) Splicing-dependent RNA Polymerase pausing in yeast. Molecular Cell. **40**(4), 582-593.

16. Bottner, C.N., Schmidt, H., Vogel, S., Michele, M. and Käufer, N.F. (2005) Multiple genetic and biochemical interactions of Brr2, Prp8, Prp31, Prp1and Prp4 kinase suggest a function in the control of activation of splicosomes in Shizosaccharomyces pombe. Current Genetics. **48**, 151-161.

Chapter 3 – Brr2 interactions with spliceosomal RNA helicases

3.1 Acknowledgement

The genetic interaction mapping experiments described in section 3.9 of this chapter were carried out in collaboration with Dr. Cosmin Saveanu, Institut Pasteur, Centre National de la Recherche Scientifique, Paris, France. While I carried out the strain preparation and validation experiments, I thank Dr. Saveanu for data collection and analysis.

3.2 Introduction

Eight RNA helicases participate in splicing and have been proposed to remodel RNA-protein or RNA-RNA interactions, thereby triggering conformational changes in splicing complexes (Chapter 1). For a productive splicing event the RNA helicases must act in a highly coordinated and sequential manner, with each helicase being required at specific step(s) [1]. However, the mechanisms which control and coordinate the activities of the spliceosomal RNA helicases remain poorly understood.

Initially sequential recruitment and release following ATP hydrolysis was suggested to be mainly responsible for determining the timely action of the different helicases throughout the splicing cycle. Several recent reports, however, show that some helicases are present in the spliceosome earlier or later than previously thought. Prp5 was proposed to remain associated with the spliceosome subsequent to its role in pre-spliceosome formation [2]. Prp16 and Prp22 have ATP-independent functions prior to their catalytic activation [3-5]. Prp43 has been suggested to disassemble spliceosomes at different stages of the splicing reaction if it fails to proceed normally [6, 7]. Finally, Brr2 remains associated with the spliceosome

throughout the splicing cycle; its activity seems to be required during both spliceosome assembly and disassembly [8]. These observations raise the question of how suppression and activation of the catalytic activities of splicing helicases can be achieved.

Several observations give reason to speculate that specifically the C-terminal helicase module of Brr2 might play a role in regulating splicing helicases: The function of the catalytically inactive C-terminal helicase module is not fully understood. Although it is thought to lack helicase activity [9], it is nevertheless crucial for Brr2 function. While deletion of the entire C-terminal module is lethal in yeast, deletion of only the C-terminal Sec63 domain is viable, yet strongly affects cell growth and Brr2 function [10]. This is likely a result of impaired or lost protein interactions. Yeast two-hybrid interaction tests have revealed a predominant role for the C-terminal helicase and Sec63 domains of Brr2 in establishing protein interactions [11, 12].

The C-terminal part of Brr2 was found to interact with splicing factors Prp8, Slu7, Snp1 and Snu66 [12]. Especially Brr2-Prp8 interactions have been studied closely, as Prp8 is thought to stimulate the activity of Brr2 (see Chapter 1) [10, 13-15]. Notably, the C-terminal domains of Brr2 also establish interactions with at least two other spliceosomal helicases, Prp2 and Prp16 [12].

Based on the various interactions of the C-terminal domains of Brr2, the existence of a protein interaction network was proposed. The establishment of distinct protein-protein interactions during splicing could regulate the activity of Brr2; in turn physical interaction with the C-terminal domains of Brr2 could contribute to the regulation of interacting proteins [12].

3.3 Y2H screen identifies *brr2* mutants with aberrant protein interaction properties

Based on the hypothesis that the C-terminus of Brr2 might participate in the catalytic regulation of other splicing helicases, I aimed at identifying and characterising determinants within the C-terminal domains of Brr2 that influence the interaction with other spliceosomal RNA helicases. To this end I devised a genetic screen based on a classical yeast two-hybrid assay, in order to identify *brr2* mutants that show aberrant protein interactions with Prp2 and/or Prp16 (Fig. 3.1, 2.9.9.2).

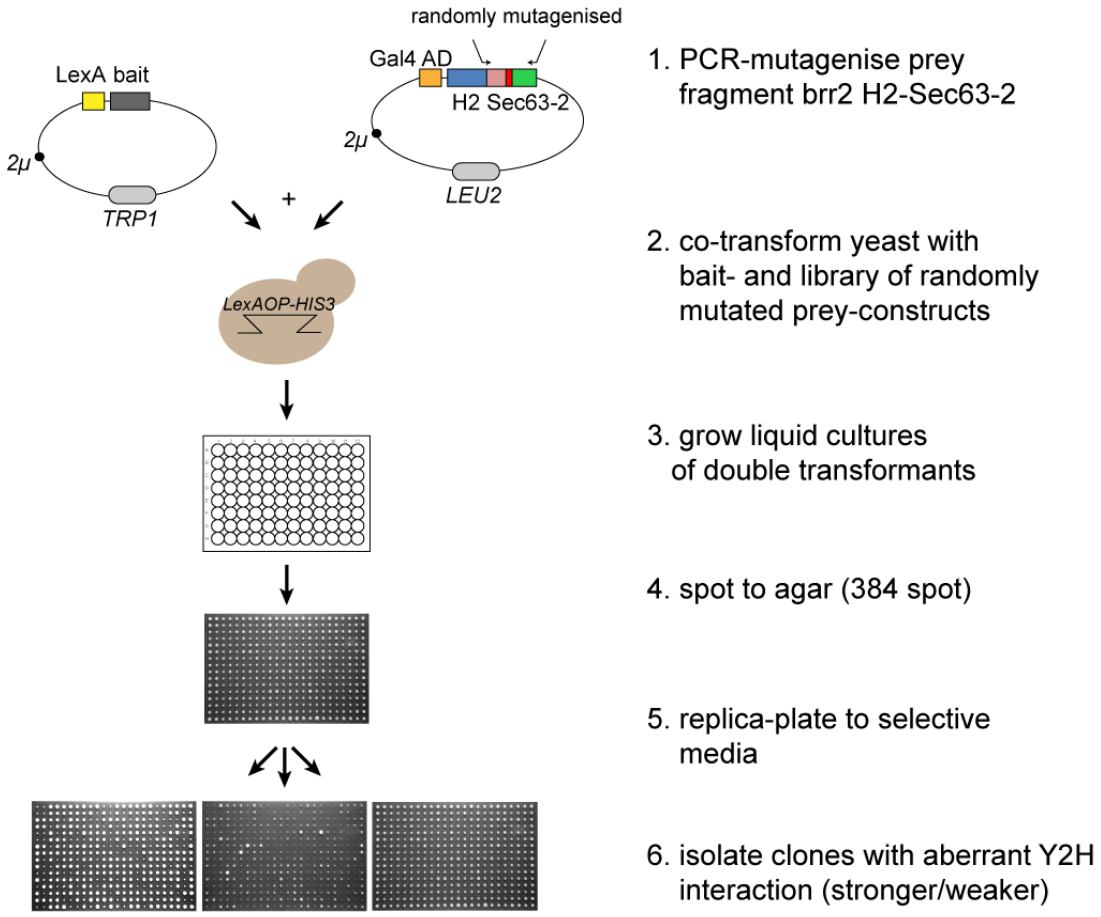

Figure 3.1 Customised Y2H screen used for the identification of *brr2* Sec63-2 mutations based on changes in protein interaction. Outline of experimental procedures used, for a more detailed description see sections 2.9.9 and 2.9.9.2.

An aberrant protein-protein interaction can manifest itself in different ways. An originally stable protein interaction can be destabilised or abolished. On the other hand a protein interaction can become abnormally stable. The Y2H interactions between two proteins should reflect these changes and hence allow identification of mutants.
Initially, several reagents were generated and their suitability verified.

3.3.1 Cloning and testing of Y2H constructs

The C-terminal domains of Brr2 have been reported to interact with the RNA helicases Prp2 and Prp16 [12]. In contrast to the previously described interactions, here a slightly different Brr2 prey construct was used. It consisted of a short N-terminal region (aa 1-113), which is thought to contain the nuclear localisation domain of Brr2, connected to the C-terminal helicase and Sec63 domains (aa 1308-2163). Hereafter, this construct will be referred to as brr2 H2-Sec63-2 (Fig. 3.2 A).

Using standard or In-Fusion cloning I generated Y2H fusion-constructs (2.11.9). brr2 H2-Sec63-2 was cloned into pACTII stop to form a Gal4-AD fusion protein. To create LexA-fusions the full length open reading frames of *PRP2* and *PRP16* were cloned into the pBTM116 bait vector. The Y2H constructs and appropriate controls were transformed into the yeast strain L40ΔG and the Y2H interactions of brr2 H2-Sec63-2 with Prp2 and Prp16 were tested (2.9.9) (Fig. 3.2 B + C). The negative controls, which expressed only one complete Y2H fusion-construct showed no growth in the absence of histidine, confirming that neither the Gal4-AD nor the LexA fusion constructs caused auto-activation of the reporter gene (Fig. 3.2 B).

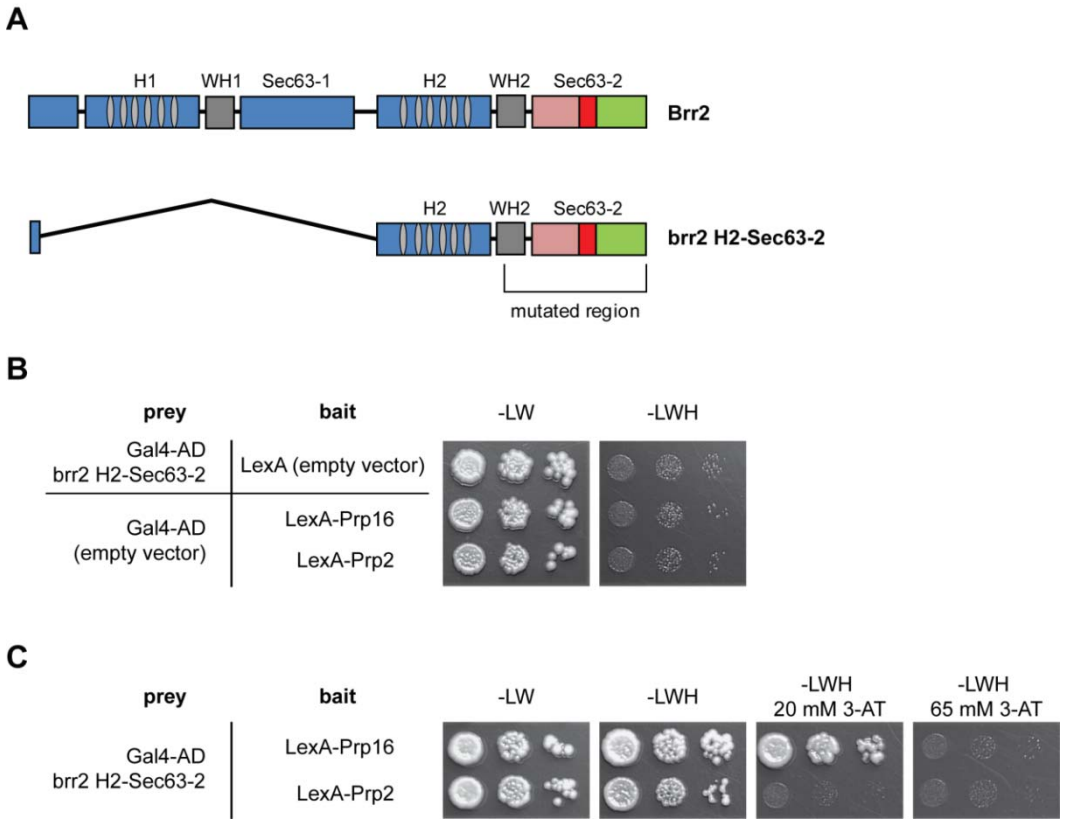

Figure 3.2 Prp16 and Prp2 interact with the C-terminal domains of Brr2 in Y2H assays. **(A)** Schematic representation of Brr2 (top) and the brr2 H2-Sec63-2 construct (bottom). **(B+C)** Pair-wise Y2H interaction tests using the Gal4-AD brr2 H2-Sec63-2 prey construct and the spliceosomal RNA helicases Prp2 and Prp16 fused to LexA as bait. Presence of bait and prey plasmids was controlled by selection on SD -LW medium. Interaction was tested in the absence of histidine by plating cells on SD -LWH medium; the presence of 3-AT increased the stringency for interaction testing (see 2.9.9). **(B)** Controls expressing only one complete Y2H construct. **(C)** Comparison of the Y2H interactions between brr2 H2-Sec63-2 and Prp2 and Prp16, respectively.

As expected, interactions between brr2 H2-Sec63-2 and Prp2 and Prp16, respectively, were confirmed by the pair-wise Y2H tests (Fig. 3.2 C). The interaction between brr2 H2-Sec63-2 and Prp16 was stronger compared to that with Prp2, as growth was supported in the presence of higher concentrations of 3-AT. The setup of these pair-wise Y2H interactions formed the basis for the screen outlined above.

3.3.2 Construction of a randomly mutated Y2H prey library

I used a combined Error prone / Megaprimer PCR approach to construct a library of Y2H brr2 H2-Sec63-2 prey constructs (a detailed description of experimental procedures is given in section 2.11.11). Residues 1762-2163 (corresponding to full-length Brr2) were subjected to random mutagenesis, encompassing most of the WH2 and the full Sec63-2 domain (Fig. 3.2 A). The conditions employed during Error prone PCR were optimised to result in 1-2 coding mutations per product. Ultra competent *E. coli* were transformed with PCR products and resulted in a total of ~ 38,000 clones. All cones were pooled and plasmid DNA extracted to create a library. In order to determine the error rate of Y2H constructs within the library, I randomly selected 50 individual clones, isolated plasmid DNA and sequenced the region previously subjected to mutagenesis. Sequence analysis revealed a mean number of 2.9 mutations per construct. In contrast the mean number of coding mutations (mutations causing an amino acid exchange) per construct was determined as 1.7.

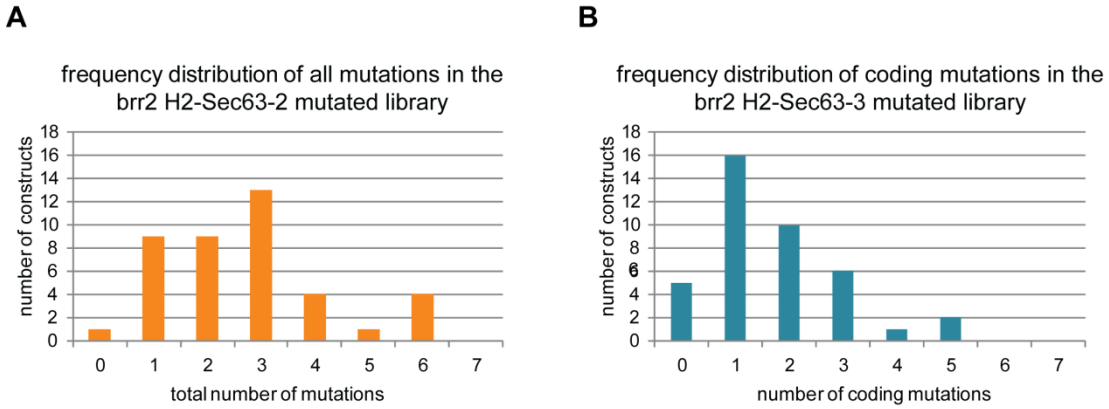

Figure 3.3 Analysis of randomly mutated brr2 H2-Sec63-2 prey library. Plasmids recovered from 50 randomly selected clones were sequenced to identify the number of mutations generated by the Error Prone PCR. **(A)** Number of mutations identified per construct (considering all nt exchanges). **(B)** Number of coding mutations (considering only mutations which cause aa exchanges) obtained per construct.

I investigated the frequency distribution of mutations (considering all nt exchanges) and coding mutations only, to find out what number of mutations per construct is found most commonly (Fig. 3.3 A, B). Constructs with one coding mutation were found most frequently, clones with two coding mutations were second most abundant. Thus, the generated library fulfilled the requirements and was used for the Y2H screen.

3.3.3 Selection of brr2 H2-Sec63-2 mutants with altered Y2H interactions

I carried out two independent screens in which either Prp16 or Prp2 was used as bait. As outlined in Fig. 3.1 yeast was co-transformed with the bait construct and the library of mutant brr2 H2-Sec63-2 prey constructs. To screen for brr2 C-terminus mutants that display interaction defects Y2H tests were performed. Here, yeast growth assays on agar plates were carried out in a 384-sample format (2.9.9.2). This allowed for a higher throughput of clones and greater spotting accuracy. The growth pattern observed in the presence of non-mutated brr2 H2-Sec63-2 served as standard to which mutants were compared. I defined conditions to select mutants with two different phenotypes (Fig. 3.4):

→ Mutants exhibiting a stronger Y2H interaction grew well in the presence of inhibitor concentrations which significantly impaired growth of the WT (≤ 65 mM 3-AT for Prp16; ≤ 20 mM 3-AT for Prp2).

→ Mutants with a weaker Y2H interaction phenotype failed to grow at the selective condition (absence of histidine) at 30°C. Lowering the temperature to 14°C restored growth, indicating a substantially weakened yet functional Y2H interaction. The selection of mutants that retained a minimal interaction prevented a preferential selection of mutants with globally mis-folded and non-functional Sec63-2 domains, e.g. due to multiple substitutions or premature termination codons.

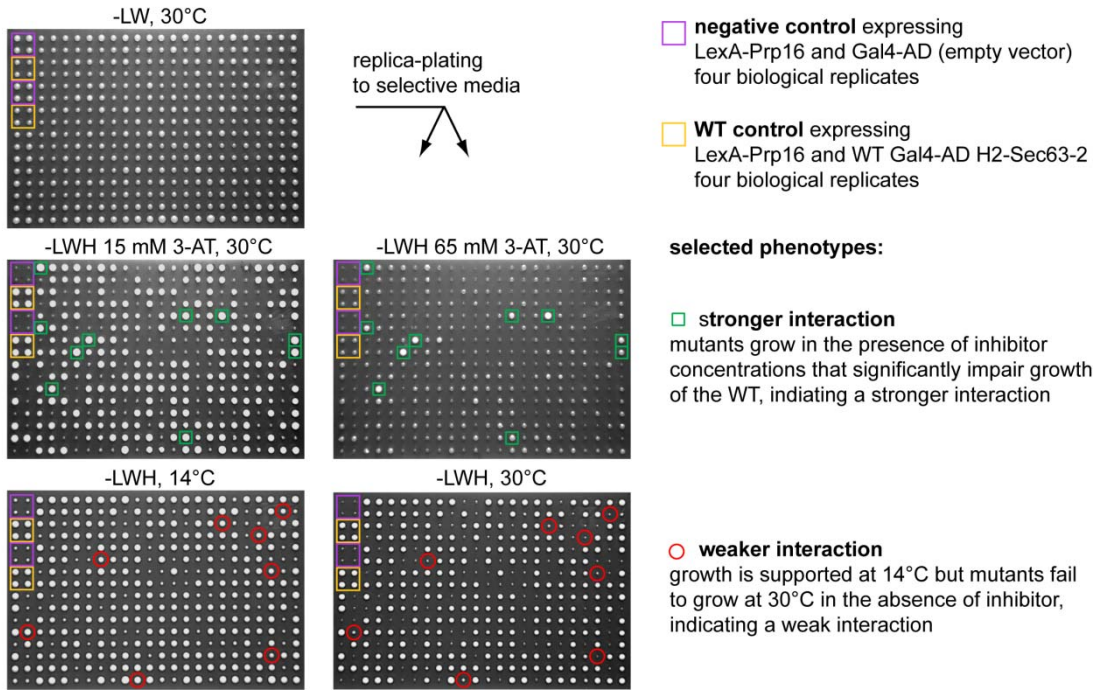

Figure 3.4 Selection of mutants causing weaker or stronger Y2H interactions. Two mutant phenotypes were selected based on their growth properties on selective media. Screens with Prp16 and Prp2 baits were carried out consecutively (the images shown serve as an example). A library of *brr2* H2-Sec63-2 two-hybrid constructs, randomly mutated across the Sec63-2 domain was co-transformed with the bait. Transformants were spotted to a master-plate, then replica-plated onto selective media. Mutations with stronger Y2H interactions exhibit resistance to higher concentrations of 3-AT than the WT. Mutations causing weaker Y2H interactions display a loss of growth in the absence of histidine at 30°C, but not at 14°C.

Clones exhibiting these growth patterns were picked from 384 spot plates. Y2H tests were repeated manually to reproduce the previously observed growth phenotype. The WH2 and Sec63-2 region of the prey constructs was PCR amplified and sequenced in order to identify the mutation(s) causing the phenotype (2.11.10; 2.11.12).

If sequencing identified one or two coding mutations the prey plasmid was rescued, re-transformed and the Y2H interaction was tested once more. This additional control served to ensure that the Y2H interaction phenotype was indeed caused by the mutation(s) in brr2 H2-Sec63-2, rather than by spontaneous changes affecting cell fitness and viability (2.11.2).

Additionally, I verified the molecular weight and equal expression-levels of bait- and prey- constructs by Western Blotting (Fig. 3.5).

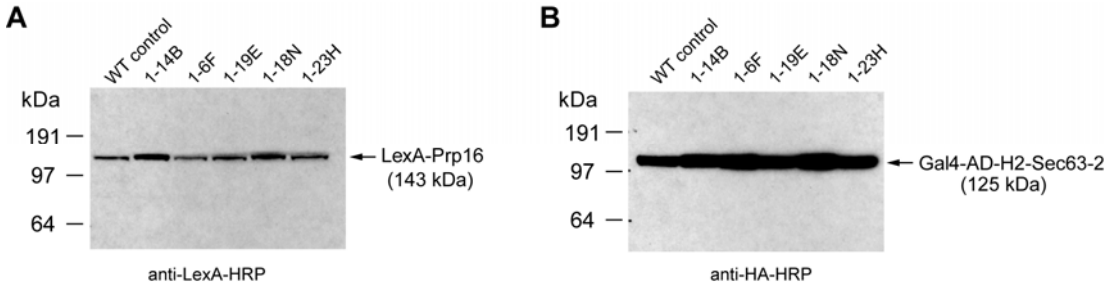

Figure 3.5 Western blotting confirms uniform expression level and expected molecular weight of Y2H constructs in isolated mutants. Representative example of a Western blot used to control expression level and molecular weight. Indicated clones were grown over night to stationary phase. Total protein was prepared from 3 OD_{600} of yeast cells, and was analysed by SDS PAGE and Western blotting. **(A)** The LexA-Prp16 bait was detected with the help of an anti-LexA-HRP monoclonal antibody. **(B)** The same membrane was stripped and reprobed. The Gal4-AD H2-Sec63-2 constructs could be detected using an anti-HA-HRP antibody (the Gal4-AD domain used here carries a 3-HA epitope tag at its C-terminus).

From approximately 4000 clones that were tested, 272 were selected and their phenotypes confirmed. With the Prp16 bait, 36 mutants exhibited a stronger Y2H interaction and 142 mutants showed a weaker Y2H interaction. With Prp2 as bait, 22 mutants with stronger and 72 mutants with weaker Y2H interactions were selected. Only mutants with one or two amino acid substitutions were considered for further characterization; these are summarised in Table 3.1.

Separation of double mutations and testing of individual single mutations

With a number of alleles sequencing revealed two amino acid substitutions. These were grouped into alleles with two substitutions in the Sec63-2 domain or with a combination of substitutions in the WH2 and Sec63-2 domains (Table 3.1). Selected substitutions were separated (i.e. plasmids with single mutations were generated by SDM) and tested individually, to find out if they were sufficient to cause the observed Y2H interaction defect.

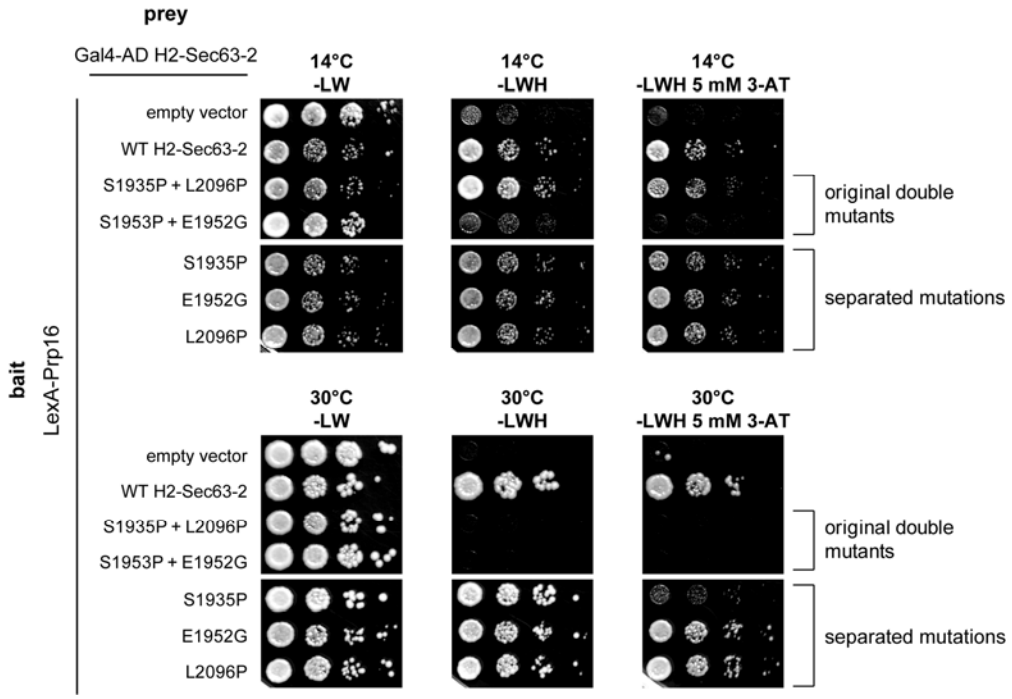

Figure 3.6 Separation of double mutations and testing Y2H interactions of individual single mutations. Pair-wise Y2H interaction tests of LexA-Prp16 bait with indicated WT or mutant brr2 H2-Sec63-2 prey constructs. aa substitutions identified in double mutants were separated and tested individually. A summary of all alleles analysed in this way is given in Table 3.1.

In most cases a single substitution was not sufficient to cause the phenotype that was initially observed in the double mutant. An example is given in Fig. 3.6. Substitution S1935P causes loss of Y2H interaction at 30°C only in combination with either L2096P or E1952G. As separated alleles the substitutions do not affect the Y2H interactions as strongly.

Reciprocal testing of *brr2* alleles indentified with the Prp2- and Prp16-baits

To assess if mutations isolated with the help of the Prp16-bait affected the interaction with Prp2 as well, and vice versa, Y2H tests with the reciprocal baits were performed. As illustrated in Fig. 3.7 A and Table 3.1, most mutations affected the Y2H interaction with both Prp2 and Prp16 and the observed interaction phenotype (e.g. stronger or weaker Y2H interaction) was generally the same. However, few mutations affected only the interaction with either Prp2 or Prp16. In these cases the mutations had only a subtle effect.

Table 3.1 *brr2* alleles with aberrant protein-protein interaction phenotype

brr2 allele[a]	origin of allele	Y2H phenotype[b] with Prp2	Y2H phenotype[b] with Prp16	*in vivo* phenotype[c]
single aa substitution, stronger Y2H interaction				
H1855R	screen with Prp16-bait	WT	stronger	nd
R1899G		stronger	stronger	WT
S1919P		weaker	stronger	nd
K1925R		WT	stronger	WT
C1769R	screen with Prp2-bait	stronger	stronger	WT
A1973N		stronger	stronger	nd
L2120V		stronger	stronger	nd
single aa substitution, weaker Y2H interaction				
L1883P	screen with Prp16-bait	weaker	weaker	ts
L1930P		weaker	weaker	ts
A1932P		weaker	weaker	ts
L1951P		weaker	weaker	ts
I2071T		weaker	weaker	WT
I2073N		weaker	weaker	WT
S2148P		weaker	weaker	ts
S2088P	screen with Prp2-bait	weaker	WT	nd
one substitution in WH2 + one substitution in Sec63-2, weaker Y2H interaction				
Y1775C + N1972D	screen with Prp16-bait	weaker	weaker	WT
L18114I + Q1931R		weaker	weaker	ts
S1795P + S1966P		weaker	weaker	ts
D1823G + W2099R		weaker	weaker	slow growth at 37°C
R1781C + V2045D		WT	weaker	WT
L1814S + L2075S	screen with Prp2-bait	weaker	weaker	ts
T1862P + D2027G		weaker	weaker	ts
V1815I + S2148P		weaker	WT	ts
one substitution in WH2 + one substitution in Sec63-2, stronger Y2H interaction				
I1763M + V1922A	screen with Prp16-bait	WT	slightly stronger	WT
D1793G + T2132A		stronger	stronger	WT
I1763T + K1925R		nd	stronger	nd
F1802S + R1899G		nd	stronger	nd
R1781P + S2098C	screen with Prp2-bait	stronger	stronger	WT
two substitutions in Sec63-2, weaker Y2H interaction				
S1871L + C2144R	screen with Prp16-bait	nd	weaker	nd
L1951P + T2087S			weaker	nd
S1935P + L2096P			weaker	nd
S1935P + E1952G			weaker	nd
L1883F + W2099R			weaker	nd
I1843V + L1880P			weaker	nd
S1868P + C2144R			weaker	nd
L1870P + K2090E			weaker	nd
L1902P + E2006G			weaker	nd
L1965H + S1966P			weaker	nd
L2101S + N2161S			weaker	nd
E2014K + C2144R	screen with Prp2-bait	weaker	nd	nd
separation of two substitutions in Sec63-2 domain				
V1922A	created by SDM	WT	WT	WT
Q1931R		weaker	WT	WT
S1935P		weaker	weaker	WT
E1952G		WT	WT	WT
S1966D		weaker	WT	nd
N1972D		weaker	weaker	nd
V2045D		slightly stronger	weaker	WT
L2096P		WT	WT	nd
W2099R		weaker	weaker	slow growth at 37°C

Table 3.1 continued

separation of mutations in WH2 domain				
I1763M	created by SDM	nd	nd	WT
W1772A				WT
Y1779A				WT
R1781P				slow growth at 37°C
D1793G				WT
S1795P				WT
L1814I				WT
L1814S				WT
V1815I				WT
D1823G				WT
N1849A				WT
S1854A				WT
G1857A				WT
T1862P				WT

aa, amino acid; WT, wild type; ts, temperature sensitive. *Only alleles with one or two aa substitutions are listed. [a] Identified aa substitutions, the given positions correspond to full length Brr2. [b] Strength of interaction as compared to WT H2-Sec63-2 (Fig. 3.4). Weaker / stronger interactions were identified based on decreased / increased resistance to 3-AT.[c] Plasmid shuffle and growth assay of indicated aa substitutions introduced to full length *BRR2*. Serial dilutions of 5-FOA selected cells were spotted to YPDA agar and incubated at 25°C, 30°C, 18°C, or 16°C.

3.4 Location of amino acid exchanges within the Sec63-2 domain

The structure of the C-terminal Brr2 Sec63 domain has been solved recently [10, 16]. It comprises three structural domains, which are contacting each other forming a triangular arrangement (Fig. 3.7) [10, 16]. Amongst the alleles identified with aberrant Y2H interactions, substitutions were found most frequently in the N-terminal helical bundle domain (residues 1859-1990). Mutations clustered especially in the region surrounding helix α4 (Fig. 3.7 A). Multiple sequence alignments reveal a high level of conservation of the mutated residues (Fig. 3.7 A bottom), indicating a particular functional significance of this area in the Sec63-2 domain. A substitution of special interest, L1951P, was found in helix α5 and conferred weaker Y2H interactions with both Prp2 and Prp16 (Fig. 3.7 A). In the context of the Sec63-1 domain this helix is referred to as "ratchet helix". Its integrity is critical for Brr2 activity [8, 16, 17]. The ratchet helix of Sec63-1 is suggested to establish direct contact to RNA substrates.

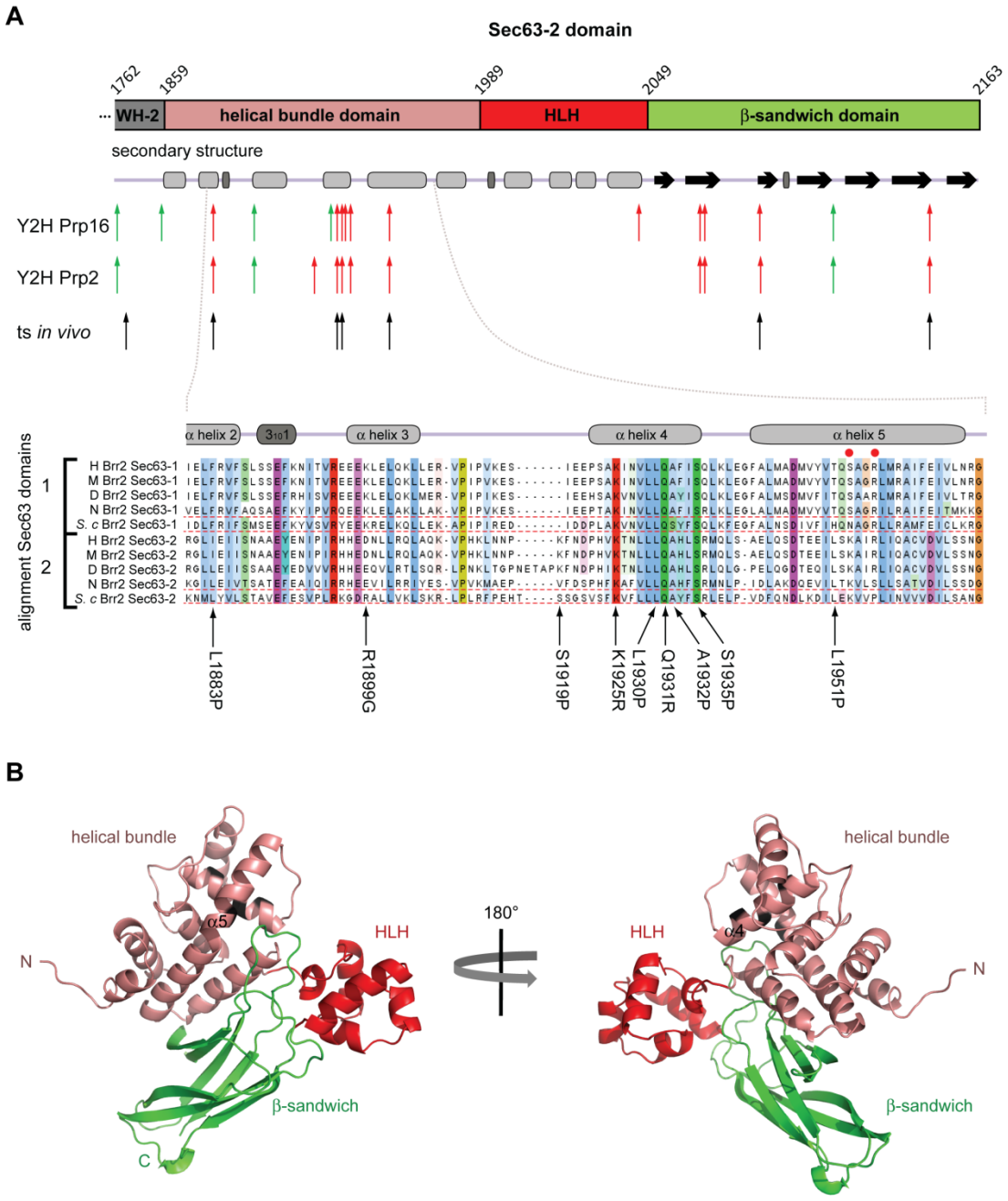

Figure 3.7 Positioning of identified single amino-acid substitutions within Sec63-2. **(A)** Schematic of the Brr2 Sec63-2 domain and its secondary structure elements. Red arrows indicate weaker, green arrows indicate stronger Y2H interactions with Prp16 and/or Prp2. Black arrows indicate substituted residues causing temperature sensitivity *in vivo* (see 3.7). **(Bottom)** Multiple sequence alignments of the indicated excerpt within the Sec63-1 and Sec63-2 domain of Brr2. H - human; M - mouse; D - *D. melanogaster*; N - *N. crassa*; *S. c.*- *S. cerevisiae*. Symbols above the alignment indicate secondary structure elements [16]. Bold colour indicates conservation. Red dots in helix α5 indicate residues of the Sec63-1 domain known to affect Brr2 function [8, 10]. **(B)** Ribbon plot of *S. cerevisiae* Brr2 Sec63-2 domain ([16], PDB ID 3IM1 P212121 form). Mutated residues in helices α4 and α5 are indicated in black. The view on the right is rotated approximately 180° compared to the view on the left.

By analogy to the helicase mechanism of the structurally related DNA helicase Hel308, the ratchet-helix was suggested to confer processivity to Brr2 [16]. Furthermore, mutations of this particular helix of the human Brr2 homologue were implicated in causing Retinitis Pigmentosa [17].
The identification of L1951P in helix α5 might suggest that this structure is functionally significant also as part of the Sec63-2 domain (see below).

Only very few alleles contained substitutions in the central helix-loop-helix domain (HLH, residues 1991-2048). The third structural domain adopts a β-sandwich fold (residues 2049-2163) (also referred to as Fibronectin 3-like structure). It is suggested to integrate the domain assembly of Sec63-2. Long loops in between β-strands link up the domain assembly and establish contacts with the helical bundle and HLH domains [16]. Substitutions identified in Y2H interaction mutants were frequently surrounded by residues known to contribute to the domain interface (e.g. W2099R and S2148P). It is thus conceivable that these particular substitutions impacted on the folding of the entire Sec63-2 domain assembly and affected the orientation adopted by the three structural domains relative to each other.

3.5 Mutations in Sec63-2 confer temperature sensitivity *in vivo*

To address whether the mutations identified by the Y2H screen described above affected the function of Brr2 *in vivo*, I tested their effects on cell growth with the help of a plasmid shuffle assay (2.9.8).

A Brr2 plasmid shuffle strain was constructed starting with a diploid W303 strain in which one genomic copy of *BRR2* was replaced with the *KanMX6* cassette [18]. Colony PCR confirmed the heterozygous deletion (2.11.10.2). Subsequently the *URA3* marked plasmid pRS316-BRR2 was introduced. Sporulation and tetrad dissection (2.9.6) allowed isolation of *brr2Δ* haploids in which growth was sustained

by the helper-plasmid (W303 brr2Δ). I constructed pRS315-BRR2 by cloning full-length *BRR2* with its natural promoter and terminator regions into an *ARS, CEN* plasmid-backbone (2.11.9.3). Subsequently I used SDM or Megaprimer PCR to generate mutant derivatives, encoding numerous *brr2* alleles (Table 2.10, 2.11.10.3, 2.11.10.4). Transformation of W303 brr2Δ with plasmids encoding wild type or mutant *BRR2* and passage over medium supplemented with 5-FOA allowed counter selection for the *URA3* marked plasmid and testing for complementation (2.9.5, 2.9.8).

In the context of the full-length protein all mutant alleles supported growth, indicating that the introduced substitutions did not alter Brr2 structure and function adversely. I tested all alleles for conditional growth defects at high and low temperatures by spot assays (2.9.7). None of the *brr2* C-terminus alleles were cold sensitive. Also, alleles that conferred a stronger interaction in the Y2H assay did not cause growth defects *in vivo*.

Of 41 *brr2* alleles tested 13 showed temperature sensitivity (Fig. 3.8 A + B). Notably, all temperature sensitive alleles presented a weakened Y2H interaction with Prp16 and Prp2. The more pronounced the reduction of the Y2H interaction of a given allele, the stronger its temperature sensitive growth defect *in vivo*. Thus, the Y2H interaction phenotype that identified theses alleles mirrored their *in vivo* growth defects (Fig. 3.8 A + B, Table 3.1, data not shown).

Several alleles contained two substitutions (Fig. 3.8 B, Table 3.1). Often a substitution in the Sec63-2 domain (aa 1858-2163) was accompanied by a substitution in the WH2 domain (aa 1750-1857) (Fig. 3.1 A). In the context of the N-terminal helicase cassette the WH1 domain is suggested to integrate the relative orientation of helicase and Sec63-1 domains via surface contacts. Substitution of hydrophobic residues at the interaction-surfaces affects cell viability and splicing [16]. The corresponding residues, which are predicted to contribute to the interaction surface between WH2, H2 and Sec63-2, were found in Y2H interaction mutants (W1772A, Y1779A, N1849A, G1857A, Table 3.1).

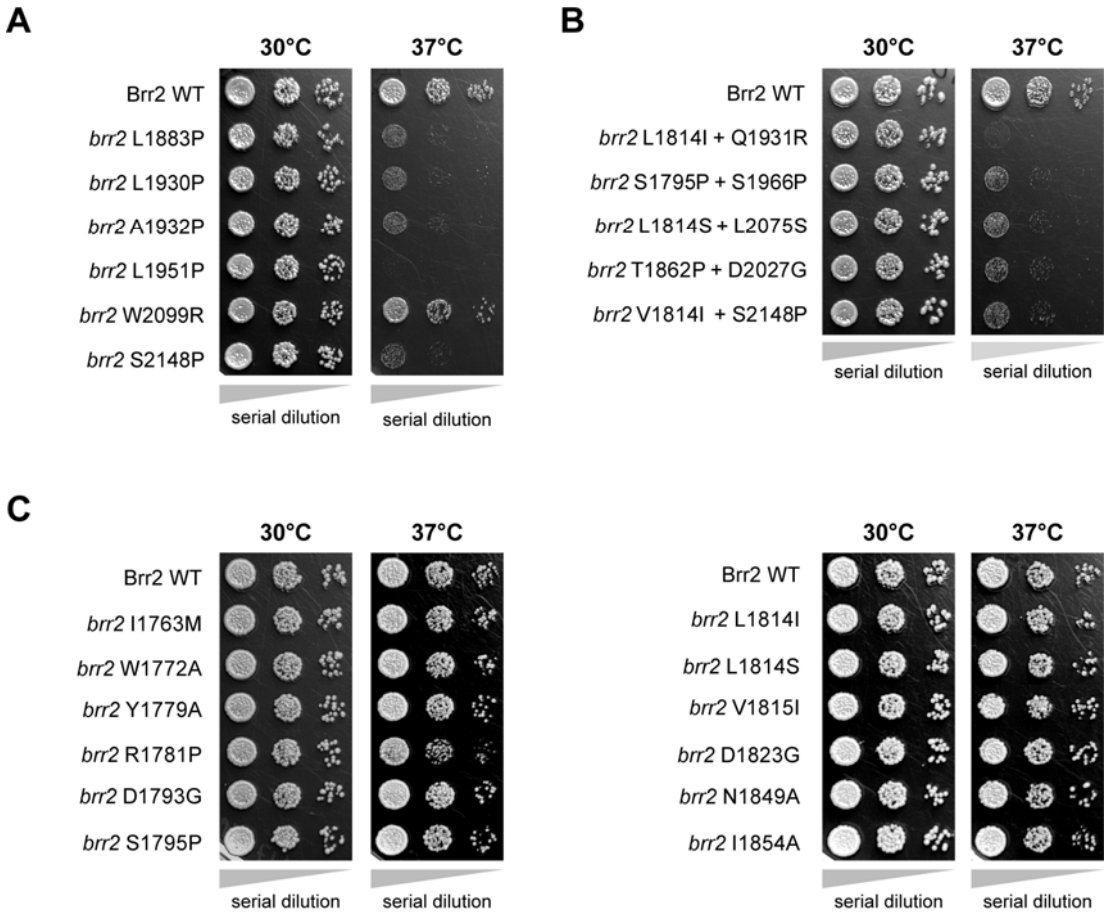

Figure 3.8 Testing for temperature sensitive growth phenotypes of *brr2* WH2 and Sec63-2 mutant alleles. W303 brr2Δ was transformed with plasmids expressing the indicated *brr2* alleles. Cultivation on 5-FOA medium evicted the helper plasmid. Thereafter cultures of all strains were grown to stationary phase and serial dilutions were spotted to YPDA medium. Plates were incubated for 2 days at the indicated temperatures. **(A)** Alleles with single aa substitutions in Sec63-2. **(B)** Alleles with double mutations in Sec63-2 and WH2. **(C)** Alleles carrying single aa substitutions in WH2. Results of all growth assays are summarised in Table 3.1.

I assessed the effect of mutations located in the WH2 domain *in vivo.* Apart from *brr2* R1781P, which displayed a mild reduction of growth at 37°C, all other substitutions in WH2 did not cause growth phenotypes (Fig. 3.8 C, Table 3.1).

3.6 Point mutations in Sec63-2 cause a splicing defect

In order to test whether the identified mutations in the C-terminal domains of Brr2 affected splicing, I selected temperature sensitive mutants, namely *brr2* L1951P and *brr2* L1815I + Q1931R and investigated the effects of temperature treatment.

To rule out that protein instability caused the growth defect, log-phase cultures carrying WT or mutant *BRR2* were shifted to the non-permissive temperature, samples were withdrawn and the Brr2 protein level was monitored by Western blotting (2.10.3, 2.10.4). Stable expression of WT and mutant Brr2, even after 4 hours (240 min) of heat treatment indicated that degradation of the mutant protein did not account for the temperature sensitive lethality (Fig. 3.9 A + B).

To monitor splicing, total RNA was prepared from a further set of samples withdrawn during the temperature shift. The abundance of pre-mRNA and mRNA of the U3 A and B transcripts was analysed by primer extensions (2.12.1.1, 2.12.9). The temperature sensitive growth of both *brr2* C-terminus mutants coincided with a splicing defect, as indicated by the accumulation of unspliced transcript observed upon shift to the non-permissive temperature (Fig. 3.9 C). Interestingly, the single aa substitution L1951P was sufficient to inhibit splicing, confirming the suspected functional importance of helix α5 in the C-terminal Sec63 domain. To assess more accurately which step of splicing was affected by the L1951P substitution I performed *in vitro* splicing assays on an *ACT1* pre-mRNA transcript (2.12.4.3; 2.12.10). *brr2* L1951P showed a general splicing defect at non-permissive temperature, as judged by the absence of splicing intermediates and mRNA (Fig. 3.9 D).

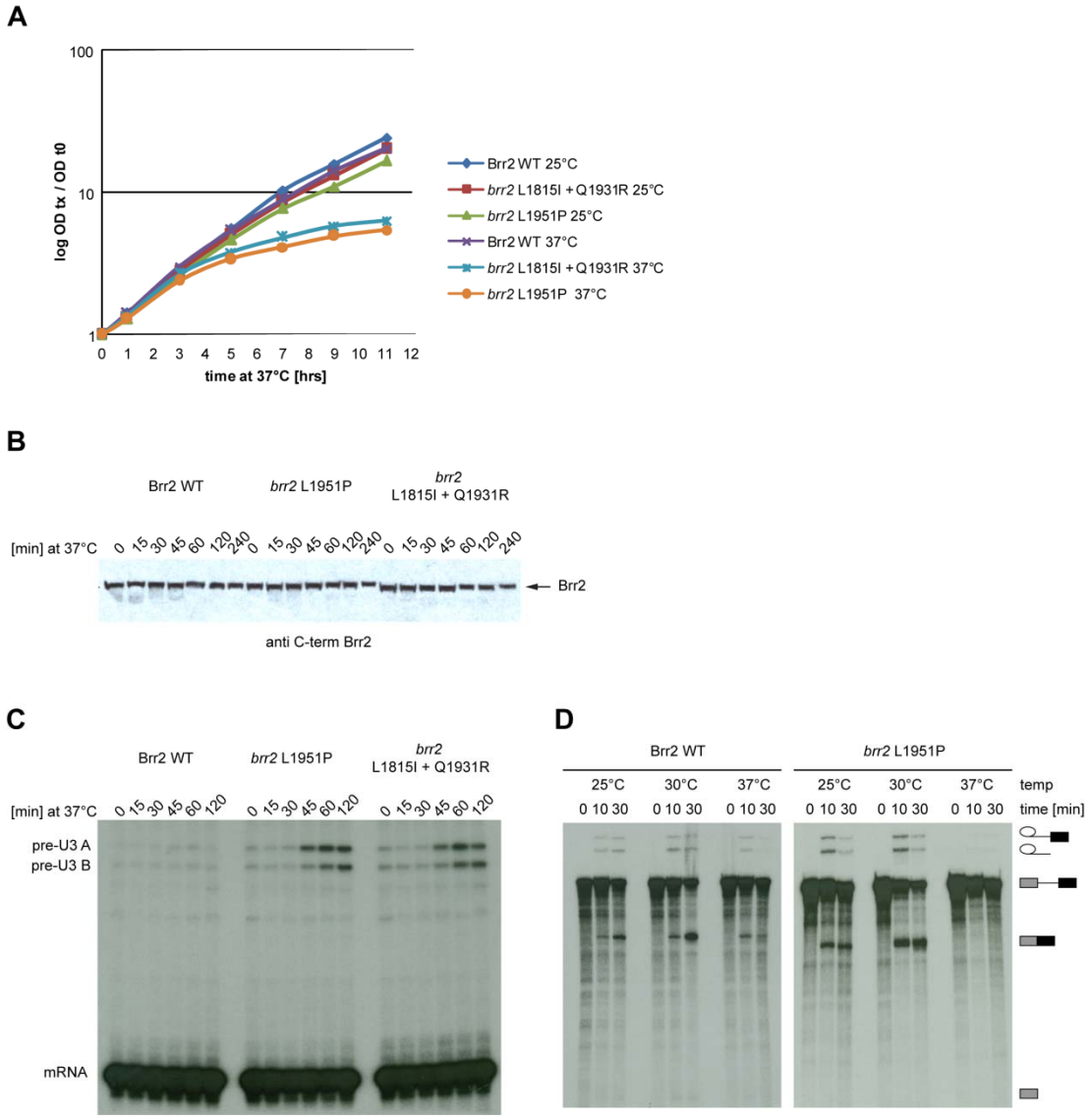

Figure 3.9 Temperature sensitive *brr2* Sec63-2 alleles exhibit splicing defect at the non-permissive condition. (A) Growth curves of WT Brr2, *brr2* L1951P and *brr2* L1815I + Q1931R. Pre-cultures were grown to log phase at 25°C, and then shifted to 37°C. Samples were withdrawn at various points during the temperature shift for subsequent RNA and protein analyses. **(B)** Protein expression levels of WT Brr2 or indicated mutants upon shift to 37°C. Total protein extracts from samples shifted to 37°C for indicated length of time were analysed by SDS PAGE and Western blotting (2.10.2; 2.10.3). Brr2 was detected using anti C-term Brr2 and anti Rabbit IgG-HRP coupled secondary antibody (Table 2.18). **(C)** *In vivo* splicing analysis of the U3 A and B transcripts by primer extension. Yeast strains expressing WT or mutant Brr2 were grown at 25°C to log-phase, and then shifted to 37°C for the indicated length of time (A). Total RNA was extracted and primer extensions performed as described in 2.12.9. **(D)** *In vitro* splicing assay of *ACT1* pre-mRNA transcript (2.12.4.3; 2.12.10). Time courses with WT and mutant extracts were performed at indicated temperatures. Migration of RNA intermediates is indicated by symbols on the right.

This suggests an inhibition of splicing prior to or at the first catalytic step, consistent with the previously suggested function of Brr2 in spliceosome activation [19]. However, this result does not rule out additional defect(s) at later stages of splicing. A defect in a component involved in spliceosome activation inhibits the splicing process as a whole and, thus, precludes the identification of defects at later stages of splicing by this assay.

3.7 Genome-wide mapping of genetic interactions of *brr2* Sec63-2 mutants

Genetic interaction mapping (GIM, [20]) is a widely used strategy for the identification of functional relationships between different factors. In an attempt to gain further insight into the potentially different effects caused by mutations in the C-terminus of Brr2 I tested two Sec63-2 mutants, *brr2* L1951P and *brr2* L1930P for genetic interactions with the complete set of non-essential gene deletion strains. A reduction in fitness of mutant combinations was measured as an increase in generation time. Both *brr2* L1930P and *brr2* L1951P, showed the strongest synthetic interactions in combination with *lin1Δ*, *snu66Δ*, or *isy1Δ* (Fig. 3.10 A).

Lin1, like Brr2, is a U5 snRNP associated protein. Since Lin1 is not present in U4/U6·U5 tri-snRNPs it was suggested to be involved in U5 snRNP biogenesis and stabilisation [21]. Conceivably, deletion of *LIN1* in conjunction with mutations in the Brr2 C-terminus lead to reduced U5 snRNP levels.

Snu66 is a U4/U6·U5 tri-snRNP specific protein. Deletion of *SNU66* or depletion of its gene product causes cold-sensitivity and inhibits splicing [12, 22, 23]. Consistent with the genetic interaction, Snu66 was found to interact with the C-terminus of Brr2 [12]. Since Snu66 is not required for tri-snRNP stabilisation [24], the synergistic interactions between *snu66Δ* and *brr2* C-terminus mutants are presumably due to a defect in spliceosome activation. Based on its interactions with various U4/U6·U5 proteins [11] Snu66 was suggested to be involved in relaying

conformational changes to the protein network of the pre-spliceosome during U4/U6 unwinding (for further discussion see Chapter 5, section 5.10.1).

Isy1 is a non-essential component of the Prp19 Complex (NTC) [25, 26]. The NTC is involved in the late stages of catalytic activation of the spliceosome, where it was suggested to affect the establishment of base-pairing interactions between snRNAs and the pre-mRNA [25]. The NTC is also part of the catalytically active spliceosome [27]. Interestingly, Isy1 is known to interact genetically with Prp16 and to affect the fidelity of 3′ splice site selection [28]. Deletion of *ISY1* exacerbated the thermo-sensitivity of several Sec63 alleles (Fig. 3.10 B). Considering that *brr2* L1930P and *brr2* L1951P show abnormal protein interactions with Prp16, it is intriguing to speculate that the C-terminus of Brr2 may also participate in regulating Prp16 during 3′ splice site selection.

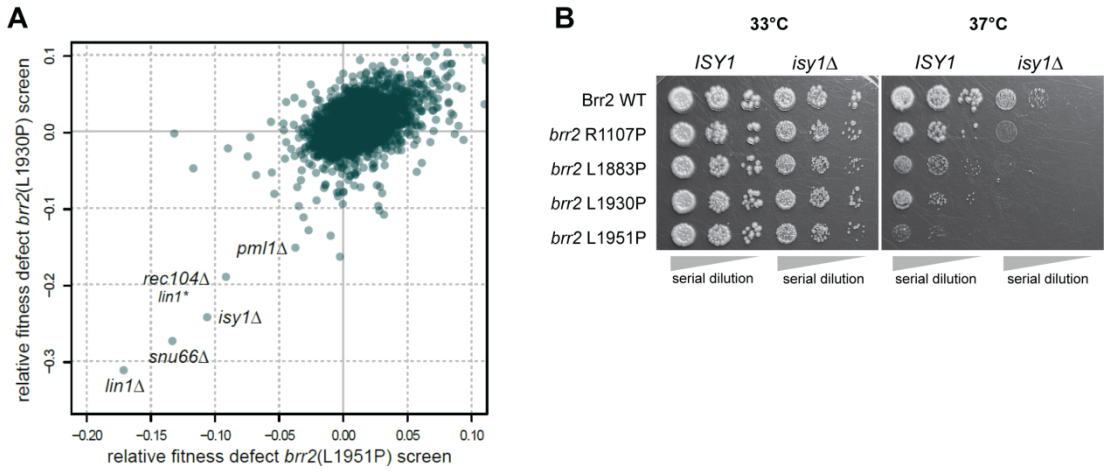

Figure 3.10 GIM screen identifies genetic interactions between *brr2* C-terminus alleles and *isy1*Δ. (A) The average values (two independent screens) for the fitness defects measured for 3864 gene deletion strains when combined with *brr2* L1930P or *brr2* L1951P as query are represented as a scatter plot [20]. Corrected fitness defects were calculated as the log2 of the ratio between the generation time for a given mutant when combined with a reference deletion and the generation time of the same mutant when combined with the query mutations. From these values, the fitness defects observed with a *brr2* (DAMP) allele were subtracted. Gene deletions that caused synthetic growth inhibition when combined with *brr2* L1930P or *brr2* L1951P have negative values and are found in the lower-left quadrant. (The *REC104* promoter region overlaps that of *LIN1* and is indicated as *lin1**). **(B)** Deletion of *ISY1* exacerbates phenotypes of *brr2* mutants. The slow-growth phenotype of substitutions in the Sec63-1 or -2 domains in combination with *isy1Δ* was confirmed on YPDA plates and increased heat sensitivity is shown at 33°C and 37°C.

The *brr2* Sec63-2 alleles also showed synthetic interactions with deletions of two other NTC components, *NTC20* and *SYF2* as well as with *ECM2*, albeit the effect on cell fitness was more subtle. *ECM2* (alternatively known as *SLT11*), encodes a factor belonging to the B^{act} complex proteins [27]. Like Brr2, it was identified in a screen searching for mutants that are synthetic lethal with U2 alleles defective in U2/U6 base-pairing [29]. A later study found that Ecm2 interacts physically and functionally with Slu7, an essential protein required for 3' ss selection (see also Chapter 5 sections 5.9 and 5.10.2) [30].

A complete list of all synthetic interactions identified is given in Table S1, which can be found on the CD accompanying this thesis. In conclusion, the genetic interactions of *brr2* Sec63-2 mutants support the known function for Brr2 in spliceosome activation, but additionally indicate a connection to factors acting during the catalytic stages of the splicing reaction.

3.8 *brr2* and *prp16* alleles interact genetically

A functional and possibly regulatory relationship between Brr2 and Prp16 should be reflected by genetic interactions of the two factors. I thus tested the viability of strains carrying wild type or mutant versions of *BRR2* and *PRP16* as the sole copy of these genes.

For this purpose W303 brr2Δ/prp16Δ, a double deletion strain was generated. Strain construction involved replacing one genomic copy of *PRP16* with the *NatNT2* cassette [31] in a diploid, heterozygous *brr2*Δ background. Growth was supported by the *URA3* marked plasmid pRS316-BRR2/PRP16, encoding wild type *BRR2* and *PRP16*. After sporulation and tetrad dissection I selected *brr2Δ/prp16*Δ haploids (W303 brr2Δ/prp16Δ). I generated pRS314-PRP16 by cloning the *PRP16* ORF including its promoter and terminator regions into pRS314 (2.11.9.3). Mutant derivatives of pRS314-PRP16 were constructed by SDM (2.11.10.3). W303

brr2Δ/prp16Δ was then co-transformed with pRS314-PRP16 and pRS315-BRR2 or mutant versions thereof, and plasmid shuffle assays were performed (2.9.8).

I chose to test conditional *prp16* mutants which carry substitutions in the functionally relevant residues of the conserved helicase motifs I, II, III and VI which compromise the specific catalytic properties that each motif conveys [32-34]: Mutations in motifs I and III affect ATP binding, substrate binding and the coordination of the ATPase and helicase activities. Substitutions in motif II and VI of Prp16 are expected to prevent ATP hydrolysis [35, 36]. *prp16*-201, *prp16*-202 and *prp16*-203 were first described as temperature sensitive alleles by Burgess & Guthrie [37]. I sequenced the coding region of these previously unmapped alleles and identified substitutions in the C-terminus of Prp16 (see legend of Table 3.2). The mutations are located in the region homologous amongst DEAH-box helicases, which is predicted to adopt a structure similar to the OB-fold described for Prp43 [38, 39]. The arrangement of the OB-fold and helicase core is critical for optimal function of DEAH-box helicases. It is thus conceivable that at high temperature *prp16-201*, *-202* and *-203* affect the domain arrangement and reduce the activity of the mutant proteins [38]. Additionally the C-terminus of Prp16 was suggested to be required for spliceosome association [32, 40].

Combinations of various temperature sensitive *brr2* Sec63-2 alleles and *prp16* mutants were tested for complementation; the results are summarized in Table 3.2. It occurred that *prp16* alleles carrying mutations in motif II and motif VI, *prp16* D473E, H476D and R686I, compromised cell viability and fitness even in combination with WT *BRR2*. Therefore, it is possible that the observed growth impairment is largely due to the expression of the defective *prp16* protein.

Co-expression of *prp16* alleles with several *brr2* Sec63-2 alleles was tolerated and generally resulted in little or no growth impairment. By contrast, deletion of the entire Sec63-2 domain resulted in more pronounced synthetic interactions. Interestingly, *brr2* Δsec63-2 affected viability and growth in an allele specific manner; especially *prp16* alleles mutated in motif VI and the C-terminus showed synthetic lethal and synthetic sick interactions.

In addition I tested two *brr2* alleles which carry mutations in the N-terminal helicase and Sec63 domain, respectively [8, 41]. While *brr2* R1107P showed mild synthetic interactions, the *rss1-1* allele showed synthetic lethality or strongly affected growth in combination with many *prp16* mutants.

Table 3.2 Genetic interactions between *brr2* and *prp16* alleles

***prp16* alleles**		***brr2* alleles**							
motif		WT	H1 (G858R) *rss1-1*	Sec63-1 R1107P	Sec63-2 Δsec63-2	Sec63-2 L1883P	Sec63-2 L1930P	Sec63-2 L1951P	Sec63-2 L1815I+ Q1931R
	Prp16 WT	+++	+++	+++	+++	+++	+++	+++	+++
I	L335F	+++	+++	+++	+++	+++	+++	+++	+++
	K379R	+++	+	+++	+++	+++	+++	+++	+++
	prp16-1	+++	-	+++	+++	+++	+++	+++	+++
II	D473E	++	+	++	++	++	++	++	++
	H476D	+	-	-	-	-	-	-	-
III	T507A	+++	+	++	+++	+++	+++	+++	+++
VI	Q686H	+++	-	++	-	+++	+++	++	+++
	R686Q	+++	-	+	-	+++	+++	++	+++
	R868I	++	-	-	-	-	-	-	-
	prp16-302	+++	+	+++	++	+++	+++	+++	+++
C-term	*prp16-201*	+++	-	+++	-	+++	+++	+++	+++
	prp16-202	+++	-	++	-	+++	+++	+++	+++
	prp16-203	+++	-	++	++	+++	+++	++	+++

Growth on medium containing 5-FOA was scored in comparison to WT after 3 days at 30°C; +++ = WT; -, synthetic lethal; *prp16-1* = Y386D; *prp16-302* = R456K + G691R; *prp16-201* = G777R; *prp16-202* = S275F + C862Y; *prp16-203* = G910R.

In conclusion, point mutations in Sec63-2 were not sufficient to cause synthetic lethality with *prp16* mutants; however more drastic changes, like deletion of the entire Sec63-2 domain, or mutating the N-terminal helicase domain of Brr2 caused synthetic interactions. Collectively these results are consistent with a functional connection between Prp16 and Brr2.

3.9 *prp16* alleles suppress the Y2H interaction defect of *brr2* H2-Sec63-2 mutants

RNA helicases that associate transiently with the spliceosome, e.g. Prp16, are released subsequent to ATP hydrolysis [42, 43]. Since the Brr2 C-terminus might be involved in the regulation of interacting helicases, I wondered whether compromising the catalytic activity of Prp16 can affect the interaction with the C-terminal domains of Brr2.

Therefore, I tested a number of functionally impaired *prp16* mutants (as described in 3.8) for their ability to interact with the C-terminal helicase module of Brr2 in pair-wise Y2H tests. Two interesting observations arose:

(1) Two alleles, *prp16-302* and *prp16* R686I, lost the ability to interact with wild type H2-Sec63-2 in the yeast two-hybrid assay (Fig. 3.11, empty ovals). Both *prp16* alleles carry mutations in motif VI. (*prp16-302* contains two mutations R456K + G691R, but G691R which lies in motif VI is sufficient to cause cold-sensitivity, however the phenotype is most severe when the two mutations are combined [28].)

(2) The interaction defect characteristic of *brr2 H2-Sec63-2* L1951P, was partially suppressed by two *prp16* alleles, which both carry a substitution in residue R686: *prp16* R686I and *prp16* R686Q (Fig. 3.11, grey ovals). While WT Prp16 did not interact with *brr2 H2-Sec63-2* L1951P, the *prp16* mutants supported growth in the presence of up to 0.2 mM 3-AT.

These observations indicate that (1) changes in the catalytic site of Prp16 can compromise its capacity to interact with H2-Sec63-2; ATP hydrolysis deficient motif VI mutants seem to be affected in particular. Furthermore, (2) the conformational change in the Sec63-2 domain caused by the L1951P mutation, which normally interferes with the interaction, can be overcome by *prp16* motif VI mutations. This might indicate that the conformational states adopted by Prp16 and the Brr2 C-terminus allow modulating the proteins' interactions.

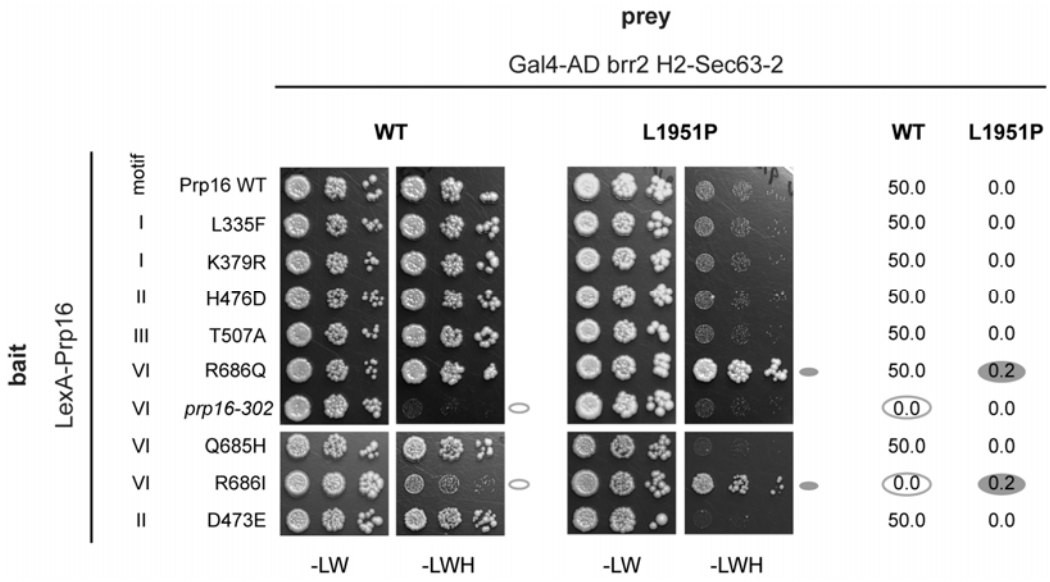

Figure 3.11 Mutations in motif VI of Prp16 partially suppress Y2H interaction defect of a *brr2* H2-Sec63-2 mutant. Direct Y2H interaction tests with the indicated *prp16* alleles (aa substitutions indicated, *prp16-302* = R456K + G691R) as bait and either WT brr2 H2-Sec63-2 or *brr2 H2-Sec63-2* L1951P as prey. Numbers to the right indicate the highest concentration [mM] of 3-AT inhibitor tolerated. Empty ovals indicate loss of Y2H interactions between WT H2-Sec63-2 and *prp16* mutants; grey ovals indicate partial suppression of the Y2H interaction defect characteristic of *brr2 H2-Sec63-2* L1951P.

3.10 Discussion

To date the precise function of the C-terminal catalytically inert helicase cassette of Brr2 is not fully understood; in particular the function of the Sec63-2

domain remains unclear. By means of a genetic screen I identified novel *brr2* alleles that carry mutations in the C-terminal Sec63 domain. The investigation of genetic interactions and the phenotypic characterisation of selected mutants provide evidence that the C-terminal domains of Brr2 exert regulation on the activity of Brr2 itself and possibly also on the activities of other spliceosomal helicases.

Structural implications: Mutations were isolated that reduced or enhanced the interaction of the C-terminal domains of Brr2 with the spliceosomal helicases Prp16 and/or Prp2 (Table 3.1). The highest incidence of mutations was found in the vicinity of helices α4 and α5 (Fig. 3.7), suggesting that this region within the Sec63-2 domain is particularly sensitive to mutagenesis. With regard to Brr2 function, helix α5 and the substitution L1951P are of special interest.

Firstly, helix α5 spans the entire length of the Sec63 domain and is thought to act as a scaffold organising the arrangement of the surrounding helices through hydrophobic interactions (Fig. 3.7 bottom) [16]. Secondly, helix α5 was recognised as a functionally important feature of the Sec63 domains in Brr2, based on structural similarity to the DNA helicase Hel308 [10, 16]. The analogous helix in Hel308 is referred to as ratchet helix, and is believed to confer helicase processivity by coupling ATPase activity and nucleic acid translocation [44]. Aromatic residues of the helix were proposed to intermittently hold on to the nucleic acid during cycles of ATP hydrolysis and conformational rearrangement. The N-terminal helicase-cassette of Brr2 was suggested to employ the same helicase mechanism utilising a ratchet helix. Mutational analyses are in agreement with this proposal [10, 16, 17]. Although the C-terminal domains of Brr2 share structural analogy with Hel308 as well, the mechanistic implications are not the same. The C-terminal helicase domain is thought to lack ATPase activity [9] and it seems unlikely that it interacts with RNA (discussed in Chapter 4). The C-terminal portion of Brr2 was thus suggested to constitute a pseudoenzyme that serves as an interaction platform [16]. But does the conserved domain architecture - including a helicase and Sec63 domain - contribute

to the specific function of the C-terminal portion of Brr2? And do the identified mutations in Sec63-2 affect the stability rather than the function of the domain?

Several observations indicate that mutations in Sec63-2 do not merely disrupt the domain (protein) organisation: (1) All mutants isolated with destabilised Y2H interactions retained a minimal interaction (Fig. 3.4). (2) Although many mutations lay in highly conserved residues, they did not necessarily disrupt protein interactions. Some mutations rendered the Y2H interaction more stable, e.g. K1925R in helix α4 (Fig. 3.5). (3) Most of the identified Sec63-2 mutations had a similar effect on the Y2H interactions with Prp2 and Prp16, however some did not (Table 3.1); again indicating that reduced interactions are presumably not resulting from global mis-folding. (4) Transferring Sec63-2 mutations into full-length *BRR2* did not affect protein stability and function adversely, since all tested alleles were viable and protein expression-levels were unaffected (Fig. 3.8, 3.9 B).

Supposedly, mutations in α4 or α5 alter the relative position of the helices. The mutations do not highlight a defined protein binding site. They rather seem to pinpoint important regulatory regions. It is conceivable that the identified mutations induce conformational changes in the conserved structural elements of the Sec63-2 domain, thereby altering its capacity to establish protein interactions. Some of the identified mutations might mimic conformational changes that occur naturally in the Brr2 C-terminus upon partner binding, constituting a conformation that is (dis)advantageous to binding of a specific interaction partner. The domain arrangement in the form of a helicase-cassette provides conformational flexibility which could contribute to the modulation of protein interactions by hiding or exposing interaction sites or by relaying regulatory signals.

Point mutations in Sec63-2 affect Brr2 function. Point mutations in Sec63-2 can cause temperature sensitivity along with a splicing defect prior to or at the first step (Fig. 3.8, 3.9). This is consistent with the suggested function for Brr2 during spliceosome activation [19]. Furthermore, it indicates that the C-terminal Sec63-2

domain is important for the functionality of the entire protein [10] and that changes within the structurally conserved parts of the Sec63-2 domain are sufficient to impair Brr2 function. The general splicing defect is also consistent with the genetic interactions between *brr2* Sec63-2 alleles and factors involved in snRNP biogenesis and spliceosome activation (Fig. 3. 10) [12, 21].

RNA analyses of splicing intermediates and products cannot determine the molecular cause of the splicing defect. One possibility is that mutations in the C-terminal Sec63 domain affect not only the interactions with Prp2 and/or Prp16, but also the interactions with other proteins. For instance the N- and C-termini of Prp8 were found to interact with Brr2 [11, 12]. Prp8 itself stably interacts with the GTPase Snu114 [45]. Both Prp8 and Snu114 are thought to regulate the activity of Brr2 [8, 10, 13, 15, 46]. Therefore, one cause of the observed splicing defect could be a failure to regulate / stimulate the activity of Brr2.

Genetic interactions support a functional connection between Brr2 and Prp16. The finding of a first step splicing defect does not rule out potential additional defect(s) at other stages of the splicing reaction. In fact results obtained by various genetic approaches support an involvement of Brr2 during the catalytic stages of splicing. Genetic interactions between *brr2* and *prp16* point towards a functional connection of the two factors (Table 3.2). *prp16* alleles mutated in motif VI or a C-terminal region corresponding to the putative OB-fold domain of Prp16 seemed most sensitive to co-expression of *brr2* mutants. Severe changes in the C-terminus of Brr2, like deletion of the Sec63-2 domain exacerbated the defects of *prp16* alleles. This is likely a result of diminished Brr2 function; deletion of the Sec63-2 domain causes loss of Brr2 ATPase activity and presumably strongly affects Brr2 protein interactions, including those with Prp8 and Snu114 [10].

Although point mutations in Sec63-2 cause splicing defects (Fig. 3.9 C + D), they were generally not sufficient to cause lethality in combination with *prp16* alleles (Table 3.2) (not considering synthetic interactions observed with *prp16*

D473E, H476D and R686I due to the strong growth defects caused by these alleles alone). The absence or mild degree of genetic interactions between *brr2* Sec63-2 and *prp16* alleles could indicate that *brr2* Sec63-2 mutations affect Brr2 regulation and thus are less penetrant than mutations that directly affect the catalytic activity of Brr2.

The observation that ATPase deficient *prp16* mutants can suppress an interaction defect induced by a mutation in the C-terminal Sec63 domain indicates that the enzymatic state or catalytic competence of Prp16 affects the interaction with the Brr2 C-terminus (Fig. 3.11). In this regard the identification of synthetic interactions between *brr2* Sec63-2 mutants and *isy1Δ* is intriguing (Fig. 3.10 A). Isy1 is thought to affect the function of Prp16 as well as the fidelity of 3' ss selection [28]. Notably, deletion of *ISY1* suppresses the defect of the cold-sensitive *prp16-302* mutant. Thus, Villa & Guthrie (2005) proposed that deletion of *ISY1* favours the premature release of Prp16 from the spliceosome, thereby promoting second-step chemistry of messages with inappropriate 3' splice sites. Consistent with this proposal, the abnormally instable interaction between Prp16 and *brr2* Sec63-2 mutants might have a similar effect. The enhanced temperature sensitivity of *brr2* Sec63 mutants in an *isy1Δ* background might result from a further destabilisation / mis-regulation of Prp16 (Fig. 3.10 B). These observations give reason to speculate that mutations in the C-terminal Sec63 domain might also affect the fidelity of splicing.

Taken together these findings support the existence of the proposed protein interaction network at the C-terminus of Brr2 [12]. Protein- and genetic interactions with different transiently associated proteins are compatible with and augment the idea of Brr2 functioning at various stages of the splicing cycle, including the Prp16-dependent steps (3.7-3.10) [12]. It is intriguing to speculate that the C-terminus of Brr2 works as a molecular sensor and switch. Subtle conformational changes within the C-terminal helicase module might be triggered by factors such as Prp8 and Snu114 which are known to affect the activity of Brr2 [8, 13, 15, 47, 48].

Furthermore, conformational rearrangements of the C-terminal domains might contribute to the sequential association and timely activation of other spliceosomal helicases, preventing premature ATP hydrolysis, RNA unwinding or RNP remodelling.

3.11 References

1. Wahl, M.C., Will, C.L. and Lührmann, R. (2009) The Spliceosome: Design Principles of a Dynamic RNP Machine. Cell. **136**, 701-718.

2. Kosowski, T.R., Keys, H.R., Quan, T.K. and Ruby, S.W. (2009) DExD/H-box Prp5 protein is in the spliceosome during most of the splicing cycle. RNA. **15**(7), 1345-62.

3. Schwer, B. and Gross, C.H. (1998) Prp22, a DExH-box RNA helicase, plays two distinct roles in yeast pre-mRNA splicing. EMBO. **17**, 2086-2094.

4. Tseng, C.K., Liu, H.L. and Cheng, S.-C. (2010) DEAH-box ATPase Prp16 has dual roles in remodeling of the spliceosome in catalytic steps. RNA. **17**(1), 145-154.

5. Koodathingal, P., Novak, T., Piccirilli, J.A. and Staley, J.P. (2010) The DEAH box ATPases Prp16 and Prp43 cooperate to proofread 5' splice site cleavage during pre-mRNA splicing. Molecular Cell. **39**(3), 385-395.

6. Pandit, S., Lynn, B. and Rymond, B.C. (2006) Inhibition of a spliceosome turnover pathway suppresses splicing defects. PNAS. **103**, 13700-13705.

7. Mayas, R.M., Maita, H. and Staley, J.P. (2006) Exon ligation is proofread by the DExD/H-box ATPase Prp22p. Nature Structural & Molecular Biology. **13**(6), 482-490.

8. Small, E.C., Leggett, S.R., Winans, A.A. and Staley, J.P. (2006) The EF-G-like GTPase Snu114p Regulates Spliceosome Dynamics Mediated by Brr2p, a DExD/H Box ATPase. Molecular Cell. **23**, 389-399.

9. Kim, H.-D. and Rossi, J. (1999) The first ATPase domain of the yeast 246-kDa protein is required for *in vivo* unwinding of the U4/U6 duplex. RNA. **5**, 959-971.

10. Zhang, L., Xu, T., Maeder, C., Bud, L.-O., Shanks, J., Nix, J., Guthrie, C., Pleiss, J.A. and Zhao, R. (2009) Structural evidence for consecutive Hel308-like modules in the spliceosomal ATPase Brr2. Nature Structural & Molecular Biology. **16**, 731-739.

11. Liu, S., Rauhut, R., Vornlocher, H.-P. and Lührmann, R. (2006) The network of protein-protein interactions within the human U4/U6.U5 tri-snRNP. RNA. **12**, 1418-1430.

12. van Nues, R. and Beggs, J.D. (2001) Functional Contacts With a Range of Splicing Proteins Suggest a Central Role for Brr2p in the Dynamic Control of the Order of Events in Spliceosomes of *Saccharomyces cerevisiae*. Genetics. **157**, 1457-1467.

13. Maeder, C., Kutach, A.K. and Guthrie, C. (2008) ATP-dependent unwinding of U4/U6 snRNAs by the Brr2 helicase requires the C terminus of Prp8. Nature Structural & Molecular Biology. **16**(1), 42-48.

14. Brow, D.A. (2009) Eye on RNA unwinding. Nature Structural & Molecular Biology. **16**(1), 7-8.

15. Kuhn, A.N., Li, Z.R. and Brow, D.A. (1999) Splicing factor Prp8 governs U4/U6 RNA unwinding during activation of the spliceosome. Molecular Cell. **3**(1), 65-75.

16. Pena, V., Mozaffari Jovin, S., Fabrizio, P., Orlowski, J., Bujnicki, J.M., Lührmann, R. and Wahl, M.C. (2009) Common Design Principles in the Spliceosomal RNA Helicase Brr2 and in the Hel308 DNA Helicase. Molecular Cell. **35**, 454-466.

17. Zhao, C., Bellur, D., Lu, S., zhao, F., Grassi, M.A., Bowne, S.J., Sullivan, L.S., Daiger, S.P., Chen, L.J., Pang, C.P., Zhao, K., Staley, J.P. and Larsson, C. (2009) Autosomal-Dominant Retinitis Pigmentosa Caused by a Mutation in *SNRNP200*, a Gene Required for Unwinding of U4/U6 snRNAs. The American Journal of Human Genetics. **85**, 617-627.

18. Longtine, M.S., McKenzie, A., 3rd, Demarini, D.J., Shah, N.G., Wach, A., Brachat, A., Philippsen, P. and Pringle, J.R. (1998) Additional modules for versatile and economical PCR-based gene deletion and modification in Saccharomyces cerevisiae. Yeast. **14**(10), 953-961.

19. Raghunathan, P.L. and Guthrie, C. (1998) RNA unwinding in U4/U6 snRNPs requires ATP hydrolysis and the DEIH-box splicing factor Brr2. Current Biology. **8**, 847-855.

20. Decourty, L., Saveanu, C., Zemam, K., Hantraye, F., Frachon, E., Rousselle, J.-C., Fromont-Racine, M. and Jacquier, A. (2008) Linking functionally related genes by sensitive and quantitative characterisation of genetic interaction profiles. PNAS. **105**(15), 5821-5826.

21. Stevens, S.W., Barta, I., Ge, H.Y., Moore, R.E., Young, M.K., Lee, T.D. and Abelson, J. (2001) Biochemical and genetic analyses of the U5, U6, and U4/U6 x U5 small nuclear ribonucleoproteins from *Saccharomyces cerevisiae*. RNA. **7**, 1543-1553.

22. Gottschalk, A., Neubauer, G., Banroques, J., Mann, M., Lührmann, R. and Fabrizio, P. (1999) Identification by mass spectrometry and functional analysis of novel proteins of the yeast [U4/U6.U5] tri.snRNP. EMBO. **18**(16), 4535-4548.

23. Stevens, S.W. and Abelson, J. (1999) Purification of the yeast U4/U6.U5 small nuclear ribonucleoprotein particle and identification of its proteins PNAS. **96**, 7226-7231.

24. Marakova, O.V., Marakov, E.M. and Lührmann, R. (2001) The 65 and 110 kDa SR-related proteins of the U4/U6.U5 tri-snRNP are essential for the assembly of mature spliceosomes. EMBO. **20**, 2553-2563.

25. Chan, S.-P., Kao, D.-I., Tsai, W.-Y. and Cheng, S.-C. (2003) The Prp19-Associated Complex in Spliceosome Activation. Science. **302**, 279-282.

26. Chan, S.-P. and Cheng, S.-C. (2005) The Prp19-associated Complex Is Required for Specifying Interactions of U5 and U6 with Pre-mRNA during Spliceosome Activation. Journal of Biological Chemistry. **280**, 31190-31199.

27. Fabrizio, P., Dannenberg, J., Dube, P., Kastner, B., Stark, H., Urlaub, H. and Lührmann, R. (2009) The Evolutionarily Conserved Core Design of the Catalytic Activation Step of the Yeast Spliceosome. Molecular Cell. **36**, 593-608.

28. Villa, T. and Guthrie, C. (2005) The Isy1p component of the NineTeen Complex interacts with the ATPase Prp16p to regulate the fidelity of pre-mRNA splicing. Genes & Development. **19**(16), 1894-1904.

29. Xu, D.M., Field, D., Tang, S.J., Moris, A. and Bobechko, B.P. (1998) Synthetic lethality of yeast slt mutations with U2 small nuclear RNA mutations suggests functional interactions between U2 and U5 snRNPs that are important for both steps of pre-mRNA splicing Molecular and Cellular Biology. **18**, 2055-2066.

30. Xu, D. and Friesen, J.D. (2000) Splicing Factor Slt11p and Its Involvement in Formation of U2/U6 Helix II in Activation of the Yeast Spliceosome. Molecular and Cellular Biology. **21**(4), 1011-1023.

31. Janke, C., Magiera, M.M., Rathfelder, N., Taxis, C., Reber, S., Maekawa, H., Moreno-Borchart, A., Doenges, G., Schwob, E., Schiebel, E. and Knop, M. (2004) A versatile toolbox for PCR-based tagging of yeast genes: new fluorescent proteins, more markers and promoter substitution cassettes. Yeast. **21**(11), 947-962.

32. Hotz, H.-R. and Schwer, B. (1998) Mutational Analysis of the Yeast DEAH Box Splicing Factor Prp16. Genetics. **149**, 807-815.

33. Schwer, B. and Guthrie, C. (1992) A Dominant negative Mutation in a Splicosomal ATPase Affects ATP Hydrolysis but Not Binding to the Splicosome. Molecular and Cellular Biology. **12**(8), 3540-3547.

34. Madhani, H.D. and Guthrie, C. (1994) Genetic interactions between the yeast RNA helicase homolog Prp16 and spliceosomal snRNAs identify candidate ligands for the Prp16 RNA-dependent ATPase. Genetics. **137**, 677-687.

35. Tanner, K.N. and Linder, P. (2001) DExD/H Box RNA Helicases: From Generic Motors to Specific Dissociation Functions. Molecular Cell. **8**, 251-262.

36. Cordin, O., Banroques, J., Tanner, K.N. and Linder, P. (2005) The DEAD-box protein family of RNA helicases. Gene. **367**, 17-37.

37. Burgess, S.M. and Guthrie, C. (1993) A Mechanism to Enhance mRNA Splicing Fidelity: The RNA-Dependent ATPase Prp16 Governs Usage of a Discard Pathway for Aberrant Lariat Intermediates. Cell. **73**, 1377-1391.

38. He, Y., Andersen, G.R. and Nielsen, K.H. (2010) Structural basis for the function of DEAH helicases. Embo Reports. **11**(3), 180-186.

39. Walbott, H., Mouffok, S., Capeyrou, R., Lebaron, S., Humbert, O., van Tilbeurgh, H., Henry, Y. and Leulliot, N. (2010) Prp43p contains a processive helicase structural architecture with a specific regulatory domain. EMBO. **29**(13), 2194-2204.

40. Wang, Y. and Guthrie, C. (1998) PRP16, a DEAH-box RNA helicase, is recruited to the splicosome primarily via its nonconserved N-terminal domain. RNA. **4**, 1216-1229.

41. Lin, J. and Rossi, J. (1996) Identification and characterization of yeast mutants that overcome an experimentally introduced block to splicing at the 3' splice site. RNA. **2**, 835-848.

42. Schwer, B. and Guthrie, C. (1991) PRP16 is an RNA-dependent ATPase that interacts transiently with the splicosome. Nature. **349**, 494-499.

43. Teigelkamp, S., McGarvey, M., Plumpton, M. and Beggs, J.D. (1994) The splicing factor PRP2, a putative RNA helicase, interacts directly with pre-mRNA. EMBO. **13**(4), 888-897.

44. Buttner, K., Nehring, S. and Hopfner, K. (2007) Structural basis for DNA duplex separation by a superfamily-2 helicase. Nature Structural & Molecular Biology. **14**, 647-652.

45. Achsel, T., Ahrens, K., Brahms, H., Teigelkamp, S. and Lührmann, R. (1998) The Human U5-220kD Protein (hPrp8) Forms a Stable RNA-Free Complex with Several U5-Specific Proteins, Including an RNA Unwindase, a Homologue of Ribosomal Elongation factor EF-2, and a Novel WD-40 Protein. Molecular and Cellular Biology. **18**(11), 6756-6766.

46. Bartels, C., Klatt, C., Luhrmann, R. and Fabrizio, P. (2002) The ribosomal translocase homologue Snu114p is involved in unwinding U4/U6 RNA during activation of the spliceosome. Embo Reports. **3**(9), 875-880.

47. Kuhn, A.N., Reichl, E.M. and Brow, D.A. (2002) Distinct domains of splicing factor Prp8 mediate different aspects of spliceosome activation. PNAS. **99**(14), 9145-9149.

48. Bellare, P., Small, E.C., Huang, X., Wohlschlegel, J.A., Staley, J.P. and Sontheimer, E.J. (2008) A role for ubiquitin in the spliceosome assembly pathway. Nature Structural & Molecular Biology. **15**(5), 444-451.

Chapter 4 – Cross-linking and cDNA analysis identifies Brr2 RNA interactions

4.1 Acknowledgement

The work described in Chapter 4 was supported by Dr. Sander Granneman who advised me on all aspects of cross-linking and cDNA library preparation. The bioinformatics analyses of high throughput sequencing data was carried out in collaboration with Dr. Grzegorz Kudla.

4.2 Introduction

Consistent with the requirement for RNA structural rearrangements in spliceosomes, DExD/H box RNA helicases play distinct and critical roles during the splicing reaction [1]. Yet, only in few cases could the precise molecular functions and the specific RNA substrates of spliceosomal helicases be determined [2, 3]. The identification of natural RNA substrates is complicated by the fact that genetic interactions are suitable to indicate functional relationships between helicase and RNA, but do not necessarily denote direct protein-RNA interactions. Also, RNA helicases lack substrate specificity *in vitro*, thus, limiting the informative value of *in vitro* assays.

For Brr2, information on possible RNA substrates was inferred from genetic and *in vitro* experiments, which suggested U4/U6 and U2/U6 helices as substrates [4-8]. As an integral U5 snRNP component Brr2 is associated with the spliceosome from assembly, throughout the catalytic phase, until disassembly. The isolation of Brr2 mutant alleles with distinct phenotypes suggests that its activity is required at several points in the splicing pathway [5, 6, 9-11]. It is therefore an immediate

question to ask: which direct RNA interactions does Brr2 establish throughout the different stages of the splicing cycle?

The unusual domain organisation of Brr2 poses another question: Which parts of Brr2 interact with RNA? As discussed in Chapter 3, the Brr2 C-terminus interacts with several proteins; however this does not preclude additional RNA interactions. Indeed, the three-dimensional organisation of Brr2 and the relative positions of the N-terminal and C-terminal helicase-cassettes remain elusive. It was suggested that the two helicase-cassettes could functionally behave like a dimer, as can be observed for oligomeric DNA helicases [12, 13]. Although it is unlikely that the C-terminal cassette hydrolyses ATP for bona fide RNA helicase activity [14], it might still bind RNA.

Answers to the foregoing questions demand the identification of the direct RNA interactions that are established by the two halves of Brr2. The use of photo-activatable nucleotides in combination with cross-linking was successfully applied to study protein-RNA interactions in the spliceosome [15-18]. However, it generally yields information only on the modified nucleotide within the RNA of choice. More recent approaches use UV cross-linking and identify direct protein-RNA interactions by sequencing. The CLIP technique (Cross-linking and immunoprecipitation) was originally developed by Darnell and colleagues [19], and is based on UV cross-linking of whole tissue samples. With the help of antibodies the protein of interest is immunoprecipitated and the covalently bound RNA can be cloned and sequenced. The method had a wide applicability and improvements and adaptations have been made since. For instance, the use of high throughput sequencing technologies now allows identification of protein-RNA interactions on a transcriptome wide scale [20-23]. Cross-linking and sequencing approaches should, thus, be suited to identify Brr2-RNA interactions.

4.3 Cross-linking and analysis of cDNA

Although CLIP could be directly applied to yeast, it would require specific antibodies directed against the protein of interest. However, in yeast epitope-tagging and the expression of modified proteins can be achieved rapidly. The TAP-tag is a widely used tool in yeast biochemistry, as it allows a tandem-affinity purification of the tagged protein [24]. A related tag, the HTP-tag (His6-TEV-Protein A, Fig. 4.1 A), offers the advantage that the second purification step can be carried out under fully denaturing conditions. Thus, a UV cross-linking and affinity purification protocol was optimised for the isolation of HTP-tagged protein-RNA complexes from yeast, and the method was named CRAC (cross-linking and analysis of cDNA) [25].

Figure 4.1 gives an overview of the procedures involved in CRAC experiments. (A detailed description of the protocol is given in section 2.12.11.) The main stages of every experiment involve, UV cross-linking of an exponentially growing yeast culture in a custom-built cross-linking apparatus. Cross-linked RNPs are purified by a two-step procedure. During the first step the Protein A moiety of the HTP tag is bound to IgG Sepharose. After TEV protease cleavage a limited RNase digestion is performed to shorten the unprotected ends of the RNA and to create an impression or "protein-footprint" on the RNA. For the second purification step the protein-RNA complex is immobilised on Ni-NTA agarose and is fully denatured to remove co-purified proteins. Several enzymatic reactions are performed consecutively to modify the RNA: Dephosphorylation of the 5′ and 3′ ends, ligation of the 3′ linker, radio-labelling and finally linker ligation at the 5′ end. Protein-RNA complexes are eluted from the beads and subjected to SDS page and Western transfer. At this stage Western blotting can be performed to monitor the success of the protein purification.

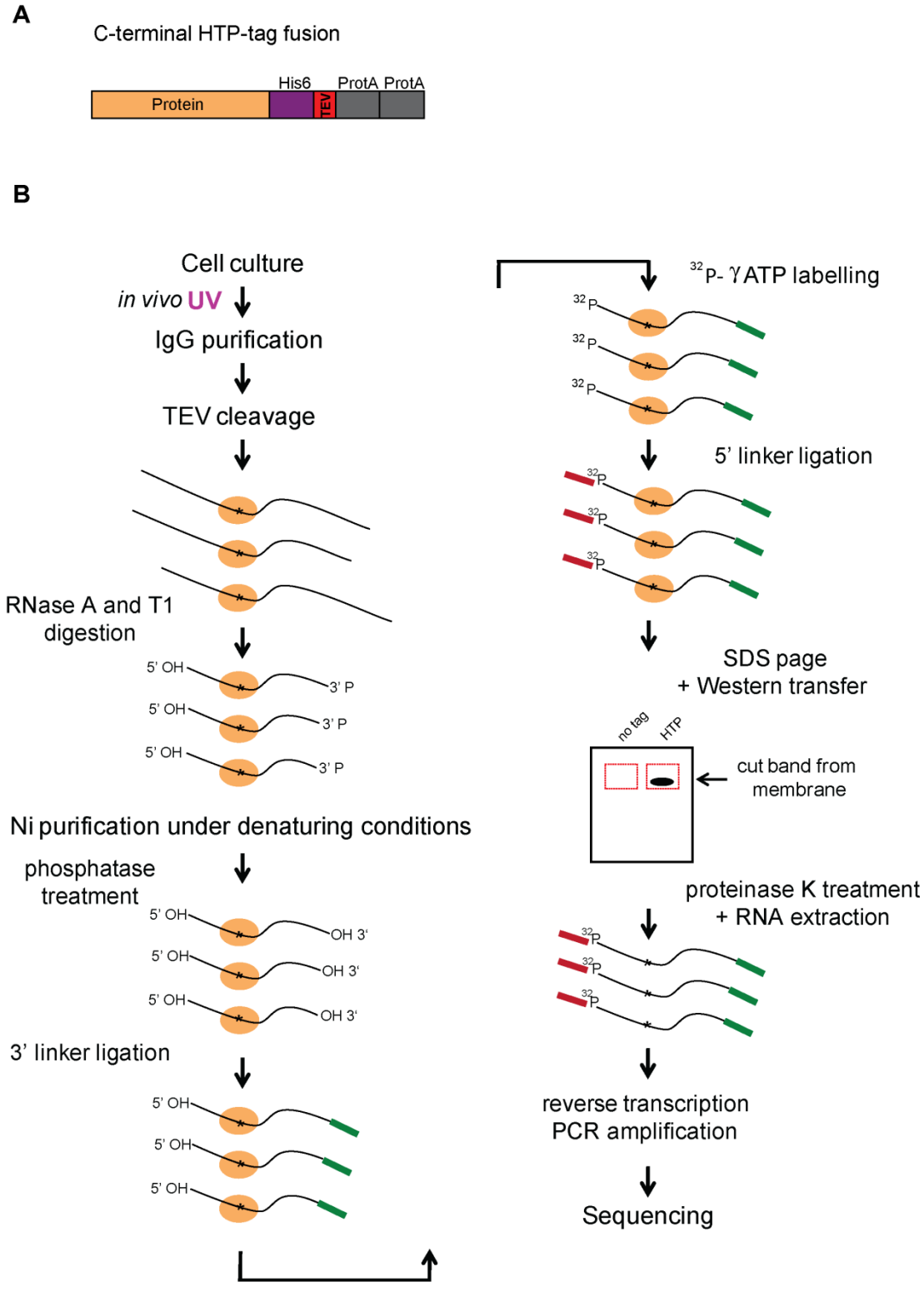

Figure 4.1 The CRAC technique. (A) Schematic showing a protein fused to the HTP-tag. **(B)** Outline of the experimental procedures and enzymatic reactions carried out during CRAC experiments.

To analyse the bound RNA, the area containing the radio-labelled protein-RNA complex is excised from the transfer membrane and the RNA is recovered by proteinase digestion. cDNA synthesis, PCR amplification of the library and sequencing complete the experiment.

4.4 The N-terminal and C-terminal portions of Brr2 complement in trans

In order to perform CRAC experiments which can distinguish RNA interactions of the N-terminal and C-terminal portions of Brr2, I generated strains in which the two halves of Brr2 were physically separated, but co-expressed. Fusing either the N-terminal or C-terminal part of Brr2 to the HTP-tag, would allow purification of the tagged part separated from the rest of the protein, and with that the identification of its RNA interactions (Fig. 4.2 A).

To facilitate this, a number of yeast expression plasmids were generated. The exact position in which the N-terminal and C-terminal Brr2 portions were separated was chosen guided by multiple sequence alignments and secondary structure prediction. These suggested that the last beta-sheet of Sec63-1 is connected to the first alpha-helix of H2 by a loop. Thus, the Brr2 fragments were separated between aa 1313 and 1314, a position that marks the middle of this loop (Fig. 4.2 A). To create a plasmid expressing the Brr2 N-terminus, a *BBR2* fragment encoding aa 1-1313 was PCR amplified and cloned into the pRS413 vector (P_{MET25}, *HIS3*, *ARS*, *CEN*), generating pRS413-brr2 N. A plasmid expressing the C-terminal half of Brr2 was produced by cloning a fragment encoding a start ATG and aa 1314-2163 into pRS413, resulting in pRS413-brr2 C. As the planned experiment required one of the Brr2 fragments to carry an affinity tag, the same *BRR2* fragments were cloned into the pRS415-HTP vector (P_{MET25}, *LEU2*, *ARS*, *CEN*), to generate C-terminally tagged HTP-fusions (pRS415-brr2 N-HTP and pRS415-brr2 C-HTP) (see Fig. 4.2). Finally,

pRS315-BRR2-HTP, which encodes a C-terminally HTP-tagged full-length Brr2, was created by integrating the HTP-tag into pRS315-BRR2 by Megaprimer PCR (2.11.10.4).

To test whether the physically separated Brr2 fragments can substitute for WT Brr2 *in vivo*, a plasmid shuffle assay was used (2.9.8). For positive controls W303 brr2Δ was transformed with constructs expressing Brr2 (non-tagged) and Brr2-HTP. Co-transformation of constructs expressing the HTP-tagged N-terminal fragment together with the non-tagged C-terminal fragment, and vice versa, gave rise to the N-HTP + C and N + C-HTP strains (Fig. 4.2 A + B). In addition, W303 brr2Δ was transformed with only the N- or C-terminal fragment; to test if either half of Brr2 is sufficient to sustain growth. Growth assays on medium containing 5-FOA showed that the two separate halves of Brr2 support growth, even if co-expressed from individual constructs (Fig. 4.2 B). This implies that the N-terminal and C-terminal fragments of Brr2 complement in trans. Consistently, the presence of only one of the Brr2 fragments was not sufficient to support growth, clearly indicating that both portions of Brr2 contribute vital functions.

In the context of full-length Brr2, mutations within alpha-helix 5, the so-called "ratchet helix", of both Sec63-1 and Sec63-2 are viable, but cause growth defects and interfere with splicing (Chapter 3) [26, 27]. I tested the consequence of introducing such mutations into the separated Brr2 fragments. I performed SDM (2.11.10.3) on the N-HTP and C-HTP constructs and placed aa substitution R1107P, L1930P or L1951P in or close to the ratchet helices of Sec63-1 and Sec63-2, respectively. Substitutions R1899G and K1925R served as controls, since they do not cause splicing defects and lie elsewhere in Sec63-2. Plasmid shuffle assays revealed that mutations within functionally important structures of the N-HTP and C-HTP fragments abrogate trans complementation (Fig. 4.2 C).

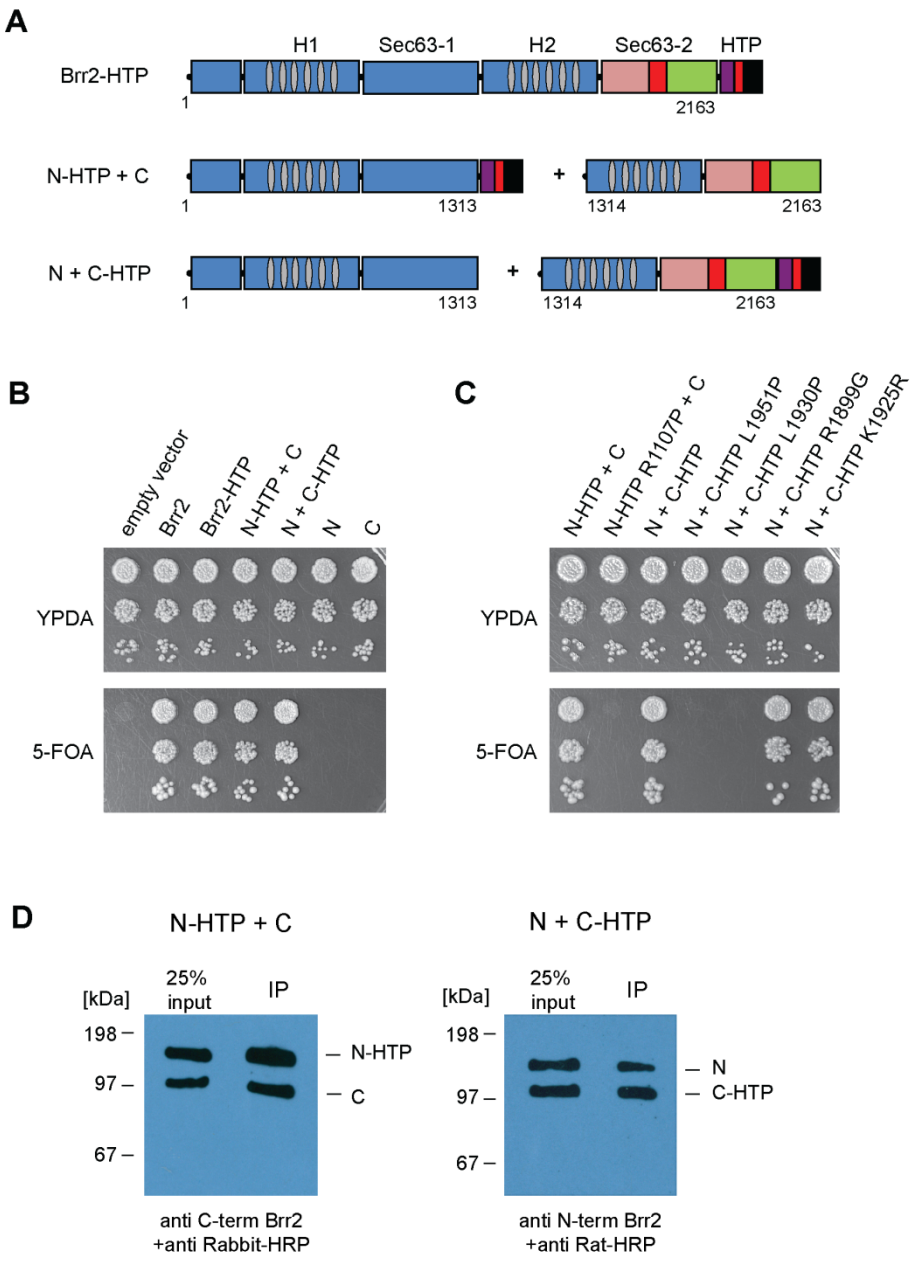

Figure 4.2 The N-terminal and C-terminal halves of Brr2 complement in trans and interact with each other. (A) Schematic representation of C-terminal HTP-fusions. Numbers indicate aa with respect to full-length Brr2 (aa 1-2163). Split Brr2 strains express the N-terminal portion of Brr2 (aa 1-1313) and the C-terminal portion (aa 1 + 1314-2163) from individual plasmids. Either the N-terminal or C-terminal fragment is HTP-tagged. **(B+C)** Plasmid shuffle assays test for viability. W303 brr2Δ was (co-)transformed with plasmids encoding the indicated proteins or protein fragments. Liquid cultures were grown to stationary phase and serial dilutions were spotted to YPDA or 5-FOA agar plates. Plates were incubated at 30°C for 2 days. **(D)** Precipitation of indicated HTP-tagged Brr2 fragments (2.10.5). Western blots were probed with antibodies raised against the N-terminus or C-terminus of Brr2 (Table 2.18) and reveal co-precipitation of the split Brr2 fragments.

This indicates that the phenotypes of mutations, which affect Brr2 function, are enhanced by the physical separation of the N-terminal and C-terminal portions of Brr2. It also implies that both halves of Brr2 must be functional to facilitate complementation.

To test whether the N-terminal and C-terminal Brr2 fragments associate with each other, pull-down assays were performed (Fig. 4.2 D). Extracts were prepared from the split Brr2 strains and the HTP-tagged fragments were precipitated with IgG Sepharose. Extensive wash steps were followed by SDS Page and Western blotting (2.10.5). In order to detect the non-tagged Brr2 fragments, Western blots were probed with antibodies that recognise different parts of Brr2. One antibody was raised against an N-terminal Brr2 peptide, and the other one was specific to a C-terminal peptide of Brr2 (Table 2.18). The Protein A moiety of the HTP-tagged fragments binds IgG, and could therefore be detected at the same time. The pull-down assays showed that the separate Brr2 fragments co-precipitated, confirming that the N-terminal and C-terminal halves of Brr2 indeed associate with each other.

The fact that the split halves of Brr2 can support growth implied that separating the protein in two fragments does not interfere with its function. Further growth assays showed that, exposing the split Brr2 strains to high or low temperatures does not affect growth-rates (Fig. 4.3 A). To test whether splicing functions normally if Brr2 is produced as two separated portions, I performed primer extension analysis of the U3 transcript to measure the abundances of pre-mRNA and mRNA (2.12.9). Strains expressing Brr2-HTP, N-HTP + C or N + C-HTP were compared to a temperature-sensitive mutant, *brr2* E909K, which is known to have a first step splicing defect at non-permissive condition [5]. Total RNA was isolated from cultures grown at 30°C, and after incubation at 37°C for 1 hour. (Fig. 4.3 B). As expected the *brr2* E909K mutant showed an accumulation of pre-mRNA. By contrast, in strains expressing Brr2-HTP, N-HTP + C and N + C-HTP no

accumulation of pre-mRNA was observed, indicating that splicing functions normally in these strains.

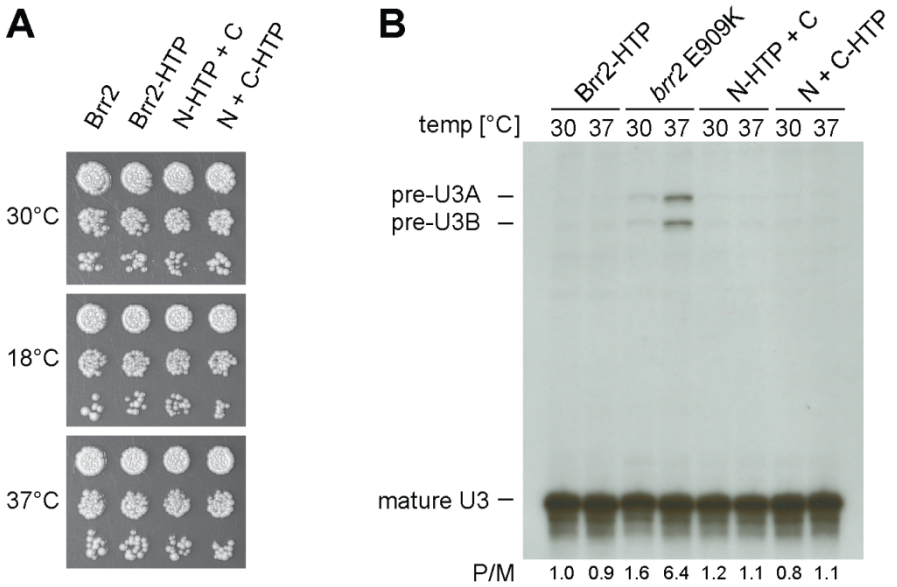

Figure 4.3 Split Brr2 strains grow at high and low temperature and do not show a splicing defect. (A) Growth assay at high and low temperatures. Strains expressing the indicated Brr2 proteins or protein fragments were grown to stationary phase. Serial dilutions were spotted to YPDA agar. Plates were incubated at indicated temperatures and photographed after 2-4 days. **(B)** Primer extension of the U3 A + B snoRNA transcripts. Exponentially growing cultures of indicated stains were incubated at 30° or 37°C for 1h before total RNA was isolated. Primer extension reactions (2.12.9) were carried out with end-labelled oligo U3 A B Exon2 (Table 2.15) and were separated on a 7% denaturing PAA gel. The heat sensitive mutant *brr2* E909K (allelic to *slt22-1* [5]) was used as positive control for a splicing defective mutant. P/M indicates the ratio between pre-mRNA and mature RNA using pre-U3 B values. Ratios were normalised such that Brr2 = 1 at 30°C.

Taken together, these observations show that the physically separated halves reconstitute normal Brr2 function and should therefore allow the analysis of Brr2 interactions with RNA.

4.5 Brr2-HTP, N-HTP and C-HTP CRAC experiments

CRAC experiments were performed with yeast strains expressing non-tagged Brr2, HTP-tagged full-length Brr2 as well as with strains expressing the split brr2 fragments with either the N-terminal or C-terminal fragment HTP-tagged.

I optimised the standard CRAC protocol for the analysis of spliceosomal proteins by amending the extract preparation and including an additional high-speed centrifugation step. This resulted in sedimentation of the heavy polysome fraction which contains a large proportion of the cells' ribosomal RNA, one of the most common contaminants in CRAC or CLIP experiments (2.12.11.1). Western blot analysis confirmed that the HTP-tagged full-length Brr2 as well as the N-terminal and C-terminal Brr2 fragments could be successfully purified by the adapted protocol (Fig. 4.4. A).

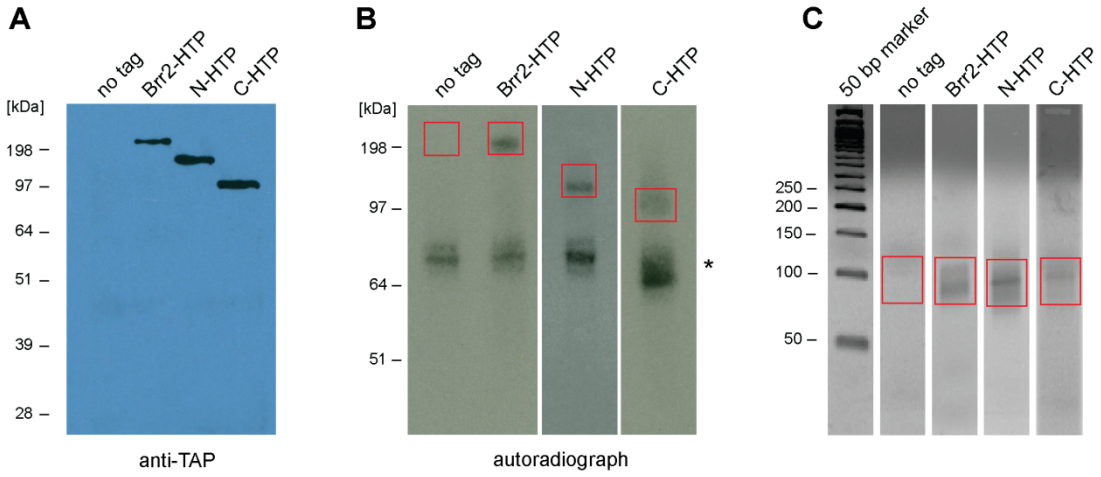

Figure 4.4 Cross-linking of full-length Brr2, N-terminal and C-terminal portions. (A) Western blot of cold (not radio-labelled) protein-RNA complexes after two-step affinity purification (as outlined in Fig. 4.1). Probing with anti-TAP antibody shows migration of tagged protein (-fragments). **(B)** Autoradiography visualises purified and radio-labelled protein-RNA complexes after two-step affinity purification and linker ligation. Red boxes indicate areas that were excised from the membrane for RNA recovery and cDNA synthesis. Asterisk marks a common contaminant approx. 80 kDa in size. SDS page for C-HTP sample was migrated further to achieve better separation. No tag control, Brr2-HTP and N-HTP show 2 hour exposures; C-HTP sample was exposed overnight. **(C)** Agarose gel electrophoresis (3%, 1xTBE) of PCR amplified cDNA libraries. Red boxes indicate areas that were excised from the gel for DNA extraction and subsequent cloning and sequencing.

After enzymatic modification the radio-labelled protein-RNA complexes were visualised by autoradiography (Fig. 4.4 B). A common contaminant of roughly 80 kDa [25] was detected in all samples. Other than that, no signal could be detected in the non-tagged control sample. For the Brr2-HTP and N-HTP samples

comparable signals were measured. The C-HTP sample co-purified less radio-labelled RNA, indicating inefficient cross-linking, but a weak signal could be visualised after overnight exposure of a high sensitivity film (Fig. 4.4 B shows 2 h exposures for Brr2-HTP and N-HTP). The indicated regions (red boxes in Fig. 4.4 B) were cut out from the membrane and cDNA libraries were prepared (Fig. 4.4 C). To assess their quality, a small fraction of each of the generated libraries was TA-cloned and analysed by Sanger sequencing. To determine whether a library is suitable for deep sequencing I surveyed parameters such as insert-length, integrity of Solexa adapter sequences, the presence and prevalence of common contaminants as well as the presence of expected RNA targets. The cDNA libraries for Brr2-HTP and N-HTP showed optimal results with insert lengths averaging around 40 nt and only a small proportion of the analysed sequences corresponded to common contaminants. By contrast, analysis of the no-tag control sample showed that the majority of all sequences mapped common contaminants (see below, 4.5).

The library generated for the C-terminal Brr2 fragment showed strong resemblance to that of the no tag control. In an attempt to cross-link and identify any specific RNA interactions of brr2 C-HTP, the experiment was repeated for a total of 5 biological replicates. In each of the experiments the recovered sequences resembled those obtained for a non-tagged control (see below, 4.5). I therefore decided to analyse only Brr2-HTP, N-HTP and no tag control samples by Solexa sequencing.

4.6 High-throughput sequencing reveals similar cross-linking pattern of Brr2-HTP and N-HTP

The bioinformatics analyses of high throughput sequencing data was carried out as described in Granneman et al. (2009). Solexa sequence reads above a certain base quality threshold were selected and the linker specific sequences were

computationally removed. The remaining sequence corresponds to the cDNA and was aligned to the yeast genome with the help of the NOVOALIGN algorithm (www.novocraft.com). The distribution of sequences along the genome could be displayed in the Affimetrix Integrated Genome Browser (www.affimetrix.com). The distribution of sequence reads, as well as substitutions and deletions in them could be plotted along the length of a particular gene or genome region with the open source software gplot (e.g. http://sourceforge.net/projects/gplot/).

For the Brr2-HTP sample a dataset of over 10 million sequence reads was obtained, out of which over 9 million sequences could be mapped to the genome. The N-HTP sample yielded a total of 9 million sequence reads, 7.5 million of which were mapped to the genome (Fig. 4.5 A + B). Sequencing of the no tag control sample resulted in less than 25 thousand reads. Unfortunately, the poor base quality of the sequencing reads interfered with their alignment to the genome. Presumably, the Solexa sequencing reaction was impaired, due to the low DNA concentration of the purified library. Low-throughput sequence data obtained during the initial quality testing showed a similar distribution of identified RNAs as compared to the high-throughput data. Therefore, sequences obtained by low-throughput sequencing are used to represent the RNAs associated with the no tag control (159 sequences) and the C-HTP sample (193 sequences) (Fig. 4.5 C + D).

The no tag and C-HTP samples showed a similar composition (Fig. 4.5 C + D). They both comprised large proportions of rRNA and tRNA sequences. Most of the hits in rRNA mapped to the 25S and 5.8S rRNAs. Due to their high abundance rRNAs and tRNAs are frequently co-purified and were previously identified as common contaminants in CRAC experiments [25, 28, 29]. Sequences assigned to the mRNA category mapped almost exclusively to highly expressed, intron-less genes. In the few cases in which sequencing reads mapped to intron-containing genes, they did not overlap the intron, indicating that they did not result from splicing related events.

Also, only a very small proportion of sequences mapped to snRNAs. Overall, this suggested that the C-terminus of Brr2 is not participating in establishing RNA interactions.

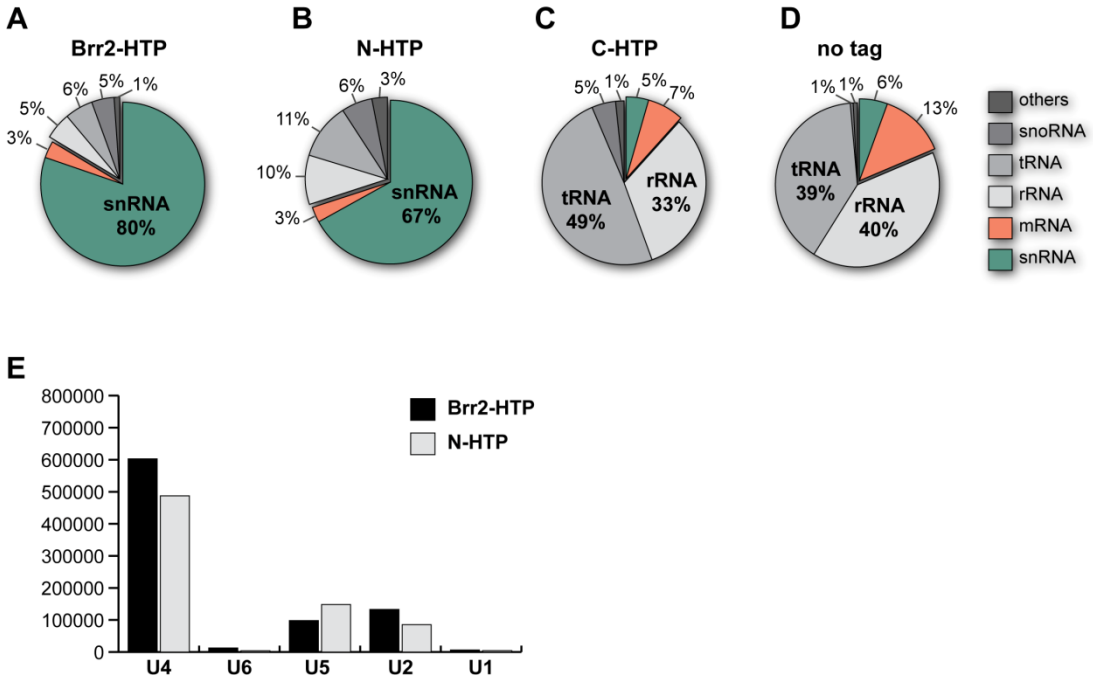

Figure 4.5 Overview of cross-linked RNAs. Summary for high-throughput **(A+B)** and low-throughput **(C+D)** sequencing data of cDNA libraries generated from RNAs cross-linked to Brr2-HTP, N-HTP, C-HTP or the no tag control sample. Sequences were matched to the genome using NOVOALIGN. Pie charts indicate the proportions of mapped reads that correspond to the different types of RNA identified in each of the samples. **(E)** Bar-diagram shows distribution of cross-links that mapped to spliceosomal snRNAs in Brr2-HTP and brr2 N-HTP datasets, respectively. Y axis indicates number of hits per 1 million sequencing reads.

By contrast, the biggest proportion of sequencing reads in the Brr2-HTP and brr2 N-HTP datasets mapped to snRNAs, highly consistent with Brr2 being a spliceosomal RNA helicase (Fig. 4.5 A + B). While the Brr2-HTP dataset contained only few contaminants, the N-HTP dataset showed a slightly larger proportion of unanticipated RNAs such as rRNAs, tRNAs and other stable RNAs, indicating a poorer signal to noise ratio.

The proportions of sequences allotted to the individual snRNAs were comparable for Brr2-HTP and N-HTP (Fig. 4.5 E). Sequences mapping to the U4 snRNA were clearly the most abundant and accounted for approx. 70% of all identified snRNAs. Notably, far fewer sequence reads were mapped to U6 snRNA, in both Brr2-HTP and N-HTP datasets. Sequences in U1 snRNA were rarer still, accounting for only 0.1% and 0.2% of all snRNA sequences in the Brr2-HTP and N-HTP datasets, respectively.

The distribution of sequences along the length of the recovered RNA indicates where the protein interacted with the RNA. The low abundance and random distribution of sequence reads along U1 (data not shown), makes it difficult to infer that they represent specific Brr2 cross-linking sites. Comparing the distribution of sequence reads along the length of the U4, U6, U5 and U2 snRNAs showed a striking similarity between the Brr2-HTP and brr2 N-HTP datasets (Fig. 4.6 A-D).

In both datasets, sequences mapped to two separate regions in the U4 snRNA, spanning nt 30-70 and nt 120-160, close to the 3' end of U4 (Fig. 4.6 A). Although hits in the U6 snRNA were less abundant, the distribution of sequence reads was reproducible between datasets. Sequences most frequently spanned nt 10-80, but showed a distinctive reduction in the signal across nt 44-48 (Fig. 4.6 B). Sequences that mapped to U5 overlapped mainly the central area of the snRNA. The most striking feature, observed in both datasets, was that roughly 50% of all sequences showed a deletion in nt U96, as indicated by the green line in Figure 4.6 C.

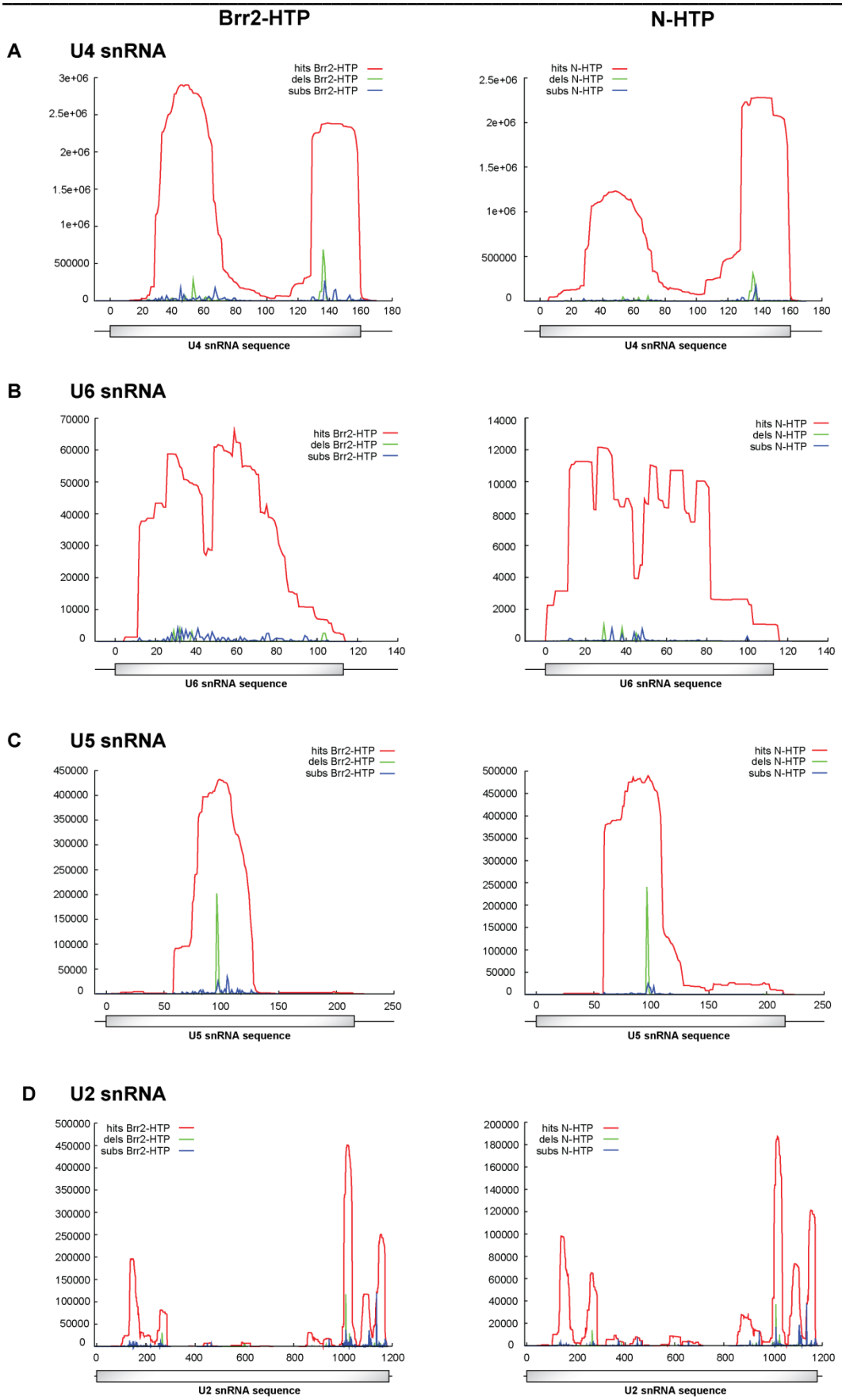
Brr2-HTP
N-HTP
A
U4 snRNA
hits Brr2-HTP
dels Brr2-HTP
subs Brr2-HTP
hits N-HTP
dels N-HTP
subs N-HTP
U4 snRNA sequence
B
U6 snRNA
U6 snRNA sequence
C
U5 snRNA
U5 snRNA sequence
D
U2 snRNA
U2 snRNA sequence

Figure 4.6 Distribution of sequencing reads in snRNAs identified by high-throughput sequence analysis of Brr2-HTP and brr2 N-HTP CRAC experiments. (A-D) The red graph represents the number of sequence reads mapped to the indicated snRNA (y axis), plotted against the snRNA sequence (x axis, numbers correspond to nt, boxes indicate the length of the snRNA, line represents 5' and 3' flanking sequences). Green line indicates the frequency of deletions, blue line the number of substitutions identified at the respective position in the snRNA sequence. Diagrams on the left show results obtained for Brr2-HTP; diagrams on the right show sequence reads of brr2 N-HTP experiment.

The accumulation of deletions and/or substitutions at a specific position can pinpoint the cross-linking site, as follows: For cDNA synthesis and library preparation RNA is released from the cross-linked protein-RNA complex by proteinase K digestion. However, at the cross-linking site, at least one amino acid remains covalently bound to the RNA. This lesion is likely to increase the mutation frequency of the reverse transcriptase, as it traverses this position [25] (Fig. 4.7).

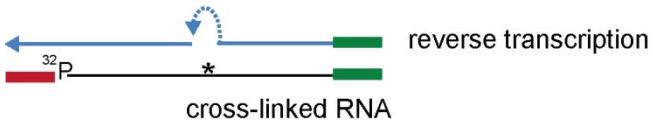

Figure 4.7 Introduction of substitutions and/or deletions at the cross-linking site. Schematic representing cDNA synthesis from cross-linked RNA. Asterisk symbolises cross-linked nucleotide which remains covalently bound to at least one amino acid after proteinase digestion. The reverse transcriptase is likely to introduce errors (dashed line) when traversing the cross-linking site.

Finally, in both datasets hits in the U2 snRNA were located in defined, well spaced out positions along the length of U2. None of the sequences mapped to the 5′ end of U2 (Fig. 4.6 D).

In conclusion these findings clearly suggest that the cross-linking patterns of full-length Brr2 and the N-terminal fragment are the same.

4.7 Discussion

The domain organisation of Brr2 is highly conserved and can be recognised in its homologues including the human U5-200K protein [4]. Taking advantage of its bipartite domain organisation, I separated the N-terminal and C-terminal portions of Brr2 and expressed them as individual polypeptides. The observation that the split fragments complemented in trans clearly illustrates the segmental design of Brr2 (Fig. 4.2 A + B). In fact, trans complementation proved robust, as C-terminal tags were tolerated on either of the fragments and splicing functioned efficiently (Fig. 4.3). Co-precipitation of the N-terminal and C-terminal fragments suggests that they associate with each other, presumably forming a complex that resembles the full-length protein (Fig. 4.2 D).

Interestingly, mutations in Sec63 domains that affect Brr2 function and cause splicing defects eliminate trans complementation (Fig. 4.2 C). Mutations in the ratchet helix of Sec63-1 (e.g. R1107P) have been suggested to impair Brr2 helicase activity and processivity, due to a failure of the mutated ratchet helix to interact with RNA [26, 27, 30]. Analogous mutations in Sec63-2 however cause abnormal protein interactions (Chapter 3). Since mutations in either of the Sec63 domains can cause lethality when introduced to the separated Brr2 fragments, it seems likely that they affect the association or "communication" of the two fragments. The C-terminal half of Brr2 was suggested to regulate the activity of Brr2, but the underlying mechanism remains unknown [7]. Hence, the split Brr2 strains could be used to study the interaction of the N-terminal and C-terminal portions further. The identification of suppressor mutations that restore viability of the split strains could give clues on the interface of the helicase-cassettes. The tagged fragments could also be used to localise the positions of the N- and C-terminal portions of Brr2 in EM projection structures of different spliceosomal particles [31].

Here, the outstanding question, which parts of Brr2 interact with RNA, was addressed by applying CRAC to the separate Brr2 fragments. The analysis of direct RNA interactions underscored the functional distinction of the N-terminal and C-terminal Brr2 portions.

The only RNAs that could be identified in association with brr2 C-HTP resembled those obtained for a negative control (Fig. 4.5 C + D). This strongly implies that the C-terminal helicase-cassette of Brr2 does not engage in specific RNA interactions *in vivo*. This result is consistent with and complements the following observations: The C-terminal helicase-cassette is devoid of ATPase activity and mutations in the conserved motives I and II of its helicase domain do not result in growth or splicing defects [14]. Although the C-terminal and N-terminal helicase cassettes are believed to possess similar overall conformations [26, 27], structural modelling predicts that the distribution of surface charges within the C-terminal cassette make it inappropriate for the interaction with RNA [26]. In conjunction with the observation that the Brr2 C-terminus engages in multiple protein-interactions (see Chapter 3), these findings suggest that the C-terminal portion of Brr2 functions solely as a protein interaction domain.

Consequently, the N-terminal portion of Brr2 should be the part of the protein that establishes all RNA interactions. The striking similarity of high-throughput sequence datasets obtained for CRAC experiments with full-length Brr2 and the N-terminal portion alone clearly supports this hypothesis (Fig. 4.5 A + B + E, Fig. 4.6). Sequence reads in snRNAs predominated in both datasets, reflecting the involvement of Brr2 and its N-terminal helicase-cassette in splicing. In particular the strong resemblance of the distribution of sequencing reads within snRNAs pointed out that the N-terminal fragment of Brr2 interacts with the same snRNAs as the full-length protein. Moreover, the positions in which substitutions and deletions occurred were virtually identical in both datasets (patterns of green and blue graphs in Fig. 4.6), indicating that brr2 N-HTP and Brr2-HTP have common cross-linking sites. The conclusions drawn from the cross-linking analyses of Brr2-HTP and

N-HTP are reinforced by the observation that the N-terminal helicase domain shares high similarity to the conserved signature motifs of DExH-box RNA helicases, and that in yeast these motifs were shown to be crucial for cell viability and Brr2 ATPase activity [10, 14].

The observation that some of the identified Brr2 interaction sites fall into poorly characterised and perhaps unanticipated regions, e.g. the 3′ ends of U4 and U2, demonstrates the applicability of this unbiased approach for the identification of Brr2-RNA interactions, as other approaches might have overlooked them. It also leads to the question whether the identified RNA interaction sites can give clues regarding the biological function(s) of Brr2. Seeking to understand the direct involvement of Brr2 in RNA rearrangements *in vivo* I characterised the identified Brr2-RNA interactions further. The functional implication of these analyses will be presented and discussed below. Cross-linking sites in U4 and U6 will be described in Chapter 5. Cross-links in U5 will be discussed in a further section of Chapter 5. Brr2 interactions with the U2 snRNA will be discussed in Chapter 6.

4.8 References

1. Wahl, M.C., Will, C.L. and Lührmann, R. (2009) The Spliceosome: Design Principles of a Dynamic RNP Machine. Cell. **136**, 701-718.

2. Schwer, B. (2008) A Conformational Rearrangement in the Spliceosome Sets the Stage for Prp22-Dependent mRNA Release. Molecular Cell. **30**, 743-754.

3. Perriman, R.J. and Ares, M. (2007) Rearrangement of competing U2 RNA helices within the spliceosome promotes multiple steps in splicing. Genes & Development. **21**(7), 811-820.

4. Laggerbauer, B., Achsel, T. and Lührmann, R. (1998) The human U5-2OOkD DEXH-box protein unwinds U4/U6 RNA duplices *in vitro*. PNAS. **95**(8), 4188-4192.

5. Xu, D.M., Nouraini, S., Field, D., Tang, S.J. and Friesen, J.D. (1996) An RNA-dependent ATPase associated with U2/U6 snRNAs in pre-mRNA splicing. Nature. **381**, 709-713.

6. Small, E.C., Leggett, S.R., Winans, A.A. and Staley, J.P. (2006) The EF-G-like GTPase Snu114p Regulates Spliceosome Dynamics Mediated by Brr2p, a DExD/H Box ATPase. Molecular Cell. **23**, 389-399.

7. Maeder, C., Kutach, A.K. and Guthrie, C. (2008) ATP-dependent unwinding of U4/U6 snRNAs by the Brr2 helicase requires the C terminus of Prp8. Nature Structural & Molecular Biology. **16**(1), 42-48.

8. Kuhn, A. and Brow, D.A. (2000) Suppressors of a Cold-Sensitive Mutation in Yeast U4 RNA Define Five Domains in the Splicing Factor Prp8 That influence Splicosome Activation. Genetics. **155**, 1667-1682.

9. Noble, S.M. and Guthrie, C. (1996) Identification of Novel Genes Required for Yeast Pre-mRNA Splicing by Means of Cold-Sensitive Mutations. Genetics. **143**, 67-80.

10. Raghunathan, P.L. and Guthrie, C. (1998) RNA unwinding in U4/U6 snRNPs requires ATP hydrolysis and the DEIH-box splicing factor Brr2. Current Biology. **8**, 847-855.

11. Lin, J. and Rossi, J. (1996) Identification and characterization of yeast mutants that overcome an experimentally introduced block to splicing at the 3' splice site. RNA. **2**, 835-848.

12. Staley, J.P. and Guthrie, C. (1998) Mechanical Devices of the Splicosome: Motors, Clocks, Springs and Things. Cell. **92**, 315-326.

13. Lohman, T.M. and Bjornson, K.P. (1996) Mechanisms of helicase-catalyzed DNA unwinding. Annual review of Biochemistry. **65**, 169-214.

14. Kim, H.-D. and Rossi, J. (1999) The first ATPase domain of the yeast 246-kDa protein is required for *in vivo* unwinding of the U4/U6 duplex. RNA. **5**, 959-971.

15. Vidal, V.P., Verdone, L., Mayers, A.E. and Beggs, J.D. (1999) Characterisation of U6 snRNA-protein interactions. RNA. **5**, 1470-1481.

16. Dix, I., Russell, C.S., O'Keefe, R.T., Newman, A.J. and Beggs, J.D. (1998) Protein-RNA interactions in the U5 snRNP of Saccharomyces cerevisiae. RNA. **4**, 1239-1250.

17. Newman, A.J., Teigelkamp, S. and Beggs, J.D. (1995) snRNA interactions at 5' and 3' splice sites monitored by photoactivated crosslinking in yeast spliceosomes. RNA. **1**, 968-980.

18. Turner, I.A., Norman, C.M., Churcher, M.J. and Newman, A.J. (2006) Dissection of Prp8 protein defines multiple interactions with crucial RNA sequences in the catalytic core of the spliceosome. RNA. **12**(3), 375-386.

19. Ule, J., Jensen, K., Ruggiu, M., Mele, A., Ule, A. and Darnell, R.B. (2003) CLIP identifies Nova-regulated RNA networks in the brain. Science. **302**, 1212-1215.

20. Ule, J., Jensen, K., Mele, A. and Darnell, R.B. (2005) CLIP: a method for identifying protein-RNA interaction sites in living cells. Methods. **37**, 376-386.

21. Konig, J., Zarnack, K., Rot, G., Curk, T., Kayikci, M., Zupan, B., Turner, D.J., Luscombe, N.M. and Ule, J. (2010) iCLIP - Transcriptome-wide Mapping of Protein-RNA Interactions with Individual Nucleotide Resolution. J Vis Exp. **50**, 2638.

22. Licatalosi, D.D., Mele, A., Fak, J.J., Ule, J., Kayikci, M., Chi, S.W., Clark, T.A., Schweitzer, A.C., Blume, J.E., Wang, X., Darnell, J.C. and Darnell, R.B. (2008) HITS-CLIP yields genome-wide insights into brain alternative RNA processing. Nature. **456**, 464-469.

23. Hafner, M., Landthaler, M., Burger, L., Khorshid, M., Hausser, J., Berninger, P., Rothballer, A., Ascano, M., Jungkamp, A.C., Munschauer, M., Ulrich, A., Wardle, G.S., Dewell, S., Zavolan, M. and Tuschl, T. (2010) PAR-CliP--a method to identify transcriptome-wide the binding sites of RNA binding proteins. J Vis Exp. **41**, pii: 2034.

24. Rigaut, G., Shevchenko, A., Rutz, B., Wilm, M., Mann, M. and Seraphin, B. (1999) A generic protein purification method for protein complex characterization and proteome exploration. Nature. **17**, 1030-1032.

25. Granneman, S., Kudla, G., Petfalski, E. and Tollervey, D. (2009) Identification of protein binding sites on U3 snoRNA and pre-rRNA by UV cross-linking and high-throughput analysis of cDNAs. PNAS. **106**(24), 9613-9618.

26. Pena, V., Mozaffari Jovin, S., Fabrizio, P., Orlowski, J., Bujnicki, J.M., Lührmann, R. and Wahl, M.C. (2009) Common Design Principles in the Spliceosomal RNA Helicase Brr2 and in the Hel308 DNA Helicase. Molecular Cell. **35**, 454-466.

27. Zhang, L., Xu, T., Maeder, C., Bud, L.-O., Shanks, J., Nix, J., Guthrie, C., Pleiss, J.A. and Zhao, R. (2009) Structural evidence for consecutive Hel308-like modules in the spliceosomal ATPase Brr2. Nature Structural & Molecular Biology. **16**, 731-739.

28. Bohnsack, M.T., Martin, R., Granneman, S., Ruprecht, M., Schleiff, E. and Tollervey, D. (2009) Prp43 bound at different sites on the pre-rRNA performs distinct functions in ribosome synthesis. Molecular Cell. **36**, 583-592.

29. Woltzka, W., Kudla, G., Granneman, S. and Tollervey, D. (2011) The nuclear RNA polymerase II surveillance system targets polymerase III transcripts. EMBO. **30**(9), 1790-1803.

30. Zhao, C., Bellur, D., Lu, S., zhao, F., Grassi, M.A., Bowne, S.J., Sullivan, L.S., Daiger, S.P., Chen, L.J., Pang, C.P., Zhao, K., Staley, J.P. and Larsson, C. (2009) Autosomal-Dominant Retinitis Pigmentosa Caused by a Mutation in *SNRNP200*, a Gene Required for Unwinding of U4/U6 snRNAs. The American Journal of Human Genetics. **85**, 617-627.

31. Häcker, I., Sander, B., Golas, M.M., Wolf, E., Karagöz, E., Kastner, B., Stark, H., Fabrizio, P. and Lührmann, R. (2008) Localzation of Prp8, Brr2, Snu114 and U4/U6 proteins in the yeast tri-snRNP by electron microscopy. Nature Structural & Molecular Biology. **15**(11), 1206-1212.

Chapter 5 – Brr2 functions during catalytic activation and the second step of splicing

5.1 Introduction

The spliceosome exhibits compositional and conformational dynamics during complex assembly, catalytic activation, active site remodelling and at last during complex disassembly. As an integral component of the U5 snRNP Brr2 is present throughout the whole sequence of events. So far a requirement for Brr2 activity has been reported for only two stages of the splicing reaction.

Catalytic activation of the assembling spliceosome requires a dramatic reorganisation of RNA and protein components which results in destabilisation and release of the U1 and U4 snRNAs and formation of the catalytic centre [1]. Spliceosome activation requires Brr2 activity and many lines of evidence indicate that Brr2 dissociates the U4/U6 snRNA duplex [2-4]. The mechanism by which duplex dissociation is realised remains unknown. It is not clear in which order the two stems of the U4/U6 duplex are opened, and whether they open in a concerted or sequential manner. Without knowledge of the direct Brr2 contact sites with these RNAs the molecular mechanism for duplex unwinding is hard to make out.

Subsequent to the catalytic phase, the spliced mRNA is released and the spliceosome is actively disassembled. Staley and co-workers reported an intron release defect in the presence of *brr2* mutants [5]. Hence, Brr2 activity is thought to be required for spliceosome disassembly. In this context U2/U6 base-pairing interactions were suggested as a Brr2 substrate.

5.2 Brr2 interactions with U4 and U6 snRNAs

Natural Brr2 substrates should be represented by the RNAs that were identified in Brr2 CRAC experiments (Chapter 4). Since many studies suggested the U4/U6 duplex as a presumed Brr2 substrate, cross-links in the U4 and U6 snRNAs were anticipated. In order to explore how U4/U6 dissociation might occur I investigated where within the predicted secondary structure the Brr2 interaction sites are located.

Brr2-U4 cross-links were highly abundant and should occur either in the U4/U6·U5 tri-snRNP or during spliceosome assembly. In both configurations U4 is (initially) base-paired to U6, thus Brr2-U4 contacts are indicated in the U4/U6 structure (Fig. 5.1 A). The identified interaction regions in U4 fall into two separate parts of the snRNA. One of these regions begins in the central domain of U4, continues into the area in which U4 and U6 base-pair to form U4/U6 stem 1 and ends in the apical loop of the U4 5′ stem-loop (SL). Interestingly, in this area substitutions and deletions were dispersed (Fig. 4.6 A), suggesting that multiple interaction sites exist within this region. The second region of interaction falls into the U4 3′ SL and extends to the 3′ end of U4. Substitutions and deletions clustered in nt U138 (Fig. 4.6 A, 5.1 A), which is bulged out from the 3′ SL; a feature that likely constitutes a preferred cross-linking site. The sequencing reads identified in CRAC experiments can extend beyond the protein-RNA interaction site. If sequences overlap the same area the minimal interaction site within this area can be deduced from the shortest sequencing reads in the alignment. In the U4 3′ domain the minimal interaction region seems to be the top half of the 3′ side of the 3′ SL (approx. nt 130-142, Fig. 5.1 A).

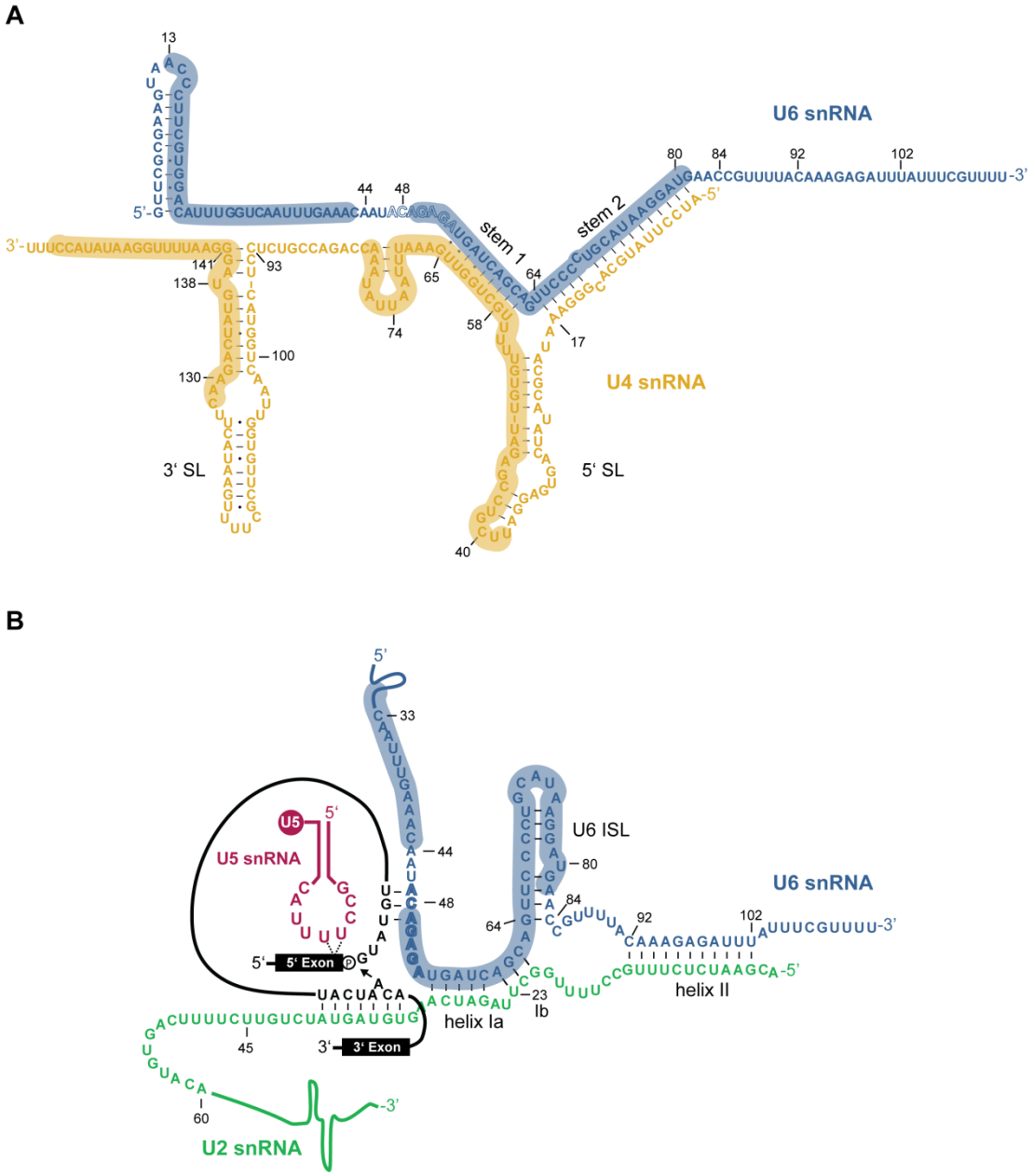

Figure 5.1 Brr2-RNA interactions in the U4 and U6 snRNAs. (A) Secondary structure of *S. cerevisiae* U4/U6 snRNA duplex according to Brow & Guthrie [6]. Shaded areas highlight Brr2-RNA interaction regions indicated by high-throughput sequencing reads obtained in CRAC experiments (Chapter 4, Fig. 4.6). **(B)** RNA-RNA interactions in the assembled spliceosome in *S. cerevisiae* prior to the first catalytic step. U6/5' ss and U2/U6 interactions are depicted according to Madhani & Guthrie [7]. Intra-molecular U6 base-pairing is shown based on Ryan & Abelson [8]. Blue shading indicates possible Brr2 interaction region in U6 (Chapter 4, Fig. 4.6). Formation of the U6 base-pairing interactions shown in B is mutually exclusive with U4/U6 stem 1 and 2.

Compared to U4, Brr2 cross-links in U6 were much rarer, which could indicate that Brr2 interacts only very transiently with U6. Interactions with U6 covered most of the snRNA, with a reduction of the signal in nt 44-48 (Fig. 4.6 B). This is in agreement with cross-linking studies based on photo-activatable cross-linkers that previously indicated a Brr2 cross-link in U6 U54 [9]. Within the U4/U6 duplex this corresponds to part of the 5' terminal SL and the central area of U6 as well as the entire region in which U6 base-pairs with U4 forming U4/U6 stems 1 and 2 (Fig. 5.1 A).

Brr2 clearly interacts with both U4 and U6 but do these interactions occur during spliceosome activation? This question is difficult to answer, in particular with regard to Brr2-U6 interactions. U6 is not only present in tri-snRNPs or pre-catalytic spliceosomes; it is also part of assembled, catalytic spliceosomes. *In vivo* cross-linking approaches do not distinguish different populations of spliceosomes; hence, it has to be considered that Brr2-U6 cross-links could occur at various points throughout the splicing cycle. Figure 6.1 B shows a schematic of the catalytic core of the activated spliceosome prior to the first transesterification reaction and where within this structure Brr2-U6 interactions could occur. The U6 snRNA is thought to undergo conformational rearrangements during the transition from the first step to the second step competent spliceosome. U6 conformations and base-paring interactions established at these stages are at present still under dispute ([10-14] and references therein).

Due to the apparent involvement of Brr2 in spliceosome activation I attempted to delineate cross-links that are established during the catalytic phase from those occurring in pre-catalytic spliceosomes. The U4 cs-1 allele hyper-stabilises U4/U6 base-pairing interactions and inhibits spliceosome activation at cold temperatures [3, 15]. It seemed like a suitable tool, for stalling spliceosomes *in vivo* before applying CRAC in order to identify Brr2-RNA interactions established under these conditions. For this purpose I generated a *BRR2,* U4 double-deletion strain by replacing one genomic copy of *snR14* (which encodes U4) with the *HphNT1* cassette

in a diploid, heterozygous *brr2*Δ background (2.9.5). Growth was supported by the *URA3* marked plasmid pRS316-BRR2/U4, harbouring wild type *BRR2* and *SNR14*. After sporulation and tetrad dissection (2.9.6) *brr2Δ*/U4Δ haploids were selected and propagated (W303 brr2Δ/U4Δ).

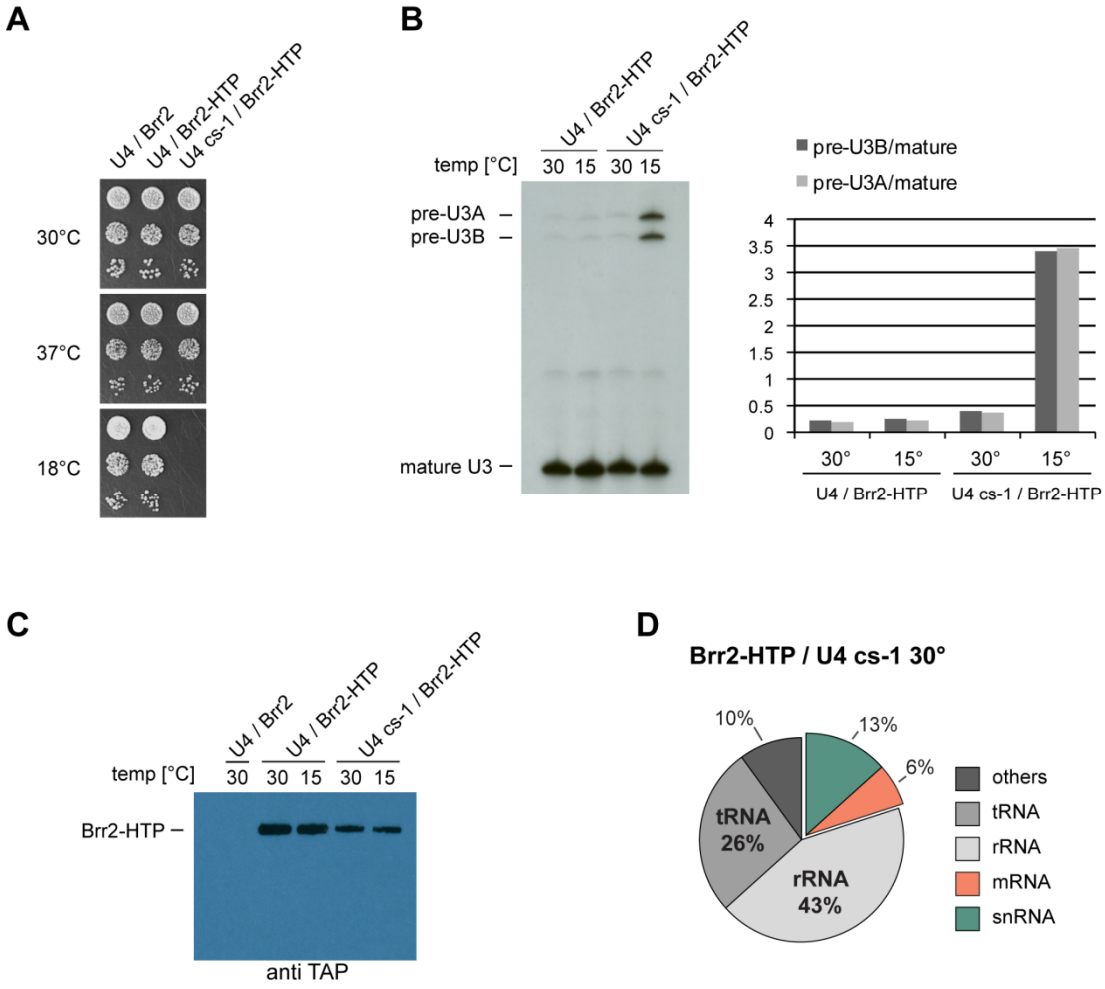

Figure 5.2 Attempted CRAC analysis of Brr2-RNA interactions in U4 cs-1 pre-catalytically stalled spliceosomes. (A) Spotting assay shows cold-sensitive growth of strain expressing the U4 cs-1 allele. Serial dilution of strains expressing the indicated *brr2* and U4 alleles were spotted to YPDA and incubated at the indicated temperature for 3 days. **(B)** Primer extension analyses of the U3 A + B transcripts in indicated strains. RNA was purified after incubation at 30°C or 15°C for 3 hours. Quantification is shown to the right. **(C)** CRAC Western blot (anti TAP) of cross-linked purified protein-RNA complexes (see Chapter 4 and 2.12.11). Prior *to in vivo* cross-linking the indicated strains were grown to log-phase and continuously incubated at 30°C or shifted to 15°C for 3 hours. **(D)** Proportion of RNAs identified by low-throughput sequencing (100 sequences) of cDNA generated for Brr2-HTP / U4 cs-1 30° sample.

Strains in which WT or mutant U4 is co-expressed with HTP-tagged Brr2 were generated by co-transforming W303 brr2Δ/U4Δ with pRS315-BRR2-HTP and either pRS413-U4 or pRS413-U4 cs-1. For a non-tagged Brr2 control pRS315-BRR2 was used. Transformants were cured of the *URA3* marked helper plasmid. The presence of the C-terminal HTP-tag was tolerated in combination with the U4 cs-1 allele and showed the expected cold-sensitive phenotype (Fig. 5.2 A + B).

I performed CRAC experiments with WT U4 and U4 cs-1 strains. Two sets of cultures were either cultivated at permissive temperature or, were shifted to non-permissive temperature. Unfortunately, it appeared that the purification of cross-linked protein-RNA complexes from strains expressing the U4 cs-1 allele was inefficient compared to strains carrying wild type U4 (Fig. 5.2 C). This and possibly other factors lead to the recovery of a large proportion (~ 70-80%) of non-specific RNAs in U4 cs-1 strains (Fig. 5.2 D). The reason for this phenomenon is unclear, as RNP purification in U4 cs-1 expressing strains was affected even at the permissive temperature at which splicing should proceed largely unaffected (Fig. 5.2 D). As yet, I was unable to optimise the experimental conditions to markedly improve the signal/noise ratio in sequencing libraries and therefore could not pursue this approach further.

5.3 The U4 3' SL is essential *in vivo*

The U4 3' domain does not directly base-pair with U6 and (in sequence) is not adjacent to other areas in U4 that do. In order to investigate the role of Brr2 interaction with the U4 3' domain, I studied genetic interactions.

Assuming that U4 structures involved in spliceosome activation should be synergistic with mutations that compromise Brr2 function, the viability of various *brr2* / U4 mutant combinations was assessed. Conditional *brr2* alleles carried mutations in the N-terminal helicase or the N-terminal or C-terminal Sec63 domains (Table 5.1). As the stability of U4/U6 stem 1 is critical for spliceosome activation [1],

I included U4 alleles that caused a destabilisation (G58A) or hyper-stabilisation (U64C,G65A and U4 cs-1) of stem 1 [15, 16]. To investigate the role of the Brr2 interaction site in the U4 3′ SL, I generated constructs carrying mutations in and around the Brr2 binding site by SDM (2.11.10.3). These included deletion of the bulged nt U138, insertions that artificially enlarge the bulge as well as various deletions in the 3′ side of the 3′ SL (Fig. 5.3 B - G).

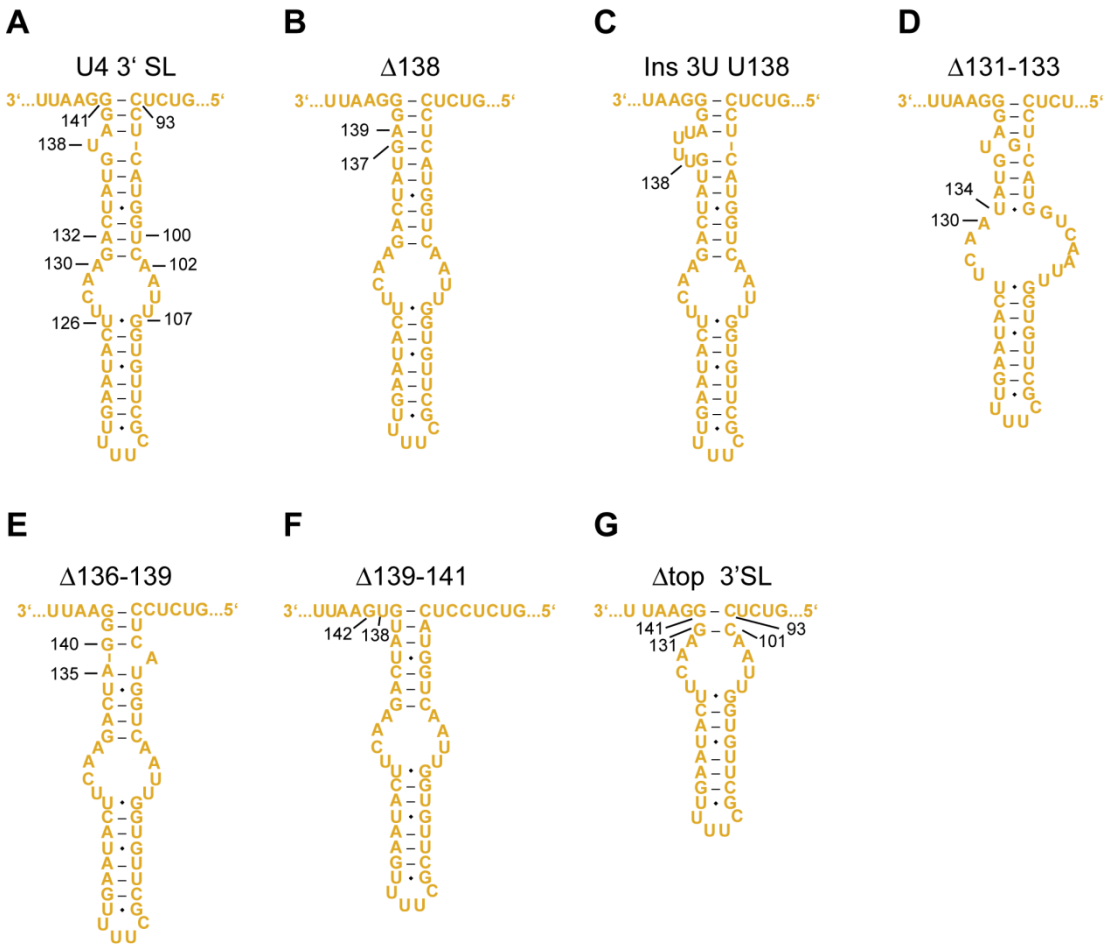

Figure 5.3 Deletions and insertions in the 3' SL of the U4 snRNA. Schematics show the wild type 3' SL of *S. cerevisiae* U4 snRNA **(A)** and mutant derivatives thereof **(B-G)**. Numbers indicate deletion and insertion sites and give nt positions relative to the full-length, wild type U4 snRNA sequence. The shown structures were predicted using the RNAfold algorithm (http://rna.tbi.univie.ac.at/cgi-bin/RNAfold.cgi).

The double-shuffle strain W303 brr2Δ/U4Δ was co-transformed with plasmids encoding the various mutant alleles. Tests for viability were carried out in triplicate

by streaking single colonies of double-transformants on 5-FOA containing medium. Representative plates are shown in Fig. 5.4; a summary of all tested allele combinations is given in Table 5.1.

As anticipated, mutations in U4/U6 stem 1 showed synthetic sickness or synthetic lethality with *brr2* mutations in the N-terminal helicase or Sec63 domains, confirming a functional connection between this region in U4 and Brr2 activity. While the *rss1-1* allele was less strongly affected, the *slt22-1* and R1107P alleles showed more severe phenotypes (Fig. 5.4 e.g. U64C, G65A, Table 5.1). By contrast, local changes in the U4 3′ SL were generally tolerated and did not show genetic interactions with *brr2* mutant alleles. Alone the Δsec63-2 allele was enhanced by some of the U4 3′ SL mutations. However deletion of the C-terminal Sec63 domain is sufficient to reduce cell fitness and causes slow growth at all temperatures [17]. U4 Δ131-133 was included since it was reported to confer cold-sensitivity [18], however, this phenotype could not be reproduced (data not shown). This discrepancy is probably caused by differences in strain background. In the original work the W303-1a stain background was used, which is generally more susceptible to developing phenotypes compared to W303.

The observation that changes in the upper area of the U4 3′ SL are not synergistic with Brr2 helicase / ATPase mutants suggests that changes in sequence or the absence of local features within this region of U4 do not adversely affect Brr2 function. It also seems unlikely that Brr2 helicase activity is needed to directly change the conformation of the U4 3′ SL. Then again, deletion of the entire U4 3′ SL is lethal (Fig. 5.4 bottom). (Lethality of U4 Δ3′ SL was confirmed in W303 U4Δ, a strain which expresses *BRR2* from the genome, data not shown). This demonstrates a requirement for the U4 3′ SL as a whole.

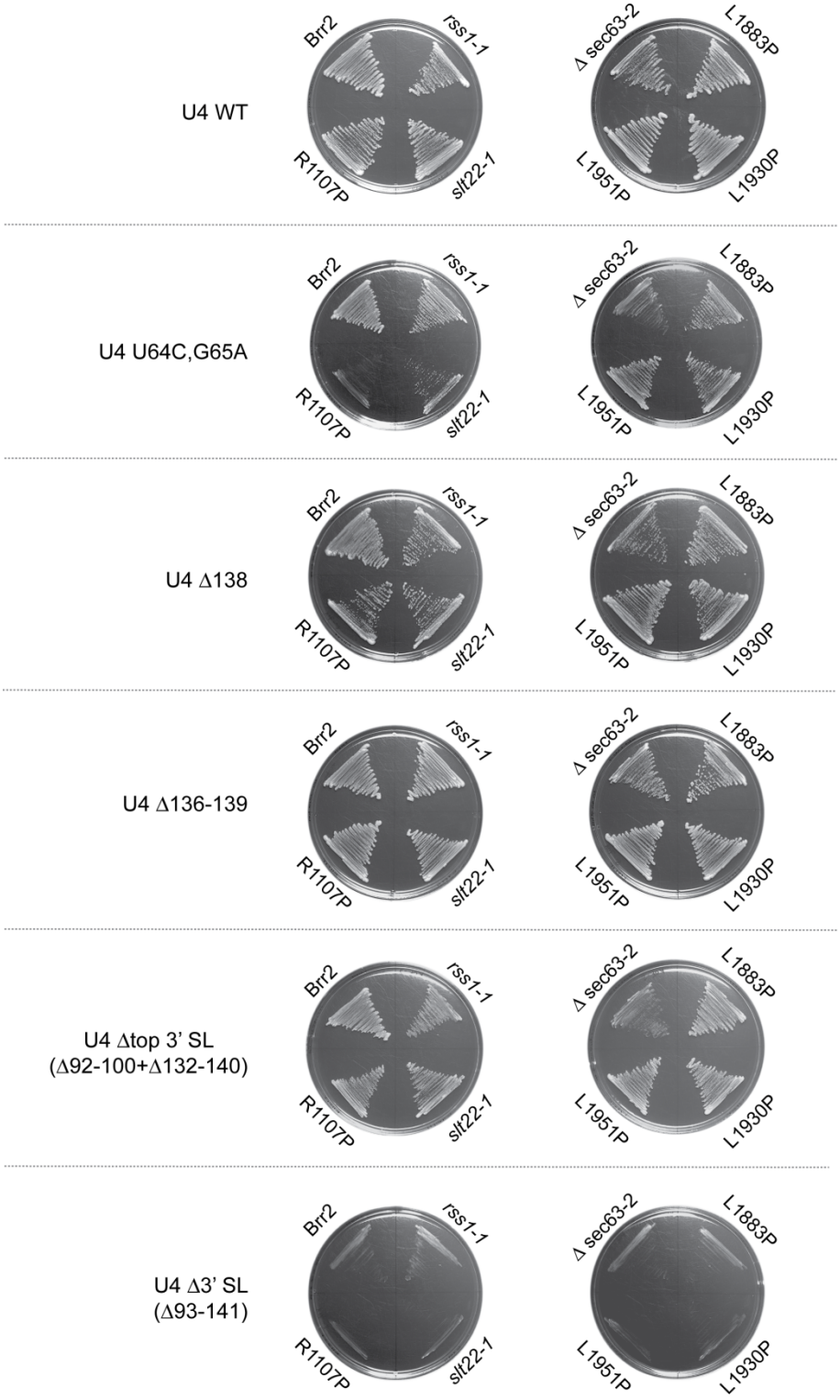

Figure 5.4 Genetic interactions between U4 and *brr2* mutant alleles. The plasmid shuffle strain W303 brr2Δ/U4Δ was co-transformed with plasmids expressing the indicated U4 **(Left)** and *BRR2* alleles **(adjacent to plate)**. To test for viability, single colonies of double-transformants were streaked to medium containing 5-FOA and were incubated for 3 days at 30°C. For each mutant-combination at least 3 clones were analysed, one representative example is shown.

Table 5.1 Genetic interactions between *brr2* and U4 alleles

U4	*brr2* alleles							
	WT	H1 (G858R) *rss1-1*	H1 (E909K) *slt22-1*	Sec63-1 R1107P	Sec63-2 L1883P	Sec63-2 L1930P	Sec63-2 L1951P	Sec63-2 Δsec63-2
WT	+++	+++	+++	+++	+++	+++	+++	++
U4 cs-1	+++	+	-	-	++	++	+++	-
U64C,G65A	+++	++	+	-	+++	+++	+++	+
G58A	+++	+	++	++	++	++	+++	+
Δ3' SL	-	-	-	-	-	-	-	-
Δtop 3' SL	+++	++	+++	+++	+++	+++	+++	+
Δ138	+++	++	++	++	+++	+++	+++	++
Δ136-139	+++	++	++	++	+++	+++	+++	++
Δ139-141	+++	+++	+++	+++	+++	+++	+++	++
Δ131-133	+++	++	++	++	+++	+++	+++	+
Ins 3U U138	+++	++	++	+++	+++	+++	+++	-

Growth was scored in comparison to WT after 3 days at 30°C; +++ = WT; -, synthetic lethal; (Δtop 3' SL = Δ94-100+Δ132-140), (Δ3' SL = Δ93-141).

5.4 Deletion of U4 3' SL affects Brr2 association with U4/U6 duplex

Since deletion of U4 3' SL was lethal and the cross-linking experiments suggested that Brr2 is in contact with this region of U4, I hypothesised that loss of the 3' SL might impair Brr2 association with the U4/U6 duplex. I thus investigated Brr2 interactions with U4/U6 *in vitro*.

Due to its large size, recombinant expression and purification of Brr2 from *E. coli* is not feasible. Therefore, I over-expressed affinity-tagged Brr2 in yeast. Yeast cells were mechanically disrupted and affinity purification of Brr2 was performed, including stringent wash steps (2.10.6). The purity and integrity of the purified protein was assessed by SDS PAGE (2.10.1) and gel-code staining (Fig. 5.5 A).

Templates for RNA *in vitro* transcription were generated by PCR amplification of U6, U4, U4 Δ138 and U4 Δ3' SL from expression plasmids. *In vitro* transcription was carried out as described in section 2.12.4. Transcripts were gel

purified and the integrity of purified transcripts was confirmed by denaturing PAGE (2.12.4.4). During transcription U6 was internally labelled to allow its detection by autoradiography. U4/U6 duplexes were prepared by denaturing and annealing equimolar amounts of (mutant) U4 and U6 transcripts (2.12.4.5). Native PAGE (2.12.7) showed that duplex formation was efficient with WT and mutant U4 transcripts (Fig. 5.5 B).

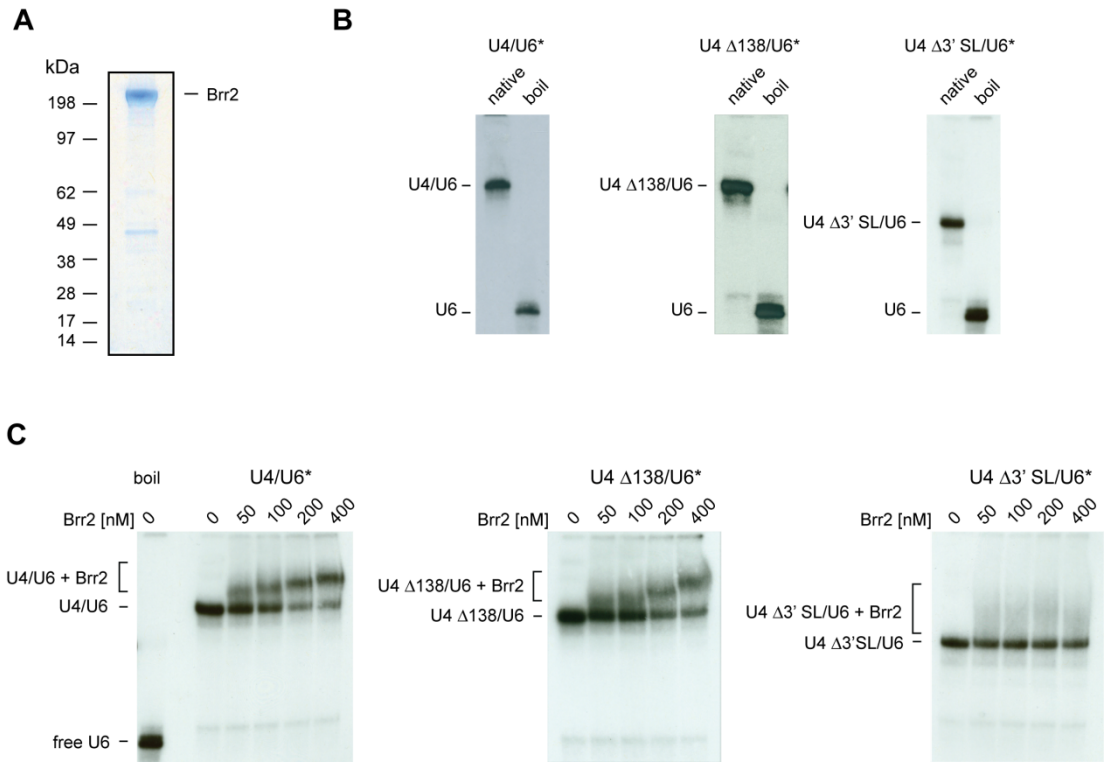

Figure 5.5 Deletion of U4 3' SL inhibits Brr2 association with U4/U6 duplex *in vitro*. (A) Gel-code strained SDS-PAGE gel showing TAP-tagged Brr2 purified from yeast (2.10.6). Numbers on the left indicate migration of MW marker. **(B)** Duplex formation of U4, U4 Δ138 and U4 Δ3' SL with internally labelled (*) U6 was analysed by native PAGE, 6% gel (2.12.7). **(C)** EMSA analysing the association of purified Brr2 with wild type and mutant U4/U6 duplexes. Indicated amounts of Brr2 were combined with 10 nM RNA duplex (2.12.8). Protein-RNA complexes were resolved by native PAGE on 6% gels.

I performed EMSAs to assess whether the presence or absence of U4 nt 138 or the U4 3′ SL influences the association of Brr2 with the U4/U6 duplex (2.12.8). Brr2 bound efficiently to WT U4/U6; and with increasing amounts of protein a larger proportion of RNA duplex was shifted (Fig. 5.5 C). A similarly efficient

binding was observed with the U4 Δ138/U6 duplex, indicating that deletion of the bulged U4 nt 138 did not affect Brr2 binding. By contrast, deletion of the entire U4 3′ SL markedly reduced Brr2 association with the RNA duplex and no clear band-shift could be detected. This suggests that the 3′ SL of U4 indeed aids Brr2 association with the U4/U6 duplex.

5.5 Brr2 interacts with U5 loop 1

Brr2 was not previously implicated in U5 interactions. Studies on *in vitro* reconstituted yeast U5 snRNPs did not detect Brr2-U5 cross-links, possibly suggesting that Brr2 does not interact with U5 in U5 snRNPs [19]. The analysis of Brr2 CRAC high-throughput sequencing data clearly suggests a cross-linking site at nt U96 of the U5 snRNA (Chapter 4, Fig. 4.6 C). Intriguingly, U96 lies in a strictly conserved and functionally very important region of U5, the U5 loop 1 (Fig. 5.6 A) [20, 21].

In order to verify a functional connection between U5 loop 1 and Brr2, I tested if mutations in loop 1 are synergistic with conditional *brr2* alleles. To allow combining different *brr2* and U5 alleles, I generated W303 brr2Δ/U5Δ in which both *BRR2* and U5 can be replaced by mutant alleles. The (*URA3* marked) helper-plasmid pRS316-BRR2/U5 was constructed by *in vivo* gap repair (2.11.9.3). I replaced one genomic copy of *SNR17* (encoding U5) with the *HphNT1* cassette in a diploid, heterozygous *brr2*Δ background (2.9.5) and transformed pRS316-BRR2/U5 to sustain growth. Subsequent to sporulation and tetrad dissection (2.9.6) I isolated *brr2Δ*/U5Δ haploids (W303 brr2Δ/U5Δ).

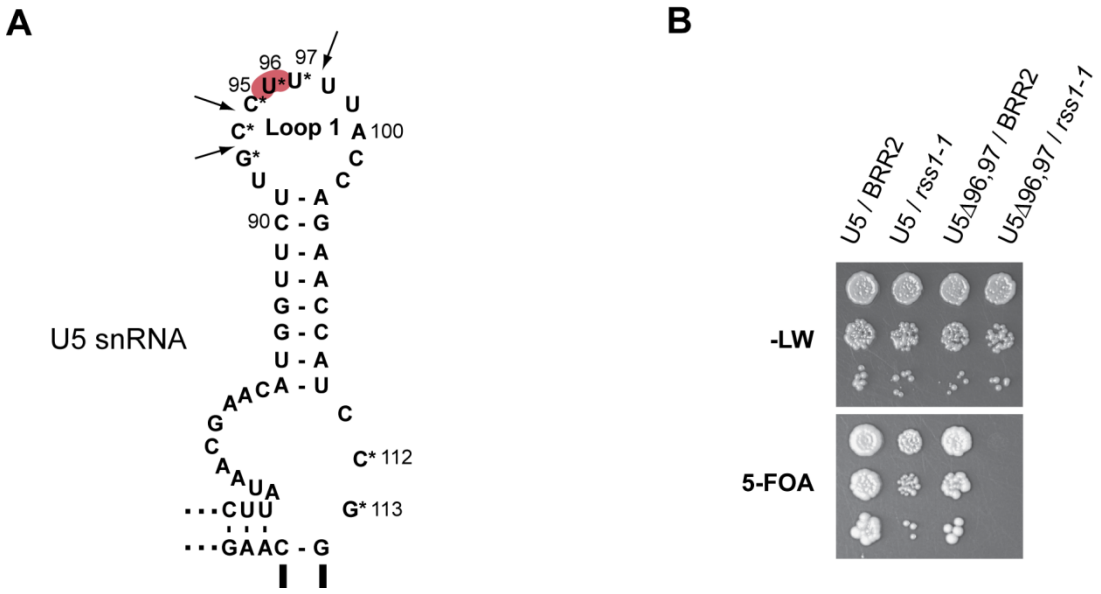

Figure 5.6 U5 loop 1 mutants interact genetically with *brr2*. (A) Schematic representation of part of the U5 snRNA, including the highly conserved loop 1 region. Numbers correspond to nt positions in full-length U5. Red shading indicates Brr2 cross-linking site identified by protein-RNA cross-linking and sequencing (Chapter 4). Arrows indicate insertion points and asterisks mark nt that were deleted (Table 5.2). **(B)** Plasmid shuffle assay tests viability of U5 / *brr2* mutant combinations. Cultures of W303 brr2Δ/U5Δ, transformed with plasmids expressing the indicated *brr2* and U5 alleles were grown to stationary phase and then spotted to the indicated media. Plates were photographed after 2-3 days of incubation at 25°C.

Despite its high degree of conservation U5 loop 1 tolerates a variety of insertions and deletions without fatal consequence [22, 23]. To test for synthetic lethal interactions W303 brr2Δ/U5Δ was first co-transformed with plasmids bearing WT or mutant *brr2* and U5 alleles, thereafter double transformants were transferred to medium containing 5-FOA to evict the *URA3* marked helper plasmid. Seven different U5 mutations were tested for interactions with six different *brr2* alleles (Fig. 5.6, Table 5.2). The genetic analysis revealed no synthetic lethal interactions between U5 loop 1 mutations and *brr2* alleles that posses substitutions in either the N-terminal or C-terminal Sec63 domains. By contrast, the *rss1-1* and *slt22-1* alleles, which carry mutations in the N-terminal helicase domain, showed synthetic lethal interactions with U5Δ96, 97 and U5 Ins 1U U97/U98 (Table 5.2).

Table 5.2 Genetic interactions between *brr2* and U5-loop 1 alleles

U5	*brr2* alleles						
	WT	H1 (G858R) *rss1-1*	H1 (E909K) *slt22-1*	Sec63-1 R1107P	Sec63-2 L1883P	Sec63-2 L1930P	Sec63-2 L1951P
WT	+++	++	+++	+++	+++	+++	+++
ΔG93	+++	+	+++	++	++	++	+++
ΔC94,C95	+++	-	+	+	+	++	+
ΔU96,U97	+++	-	-	++	+	+	++
ΔC112,G113	+++	+	++	+	+	++	++
Ins 1U G93/C94	+++	-	++	+	++	++	+++
Ins 1U C94/C95	+++	-	+	+	+	+	++
Ins 1U U97/U98	+++	-	-	++	++	++	+++

Growth scored in comparison to WT after 3 days at 30°C; +++, WT; -, synthetic lethal interaction.

Both U5 alleles comprise mutations at or adjacent to the Brr2 interaction site identified in cross-linking experiments (Fig. 5.6). Notably, the *rss1-1* allele was particularly sensitive to changes in U5 loop 1 and showed synthetic lethality with five of the seven alleles tested.

These findings are in clear agreement with the Brr2-U5 cross-linking data and indicate a functional link between U5 loop 1 and the N-terminal helicase domain of Brr2.

5.6 The *rss1-1* allele causes a reduction in second step efficiency

Intrigued by the severity of genetic interactions between U5 loop 1 and the *rss1-1* allele I decided to investigate the phenotype of this *brr2* allele further. *rss1-1* causes slow growth at 23°-25°C and a temperature sensitive growth phenotype at 33°C or above [24] (e.g. Fig. 5.6 B; 5.8 C).

Although a moderate decrease in mRNA of different intron-containing transcripts upon shift to high temperatures had been reported [24], the exact nature of the splicing defect caused by the *rss1-1* allele remained unknown. To test for splicing defects *in vivo* I performed primer extension analyses on the U3 A and B transcripts. In a *brr2Δ* background plasmids expressing WT Brr2, the temperature sensitive *brr2* L1951P allele or the *rss1-1* allele were the sole copy of the gene. Cultures were grown to logarithmic-phase at 25°C, and then shifted to 37°C for 1 hour. Total RNA was prepared from aliquots withdrawn before and after temperature shift. Primer extensions revealed that *brr2* L1951P accumulated pre-mRNA as expected; surprisingly, in the *rss1-1* strain no accumulation of pre-mRNA was detectable (Fig. 5.7 A + B). This suggested that unlike other *brr2* mutant alleles, *rss1-1* did not develop a first step defect at the restrictive condition.

Since primer extension of U3 transcripts does not allow detection of first step products, I utilized the pMA reporter plasmid harbouring the WT *ACT1* 5′ exon, intron and a small portion of 3′ exon fused in frame to the *CUP1* gene [25]. Primer extension with an oligo complementary to the downstream exon allows detection of pre-mRNA, mRNA and first step intermediate at the same time. Strains expressing WT or mutant *brr2* were transformed with pMA. To rule out that one hour of the heat treatment was insufficient to initiate the *rss1-1* defect, I shifted exponentially growing cultures to 37°C for 3 hours and withdrew samples after 30 minutes, one, two and three hours. RNA analysis and quantification confirmed the first step defect of *brr2* L1951P, and showed an accumulation of pre-mRNA at the expense of mRNA and intron-lariat exon 2 intermediate (IL-E2) over time (Fig. 5.7 C). Once again, the *rss-1* allele did not cause accumulation of pre-mRNA. Instead, it caused a higher abundance of IL-E2 along with a slight reduction of mRNA (Fig. 5.7 C). This indicated a defect before or at the second step of splicing.

An approximation of the first and second step efficiencies can be deduced from the relative abundances of the various RNA species [26]. First step efficiency can be calculated as (mRNA+IL-E2)/(pre-mRNA+mRNA+IL-E2) and second step

efficiency as mRNA/(mRNA+IL-E2). Although these analyses do not account for variations in stability of the different RNA species, they show the expected reduction in first step efficiency for *brr2* L1951P and a reduction in second step efficiency for *rss1-1*, respectively (Fig. 5.7 D).

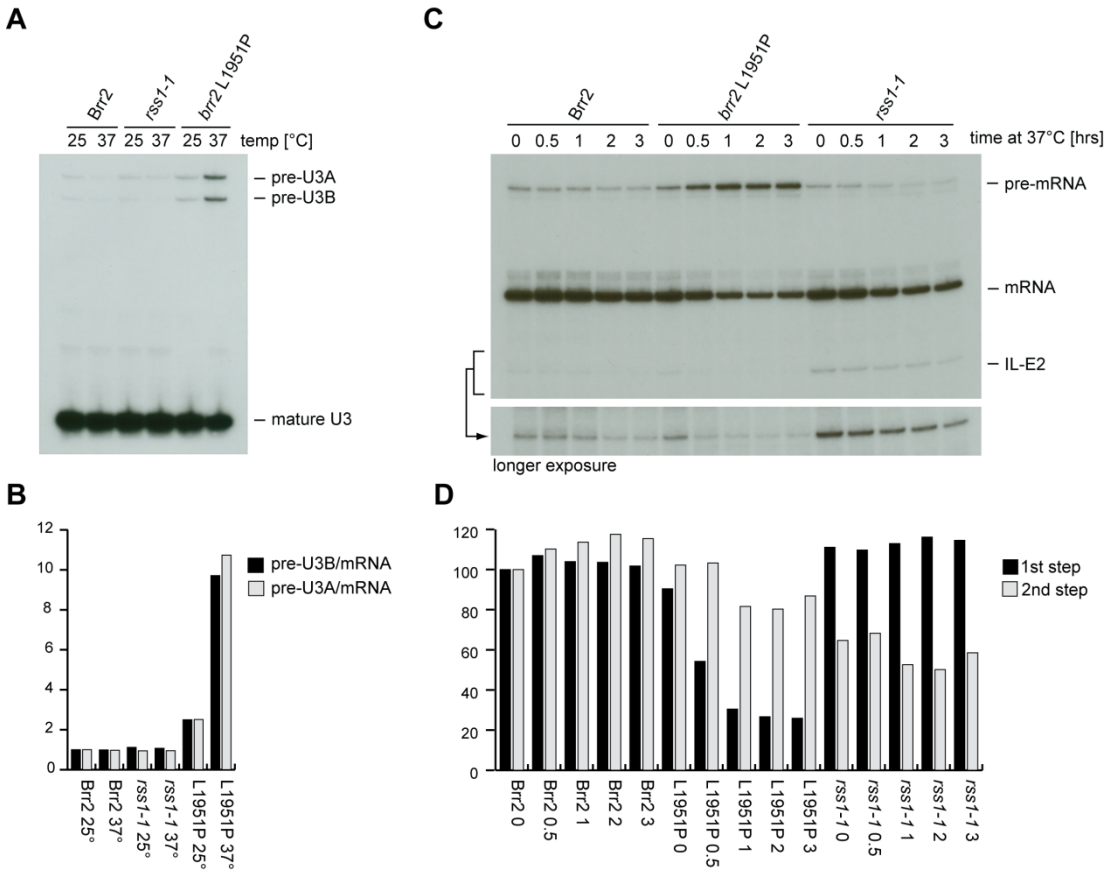

Figure 5.7 *rss1-1* does not have a first step splicing defect, but shows reduced second step efficiency. (A) Primer extension of U3 A + B transcripts. Cultures of strains carrying the indicated *brr2* alleles were incubated at 25° or 37°C for 1h before RNA was isolated. Primer extension reactions (2.12.9) were carried out with oligo U3 A B Exon2. **(B)** Quantification of results in (A). Values indicate the ratio between pre-mRNA and mRNA. **(C)** Primer extension of *ACT1-CUP* 1 reporter transcript expressed in strains carrying the indicated *brr2* alleles. Strains were shifted to 37°C for indicated time before RNA isolation. Primer extensions were carried out and quantified according to Query & Konarska [26]. **(D)** Quantification of experiment shown in (C). For each reaction the first and second step efficiencies were calculated. First step efficiency (dark bars) was calculated as (mRNA+IL-E2)/(pre-mRNA+mRNA+IL-E2) normalised to the value of the WT Brr2 strain at permissive condition, set at 100. Second step efficiency (light bars) was calculated as mRNA/(mRNA+IL-E2), normalised to second step efficiency of WT Brr2, set at 100.

The reduced abundance of all of the various RNA species observed in the *rss1-1* strain over time is very likely a consequence of cell death, as this strain rapidly ceases to grow when shifted to 37°C (Fig. 5.7 C, data not shown). Primer extension analyses of steady state RNA levels did detect an elevated level of IL-E2 already at permissive condition, but did not allow monitoring of the onset of the processing defect.

To get a clearer understanding of the origin of the *rss1-1* defect, splicing of an inducible reporter transcript was analysed kinetically. The RIBO1 strain harbours an *ACT1-PGK1* reporter gene, which is under the control of a tetON promoter. It also expresses tetracycline-responsive repressor and *trans*-activator proteins. This setup facilitates very low levels of basal expression, but rapid induction of the reporter gene upon addition of tetracycline (or doxycycline, as used here) (for further details see

[27]).

I constructed RIBO1 *GalS::brr2* in which the *GalS* promoter is integrated at the *BRR2* locus, which allows depletion of genomically encoded Brr2 in the presence of Glucose. Sensitivity to Glucose was confirmed and growth curves showed that, compared to RIBO1, RIBO1 *GalS::brr2* developed a significantly reduced growth rate after 4-6 hours of depletion (Fig. 5.8 A + B). Both strains were transformed with plasmids expressing WT Brr2, *brr2* L1951P and *rss1-1*, respectively. Growth assays demonstrated that the temperature sensitive growth phenotypes characteristic of *brr2* L1951P and *rss1-1* emerged in the presence of Glucose, indicating that under this condition growth is supported by the plasmid-borne copies of *brr2* (Fig. 5.8 C).

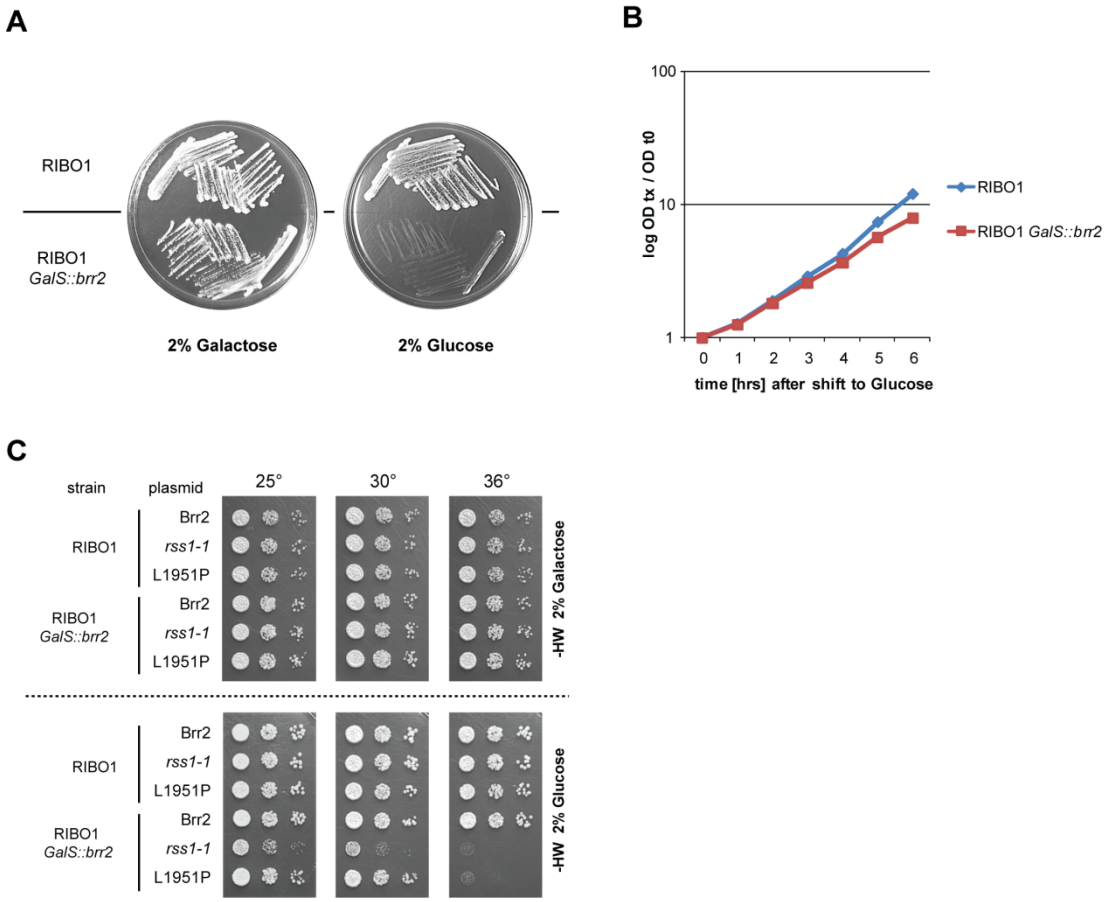

Figure 5.8 Construction and testing of RIBO1 *GalS::brr2*. (A) Test for Glucose sensitivity of RIBO1 and RIBO1 *GalS::brr2*. **(B)** Growth curve of RIBO1 and RIBO1 *GalS::brr2*. Both strains were pre-grown in YP Gal and shifted to YPDA (2% Glucose) for the indicated length of time. **(C)** RIBO1 and RIBO1 *GalS::brr2* were transformed with plasmids expressing the indicated *brr2* alleles. Transformants were grown to stationary phase in SD -HW 2% Galactose, serial dilutions were spotted to SD -HW containing either 2% Glucose or 2% Galactose and were incubated at the indicated temperatures for 2 days.

For kinetic analysis of splicing intermediates pre-cultures of RIBO1 *GalS::brr2* transformed with Brr2 or *rss1-1* expression plasmids were grown to log-phase in SD -WH 2% Galactose. The cultures were then shifted to medium containing 2% Glucose and endogenous Brr2 was depleted for 7 hours. Thereafter, the cultures were subjected to a mild temperature treatment for 1 hour at 33°C. Finally, the reporter gene was induced by the addition of doxycycline and samples were withdrawn every 2.5 minutes for 30 minutes. Total RNA was extracted and cDNA synthesised with RIBO1 specific oligonucleotides (2.12.1, 2.12.12, Fig. 5.9). RT-qPCR

was performed using primer sets that distinguish the different intermediate products of the splicing reaction, as described in the legend to Fig. 5.9 A.

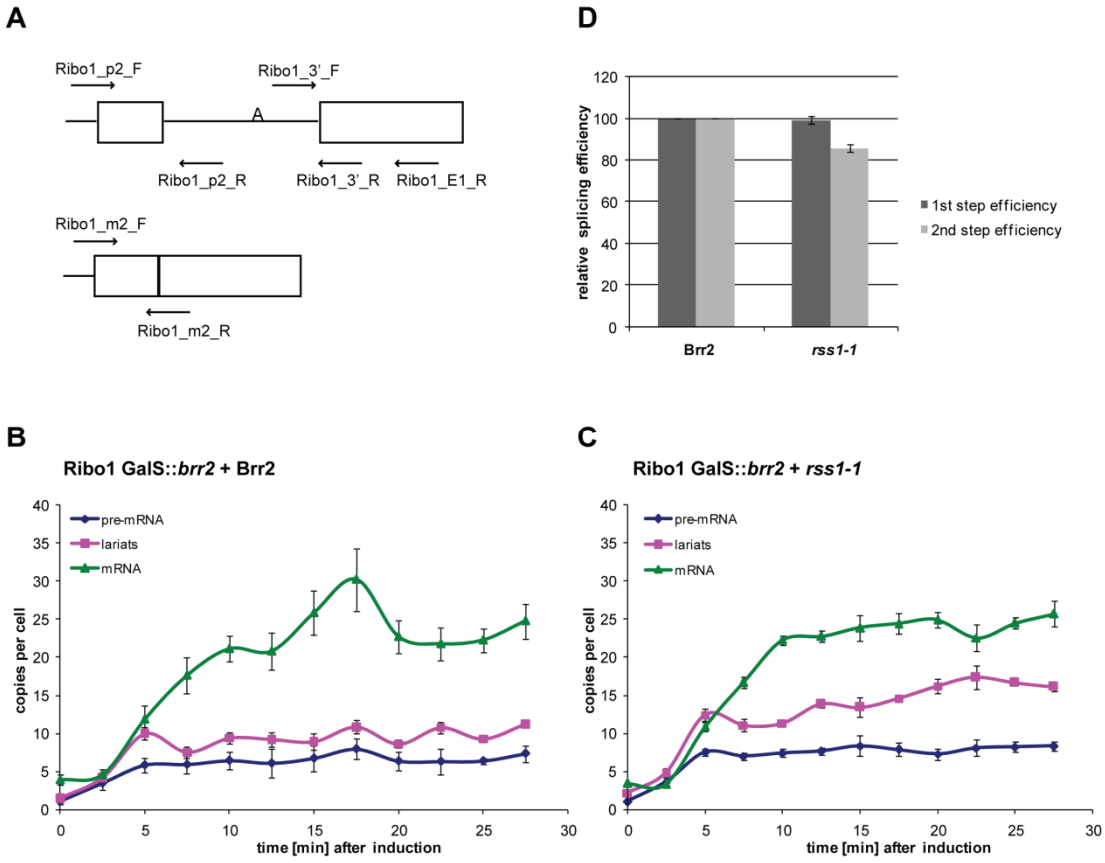

Figure 5.9 Kinetic analysis of *rss1-1* splicing defect by RT-qPCR of the RIBO1 reporter transcript. (A) Schematic representation of RIBO1 transcript and mRNA. Arrows indicate the oligonucleotides used to measure the abundances of different RNA species. Primers p2_F and p2_R amplify the 5′ ss region of unspliced pre-mRNA. Exon specific primers m2_F and m2_R are used to quantify mRNA and do not produce product from pre-mRNA. The intron-containing products of the first and second steps of splicing are lariat structures, containing a 2′-5′ phosphodiester bond, which blocks reverse transcription. The intron-lariat exon 2 species can be measured by the product produced with primers 3'_F and 3'_R flanking the 3′ ss. The product represents the sum of pre-mRNA and intron-lariat exon 2 species, thus the RT-qPCR product generated with primers p2_F and p2_R needs to be mathematically subtracted to measure the abundance of the intron-lariat exon 2 species. **(B+C)** RT-qPCR analysis of RIBO1 *GalS::brr2* + Brr2 or + *rss1-1*. Cultures were pre-grown to log-phase in SD -HW 2% Galactose and were then shifted to SD-HW 2% Glucose for 7 hours. Thereafter, cultures were shifted to 33°C for 1 hour. Time course was performed at 33°C and samples were withdrawn at 2.5 minute intervals after induction with doxycyclin. Diagrams represent biological duplicates with 6 technical repeats. RT-qPCR values were converted to copies per cell according to [27]. **(D)** Calculation of 1st and 2nd step splicing efficiencies as in Fig. 5.7 D, based on RT-qPCR values averaged across the time course.

Figures 5.9 B + C show the abundances of the different intermediate RNA species following induction of the reporter gene in the presence of Brr2 and *rss1-1*, respectively. Time point 0 indicates the abundance of pre-existing RNAs which are produced as a result of promoter leakage. The addition of doxycycline triggers transcription, consequently the level of pre-mRNA increases. The pre-mRNA is rapidly processed, leading to an initial increase in lariat intermediate which is then converted to mRNA. In the presence of WT Brr2 both steps of splicing occur efficiently as the abundances of pre-mRNA and first step intermediate level off shortly after induction, while the mRNA abundance increases steadily (Fig. 5.9 B).

In the presence of *rss1-1* the amount of pre-existing intron-lariat species is slightly higher compared to the WT, and upon induction it increases rapidly. The continuous increase of mRNA demonstrates that both steps of splicing occur. However, the conversion of IL-E2 to mRNA seems to be inefficient as the signal detected for lariat intermediates does not drop, but remains high and increase with time (Fig. 5.9 C).

Based on RT-qPCR values the first and second step efficiencies were calculated (Fig. 5.9 D). The *rss1-1* expressing strain showed no reduction of first step efficiency, but its second step efficiency was reduced to 82% compared to WT Brr2. These results are in agreement with the primer extension analyses and showcase that *rss1-1* causes a mild, but reproducible inhibition of the second step of splicing, while the first step is unaffected.

5.7 Synthetic lethality of U5 loop 1 mutant and *rss1-1* coincides with inhibition of second step

U5 loop 1 is thought to function in 5′ exon tethering and in exon alignment, the latter being specifically important during the second catalytic step [23, 28-30]. In the light of the reduced second step efficiency caused by the *rss1-1* allele, it was

interesting to ask if an insufficiency of the second step provoked the synthetic lethality observed upon combining *rss1-1* and U5 loop 1 mutations (Table 5.2).

In order to identify what splicing defect the presence of *rss1-1* induced in a U5 mutant strain, I used a Brr2 depletion and reconstitution approach. I constructed a strain in which WT U5 can be exchanged for mutant versions by plasmid shuffle. At the same time expression of the genomic copy of *BRR2* can be repressed, making the strain gradually dependent on a second, plasmid-borne copy of WT or mutant *BRR2*.

To achieve this I modified a U5-shuffle strain (U5KO, kindly provided by R. O'Keefe) and integrated a *GalS::3HA* promoter cassette at the *BRR2* locus. Correct integration of the promoter cassette was confirmed by colony PCR (2.11.10.2); and, as expected, U5KO *GalS::3HA-brr2* was sensitive to Glucose (Fig. 5.10 A).

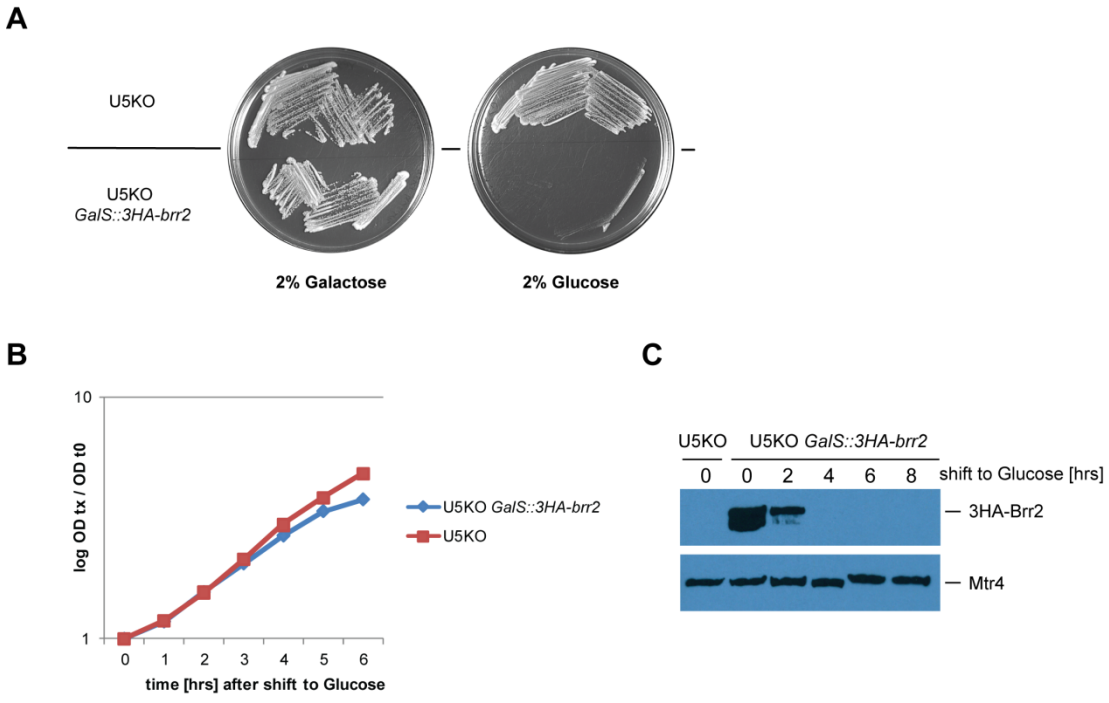

Figure 5.10 Construction of U5-shuffle / brr2 shut-off strain. (A) Testing of Glucose sensitivity of U5KO and U5KO *GalS::3HA-brr2*. **(B)** Growth curve shows that U5KO *GalS::3HA-brr2* develops a decreased growth-rate in the presence of Glucose, **(C)** samples withdrawn at indicated points were tested by Western blot analysis for the presence of 3HA-Brr2. The same membrane was reprobed with anti-Mtr4 antiserum, to control for equal loading.

Shift to Glucose resulted in a reduction of growth rate after four hours, which was accompanied by efficient depletion of 3HA-Brr2, as confirmed by Western blotting (Fig. 5.10 B + C). Next, U5KO *GalS::3HA-brr2* was transformed with plasmids encoding either WT U5 or U5Δ96,97. The U5 helper-plasmid was cured by cultivating transformants on 5-FOA, 2% Galactose medium. Subsequently, both strains were transformed with plasmids encoding WT Brr2 or *rss1-1*. This gave rise to four strains in which either WT or mutant U5 were combined with WT or mutant Brr2. Isogenic control strains were generated by introducing the same plasmids to the parental U5KO strain (Fig. 5.11 A). Finally, all strains were transformed with the pMA reporter plasmid to facilitate inspection of splicing *in vivo* (see above).

As opposed to the U5KO background, in U5KO *GalS::3HA-brr2* the synthetic lethal interaction between U5Δ96,97 and *rss1-1* (Fig. 5.6 B) should manifest itself in the presence of Glucose. Growth assay confirmed the expected phenotype, as shown in Fig. 5.11 A. To investigate splicing, cultures of all strains were grown at 25°C, in SD 2% Galactose medium to log-phase. Then the strains were shifted to SD 2% Glucose medium and their growth was monitored over 10 hours (Fig. 5.11 B - E). Cultures were diluted if needed, to maintain exponential growth. The growth curves mirrored the results of the spotting assay. All strains continued to grow, except U5KO *GalS::3HA-brr2* + U5Δ96,97 + *rss1-1*, which gradually stopped growing after eight hours of depletion (Fig. 5.11 E). I withdrew aliquots from U5KO *GalS::3HA-brr2* cultures before and during depletion. I isolated total RNA and performed primer extension of the *ACT1-CUP1* transcript (Fig. 5.12 A + B). With continuous depletion all strains showed an accumulation of pre-mRNA, even in the presence of WT Brr2 / U5. This indicates an overall reduction of splicing activity in this strain background, presumably as a consequence of the extensive manipulations required throughout the experiment (reconstitution of two essential genes from plasmid, cultivation in triple drop-out medium to maintain plasmid selection whilst changing carbon source to deplete genomic *BRR2*).

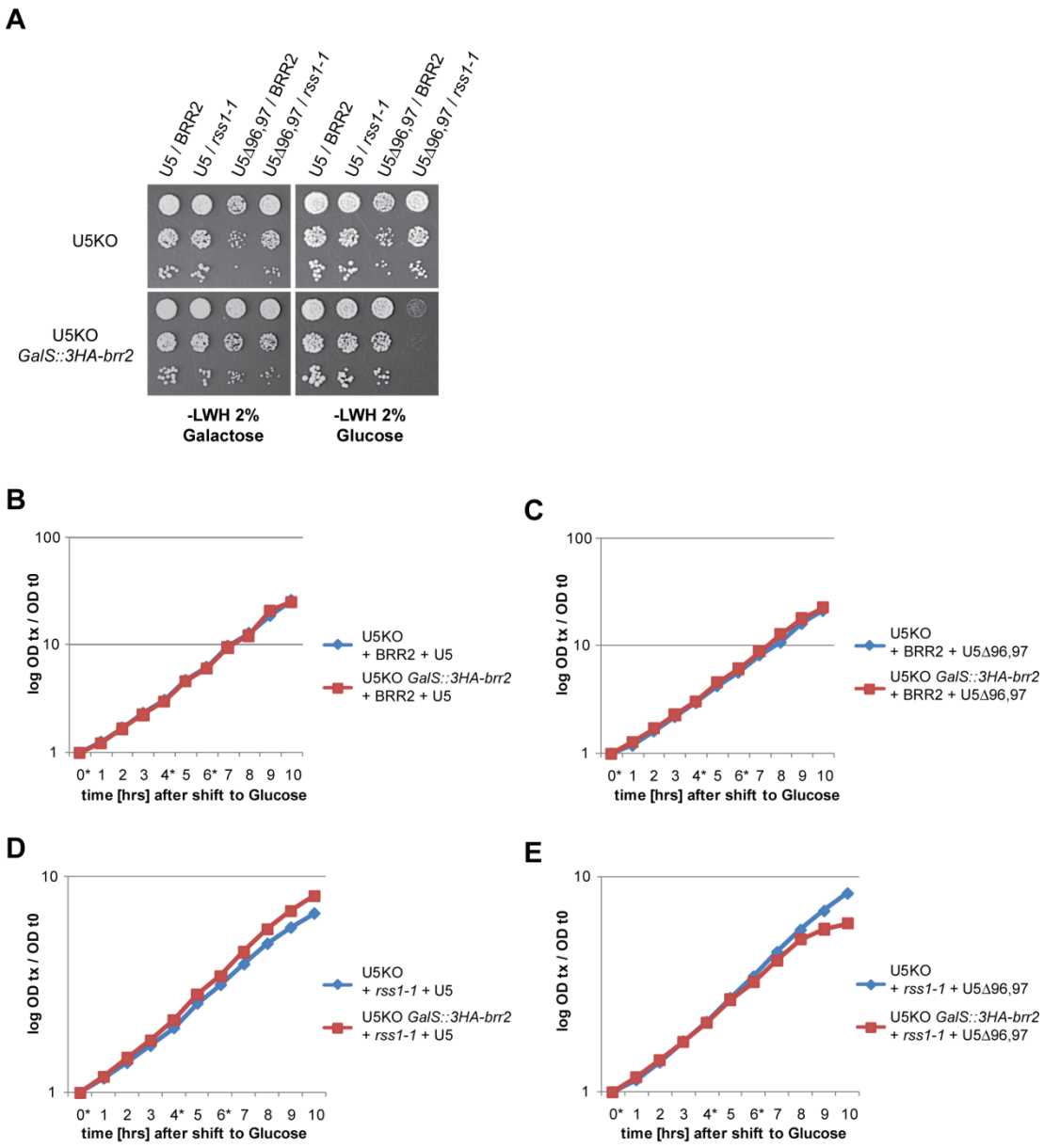

Figure 5.11 Depletion of 3HA-Brr2 is lethal only in the presence of U5Δ96,97 and *rss1-1*. (A) Growth assay (25°C) of U5KO and U5KO *GalS::3HA-brr2* transformed with plasmids expressing the indicated *brr2* and U5 alleles. In addition all strains carry the pMA reporter plasmid. Serial dilutions of stationary phase cultures were spotted to SD -LWH medium containing either 2% Galactose or 2% Glucose. **(B-E)** Growth curves of strains shown in A. Pre-cultures were grown to log-phase in SD -LWH 2% Galactose. Cultures were then shifted to SD -LWH 2% Glucose and OD_{600} readings were monitored over 10 hours. Asterisks mark time points at which samples were withdrawn from U5KO *GalS::brr2* cultures for analysis of RNA (see Fig. 5.12).

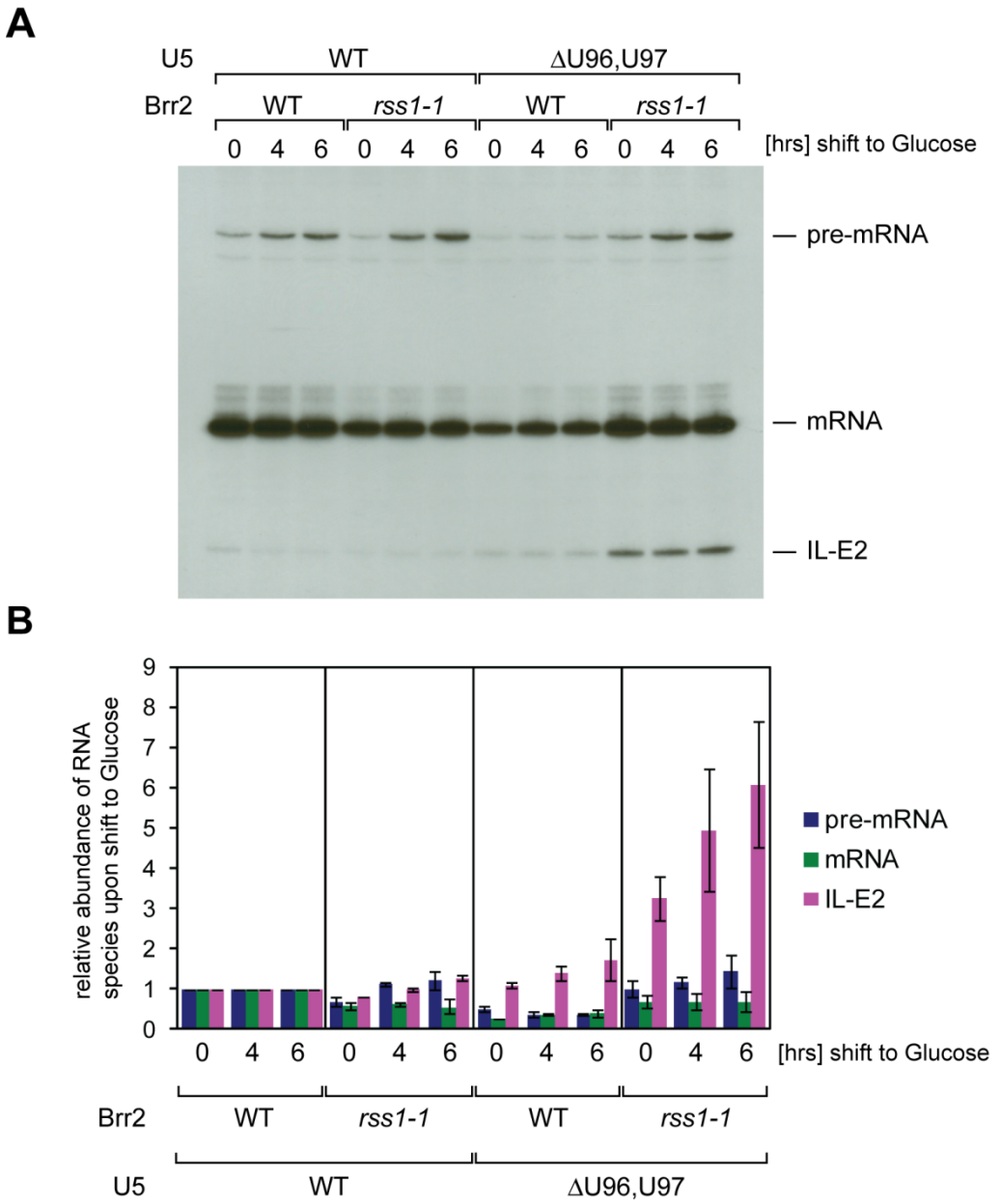

Figure 5.12 Combination of *rss1-1* and U5Δ96,97 exacerbates accumulation of first step intermediate. (A) U5KO *GalS::3HA-brr2* transformed with plasmids expressing the indicated *brr2* and U5 alleles and pMA (encoding the *ACT1-CUP1* reporter gene) were shifted to Glucose containing medium for indicated length of time (see Fig. 5.11). Total RNA was prepared and analysed by primer extension of *ACT1-CUP1* reporter transcript. Extension products were resolved by denaturing 7% PAGE. Signal intensities were determined by phosphorimaging. The experiment was carried out in biological triplicate, A shows one representative gel. **(B)** Quantification of PE described in A. Bar diagram shows average values obtained in three independent experiments. Error bars indicate SDV. Values for each time point are normalised relative to WT Brr2 / U5 strain at the corresponding time, set at 1.

The strain bearing U5Δ96,97 in combination with WT Brr2 reproducibly showed lower signals for pre-mRNA and mRNA, although IL-E2 levels were slightly higher compared to WT Brr2 / U5. The basis for this effect is unclear.

Nevertheless, the primer extension analysis confirmed that combination of *rss1-1* and U5Δ96,97 affects the second step of splicing, as a clear accumulation of lariat intermediate could be observed. The double-mutant strain showed a high basal level of IL-E2 at time point 0, indicating that *rss1-1* is dominant over WT 3HA-Brr2 when combined with a U5 loop 1 mutation, even at 25°C. Gradual depletion of 3HA-Brr2 caused a further increase in the abundance of IL-E2, which reached levels up to 6-fold higher than those of the WT Brr2 / U5 strain (Fig. 5.12 B). This demonstrated a clear effect on the second step of splicing and underscored the functional connection between Brr2 and U5 loop 1.

5.8 Brr2 cross-links specifically to intron-containing transcripts

Cross-linking studies demonstrated that U5 loop 1 interacts with the 5′ exon early and throughout the first step of splicing; prior to exon ligation loop 1 also establishes interactions with the 3′ exon [23, 29]. As shown above, Brr2 and U5 loop 1 interact genetically and physically, and mutations in both adversely affect the second catalytic step. In conjunction with Brr2 being an RNA helicase these observations provoked the question whether Brr2 might function in mediating changes that facilitate or influence U5-exon interactions at the second step of splicing. This assumption would require Brr2 to directly interact with the pre-mRNA. I thus inspected if the high-throughput sequencing data obtained in Brr2 CRAC experiments supported this hypothesis.

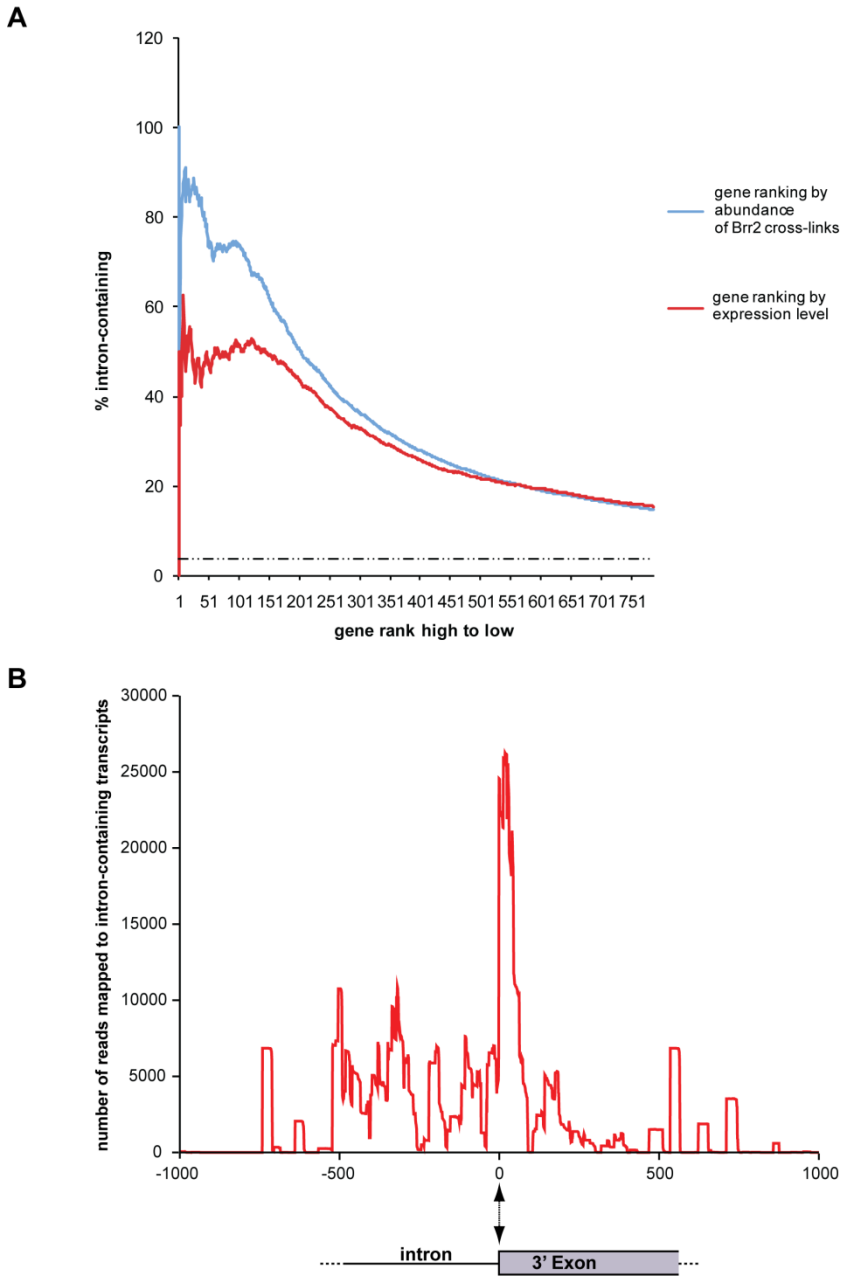

Figure 5.13 Brr2 interactions with intron-containing transcripts. (A) Gene ranking indicates enrichment of Brr2 cross-links in intron-containing transcripts. Based on Brr2 CRAC high-throughput sequence data, the blue graph ranks genes according to the number of sequencing reads that could be aligned; the higher the number of reads, the higher the rank. The red graph ranks genes according to their expression level based on Holstege *et al.* (1998) [32]. The y axis indicates the % of genes that contain introns. The dashed line indicates % of genes with introns genome-wide. **(B)** Distribution of Brr2 interaction sites in intron-containing transcripts. The number of sequencing reads mapped to intron-containing genes is plotted against the nt sequence. Sequences are positioned relative to the 3' intron-exon border.

In datasets obtained with full-length Brr2 and the N-terminal Brr2 portion 3% of sequencings reads were classified as mRNAs (Chapter 4, Fig. 4.5 A + B). This classification, however, does not take into account whether genes are intron-containing or intron-less. Certainly, Brr2 is expected to interact with intron-containing transcripts, but abundant messages have been identified as contaminants in other CRAC experiments [31]. To rule out that Brr2-mRNA interactions occur randomly, the propensity for cross-linking in intron-containing transcripts was analysed. In doing so, it must be considered that the cross-linking frequency is biased by the expression level of any given transcript. High transcript abundance increases the likelihood for physical interactions to occur. Moreover, if splicing is required a highly expressed transcript engages a larger proportion of the cell's splicing machinery in processing, consequently cross-links and sequencing reads will be more abundant.

To control for this effect genes were ranked based on two different criteria. Firstly, all genes were sorted according to their expression level. Concomitantly, it was assessed whether genes of any given expression level were intron-containing or not. This information was compiled in a graph, as shown in Fig. 5.13 A (red graph). As expected, this analysis showed that the most highly expressed genes are quite often (in 50-60%) intron-containing; genes encoding ribosomal proteins are prominent examples. Secondly, genes were ranked based on the number of sequencing reads that were mapped to them, and whether these genes were intron-containing (Fig. 5.13 A, blue graph). Comparison of the two graphs showed a correlation between expression level and cross-linking frequency. However, Brr2 cross-links showed a clear enrichment in intron-containing transcripts, which exceeded the expression level. For example, of the 40 most frequently cross-linked transcripts over 80% are intron-containing. This illustrates that sequencing reads classified as mRNAs were found predominantly in intron-containing transcripts, suggesting that they represent Brr2-specific cross-linking events.

I next asked where within transcripts Brr2 interacted, and whether preferential interaction sites existed. For this purpose, the distribution of all sequencing reads that mapped to intron-containing transcripts was analysed. Sequences spanning splice junctions were extremely rare and negligible, suggesting that Brr2 interacts with pre-mRNA or splicing intermediates, rather than with spliced mRNA (data not shown). Sequencing reads overlapped 5′ ss relatively infrequently and only in rare cases aligned to introns. Intriguingly, an enrichment of sequencing reads in the vicinity of the 3′ intron-exon border became apparent (Fig. 5.13 B). Frequently, sequences aligned in the 3′ exon immediately downstream of the 3′ ss.

This observation substantiates the assumption that Brr2 functions during the second catalytic step of splicing and can be reconciled with an involvement in mediating exon rearrangements.

5.9 *rss1-1* interacts genetically with other second step factors

In a first survey I wanted to test if depletion of known second step factors Slu7 and Prp18 can suppress or alleviate the mutant phenotype of *rss1-1*. I thus constructed W303 brr2Δ/*GalS::3HA-prp18* and W303 brr2Δ/*GalS::3HA-slu7* in which the WT copy of *BRR2* can be exchanged for the *rss-1* allele and at the same time the expression of 3HA-Prp18 and 3HA-Slu7, respectively, can be regulated by the addition of Glucose or Galactose to the culture medium.

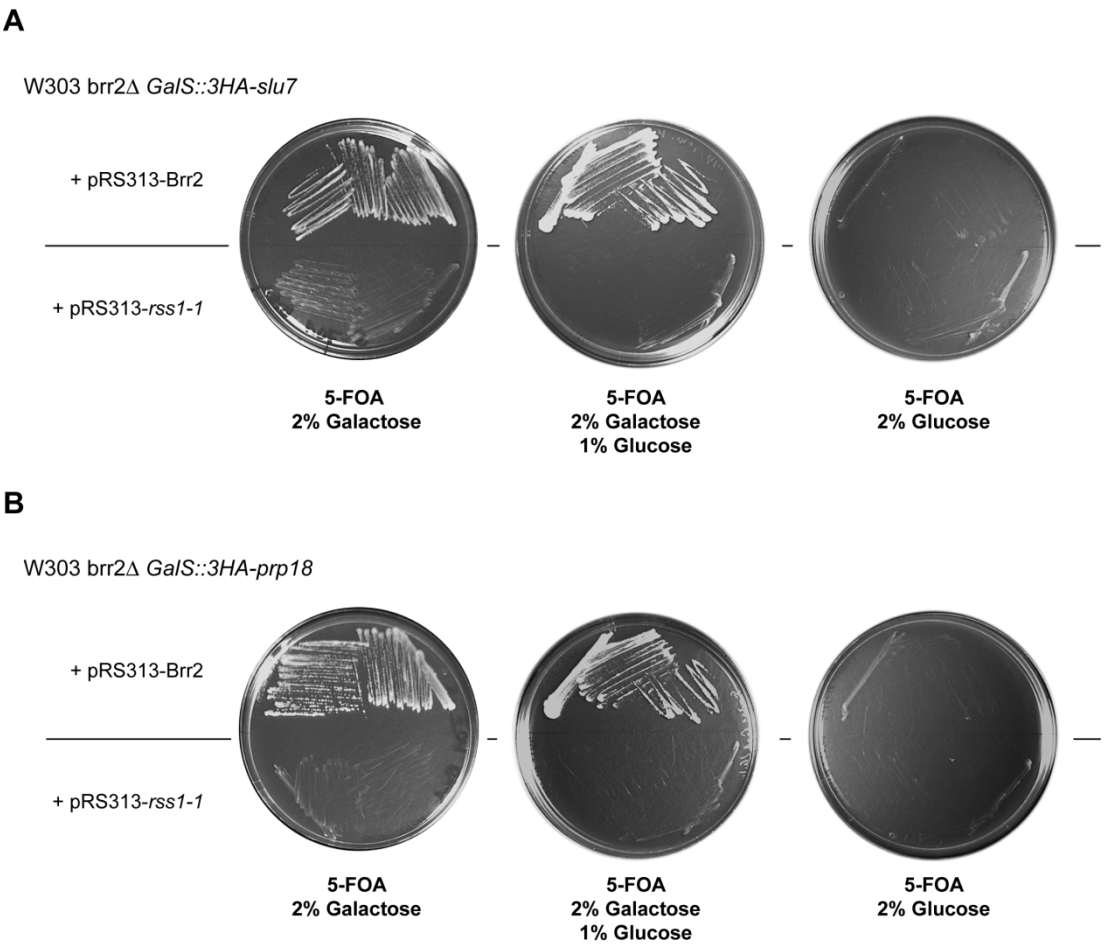

Figure 5.14 Expression of the second step factors *SLU7* and *PRP18* from a *GalS* promoter is detrimental in the presence of *rss1-1*. Brr2-shuffle strains in which *SLU7* **(A)** or *PRP18* **(B)** were under the control of a *GalS* promoter were transformed with plasmids expressing either wild type Brr2 or the *rss1-1* mutant. Transformants were streaked on 5-FOA containing medium to cure the helper plasmid. Increasing Glucose concentrations result in reduced expression levels of the *GalS* promoter.

The *GalS::3HA* cassette was PCR amplified with oligos providing the required sequences complementary to the *PRP18* or *SLU7* loci and W303 brr2Δ was transformed with the PCR product. Colony PCR and test for Glucose sensitivity confirmed the correct integration of the *GalS* promoter (data not shown). The obtained strains were transformed with pRS313-Brr2 or pRS313-*rss1-1*. In order to counter select the helper plasmid I streaked transformants on medium containing 5-FOA. The medium contained 2% Galactose to allow expression of *RPP18* and *SLU7*, respectively. While the strains expressing wild type *BRR2* from plasmid grew

readily, no growth could be observed when plasmids encoding *rss1-1* were used (Fig. 5.14). In the absence of Glucose the *GalS* promoter is not repressed and reaches a high level of expression. To test, whether the expression level caused the apparent lethality in the presence of *rss1-1* I tested various concentrations of Glucose and Galactose. However, titrating Galactose and Glucose to reduce the *GalS* expression level did not restore viability in the presence of *rss1-1*.

Possibly the N-terminal 3HA-tag is detrimental. As described above, this result suggests that malfunctioning second step factors aggravate the mutant phenotype of *rss1-1*. Certainly, this phenomenon needs further investigation to work out what exactly causes the observed lethality.

5.10 Discussion

5.10.1 Brr2-mediated U4/U6 unwinding

Processes contributing to spliceosome assembly and catalytic activation have been studied extensively. In conjunction with the Brr2 cross-linking analysis presented here, an increasingly detailed picture of the complex chain of events, and the conformational intermediates involved, is emerging. Below, I give a synopsis of these events and discuss the mechanistic insight provided by Brr2-RNA interactions.

Brr2 interactions in the 3′ SL of U4 might occur in the tri-snRNP. Brr2 cross-links in the U4 3′ SL were unexpected, as this region is not involved in base-pairing interactions with U6 and has not been implicated in spliceosome activation. The lack of genetic interactions between Brr2 and the U4 3′ SL (Fig. 5.3, 5.4 Table 5.1) is consistent with other studies in which point mutations in the yeast U4 3′ SL were uniformly functional [18]. However, a complete deletion of the U4 3′ SL was inviable (Fig. 5.4 [33]). Deletion of the equivalent structures from the human U4atac

[34] and U4 in *Xenopus* oocytes are also detrimental [35], suggesting that the 3′ SL does contribute to U4 function *in vivo*. I cannot rule out that lethality is caused by interference with the Sm binding site, which is usually flanked by stem-loop elements [36]. On the other hand it is possible that the U4 3′ SL plays a role in efficient assembly of the tri-snRNP and in positioning of Brr2 with respect to the U4/U6 substrate. The observation that deletion of the U4 3′ SL reduces the association of Brr2 with the U4/U6 duplex *in vitro* (Fig. 5.5 C) is consistent with results presented by Pena *et al.* (2009), who showed that Brr2 associates much less efficiently with a truncated duplex consisting only of U4/U6 stems 1 and 2 and the U4 5′ SL [37]. Structural probing demonstrated the existence of the U4 3′ SL in isolated tri-snRNP particles [38]. Brr2 cross-links in the 3′ SL might reflect a Brr2-U4 interaction in an early or "disengaged" state, i.e. in free tri-snRNPs. Accordingly, the Brr2 interaction with the 5′ portion of U6 could represent an interaction established at the same time, while the remaining part of U6 might interact with Brr2 at later stages.

Brr2-mediated unwinding of U4/U6 stem 1 initiates spliceosome activation. In order to understand how U4/U6 dissociation is achieved, one must consider which parts of the duplex constitute the Brr2 substrate. Based on its similarity to other SF 2 helicases, Brr2 is expected to have 3′ to 5′ unwinding directionality [37, 39]. With regard to U4/U6 unwinding this allows for two different options: (1) Brr2 might translocate on U6 to sequentially disrupt U4/U6 stem 2 and stem 1. Translocation along U6 would require high processivity, however at present there is no direct evidence for processivity of Brr2. Also, unwinding of stem 2 is hard to reconcile with the fact that no Brr2 cross-links were found in the U4 side of stem 2 (Fig. 5.1 A). (2) Alternatively, Brr2 might translocate along U4 and unwind U4/U6 stem 1. This is highly consistent with cross-links found in this region of U4 and U6. Several other observations are also in favour of the latter option, as outlined below.

To start spliceosome activation, U4/U6 unwinding must occur coordinated with the exchange of U1 for U6 at the 5′ ss. Prp28 helicase activity is required for the disruption of U1/5′ ss interactions [40] to allow formation of the mutually exclusive interactions of U6 with the 5′ ss (Fig. 5.16 C). Therefore, Brr2 and Prp28 are thought to act in a concerted manner [41]. Notably, not only hyper-stabilisation of U1/5′ ss interactions, but also of U4/U6 inhibits the formation of U6/5′ ss interactions and locks the spliceosome in an inactive state, unable to release U1 and U4 [3, 42, 43]. The triple nt substitution of the U4 cs-1 allele (U4 ^{44}AAA^{46} to ^{44}UUG^{46}), is located immediately downstream of the region that forms U4/U6 stem 1 and results in extended base-pairing between U4 and U6. This sequesters U6 nt that ultimately pair with the 5′ ss (Fig. 5.15 A underlined) [15]. Notably, hyper-stabilisation of stem 1 causes synthetic lethality when combined with *brr2* helicase mutants (Table 5.1, [43]). In conjunction with the Brr2 interaction sites identified in the central domain and stem 1 of U4 (Fig. 5.1 A, 4.6), these observations strongly support the hypothesis that Brr2 translocates along U4 and unwinds U4/U6 stem 1 (Fig. 5.15 B). They also suggest that Brr2-mediated disruption of stem 1 is a primary event, and if inhibited, all concomitant and subsequent events of the activation sequence cannot occur.

Cheng and co-workers report that in pre-activated spliceosomes - which still contain U4 - extended base-pairing can be observed between the 5′ ss and U6 [44, 45]. The initial base pairing involves two sets of ACA tri-nucleotides U6 42-44 and 47-49 of U6 with the UGU at positions +4 to +6 of the intron. Remarkably, this coincides with the area of U6 in which reduced Brr2 interactions were detected (Fig. 5.1, 4.6 B), suggesting that this region of U6 is not in contact with Brr2. Upon dissociation of U4 and binding of the NTC complex the interaction region becomes confined to nt 47-49 in the conserved ACAGA box.

A yeast *trans*-splicing system has demonstrated the existence of U4/5′ ss interactions *in vitro* (Fig. 5.15 C, red dotted arrows). The intron +2 residue cross-links to nt 75, 78 and 82 of U4, demonstrating that during spliceosome assembly U4 comes into close contact with the pre-mRNA [46]. The establishment of U4/5′ ss

cross-links is ATP-dependent and was hence suggested to require Brr2 activity. Based on the Brr2-U4 interaction sites identified in CRAC experiments (Fig. 4.6, 5.15 A), it is feasible that Brr2 translocates along U4 and concomitantly to opening U4/U6 stem 1 frees the central domain of U4 for 5′ ss interactions (Fig. 5.15 C). The U4 and U6 snRNAs are thought to cooperate such that both the U4 central domain and the U6 ACAGA region are dynamically in contact with the 5′ ss (Fig. 5.15 C) [45, 46]. Discontinuous unwinding of the U4/U6 duplex might allow proof-reading of U6/5′ ss contacts, before U4 fully dissociates and formation of the U6 ISL can take place.

Analogy to the minor spliceosome supports discontinuous U4/U6 unwinding. Further evidence for a discontinuous U4/U6 unwinding mechanism comes from studies of the minor spliceosome. During activation the U4atac and U6atac snRNAs of the U12-dependent spliceosome engage in analogous snRNA-snRNA and snRNA-pre-mRNA interactions and therefore represent functional analogs of U4 and U6 snRNAs [47]. Since the minor and major spliceosomes share the same U5 snRNP, the activation processes must be conserved and the same components (including Brr2) must carry out identical functions during catalytic activation.

Intricate psolaren cross-linking experiments demonstrated that activation of the minor spliceosome indeed proceeds via sequential dissociation of U4atac/U6atac stem 1, followed by disruption of U4atac/U6atac stem 2 [48]. An intermediate complex was detected, in which stem 1 is disrupted and a (partial) U6atac/U12 helix I is established [48]. The analogous complex that might form in the major splicosome due to disruption of U4/U6 stem 1 is depicted in Fig. 5.15 D.

Interestingly, the activity of Brr2 is thought to be necessary for stable association of the tri-snRNP with the spliceosome [2, 49]; consistently partial unwinding of the U4/U6 snRNA might aid the early recognition of the 5′ ss and would allow formation of U2/U6 interactions. In this view, formation of complex B and the transition to complex C does not reflect “recruitment” but rather a

stabilisation of RNA-RNA interactions that occur as a consequence of Brr2 (and Prp28) activity [49].

Brr2 might mediate dissociation of U4/U6 stem 2 indirectly. This intermediate complex is inactive until the U6 ISL has formed; this requires disruption of U4/U6 stem 2 (Fig. 5.15 D, E). Apart from Brr2 activity, snRNA binding proteins likely play a key role in destabilising U4/U6 stem 2. Formation of U4/U6 stem 2 and U6 ISL are in competition [50, 51], therefore stem 2 can only be established and maintained with the help of protein factors. U4/U6 annealing requires Prp24 to wedge open the U6 ISL structure to facilitate base-pairing to U4 [52]. Also, the oligomeric Lsm complex aids formation and stabilisation of the U4/U6 duplex [53]. In the U4/U6·U5 tri-snRNP an intricate protein-protein network is established that preserves the U4/U6 conformation [54]. Structural and chemical probing of tri-snRNPs demonstrated that U4/U6 stem 2 and parts of the U4 5′ SL are highly protected against modification and cleavage (Fig. 5.15 A) [38, 55, 56].

Binding of Snu13 (human 15.5K) to the U4 5′ SL results in a sharp bend in the apical stem-loop-stem structure and sequesters single stranded regions into a K-turn [57]. By fastening this conformation, Snu13 acts as a nucleation factor for the assembly and stabilisation of Prp31, Prp3 and Prp4 (analogous to human 61K, 90K and 60K) [58]. Together these proteins (and possibly further U4/U6 specific factors) bridge the U4 5′ SL with U4/U6 stem 2 (Fig. 5.15). Importantly, U4/U6 stem 1 is not required for binding of these proteins, which is consistent with the proposed step wise dissociation of U4/U6 stems 1 and 2 [58].

Prp31 is believed to play an active role in U4/U6 unwinding. Interestingly, a mutant allele *prp31-1* is synthetic lethal with U4 cs-1 [59]. The Nop domain of Prp31 interacts concomitantly with Snu13 and the U4 snRNA, reinforcing their interaction [60]. In tri-snRNPs the 15.5K protein is inaccessible for reaction with antibodies or capture oligos.

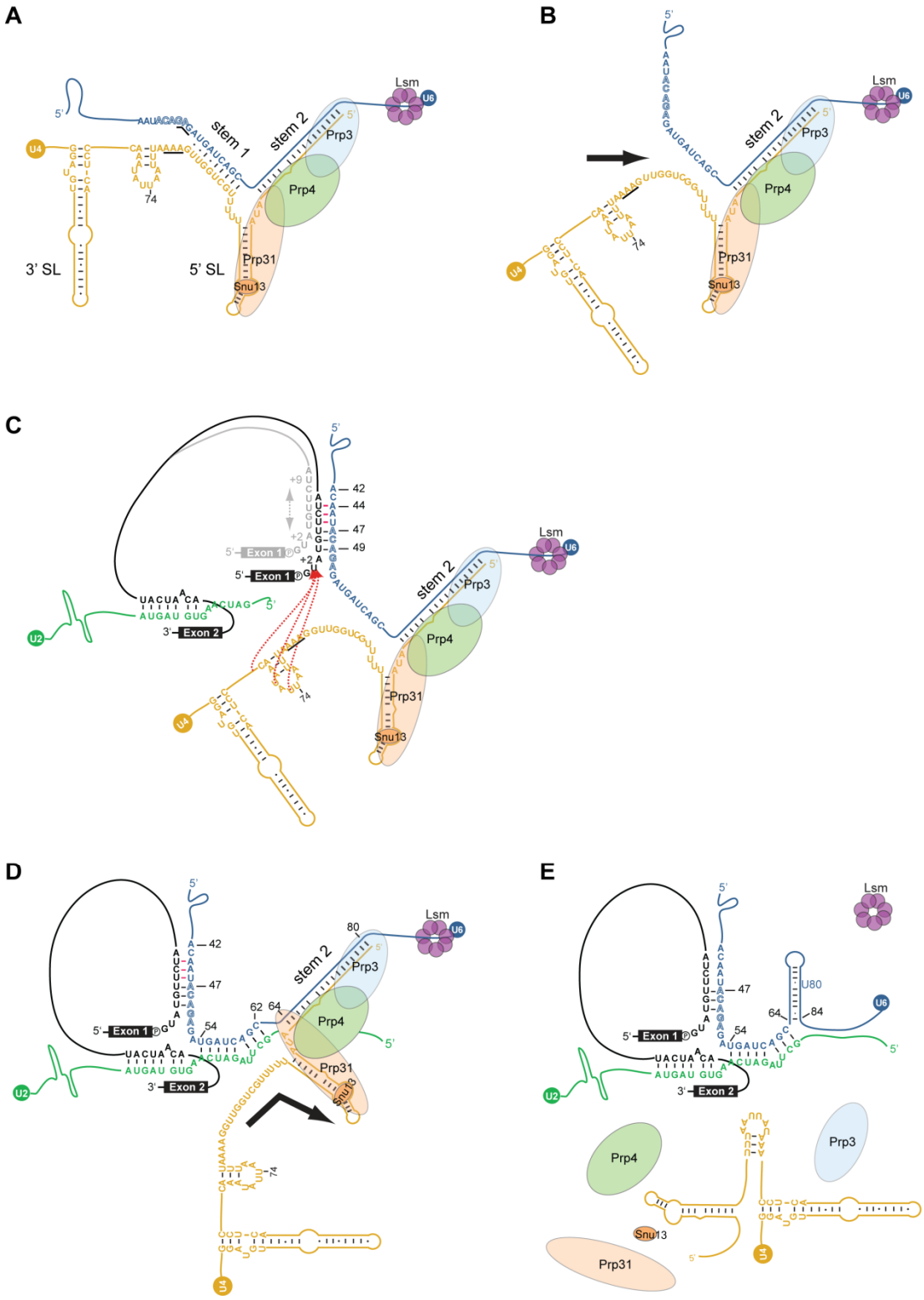

Figure 5.15 Model for Brr2-mediated discontinuous U4/U6 unwinding during spliceosome activation. During spliceosome activation the U4/U6 duplex **(A)** needs to be dissociated to allow the establishment of mutually exclusive base-pairing interactions that are found in a catalytically competent spliceosome **(E).** Legend continues on following page.

Study of Brr2-RNA interaction sites and numerous other studies are consistent with and indicative of a stepwise dissociation of U4/U6 base-pairing which might proceed via the intermediates shown in **B-D** (see Text for details). Bold black arrows **(A+D)** indicate Brr2-mediated conformational changes. Underlined AAA tri-nucleotide in U4 indicates positions substituted in the U4 cs-1 mutant allele and the bases they pair with in U6 **(A-C)** [15]. Dotted red arrows **(D)** indicate U4 cross-links to the +2 residue of the intron [46]. U6/5' ss base-pairing interactions in C and D are shown according to Chan *et al.* (2005), red lines indicate transient interactions detected in U4 associated pre-catalytic spliceosomes. For simplicity, U5-exon interactions were omitted.

However, upon formation of complex B - that is integration of the tri-snRNP into the spliceosome - it becomes accessible [61]. The observed changes in accessibility could be a direct result of Brr2-mediated structural changes in the U4 5′ SL, as suggested by the Brr2-U4 interactions with U4 nt 65-35 (Fig. 5.1 A, 5.15 D). Consistent with this, Pena *et al*. (2009) show that excess Snu13 can reduce Brr2 association to a truncated U4/U6 duplex *in vitro* [37].

The above is compatible with a model in which Brr2 interactions with the U4 5′ SL trigger conformational rearrangements in U4 that directly counteract stable binding of Prp31, Snu13 and the associated protein-RNA network. The resulting destabilisation allows release of U4 and the U4/U6 specific proteins and gives way for the formation of the U6 ISL (Fig. 5.15 E).

Finally, it remains unclear if the events outlined above happen in the suggested order [1, 62]. Alternative pathways are feasible in which these events might occur simultaneously or in a different sequence. Flexibility in the establishment of RNA-RNA interactions that eventually attain the same catalytic configuration might be advantageous, as it would confer additional opportunities for regulation [48].

5.10.2 A possible function for Brr2 in 3' ss selection and exon alignment

Apart from the suggested function of Brr2 in spliceosome activation, I found conclusive evidence for an involvement of Brr2 in the second catalytic step of splicing.

To render the spliceosome competent for second step catalysis several rearrangements must take place (reviewed in [63]). The spliceosome was proposed to have a single active site [64], consequently the product of the first reaction, the branch structure, must be displaced from the catalytic centre. Subsequently, the 3' ss of the intron-lariat intermediate must be positioned at the active site (Fig. 5.16 A). Efficient second step catalysis requires the sites of chemistry to be in close proximity. To achieve this, a number of protein and RNA components need to collaborate:

The U5 loop 1 is of critical importance, because it establishes interactions with both exons and is thought to align them [28, 65]. Earlier models suggested that the terminal nt of both exons base-pair with U5 nt U96; a more recent model suggests that upon positioning of exon 2 the loop nt U96 base-pairs only with the terminal nt of exon 2 (Fig. 5.16 B) [28, 66]. Remarkably, *in vivo* cross-linking and CRAC analysis revealed Brr2 interactions with both U5 nt U96 and the terminal region in exon 2 (Fig. 5.6, 5.13, 5.16 B). Moreover, the size of U5 loop1 influences the arrangement of the exons and their relative positions. For example deletion of nt U96,97,98 was reported to result in exons cross-linking to non-contiguous nt of the loop, thereby keeping the exons at a distance and impairing second step chemistry [23]. The fact that several U5 deletion alleles, including U5ΔU96,97 are synthetic lethal with *brr2* H1 mutants suggests that lack of Brr2 activity adversely affects exon positioning (Fig. 5.6, Table 5.2, [67]). This suggestion is corroborated by the observation that in a U5Δ96,97 background WT Brr2 depletion and reconstitution with *rss1-1* caused a marked inhibition of the second step (Fig. 5.12). These observations are relevant, considering that it remains poorly understood how the

splicing machinery can accomplish the molecular movements needed for 3′ ss positioning and exon 2 alignment relative to U5 loop 1 (Fig. 5.16 A + B).

To achieve positioning of exon 2 it was proposed that U6/5′ ss and U2/U6 base-pairing needs to be disrupted transiently (Fig. 5.16 A, dashed base-pairing) [11, 12]. Genetic experiments implicated the activity of Prp16 in these rearrangements [12, 68], but physical interaction of Prp16 with any of these RNAs has not been demonstrated. Instead, *in vitro* cross-linking studies indicate that Prp16 and Prp22 interact sequentially with different parts of the 3′ ss region [69, 70]. Subsequent to first step catalysis Prp16 interacts with the terminal nt of the intron as well as with up to 13 nt of exon 2 [69, 71]. Subsequent to ATP hydrolysis Prp16 dissociates and Prp22 interacts with the intron region just upstream of the 3′ ss, however it does not interact with exon 2. Binding of Prp22 is thought to represent a transient intermediate prior to the second step in which Prp22 functions independent of ATP hydrolysis to bind to and organize the structure of the last eight intron nucleotides [69, 72]. Brr2 interactions with the 3′ exon (and other sites within the lariat, Fig. 5.14) might occur at the same time, subsequent to Prp16 activity. In this context it is interesting to note that the *rss1-1* allele interacts genetically with several *prp16* helicase/ATPase mutants (Chapter 3, Table 3.2), consistent with both proteins influencing the same process. First biochemical evidence indicates that the physical interaction of Prp16 and Brr2 contributes to regulation of Prp16 activity (O. Cordin unpublished, [73], see Chapter 3).

Three additional factors, namely Prp17, Prp18 and Slu7, are required for the second step. Mutant alleles of all three factors interact with each other and with mutations in U5 loop 1 [74]. Slu7 interacts with and mediates association of Prp18 and Prp22; it also interacts with Brr2 in yeast two-hybrid assays. The latter interaction is thought to allow the initial binding of Slu7 to the spliceosome [73, 75]. Furthermore, Slu7 affects 3′ ss selection [74], and subsequent to ATP hydrolysis by Prp16, Slu7 can also be cross-linked to the 3′ ss [70]. Prp18 functions in stabilising U5 loop 1-exon interactions [66, 76, 77]. Notably, deletion of a highly conserved

region within Prp18 (*prp18ΔCR*) results in a slowed but not abolished second step [77], similar to the defect observed with the *rss1-1* allele (Fig. 5.9). Since overexpression of *SLU7* can suppress the temperature sensitive growth defect of *prp18-1* [78], I attempted to see whether higher or lower expression levels of *SLU7* or *PRP18* affect the *rss1-1* phenotype. However, expression of N-terminally 3HA-tagged Prp18 or Slu7 from a *GalS* promoter was not tolerated in the presence of *rss1-1* (Fig. 5.14). This observation in itself is intriguing, but further experimentation will be required to elucidate the mechanistic basis of this defect.

Interestingly, Slu7 and Prp18 are dispensable for splicing *in vitro* if the 3′ ss is in close proximity to the branch point, i.e. ≤ 9. If the distance between branch point and 3′ ss exceeds 12 nt splicing depends on the presence of both factors [79, 80]. It would be interesting to test if a similar requirement applies to Brr2, and whether the *rss1-1* allele affects splicing of messages with long BP to 3′ ss distances more severely.

The phenotype of the *rss1-1* allele stands out; to my knowledge it is the only known *brr2* allele that inhibits splicing without conferring a clear first step defect (Fig. 5.7, 5.9). Hence, it can be viewed as a separation-of-function mutant.

Sequence comparisons and structural modelling indicated that the Brr2 N-terminal helicase cassette bears strong resemblance to the DNA helicase Hel308 [17, 37]. The structural analogy gave reason to speculate that both factors share a common helicase mechanism. Hel308 features a β-hairpin loop that inserts between the DNA strands, forcing them apart as the helicase translocates [81]. An analogous structure was predicted to exist in the N-terminal helicase-cassette of Brr2 (Fig. 5.17 A) [17, 37]. Remarkably, *rss1-1* carries a single aa substitution, G858R, in the centre of the putative strand separation loop (Fig. 5.17). Pena *et al.* (2009) suggested that the strand separation loop is required for processive unwinding of U4/U6 stems 2 and 1; however this suggestion is hard to reconcile with the *rss1-1* phenotype and the data discussed above.

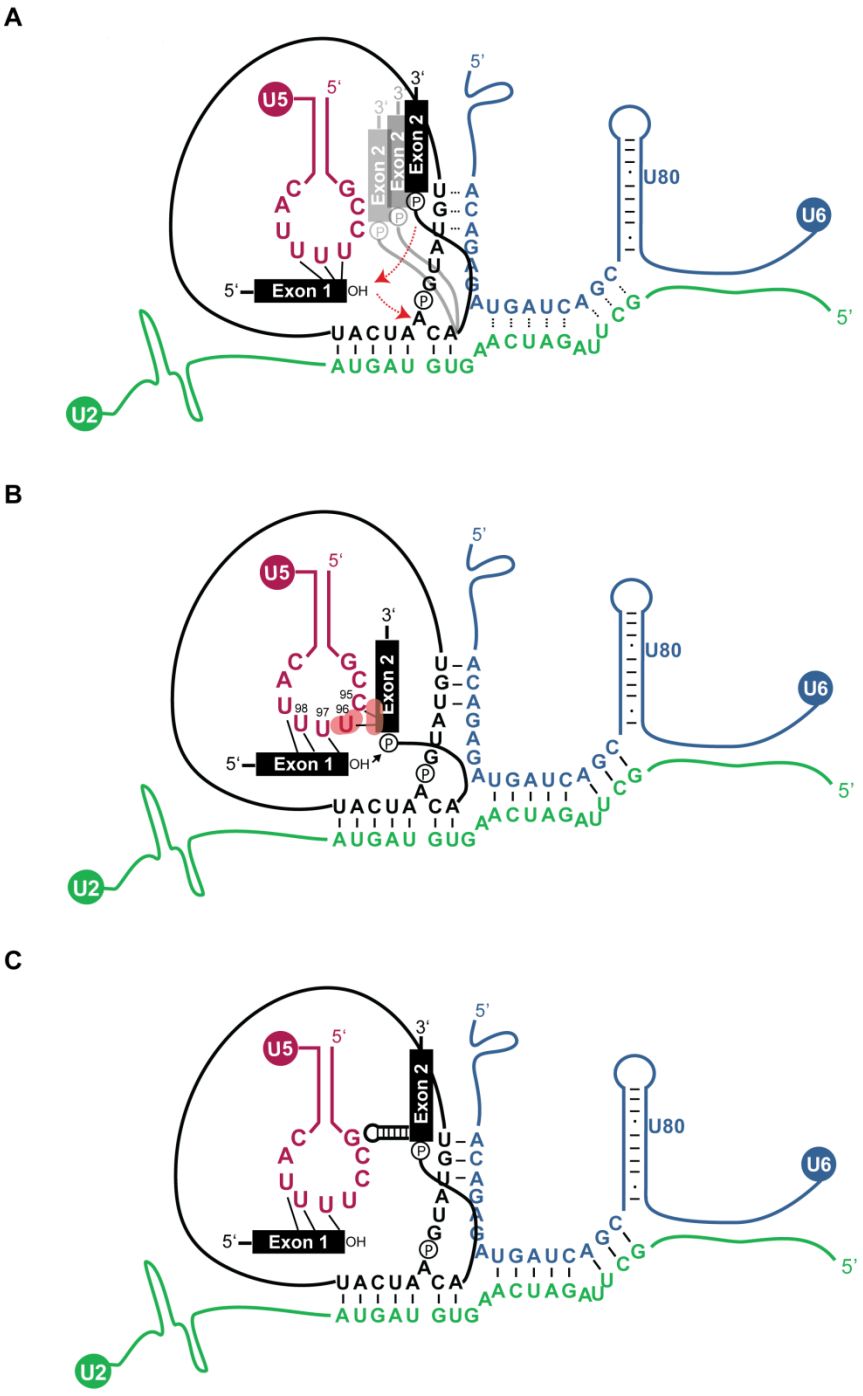

Figure 5.16 Model for Brr2 involvement during the second catalytic step of splicing. **(A)** Subsequent to first step chemistry the catalytic centre of the spliceosome undergoes remodelling. To facilitate the second step, the branch structure must be removed and the 3' ss must be positioned at the catalytic centre (dashed red arrows). Potentially, U6/5' ss and U2/U6 base-pairing needs to be disrupted in order to allow these movements [11, 12] (dashed base-pairing). **(B)** The U5 loop interacts with and aligns the exons, thereby bringing the 3' ss into close proximity to the 3' hydroxyl of exon 1. Figure legend continued on next page.

Red shading indicates Brr2 cross-linking sites. **(C)** Secondary structure in exon 2 might interfere with 3' ss recognition and efficient exon positioning. The observation that Brr2 directly interacts with nt U96 and exon 2 close to the 3' ss suggests its involvement in exon positioning. Brr2 could be required to facilitate exon movement and might resolve secondary structures that interfere with exon alignment (see text for details).

Instead, it seems more likely that an intact strand separation loop of Brr2 fortifies formation of a second step competent spliceosome by aiding 3′ exon positioning.

Several observations suggest that the requirement for Brr2 and the deficiency of *rss1-1* in second step catalysis might be connected to RNA secondary structure elements: The sequence environment of a splice site can affect the efficiency of its usage. In yeast the choice of 3′ ss is believed to be dictated by the distance between BP and the 3′ ss. The formation of secondary structure can, however change the effective distance between BP and 3′ ss. Structural motifs placed between BP and 3′ ss can inhibit the second step of splicing and can impact 3′ ss utilisation [82, 83]. Likewise, introduction of secondary structure elements immediately downstream of the 3′ ss has been shown to inhibit the second step of splicing [24]. Secondary structural elements are thought to hinder the accessibility of sequences to the splicing machinery, and consequently interfere with the juxtaposition of the 3′ ss with the 3′ hydroxyl of exon 1 (Fig. 5.16 C). These considerations could be relevant to the function of Brr2, because the *rss1-1* allele was originally isolated as a trans-acting suppressor of a secondary structure at the 3′ ss, which blocked the second step of splicing [24]. However, suppression was strongly dependent on the secondary structure. While a large 74 nt mutant ribozyme hammerhead structure was suppressed by *rss1-1*, a stem consisting of eight GC base-pairs was not suppressed, instead it exacerbated the second step defect. The mechanism of suppression is thus unknown. One possible explanation is that in the large structure a cryptic 3′ ss could be used efficiently, but the small, perfect stem prevented usage of an alternative AG. Further experimentation is underway, to test whether in the presence of *rss1-1* cryptic 3′ ss are utilised more frequently.

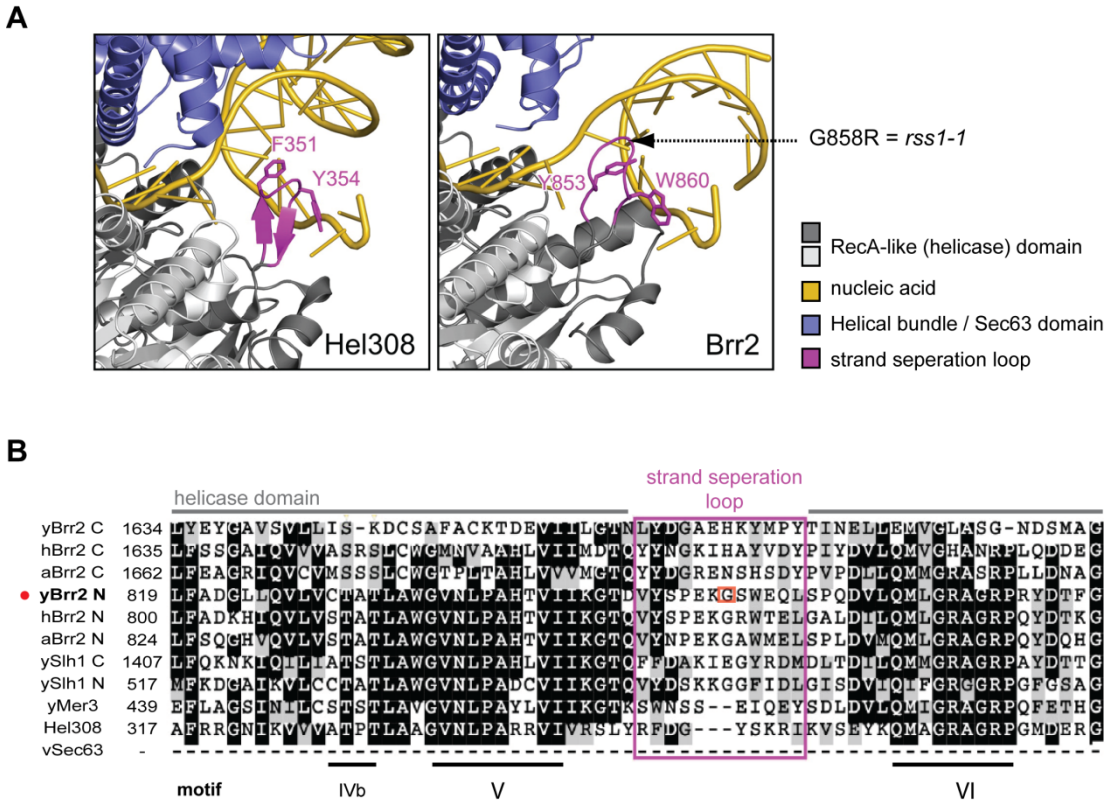

Figure 5.17 Structural model predicts strand separation loop in Brr2 helicase domain. **(A)** Close-up views of **(Left)** ribbon plot of Hel308 DNA helicase [81] (PDB ID 2P6R) and **(Right)** ribbon plot of structural model of Brr2 N-terminal helicase-cassette, including nucleic acid molecule [37]. Arrow indicates position of G858R substitution, which is allelic to *rss1-1*. **(B)** Multiple sequence alignment shows conservation of putative strand separation loop. Comparison of N- and C-terminal cassettes of Brr2 and homologous proteins Slh1 (N- and C-terminal cassettes), Mer3/Hfm1, Hel308 and Sec63. y - yeast; h - human; a - *Arabidopsis thaliana*; Hel308 is from *Archaeglobus fulgidus*. Increasing darkness of background indicates higher degree of conservation. Red circle indicates G858 in the sequence of the N-terminal helicase-cassette of yeast Brr2. A + B are modified from [37].

Regions in 3′ exons to which Brr2 cross-linked in some, but not all cases, correlated to areas with lower free energy (data not shown), indicating that Brr2 might interact with regions prone to the formation of secondary structures. If the putative strand separation loop of Brr2 is needed for resolving secondary structure elements that occur in natural messages, these structures should be stabilised and possibly detectable in the presence of *rss1-1*. Efforts to test this hypothesis are currently ongoing.

Taking all of the above observations into consideration, I suggest that Brr2 aids 3′ exon positioning. Potentially, Brr2 mediates access of factors such as Slu7 and Prp18 to exon sequences. Thereby it helps in bridging the distance between 3′ ss and the active site and contributes to stabilisation of U5-exon interactions.

5.11 References

1. Brow, D.A. (2002) Allosteric cascade of spliceosome activation. Annual Review of Genetics. **36**, 333-360.
2. Raghunathan, P.L. and Guthrie, C. (1998) RNA unwinding in U4/U6 snRNPs requires ATP hydrolysis and the DEIH-box splicing factor Brr2. Current Biology. **8**, 847-855.
3. Kuhn, A.N., Li, Z.R. and Brow, D.A. (1999) Splicing factor Prp8 governs U4/U6 RNA unwinding during activation of the spliceosome. Molecular Cell. **3**(1), 65-75.
4. Laggerbauer, B., Achsel, T. and Luhrmann, R. (1998) The human U5-2OOkD DEXH-box protein unwinds U4/U6 RNA duplices *in vitro*. PNAS. **95**(8), 4188-4192.
5. Small, E.C., Leggett, S.R., Winans, A.A. and Staley, J.P. (2006) The EF-G-like GTPase Snu114p Regulates Spliceosome Dynamics Mediated by Brr2p, a DExD/H Box ATPase. Molecular Cell. **23**, 389-399.
6. Brow, D.A. and Guthrie, C. (1988) The spliceosomal RNA U6 is remarkably conserved from yeast to mammals. Nature. **334**, 213-218.
7. Madhani, H.D. and Guthrie, C. (1992) A novel base-pairing interaction between U2 and U6 snRNAs suggests a mechanism for the catalytic activation of the spliceosome. Cell. **71**, 803-817.
8. Ryan, D.E. and Abelson, J. (2002) The conserved central domain of yeast U6 snRNA: Importance of U2-U6 helix I_a in spliceosome assembly. RNA. **8**, 997-1010.
9. Turner, I.A., Norman, C.M., Churcher, M.J. and Newman, A.J. (2006) Dissection of Prp8 protein defines multiple interactions with crucial RNA sequences in the catalytic core of the spliceosome. RNA. **12**(3), 375-386.
10. Rhode, B.M., Hartmuth, K., Westhof, E. and Lührmann, R. (2006) Proximity of conserved U6 and U2 snRNA elements to the 5' splice site region in activated spliceosomes. EMBO. **25**, 2475-2486.
11. Konarska, M.M., Vilardell, J. and Query, C.C. (2006) Repositioning of the Reaction Intermediate within the Catalytic Center of the Spliceosome. Molecular Cell. **21**, 543-553.
12. Mefford, M.A. and Staley, J.P. (2009) Evidence that U2/U6 helix I promotes both catalytic steps of pre-mRNA splicing and rearranges in between these steps. RNA. **15**, 1386-1397.
13. Hilliker, A.K. and Staley, J.P. (2004) Multiple functions for the invariant AGC triad of U6 snRNA. RNA. **10**, 921-928.
14. Sashital, D.G., Cornilescu, G., McManus, J., Brow, D.A. and Butcher, S.E. (2004) U2/U6 RNA folding reveals a group II intron-like domain and a four-helix junction. Nature Structural & Molecular Biology. **11**, 1237-1242.
15. Li, Z. and Brow, D.A. (1996) A spontaneous duplication in U6 spliceosomal RNA uncouples the early and late functions of the ACAGA element in vivo. RNA. **2**, 879-894.

16. Novak Frazer, L., Lovell, S. and O'Keefe, R.T. (2009) Analysis of Synthetic Lethality Reveals Genetic Interactions Between the GTPase Snu114p and snRNAs in the Catalytic Core of the *Saccharomyces cerevisiae* Spliceosome. Genetics. **183**, 497-515.

17. Zhang, L., Xu, T., Maeder, C., Bud, L.-O., Shanks, J., Nix, J., Guthrie, C., Pleiss, J.A. and Zhao, R. (2009) Structural evidence for consecutive Hel308-like modules in the spliceosomal ATPase Brr2. Nature Structural & Molecular Biology. **16**, 731-739.

18. Hu, J., Xu, D., Schappert, K., Xu, Y. and Friesen, J.D. (1995) Mutational Analysis of *Saccharomyces cerevisiae* U4 Small Nuclear RNA Identifies Functionally Important Domains. Molecular and Cellular Biology. **15**(3), 1274-1285.

19. Dix, I., Russell, C.S., O'Keefe, R.T., Newman, A.J. and Beggs, J.D. (1998) Protein-RNA interactions in the U5 snRNP of Saccharomyces cerevisiae. RNA. **4**, 1239-1250.

20. Frank, D.N., Roiha, H. and Guthrie, C. (1994) Architecture of the U5 small nuclear RNA. Molecular and Cellular Biology. **14**, 2180-2190.

21. Newman, A.J. (1997) The role of U5 snRNP in pre-mRNA splicing. EMBO. **16**(19), 5797-5800.

22. O'Keefe, R.T., Norman, C.M. and Newman, A.J. (1996) The Invariant U5 snRNA Loop1 Sequence Is Dispensable for the First Catalytic Step of pre-mRNA Splicing in Yeast. Cell. **86**, 679-689.

23. O'Keefe, R.T. and Newman, A.J. (1998) Functional analysis of the U5 snRNA loop 1 in the second catalytic step of yeast pre-mRNA splicing. EMBO. **17**(2), 565-574.

24. Lin, J. and Rossi, J. (1996) Identification and characterization of yeast mutants that overcome an experimentally introduced block to splicing at the 3' splice site. RNA. **2**, 835-848.

25. Lesser, C.F. and Guthrie, C. (1993) Mutational analysis of pre-mRNA splicing in *S. cerevisiae* using a sensitve new reporter gene, CUP1. Genetics. **133**, 851-863.

26. Query, C.C. and Konarska, M.M. (2004) Suppression of Multiple Substrate Mutations by Spliceosomal *prp8* Alleles Suggests Functional Correlations with Ribosomal Ambiguity Mutants Molecular Cell. **14**, 343-354.

27. Alexander, R., Barras, D., Dichtel, B., Kos, M., Obtulowicz, T., Koper, M., Karkusiewicz, I., Marikinti, L., Tollervey, D., Dichtel, B., Kufel, J., Bertrand, E. and Beggs, J.D. (2010) RiboSys, a high-resolution, quantitative approach to measure the *in vivo* kinetics of pre-mRNA splicing and 3'-end processing in *Saccharomyces cerevisiae*. RNA. **16**(12), 2570-2580.

28. Newman, A.J. and Norman, C.M. (1992) U5 snRNA interacts with exon sequences at 5' and 3' splice sites. Cell. **68**, 743-754.

29. Sontheimer, E.J. and Steitz, J.A. (1993) The U5 and U6 small nuclear RNAs as the active site components of the spliceosome. Science. **262**, 1989-1996.

30. Newman, A.J., Teigelkamp, S. and Beggs, J.D. (1995) snRNA interactions at 5' and 3' splice sites monitored by photoactivated crosslinking in yeast spliceosomes. RNA. **1**, 968-980.

31. Wlotzka, W., Kudla, G., Granneman, S. and Tollervey, D. (2011) The nuclear RNA polymerase II surveillance system targets polymerase III transcripts. EMBO. **30**(9), 1790-1803.

32. Holstege, F.C., Jennings, E.G., Wyrick, J.J., Lee, T.I., Hengartner, C.J., Green, M.R., Golub, T.R., Lander, E.S. and Young, R.A. (1998) Dissecting the regulatory circuitry of a eukaryotic genome. Cell. **95**(5), 717-728.

33. Bordonne, R., Banroques, J., Abelson, J. and Guthrie, C. (1990) Domains of yeast U4 spliceosomal RNA required for PRP4 protein binding, snRNP-snRNP interactions, and pre-mRNA splicing. Genes & Development. **4**, 1185-1196.

34. Shukla, G.C., Cole, A.J., Dietrich, R.C. and Padgett, R.A. (2002) Domains of human U4atac snRNA required for U12-dependent splicing *in vivo*. Nucleic Acids Research. **30**(21), 4650-4657.

35. Vankan, P., McGuigan, C. and Mattaj, I.W. (1990) Domains of U4 and U6 snRNAs required for snRNP assembly and splicing complementation in *Xenopus* oocytes. EMBO. **9**, 3397-3404.

36. Guthrie, C. and Patterson, B. (1987) Spliceosomal snRNAs. Annual Review of Genetics. **22**, 387-419.

37. Pena, V., Mozaffari Jovin, S., Fabrizio, P., Orlowski, J., Bujnicki, J.M., Lührmann, R. and Wahl, M.C. (2009) Common Design Principles in the Spliceosomal RNA Helicase Brr2 and in the Hel308 DNA Helicase. Molecular Cell. **35**, 454-466.

38. Mougin, A., Gottschalk, A., Fabrizio, P., Luhrmann, R. and Branlant, C. (2002) Direct probing of RNA structure and RNA-protein interactions in purified HeLa cell's and yeast spliceosomal U4/U6.U5 tri-snRNP particles. J Mol Biol. **317**(5), 631-49.

39. Hopfner, K. and Michaelis, J. (2007) Mechanisms of nucleic acid translocaes: lessons from structural biology and single-molecule biophysics. Current Opinion in Structural Biology. **17**, 87-95.

40. Chen, J.Y.-F., Stands, L., Staley, J.P., Jackups, R.R., Latus, L.J. and Chang, T.-H. (2001) Spcific Alterations of U1-C Protein or U1 Small Nuclear RNA Can Eliminate the Requirement of Prp28p, an essential DEAD Box Splicing Factor. Molecular Cell. **7**, 227-232.

41. Murray, H.L. and Jarrell, K.A. (1999) Flipping the Switch to an Active Spliceosome. Cell. **96**, 599-602.

42. Staley, J.P. and Guthrie, C. (1999) An RNA Switch at the 5' Splice Site Requires ATP and the DEAD Box Protein Prp28p. Molecular Cell. **3**, 55-64.

43. Kuhn, A. and Brow, D.A. (2000) Suppressors of a Cold-Sensitive Mutation in Yeast U4 RNA Define Five Domains in the Splicing Factor Prp8 That influence Splicosome Activation. Genetics. **155**, 1667-1682.

44. Chan, S.-P., Kao, D.-I., Tsai, W.-Y. and Cheng, S.-C. (2003) The Prp19-Associated Complex in Spliceosome Activation. Science. **302**, 279-282.

45. Chan, S.-P. and Cheng, S.-C. (2005) The Prp19-associated Complex Is Required for Specifying Interactions of U5 and U6 with Pre-mRNA during Spliceosome Activation. Journal of Biological Chemistry. **280**, 31190-31199.

46. Johnson, T.L. and Abelson, J. (2001) Characterization of U4 and U6 interactions with the 5' splice site using a *S. cerevisiae* in vitro *trans*-splicing system. Genes & Development. **15**, 1957-1970.

47. Tarn, W.Y. and Steitz, J.A. (1997) Pre-mRNA splicing: the discovery of a new spliceosome doubles the challenge. Trends in Biochemical Sciences. **22**, 132-137.

48. Frilander, M.J. and Steitz, J.A. (2001) Dynamic Exchanges of RNA interactions Leading to Catalytic Core Formation in the U12-dependent Spliceosome. Molecular Cell. **7**, 217-226.

49. Maroney, P.A., Romfo, C.M. and Nilsen, T.W. (2000) Functional recognition of the 5' splice site by the tri-snRNP defines a novel ATP-dependent step in early spliceosome assembly. Molecular Cell. **6**, 317-328.

50. McManus, J., Schwartz, M.L., Butcher, S.E. and Brow, D.A. (2007) A dynamic bulge in the U6 RNA internal stem-loop functions in spliceosome assembly and activation. RNA. **13**, 2252-2265.

51. Brow, D.A. and Vidaver, R.M. (1995) An element in human U6 snRNA destabilizes the U4/U6 spliceosomal RNA complex. RNA. **1**, 122-131.

52. Martin-Tumasz, S., Reiter, N.J. and Brow, D.A. (2010) Structure and functional implications of a complex containing a segment of U6 RNA bound by a domain of Prp24. RNA. **16**, 792-804.

53. Achsel, T., Brahms, H., Kastner, B., Bachi, A., Wilm, M. and Lührmann, R. (1999) A doughnut-shaped heteromer of human Sm-like proteins binds to the 3'-end of U6 snRNA, thereby facilitating U4/U6 duplex formation. EMBO. **18**(22), 5789-5802.

54. Liu, S., Rauhut, R., Vornlocher, H.-P. and Lührmann, R. (2006) The network of protein-protein interactions within the human U4/U6.U5 tri-snRNP. RNA. **12**, 1418-1430.

55. Xu, Y., Petersen-Bjorn, S. and Friesen, J.D. (1990) The PRP4 (RNA4) protein of *Saccharomyces cerevisiae* is associated with the 5' portion of the U4 small nuclear RNA. Molecular and Cellular Biology. **10**, 1217-1225.

56. Black, D.L. and Steitz, J.A. (1986) Pre-mRNA splicing *in vitro* requires intact U4/U6 small nuclear riobonucleoprotein. Cell. **46**, 697-704.

57. Vidovic, I., Nottrott, S., Hartmuth, K., Lührmann, R. and Ficner, R. (2000) Crystal structure of the spliceosomal15.5kD protein bound to a U4 snRNA fragment. Molecular Cell. **6**, 1331-1342.

58. Nottrott, S., Urlaub, H. and Lührmann, R. (2002) Hierarchical, clustered protein interactions with U4/U6 snRNA: a biochemical role for U4/U6 proteins. EMBO. **12**(20), 5527-5538.

59. Kuhn, A.N., Reichl, E.M. and Brow, D.A. (2002) Distinct domains of splicing factor Prp8 mediate different aspects of spliceosome activation. PNAS. **99**(14), 9145-9149.

60. Liu, S., Li, P., Dybkov, O., Nottrott, S., Hartmuth, K., Lührmann, R., Carlomango, T. and Wahl, M.C. (2007) Binding of the Human Prp31 Nop Domain to a Composite RNA-Protein Platform in U4 snRNP. Science. **316**, 115-120.

61. Nottrott, S., Hartmuth, K., Fabrizio, P., Urlaub, H., Vidovic, I., Ficner, R. and Lührmann, R. (1999) Functional interaction of a novel 15.5kD [U4/U6·U5] tri-snRNP protein with the 5' stem-loop of U4. EMBO. **18**(21), 6119-6133.

62. Fortner, D.M., Troy, R.G. and Brow, D.A. (1994) A stem/loop in U6 small nuclear RNA defines a conformational switch required for pre-mRNA splicing. Genes & Development. **8**, 221-233.

63. Umen, J.G. and Guthrie, C. (1995) The second catalytic step of pre-mRNA splicing. RNA. **1**, 869-885.

64. Steitz, T.A. and Steitz, J.A. (1993) A general two-metal-ion mechanism for catalytic RNA. PNAS. **90**, 6498-6502.

65. Newman, A.J. and Norman, C.M. (1991) Mutations in yeast U5 snRNA alter the specificity of 5' splice-site cleavage. Cell. **65**, 115-123.

66. Crotti, L.B., Bacikova, D. and Horovitz, D.S. (2007) The Prp18 protein stabilizes the interaction of both exons with the U5 snRNA during the second step of pre-mRNA splicing. Genes & Development. **21**, 1204-1216.

67. Field, D. and Friesen, J.D. (1996) Functionally redundant interactions between U2 and U6 spliceosomal snRNAs. Genes & Development. **10**, 489-501.

68. Madhani, H.D. and Guthrie, C. (1994) Genetic interactions between the yeast RNA helicase homolog Prp16 and spliceosomal snRNAs identify candidate ligands for the Prp16 RNA-dependent ATPase. Genetics. **137**, 677-687.

69. McPheeters, D.S. and Muhlenkamp, P. (2003) Spatial Organization of Protein-RNA Interactions in the Branch Site-3' Splice Site Region during pre-mRNA Splicing in Yeast. Molecular and Cellular Biology. **23**(12), 4174–4186.

70. Umen, J.G. and Guthrie, C. (1995) Prp16p, Slu7p, and Prp8p interact with the 3' splice site in two distinct stages during the second catalytic step of pre-mRNA splicing RNA. **1**, 584-597.

71. Schwer, B. and Guthrie, C. (1992) A conformational rearrangement in the splicosome is dependent on PRP16 and ATP hydrolysis. EMBO. **11**(13), 5033-5039.

72. Schwer, B. and Gross, C.H. (1998) Prp22, a DExH-box RNA helicase, plays two distinct roles in yeast pre-mRNA splicing. EMBO. **17**, 2086-2094.

73. van Nues, R. and Beggs, J.D. (2001) Functional Contacts With a Range of Splicing Proteins Suggest a Central Role for Brr2p in the Dynamic Control of the Order of Events in Spliceosomes of *Saccharomyces cerevisiae*. Genetics. **157**, 1457-1467.

74. Frank, D.N. and Guthrie, C. (1992) An essential splicing factor, *SLU7*, mediates 3' splice site choice in yeast. Genes & Development. **6**, 2112-2124.

75. James, S.-A., Turner, W. and Schwer, B. (2002) How Slu7 and Prp18 cooperate in the second step of yeast pre-mRNA splicing. RNA. **8**, 1068-1077.

76. Bacikova, D. and Horovitz, D.S. (2005) Genetic and functional interaction of evolutionarily conserved regions of the Prp18 protein and the U5 snRNA. Molecular and Cellular Biology. **25**, 2107-2116.

77. Bacikova, D. and Horovitz, D.S. (2002) Mutational analysis identifies two separable roles of the *Saccharomyces cerevisiae* splicing factor Prp18. RNA. **8**, 1280-1293.

78. Jones Haltiner, M., Frank, D. and Guthrie, C. (1995) Characterisation and functional ordering of Slu7p and Prp17p during the second step of pre-mRNA splicing in yeast. PNAS. **92**, 9687-9691.

79. Zhang, X. and Schwer, B. (1997) Functional and physical interaction between the yeast splicing factors Slu7 and Prp18. Nucleic Acids Research. **25**(11), 2146-2152.

80. Brys, A. and Schwer, B. (1996) Requirement for SLU7 in yeast pre-mRNA splicing is dictated by the distance between the branchpoint and the 3' splice site. RNA. **2**, 707-717.

81. Buttner, K., Nehring, S. and Hopfner, K. (2007) Structural basis for DNA duplex separation by a superfamily-2 helicase. Nature Structural & Molecular Biology. **14**, 647-652.

82. Deshler, J.O. and Rossi, J. (1991) Unexpected point mutations activate cryptic 3' splice sites by perturbing a natural secondary structure within a yeast intron. Genes & Development. **5**, 1252-1263.

83. Liu, Z.-R., Laggerbauer, B., Lührmann, R. and Smith, C.W.J. (1997) Crosslinking of the U5 snRNP-specific 166-kDa protein to RNA hairpins that block step 2 of splicing. RNA. **3**, 1207-1219.

Chapter 6 – CLASH analysis of Brr2-U2 interactions

6.1 Acknowledgement

The work presented in Chapter 6 was performed in collaboration with Dr. Sander Granneman and Dr. Grzegorz Kudla, Wellcome Trust Centre for Cell Biology, University of Edinburgh. Special credit needs to be given to Dr. Kudla whose invaluable knowledge in the development and employment of bioinformatics tools form the basis for the analyses described below. All experimental procedures were carried out by me. Part of the work presented in Chapter 6 was published [1].

6.2 Introduction

The identification of RNA-RNA interactions is essential for a detailed understanding of many biological processes. Almost all RNAs must be correctly folded in order to function. Base-pairing between different RNA molecules underlies many pathways of RNA metabolism, including pre-mRNA splicing [2]. As described in Chapter 1 pre-mRNA splicing requires five snRNAs which, during the splicing process, engage in base-pairing interactions with themselves, with one-another and with the pre-mRNA substrate. Key to the splicing reaction is the dynamic but highly ordered establishment and/or disruption of these base-pairing interactions [3]. Classical approaches for studying such RNA-RNA interactions range from X-ray crystallography, NMR and psoralen cross-linking to genetic analyses. Some of these methods, e.g. X-ray crystallography and NMR are labour intensive and very difficult to apply to dynamic RNA-RNA interactions, let alone in

the context of large RNPs. Psolaren cross-linking studies require prior knowledge of the interacting partners and are limited in resolution. Although genetic analyses have been instrumental in studying the spliceosome, they rely on the occurrence of detectable phenotypes, and often information derived from genetic analyses cannot be interpreted unambiguously. Alternatively, RNA base-pairing can be inferred from a combination of bioinformatics and evolutionary analyses. However, computational methods are applicable only to evolutionarily conserved interactions and, on their own provide little information.

A second important element in understanding RNP function and architecture is the identification of protein-RNA interactions. Recently, cross-linking and sequencing approaches have lead to substantial progress in this area [4, 5]. However, knowledge of protein-RNA binding sites is most informative when it can be combined with information on RNA secondary structure.

As described below, a novel approach uses sequence information from protein-RNA cross-linking experiments to infer the secondary structure of RNA that is directly associated with the protein analysed. It thus provides information about RNA-RNA interactions in RNPs, *in vivo* [1].

6.3 CLASH identifies RNA secondary structure

As described in Chapter 4 the CRAC procedure involves *in vivo* UV cross-linking and affinity purification of protein-RNA complexes (section 4.3, Fig. 4.1). The ligation of oligonucleotide linkers to the immobilized RNA allows generating cDNA libraries that are compatible with high-throughput sequencing [6].

Basic to the identification of protein-associated RNA secondary structure is the following notion: Cross-linking of (partially) base-paired RNA molecules, or cross-linking of two RNA molecules in very close proximity, can arrest the (relative) position of these RNA molecules on the protein. Limited RNase digestion can generate ends compatible for ligation. In the presence of RNA ligase these ends can

then be joined, generating chimeric RNAs (Fig. 6.1). The two remaining ends of the chimeric RNAs are available for linker ligation, allowing subsequent cDNA synthesis, PCR amplification and sequencing. In the end, the structural and positional information of the cross-linked RNAs is contained in the chimeric sequence.

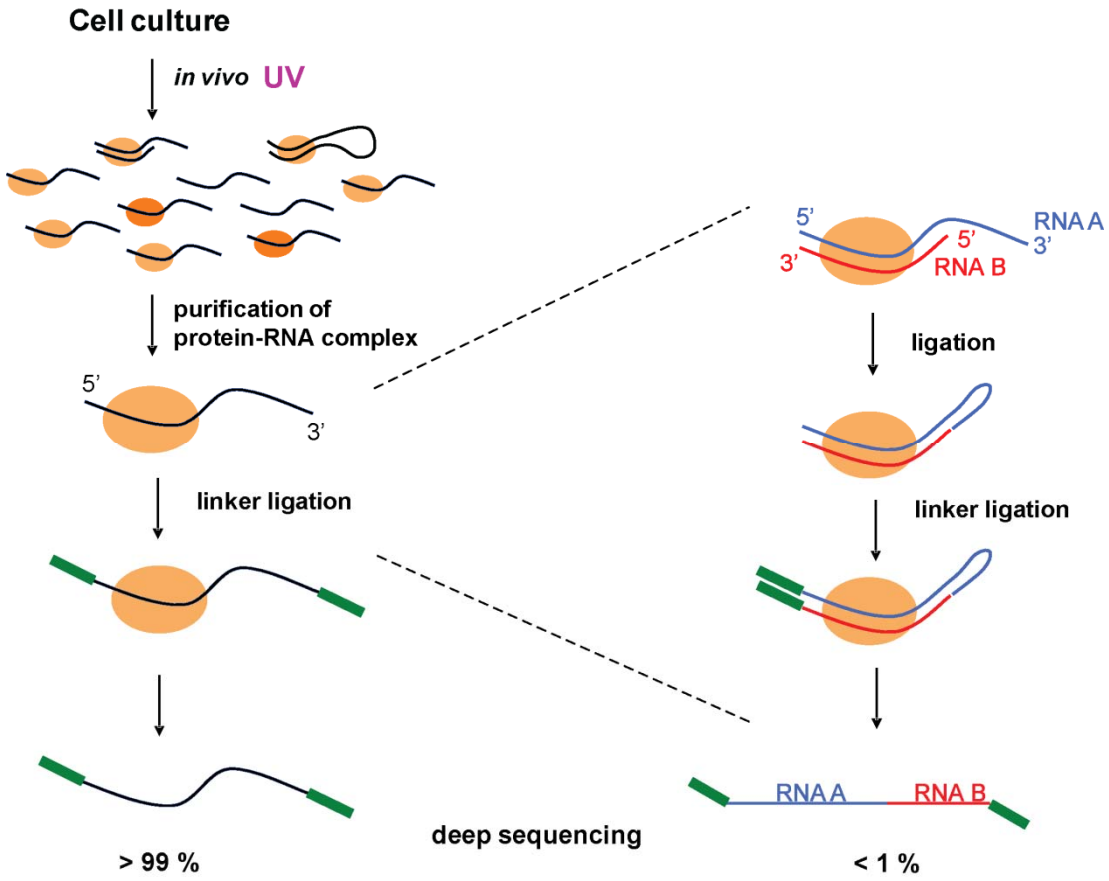

Figure 6.1 Generation of chimeric RNAs in cross-linking and cloning experiments. (Left) During *in vivo* UV cross-linking protein and RNA can be covalently joined, allowing purification of RNA-protein complexes. Ligation of oligonucleotide linkers to the cross-linked RNA allows generation of a cDNA library (CRAC). **(Right)** In rare events free ends of different RNA molecules or different parts of one RNA molecule can be ligated together, resulting in a chimeric RNA. Its remaining free ends are available for ligation of cloning linkers, which allows cDNA synthesis and sequencing of the chimeric molecule.

In CRAC experiments carried out under standard conditions the formation of chimeric cDNAs is a rare event and generally accounts for less than 1% of all sequence reads. Ligation of free RNA ends is most easily realized if the two RNA fragments are stably base-paired, providing free ends in close proximity yet long enough to make contact to each other [1]. Chimeric sequences can be distinguished from non-chimeric sequences computationally. The approach to identifying and analyzing such chimeric sequences has been described as "Cross-linking, ligation and sequencing of hybrids" (CLASH) [1].

Here the computational identification of chimeric sequences associated with the Brr2 helicase was used to study features of RNA secondary structure in the spliceosome.

6.4 Brr2-associated chimeric sequences

To identify chimeric reads CLASH analysis was applied to high-throughput sequence data derived from cross-linking experiments with brr2 N-HTP and Brr2-HTP (Chapter 4). Sequencing reads were analyzed using stringent quality filters, selecting only those reads that were composed of two distinct fragments that could be mapped separately, either to different RNA molecules or to distinct regions of the same molecule. 0.62 % of all reads from the brr2 N-HTP dataset and 0.83% of the full-length Brr2 dataset met these criteria (Table 6.1).

Table 6.1 Brr2-associated chimeric sequence reads

sequence type / abundance	brr2 N-HTP	Brr2-HTP
total number of reads	9,291,740	10,982,673
total number chimeric reads	57,666	81.204
% chimeric reads	0.62%	0.83%

Table 6.2 Brr2-associated snRNA-snRNA chimeras

snRNA-snRNA hybrids	*brr2 N-HTP*	*Brr2-HTP*
∑	**43522**	**74609**
U2-U2	43126	74585
U4-U6	372	5
U4-U4	14	10
U4-U2	10	9

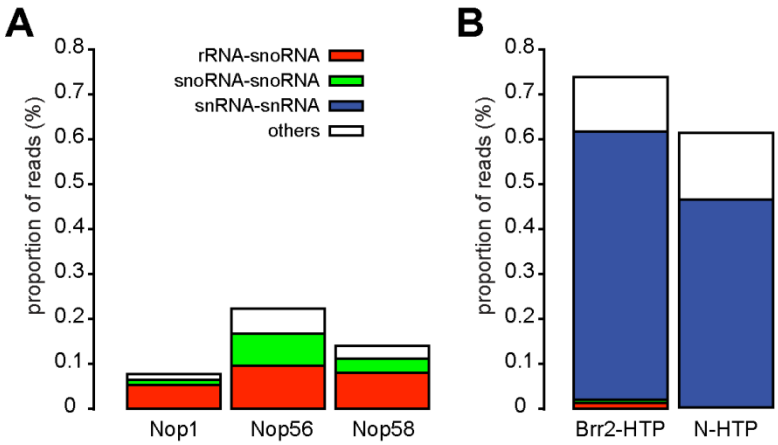

Figure 6.2 snRNA-snRNA hybrids account for the majority of Brr2-associated chimeric sequences. Classification of chimeric reads that were identified in sequence datasets of cross-linking experiments of the pre-rRNA processing factors Nop1, Nop56 and Nop58 (S. Granneman) **(A)** as well as of Brr2-HTP and brr2 N-HTP **(B)**. Modified from [1].

None of the chimeric reads could be fully aligned to a database of spliced yeast transcripts, indicating that the chimeras do not represent conventional splicing events. In most cases, the two mapped fragments were directly fused in the read. Chimeric reads previously identified by high-throughput sequencing have been attributed to reverse transcriptase template switching. However, comparison of the two regions of the chimeras did not exhibit the short sequence homology that is indicative of template switching [7]. This suggests that template switching was not the main source for the chimeric sequences identified here.

The formation of chimeric sequences does not seem to occur by random events, as the types of chimeric sequences identified clearly reflect the biological

function of the protein in question. The vast majority of Brr2 associated chimeric sequences stemmed from snRNA-snRNA ligation events, highly consistent with Brr2 being a spliceosomal RNA helicase (Table 6.2, Fig. 6.2). By comparison, the chimeric reads identified for the pre-rRNA processing factors Nop1, Nop56 and Nop58 (S. Granneman) show mainly snoRNA-rRNA and snoRNA-snoRNA chimera, reflecting these proteins' involvement in pre-ribosome biogenesis [1].

Amongst all snRNA-snRNA chimeras obtained with Brr2-HTP or brr2 N-HTP only very few stemmed from the ligation of U4-U6, U4-U4 or U2-U4 fragments (Table 6.2). In contrast, chimeric sequences composed of U2-U2 fragments were most abundant, accounting for > 90% of all snRNA-snRNA hybrids. Notably, precisely the same U2-U2 ligation events were identified in the brr2 N-HTP and Brr2-HTP datasets (data not shown), indicating that they represent meaningful U2-U2 and Brr2-U2 interactions. Because the identified sequences were located in poorly characterised regions of U2, they were investigated further.

6.5 U2-U2 hybrids suggest revised U2 structure

The distribution and frequency of all U2-U2 chimeras found in the Brr2-HTP dataset are shown in Fig. 6.3. The heat-map depicts the ligation points by indicating the end point of the first fragment (x axis) and the start point of the second fragment that was joined to it (y axis), relative to the U2 snRNA sequence. Plotted in this way, the U2-U2 chimeras formed three major clusters. These were interpreted to represent two intra-molecular stems within U2 (stems IV and V), with stem V recovered in both orientations (Fig. 6.3). This interpretation is supported by the propensity of chimeric sequences within U2 to form stable stems *in silico*. The hybrid-ss-min folding [8] algorithm was applied to *S. cerevisiae* U2, using the predicted stems as structural constraints. The structure shown in Fig. 6.3 (Bottom) was obtained.

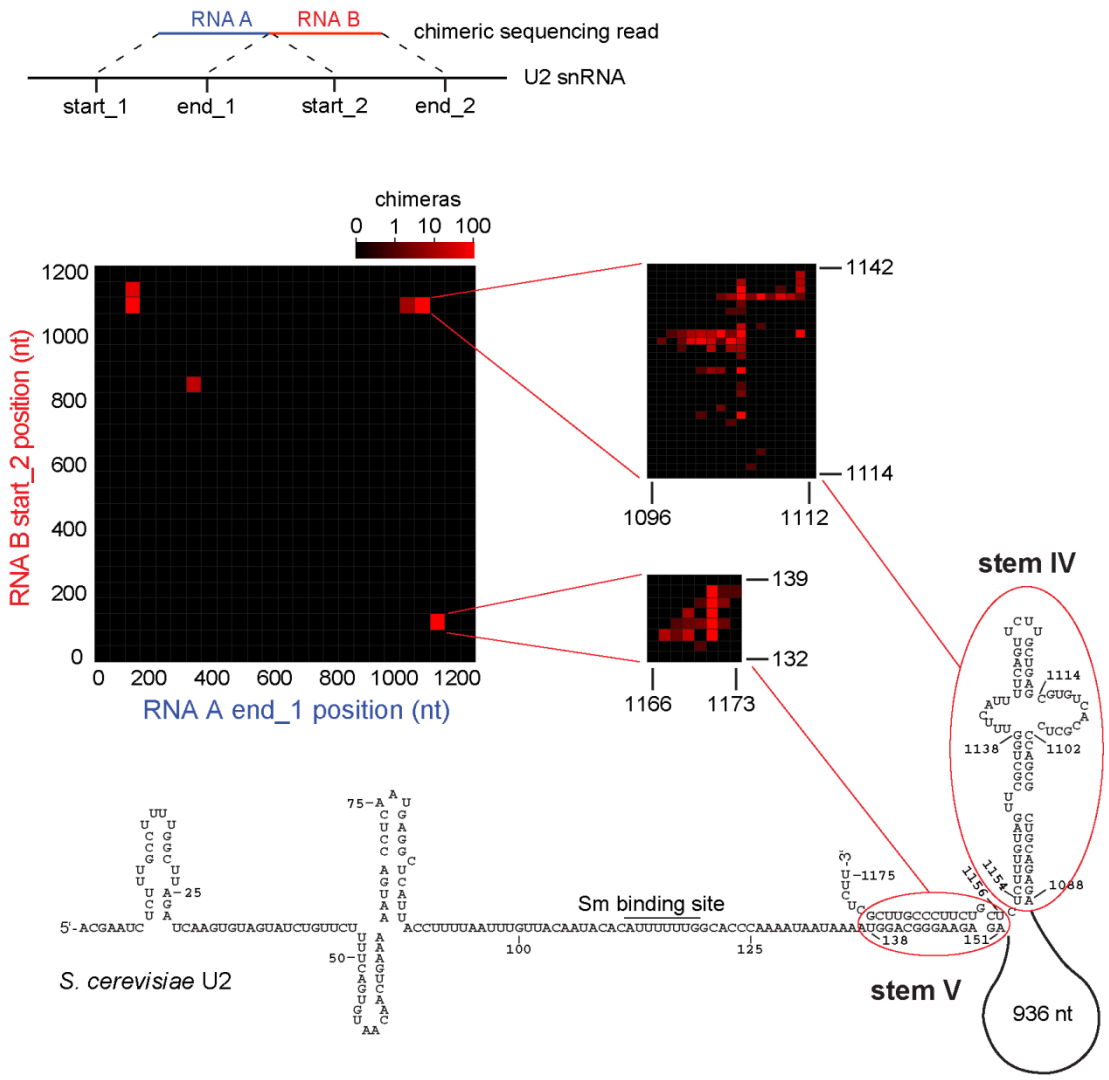

Figure 6.3 Chimeric U2-U2 sequence reads suggest secondary structure of U2 3' domain. (Top) The diagram indicates the positions of U2 fragments found in chimeric sequences. **(Middle)** Heat-map depicts ligation points of U2-U2 chimeric reads. The x axis represents the end position (nt) in U2 where the first fragment of the chimera was mapped. The y axis shows the start position (nt) of the second fragment. Red colour intensity indicates the number of chimeric reads identified. The insets show the main peaks at higher resolution. The peaks in the lower right and upper left corners correspond to the same stem ligated at the opposite ends. **(Bottom)** Secondary structure of U2 inferred from the chimeric reads. Figure modified from [1].

The novel structure is substantially different from previously proposed structures for the 3' domain of yeast U2, but more similar to mammalian U2 (Fig. 6.4 A + B) [9, 10]. A significant difference is that in the revised folding the 3' region is engaged in a stable stem structure termed stem IV. This feature can be found in many U2 homologues, including mammalian and Trypanosoma U2, and is expected to help

stabilize the RNA [11]. An internal bulge in stem IV contains a stretch of conserved nucleotides homologous to the loop sequence of the 3′ stem in human U2, which binds the hU2B′′ protein (nt 1103-1114, Fig. 6.3) [12]. Another significant difference is observed in stem V. Stem V is formed by a long-range interaction that brings the extreme 3′ end and the 5′ domain into close proximity (Fig. 6.4). The large 936 nt central region is shown "looped-out" of the structure.

6.6 Distribution of non-chimeric sequencing reads in U2 matches chimeric reads

In yeast the U2 snRNA is 1175 nt long, much larger than e.g. human U2 (187 nt). It contains a central region (nt 123-1068) which can be deleted without affecting cell viability [13, 14]. Even splicing can function in the absence of the central domain [9, 10]. Interestingly, all Brr2 interaction sites in the U2 snRNA were found within this central domain, or 3′ to it.

Figure 6.4 C shows the non-chimeric Brr2 interaction sites identified in U2 (here showing only reads for full-length Brr2, which were strikingly similar to brr2 N-HTP reads; see Chapter 4 for details). Interaction sites were found in defined positions, indicated by five sharp peaks. Coloured regions highlight where these areas are located within the U2 secondary structures (Fig. 6.4 A + B). When comparing chimeric and non-chimeric Brr2 interaction sites in U2, it appears that three out of the five major interaction sites contain sequences that can be found as part of chimeras (Fig. 6.4 red and blue colour). Thus, Brr2 cross-linking sites in U2 are highly compatible with the U2-U2 chimeras and the secondary structure inferred from them.

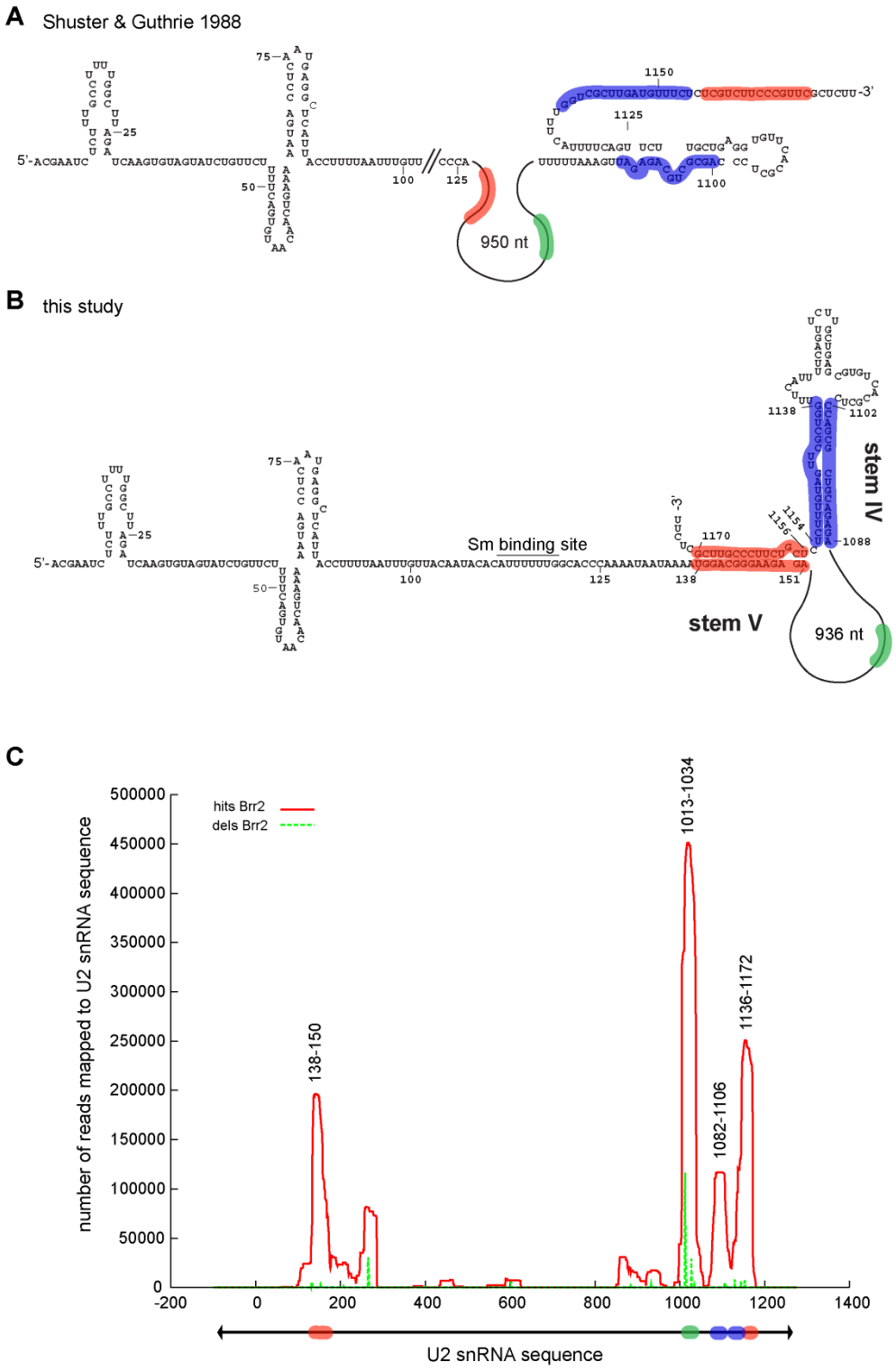

Figure 6.4 Non-chimeric Brr2 cross-links are consistent with revised model of U2 3' domain. Comparison of *S. cerevisiae* U2 secondary structures. **(A)** Previously suggested structure based on Shuster & Guthrie (1988). **(B)** Revised structure, predicted by CLASH analysis of U2-U2 hybrid sequences. **(C)** Distribution of non-chimeric Brr2 sequence reads mapped to U2 snRNA. Coloured shading indicates that 3 out of the five main Brr2 cross-linking sites correspond to the predicted stems IV and V in the 3' domain of U2.

However, not all identified Brr2-U2 cross-links lead to the formation of chimeras. In fact, the most abundant interaction site in nt 1013-1034 (green in Fig. 6.4) was not identified as part of a chimeric sequence.

6.7 Phylogenetic analysis supports revised structure of U2 3' domain

The comparative analysis of homologous RNAs can be used to assess the conservation of RNA secondary structure. It assumes that the biological function of homologous RNAs has been conserved in evolution by retaining the same folding architecture. Consequently, a consensus secondary structure can be derived from the alignment of homologous RNAs.

To validate the U2 secondary structure inferred from the CLASH analysis (Fig. 6.3) the evolutionary conservation of U2 sequences from different yeast species was analyzed. U2 sequences of *Saccharomyces mikatae* and *Saccharomyces kudriavzevii* were aligned to the *S. cerevisiae* U2, based on sequence similarity. The pfold secondary structure prediction algorithm was then applied to the alignment [15]. Conservation of stems IV and V predicted in the U2 3' domain was supported in all three species. None of the base substitutions in *Saccharomyces mikatae* and *Saccharomyces kudriavzevii* were predicted to interfere with stem formation, while the occurrence of compensatory base changes strongly supports the predicted secondary structure (Fig. 7.5 *Saccharomyces mikatae* (blue boxes) and *Saccharomyces kudriavzevii* (red boxes)). By contrast, the previously suggested *S. cerevisiae* U2 structure (Shuster & Guthrie, 1988) was not supported by evolutionary analysis (Fig. 6.5).

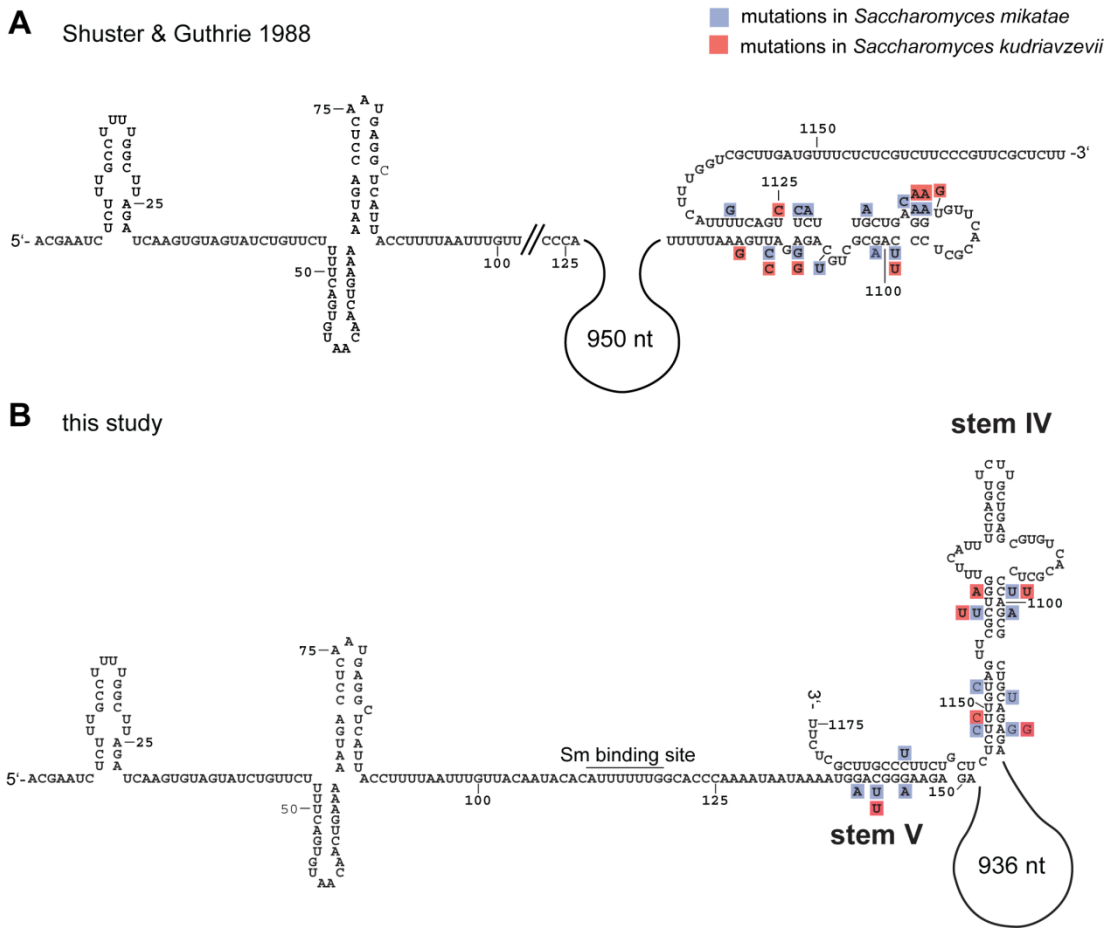

Figure 6.5 Compensatory base changes support revised U2 structure. Comparative analysis of *S. cerevisiae, S. mikatae* and *S. kudriavzevii* U2 snRNA by sequence alignment and pfold secondary structure prediction [15]. Compensatory base changes identified in *S. mikatae* and *S. kudriavzevii* are indicated by blue and red boxes, respectively. **(A)** Shows previously suggested structure of *S. cerevisiae* U2 [14], **(B)** shows revised U2 structure [1].

6.8 Mutations in U2 3' domain cause mis-processing

For further validation of the predicted folding, the phenotypes of mutations expected to interfere with formation of stem IV and/or stem V were analyzed. In order to replace WT U2 with mutant versions, a U2 plasmid-shuffle strain (W303 U2Δ, Table 2.6) was created. W303 U2Δ was constructed by replacing one genomic copy of the snR20 gene (encoding the U2 snRNA) with the *KanMX6* cassette in a diploid W303 strain (2.9.5). Colony PCR (2.11.10.2) confirmed the heterozygous deletion. Subsequently the *URA3* marked plasmid pRS416-U2 was introduced and

snR20Δ haploids (W303 U2Δ) were obtained by sporulation and tetrad dissection (2.9.6). The wild type snR20 gene was cloned into pRS314 to create pRS314-U2 (Table 2.10). Mutant derivatives of pRS314-U2 were generated by SDM (2.11.10.3). Transformation of W303 U2Δ with plasmids encoding WT or mutant U2 snRNA and cultivation on 5-FOA containing medium (2.2.2) allowed counter selection of the *URA3* marked plasmid and testing for complementation by plasmid-shuffle (2.9.8). All U2 mutant alleles tested supported growth on 5-FOA and were viable (Table 6.3).

When point mutations were introduced to stem IV (Fig. 6.6), no measurable effect on yeast growth rates (at high or low temperature) could be observed (Table 6.3). The stability and abundance of the U2 snRNA was assessed by Northern blot analyses (2.12.6). Single point mutations or combinations of mutations (Fig. 6.6) introduced to stem IV showed no apparent effect (Fig. 6.7 A, Table 6.3).

Although deleting the 5′ branch of stem V had no effect on growth rates (Table 6.1, Fig. 6.9), Northern blot analysis showed the appearance of a truncated 5′ fragment of U2 ~130 nt in size (Fig. 6.7 B). To examine the requirement for stem V further, the 5′ and 3′ branches of stem V were individually replaced with scrambled sequence in order to prohibit normal formation of stem V. The sequences used to substitute the 3′ and/or 5′ branches of stem V were designed to be non-complementary to the opposite WT branch or any other region in U2, but to restore base-pairing when combined. Further, the sequences were chosen to achieve a comparable number of base-pairs and a folding energy similar to that of the WT stem (Fig. 6.6). When scrambled sequence was introduced to either the 3′ or 5′ side of stem V, a short U2 5′ fragment was observed. Restoring base-pairing in stem V with synthetic sequence reduced the abundance of the U2 5′ fragment, although it could not be reduced to WT level.

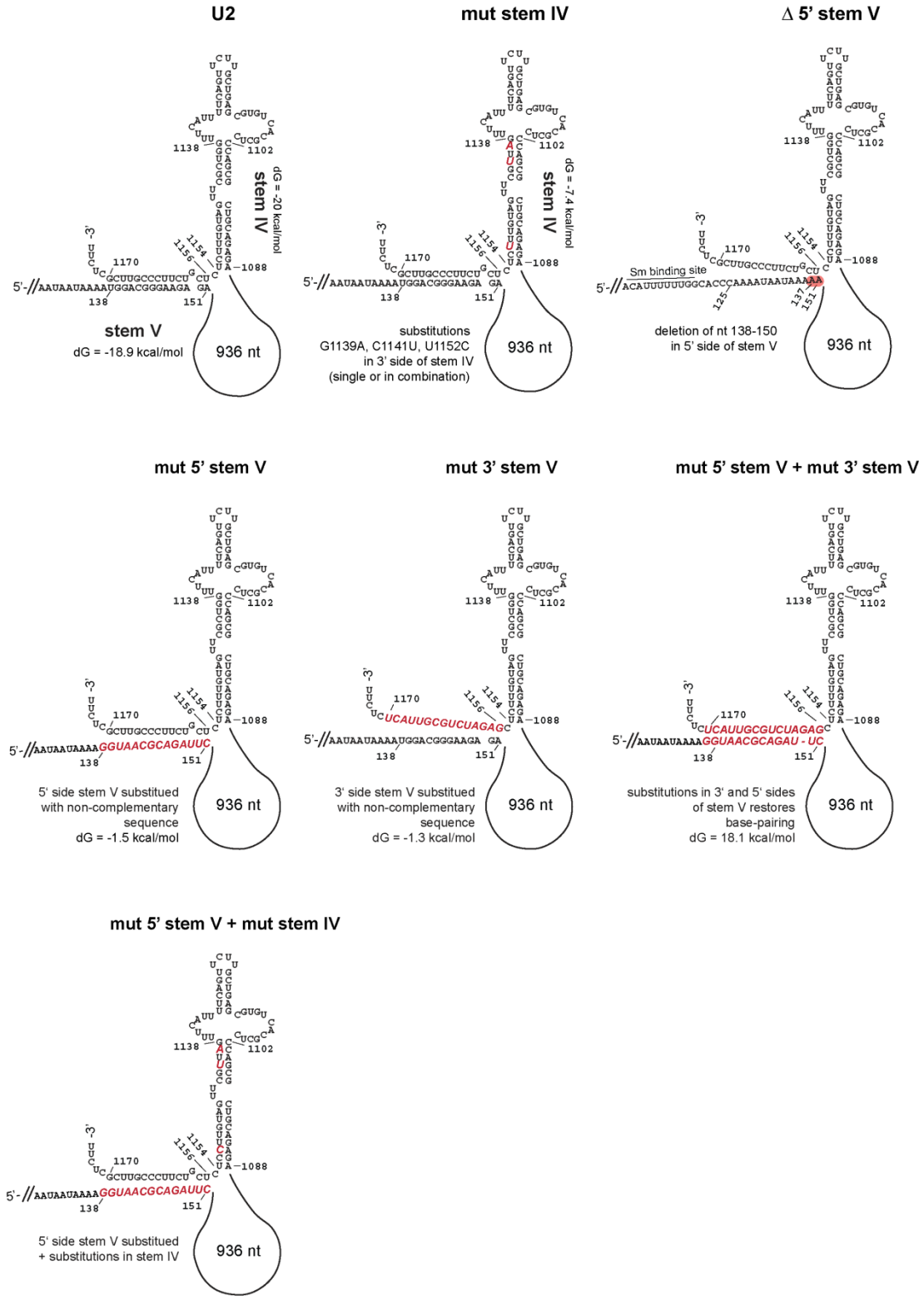

Figure 6.6 Changes introduced to the U2 3' domain. U2 (top, left) shows predicted folding of the WT U2 3'domain. All changes introduced to mutants are indicated by red shading or lettering. dG values were predicted using the mfold algorithm and indicate the folding energies calculated for stem IV and V and mutant versions thereof.

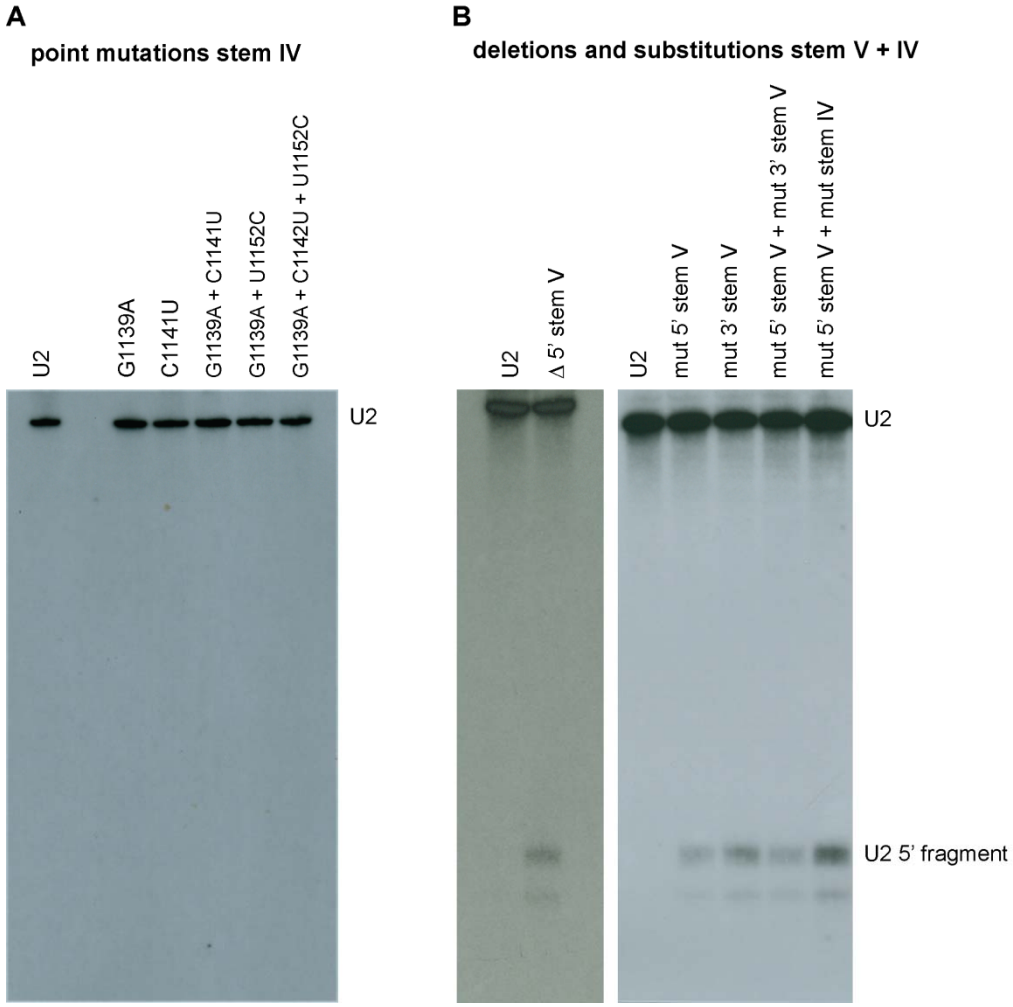

Figure 6.7 Mutations in U2 3' domain cause occurrence of a U2 5' fragment. Northern blot analysis (2.12.6) of total RNA obtained from strains carrying the indicated U2 mutant alleles (see Fig. 6.6 for details). An end-labelled probe complementary to nt 15-37 of U2 was used for hybridisation. **(A)** Point mutations introduced to stem IV do not affect U2 stability or abundance. **(B)** Deletions and substitutions introduced to the 3' and 5' branches of stem V (and IV) lead to the occurrence of a ~130 nt 5' fragment of U2.

Combining mutations in stems IV and V exacerbated the phenotype. It is thus likely that the extent to which the truncated U2 fragment is generated coincides with the degree to which the secondary structure in the U2 3′ domain is disturbed.

It is noteworthy that Shuster & Guthrie (1988) observed a ~ 132 nt 5′ fragment of U2 in some deletion-mutants that were lacking large regions within the non-essential, central part of *S. cerevisiae* U2 [14]. The basis of this effect was unclear.

Inspection of the sequences deleted in the light of the revised U2 secondary structure, indicates that they interfered with formation of the terminal stem V.

To determine the exact length and 3′ end(s) of the short U2 fragment, a home-made version of a 3′ RACE PCR was used (2.12.13). Total RNA obtained from yeast cells harbouring the "U2 mut 5′ stem V + mut stem IV" allele was ligated to a cloning linker and cDNA was synthesized. With the help of a U2 specific forward oligo (Table 2.15) and a linker specific reverse oligo the U2 5′ fragment was PCR amplified (Fig. 6.8). The PCR product was TA-cloned and DNA isolated from 20 clones was sequenced (2.11.1, 2.11.12). Eight clones contained an insert, which in all cases mapped to the 5′ region of U2. The 3′ ends mapped to nt 128-137. Thus, the 3′ ends were close to the binding site of the hexameric Sm-ring (112-119) (Fig. 6.8). The fact that 6 out of 8 mapped 3′ ends were unique with single nt size-difference suggested that the truncated U2 fragments were generated by exonucleolytic 3′ to 5′ processing. The Sm-ring presumably protects the U2 fragments from further degradation.

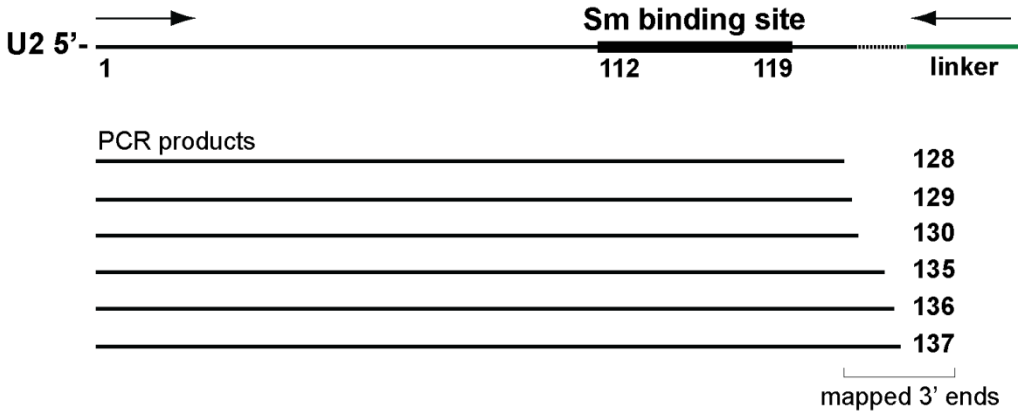

Figure 6.8 Mapping 3' ends of truncated U2 fragments. A mirCAT cloning linker was ligated to total RNA of a U2 mut 5' stem V + mut stem IV mutant. PCR amplification with oligos complementary to the linker and U2 5' end (arrows), cloning and sequencing allowed identification of 3' ends (for details see 2.12.13). Numbers on the right indicate the terminal nt identified.

6.9 Mutations in the 3' domain of U2 are synergistic with U2-U23G

The deletion of the non-essential region of U2 (nt 123-1068) alone does not interfere with splicing [10], however when combined with the U23G substitution leads to growth and splicing defects [16]. The U2-U23G mutation reduces base-pairing stability between U2 and U6 snRNAs in helix Ib. It was therefore proposed that the non-essential region in U2 stabilises U2/U6 helix Ib.

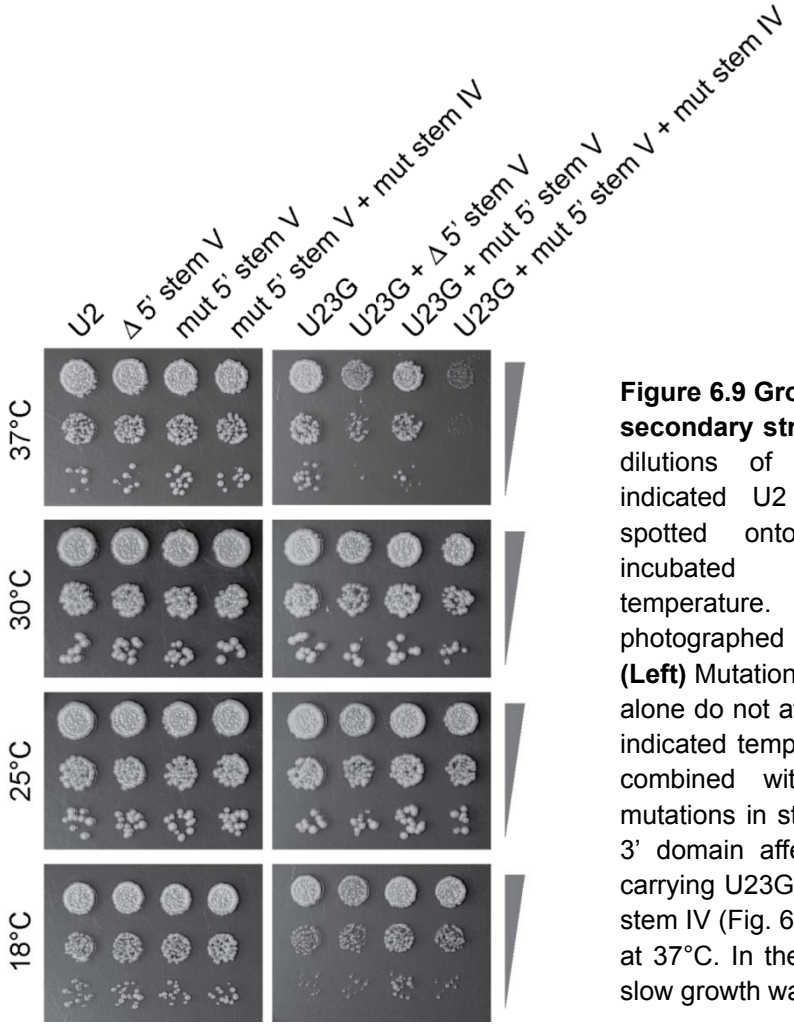

Figure 6.9 Growth phenotypes of U2 secondary structure mutants. Serial dilutions of strains carrying the indicated U2 mutant alleles were spotted onto YPDA agar and incubated at the indicated temperature. Plates were photographed after 2-5 days (18°C). **(Left)** Mutations in the 3' domain of U2 alone do not affect growth rates at the indicated temperatures. **(Right)** When combined with substitution U23G, mutations in stem V and VI of the U2 3' domain affect growth rates. Cells carrying U23G + mut 5' stem V + mut stem IV (Fig. 6.6) show heat sensitivity at 37°C. In the presence of U2-U23G slow growth was observed at 18°C.

To determine whether the observed synergistic phenotype was in fact due to disruption of stems IV and/or V, stem mutations were combined with U2-U23G (Fig. 6.9).

The U2-U23G substitution was introduced to plasmids encoding secondary structure mutants by SDM (2.11.10.3). W303 U2Δ was transformed with plasmids encoding the indicated U2 alleles and transformants were cured of the helper plasmid (2.9.8). Yeast cultures were grown to stationary phase and serial dilutions were spotted onto rich medium for growth assays at high, medium and low temperatures (2.7.9). Mild temperature sensitivity was seen on combination of U2-U23G with either the deletion or mutation of the 5′ side of stem V. Heat-sensitive lethality was seen when stem IV was additionally perturbed by mutations in its 3′ side (Fig. 6.9, 6.6).

Table 6.3 Summary of U2 alleles tested

U2 allele	*mutation(s)*	*growth on 5-FOA*	*growth defect*	*Northern*
U2	-	+++	WT	WT signal
G1139A	G1139A	+++	WT	WT signal
C1141U	C1141U	+++	WT	WT signal
G1139, C1141U	G1139, C1141U	+++	WT	WT signal
G1139A, U1152C	G1139A, U1152C	+++	WT	WT signal
G1139A, C1141U, U1152C	G1139A, C1141U, U1152C	+++	WT	WT signal
G143A, G145A	G143A, G145A	+++	WT	WT signal
Δ 5' stem V	deletion of nt 138-150	+++	WT	U2 + 5' fragment
mut 5' stem V	nt 138-151 to 5'GGUAACGCAGAUUC	+++	WT	U2 + 5' fragment
mut 5' stem V+ mut stem IV	G1139A, C1141U, U1152C + nt 138-151 to 5'GGUAACGCAGAUUC	+++	WT	U2 + 5' fragment
mut 3'stem V	nt 1156-1170 to 5'GAGAUCUGCGUUACU	+++	WT	U2 + 5' fragment
mut 5' stem V + mut 3' stem V	nt 138-151 to 5'GGUAACGCAGAUUC + nt 1156-1170 to 5'GAGAUCUGCGUUACU	+++	WT	U2 + 5' fragment
U23G	U23G	+++	sg 18°C	WT signal
U23G + Δ 5'LR	U23G + deletion of nt 138-150	+++	sg 37°C, 18°C	U2 + 5' fragment
U23G + mut 5‘ stem V	U23G + nt 138-151 to 5'GGUAACGCAGAUUC	+++	sg 18°C	U2 + 5' fragment
U23G + mut 5' stem V + mut stem IV	U23G + G1139A, C1141U, U1152C + nt 138-151 to 5'GGUAACGCAGAUUC	++	ts, 37°C, sg 18°C	U2 + 5' fragment

+++ growth on 5-FOA like WT; conditional growth defects were tested at 25°, 30°, 37°, 18°C; ts = temperature sensitive; sg = slow growth.

A summary of all U2 alleles tested and the phenotypes observed is given in Table 6.3. Taken together, these results confirm that U2 stems IV and V form *in vivo* and act to stabilize U2.

6.10 Discussion

Generally, CLASH analysis provides an alternative to existing experimental and bioinformatics methods. It allows high-throughput identification of RNA interacting partners and interaction sites without prior knowledge of their existence. Importantly, because cross-linking is carried out *in vivo*, the recovered chimeras should reflect the native state of the RNP and report RNA-RNA interactions that occur under physiological conditions.

CLASH analysis of Brr2 sequencing reads identified inter-molecular chimeras, which result from ligation of different RNAs (U4-U6), and intra-molecular chimeras, in which two fragments of the same RNA were ligated (U4-U4 and U2-U2). Intra-molecular chimeras were found far more frequently (> 99%), confirming that stable base-pairing strongly aids the formation of chimeric sequences, but also that RNA duplexes can be directly recovered as chimeric sequences.

The prevalence of U2-U2 chimera might suggest that the secondary structure formed by U2 interacts with the Brr2 protein in a way that is favourable to the formation of chimeric RNAs. The affinity purification steps recover only RNA-RNA hybrids located close to the protein-binding site, limiting the interactions identified in any specific experiment.

Chimeric and non-chimeric reads identified in cross-linking experiments with full-length Brr2 and the N-terminal portion are consistent with a revised secondary structure for the U2 3′ domain (Fig. 6.3, 6.4). In previous secondary structure models for *S. cerevisiae* U2 [14] the 5′ region closely resembled metazoan U2, whereas the 3′ domain appeared quite different, with a long, single-stranded

3'sequence. The revised model for *S. cerevisiae* U2 shows greater similarity in overall fold, with the large additional domain clearly looped-out and a structured 3' domain (Fig. 6.4).

It cannot be ruled out that Brr2 is involved in establishment of the U2 structure, however Brr2 is a U5 snRNP component and outside of the assembled spliceosome not normally found associated with the U2 RNA [17]. Thus, it seems more likely, that Brr2-U2 interactions are established in the spliceosome, possibly during the splicing reaction itself (see below). The processing defect that was observed upon disruption of structural elements in the U2 3' domain presumably occurs during biogenesis of the U2 snRNP. If the 3' domain cannot adopt the correct conformation, association of proteins might be inefficient, targeting at least a fraction of particles synthesised for degradation. Consistently, the truncated U2 fragment was more abundant when formation of both stems was perturbed (Fig. 6.7). The fact that the synthetic stem V (mut 5' stem V + mut 3' stem V, Fig. 6.6, 6.7) could only partially compensate the processing defect might indicate that optimal U2 snRNP formation requires a correctly structured 3' domain and a specific RNA sequence.

The U2 snRNA (nt 33-39) binds and activates the branch point for first step chemistry and 5' splice site cleavage [18]. Base-pairing interactions with the U6 snRNA form helices U2/U6 II and III as well as U2/U6 Ia and Ib which are integral parts of the catalytic spliceosome [19]. U2 nt 21-30 participate in formation of U2/U6 helices Ia and Ib.

The Brr2 mutant allele *slt22-1* is synthetic lethal with U2 mutations that affect the correct formation of U2/U6 helix I. This lead to the suggestion that Brr2 helicase activity is required to proof-read or unwind base-pairing interactions in U2/U6 helices Ia and Ib during assembly or disassembly of the spliceosome [20-22]. However, the Brr2 interaction sites identified in U2 do not include U2 nt 21-30, or any other nucleotides that base-pair to U6 or the branch point (Fig. 6.4). This

contradicts a direct interaction of Brr2 with U2/U6 helix I. Based on the lack of physical interactions with these U2 regions an indirect effect seems more plausible. Substitution U2-U23G introduces a mismatch to U2/U6 helix Ib. Although decreasing the stability of U2/U6 helix Ib, U2-U23 mutants behave like WT at temperatures of 25°C or above [23]. Notably, genetic studies by Hilliker & Staley (2004) showed that U2-U23G causes growth and splicing defects, if U2 is devoid of the non-essential central region (nt 123-1068). This phenotype could be partially suppressed by restoring base-pairing in helix Ib through compensatory mutations. Accordingly, the interpretation was that the non-essential region of U2 stabilizes base-pairing in U2/U6 helix Ib [16]. The finding that U2-U23G in combination with mutations in stems IV and V of the 3′ domain causes heat sensitivity is consistent with these results and further supports the revised U2 secondary structure (Fig. 6.9). Perhaps the secondary structure provided by the non-essential region of *Saccharomyces* U2 (including the 3′ domain) functionally substitutes for additional proteins found in higher Eukaryotes, which have evolved to stabilize spliceosomal conformations.

The Brr2-U2 interactions identified by cross-linking experiments show, that the structured U2 3′ domain and some parts of the non-essential region are in close proximity to Brr2 (Fig. 6.3, 6.4) and with that also close to the catalytic centre of the spliceosome. It is possible that, during splicing Brr2-U2 interactions hold the 3′ domain in place or preserve the folding of U2, thereby indirectly affecting the stability of U2/U6 base-pairing. During spliceosome disassembly, Brr2 might trigger changes in the 3′ domain of U2, e.g. through loss of interaction or by actively changing the conformation of the 3′ domain, which in turn destabilizes U2/U6. Extending the CRAC / CLASH analyses to other U2-associated proteins and proteins implicated in affecting U2/U6 helix I formation, may reveal conformational changes in U2 during the splicing cycle.

6.11 References

1. Kudla, G., Granneman, S., Hahn, D., Beggs, J.D. and Tollervey, D. (2011) Cross-linking, ligation, and sequencing of hybrids reveals RNA-RNA interactions in yeast. PNAS. **108**(24), 10010-10015.
2. Toor, N., Keating, K.S. and Pyle, A.M. (2009) Structural insight to RNA splicing. Current Opinion in Structural Biology. **19**(3), 260-266.
3. Wahl, M.C., Will, C.L. and Lührmann, R. (2009) The Spliceosome: Design Principles of a Dynamic RNP Machine. Cell. **136**, 701-718.
4. Ule, J., Jensen, K., Mele, A. and Darnell, R.B. (2005) CLIP: a method for identifying protein-RNA interaction sites in living cells. Methods. **37**, 376-386.
5. Granneman, S., Kudla, G., Petfalski, E. and Tollervey, D. (2009) Identification of protein binding sites on U3 snoRNA and pre-rRNA by UV cross-linking and high-throughput analysis of cDNAs. PNAS. **106**(24), 9613-9618.
6. Bohnsack, M.T., Martin, R., Granneman, S., Ruprecht, M., Schleiff, E. and Tollervey, D. (2009) Prp43 bound at different sites on the pre-rRNA performs distinct functions in ribosome synthesis. Molecular Cell. **36**, 583-592.
7. Li, X., Zhao, L., Jiang, H. and Wang, W. (2009) Short homologous sequences are strongly associated with the generation of chimeric RNAs in eukaryotes. Journal of Molecular Evolution. **68**, 56-65.
8. Markham, N.R. and Zuker, M. (2005) DINAMelt web server for nucleic acid melting prediction. Nucleic Acids Research. **33**(W577-W582).
9. Shuster, E.O. and Guthrie, C. (1990) Human U2 snRNA can function in pre-mRNA splicing in yeast. Nature. **345**, 270-273.
10. Igel, A.H. and Ares, M. (1988) Internal sequences that distinguish yeast from metazoan U2 are unnecessary for pre-mRNA splicing. Nature. **334**, 450-453.
11. Guthrie, C. and Patterson, B. (1988) Spliceosomal snRNAs. Annu Rev Genet. **22**, 387-419.
12. Scherly, D., Boelens, W., Dathan, N.A., van Venrooij, W.J. and Mattai, I.W. (1990) Major determinants of the specificity of interaction between small nuclear ribonucleoproteins U1A and U2B″ and their cognate RNAs. Nature. **345**, 502-506.
13. Ares, M.J. (1986) U2 RNA from yeast is unexpectedly large and contains homology to vertebrate U4, U5, and U6 small nuclear RNAs. Cell. **47**, 49-59.
14. Shuster, E.O. and Guthrie, C. (1988) Two conserved domains of yeast U2 snRNA are separated by 945 nonessential nucleotides. Cell. **55**(1), 41-48.
15. Knudsen, B. and Hein, J. (2003) Pfold: RNA secondary structure prediction using stochastic context-free grammars. Nucleic Acids Research. **31**(13), 3423-3428.
16. Hilliker, A.K. and Staley, J.P. (2004) Multiple functions for the invariant AGC triad of U6 snRNA. RNA. **10**, 921-928.
17. Stevens, S.W., Barta, I., Ge, H.Y., Moore, R.E., Young, M.K., Lee, T.D. and Abelson, J. (2001) Biochemical and genetic analyses of the U5, U6, and U4/U6 x U5 small nuclear ribonucleoproteins from *Saccharomyces cerevisiae*. RNA. **7**, 1543-1553.
18. Parker, R., Silicano, P.G. and Guthrie, C. (1987) Recognition of the TACTAAT box during mRNA splicing in yeast involves base pairing to the U2-like snRNA. Cell. **49**, 229-239.
19. Field, D. and Friesen, J.D. (1996) Functionally redundant interactions between U2 and U6 spliceosomal snRNAs. Genes & Development. **10**, 489-501.

20. Small, E.C., Leggett, S.R., Winans, A.A. and Staley, J.P. (2006) The EF-G-like GTPase Snu114p Regulates Spliceosome Dynamics Mediated by Brr2p, a DExD/H Box ATPase. Molecular Cell. **23**, 389-399.

21. Xu, D.M., Nouraini, S., Field, D., Tang, S.J. and Friesen, J.D. (1996) An RNA-dependent ATPase associated with U2/U6 snRNAs in pre-mRNA splicing. Nature. **381**, 709-713.

22. Xu, D.M., Field, D., Tang, S.J., Moris, A. and Bobechko, B.P. (1998) Synthetic lethality of yeast slt mutations with U2 small nuclear RNA mutations suggests functional interactions between U2 and U5 snRNPs that are important for both steps of pre-mRNA splicing Molecular and Cellular Biology. **18**, 2055-2066.

23. Madhani, H.D. and Guthrie, C. (1994) Genetic interactions between the yeast RNA helicase homolog Prp16 and spliceosomal snRNAs identify candidate ligands for the Prp16 RNA-dependent ATPase. Genetics. **137**, 677-687.

Chapter 7 – Final Discussion

7.1 Brr2 multi-domain and multi-functional RNA helicase

Brr2 is a large, multi-domain and apparently multi-functional protein. Brr2 features two helicase cassettes each comprising a helicase, WH and Sec63 domain (Fig. 7.1). The two cassettes seem to function as independent units, as they can be expressed as individual protein fragments that complement in trans and associate with each other *in vivo*. The contribution of both units is crucial for Brr2 function (section 5.4). Although suggested to have an overall very similar structure [1, 2], the two helicase cassettes of Brr2 seem to serve different functions (Fig. 7.1) [3].

7.2 The C-terminal helicase cassette of Brr2 functions as an inbuilt regulatory unit

Several observations suggest that the C-terminal helicase cassette functions as a specialised protein interaction domain. It is the part of the protein that engages in protein interactions [4, 5]. Consistently, protein-RNA cross-linking experiments with the C-terminal helicase cassette of Brr2 failed to detect specific cross-links with snRNAs or pre-mRNAs (section 4.5), indicating that the C-terminal helicase cassette has adapted to exclusively interact with protein and does not contribute to Brr2-RNA interactions.

It seems likely that the C-terminal portion of Brr2 functions as a regulatory unit. As Brr2 is a stable U5 component and its activity is required repeatedly throughout the splicing cycle [3], the C-terminal helicase cassette might have evolved to serve as an inbuilt accessory and regulatory domain.

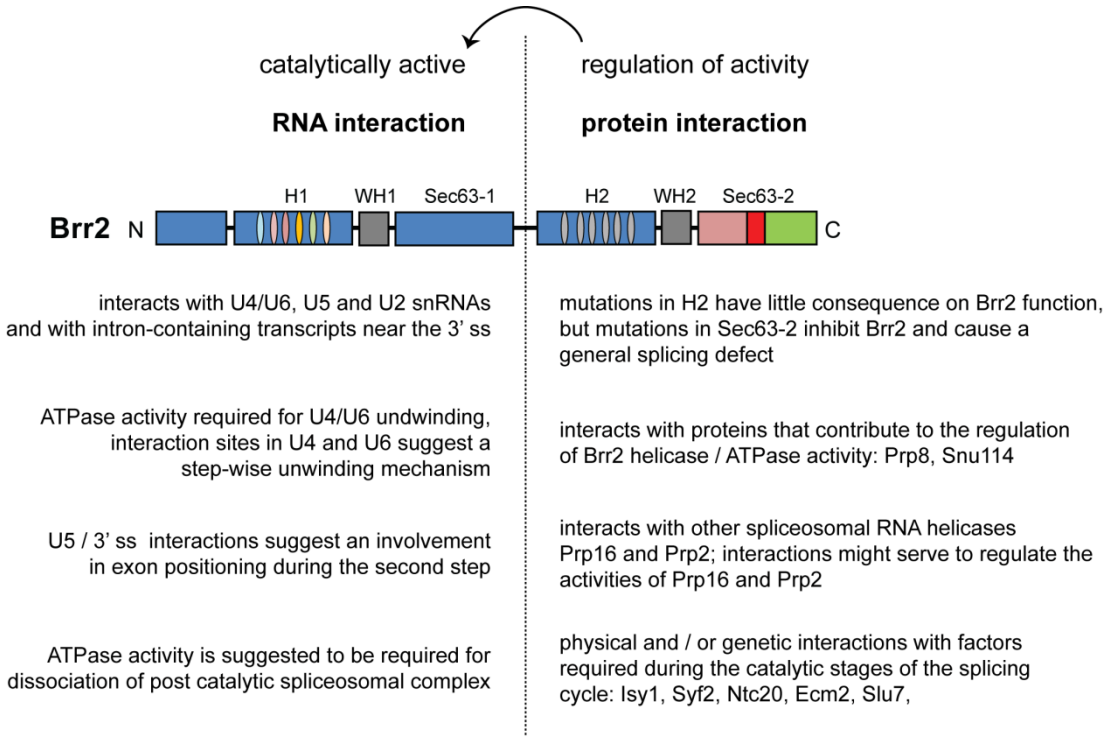

Figure 7.1 Functional distinctions of the N- and C-terminal helicase cassettes of Brr2. Brr2 comprises an N-terminal domain of unknown function, an N-terminal helicase cassette (H1, WH1 and Sec63-1) and a C-terminal helicase cassette (H2, WH2 and Sec63-2). The figure lists the key findings and indicates the suggested functional contributions of the respective parts of Brr2 outlined in Chapters 1 and 3-6 (including the referenced literature). While the N-terminal helicase cassette has catalytic activity, the C-terminal helicase cassette is catalytically inert. The N-terminal cassette engages in RNA interactions (left); however the C-terminal cassette does not. Instead it functions as a protein interaction domain (right). The C-terminal cassette seems to be involved in regulating the activity of the N-terminal helicase cassette (arched arrow) and potentially also regulates the activities of other interacting helicases, Prp2 and Prp16.

Interactions established between the C-terminal helicase cassette of Brr2 and other splicing factors seem to play crucial roles in the regulation of spliceosome dynamics.

Clearly, interactions with Prp8 and Snu114 play key roles in the regulation of Brr2 activity [6-11]. A complete deletion of the Sec63-2 domain disrupts these interactions, resulting in loss of ATPase activity [2]. Point mutations in structurally and evidently functionally relevant regions within the Sec63-2 domain, such as the putative ratchet helix (section 3.4), are sufficient to elicit a general splicing defect, demonstrating that an intact C-terminal Sec63 domain is important for normal Brr2

function (section 3.5-3.6). Taken together these observations suggest that the C-terminal domains of Brr2 regulate the activity of the N-terminal helicase cassette.

Currently, it remains unclear by which mechanism protein interactions at the C-terminus of Brr2 can modulate the activity of its N-terminal helicase cassette, and how this regulation is realised *in vivo*. Interestingly, when physically separated the N- and C-terminal halves of Brr2 trans complement only when both cassettes are sound in condition, i.e. free of mutations. Point mutations in either cassette abrogate trans complementation, such that the two halves of Brr2 no longer function in unity (section 4.4). Therefore, it will be revealing to learn more about how the two helicase cassettes are arranged with respect to one another in the full-length protein and how this arrangement contributes to communicating regulatory signals between the C- and N-termini. The tandem helicase-cassette design of Brr2 might facilitate conformational flexibility, as a means to controlling spliceosomal dynamics.

In addition, this work has provided the first evidence for a regulatory interplay between the C-terminal domains of Brr2 and the spliceosomal RNA helicases Prp2 and Prp16 (section 3.7-3.9). Protein interactions seem to depend on both the conformational state of the C-terminal portion of Brr2 and on the catalytic state of its helicase partner (section 3.9). Accompanying studies conducted by O. Cordin in the lab provided further evidence for the regulatory function of the C-terminal helicase cassette of Brr2: Biochemical approaches showed that the presence of the C-terminal Sec63 domain modulates the ATPase activities of Prp2 and Prp16 *in vitro*. The C-terminus of Brr2 interacts directly with both helicases. As these interactions are affected by the presence of RNA, we hypothesise that the interaction with the C-terminal domains of Brr2 might regulate whether / when interacting helicases have access to their RNA substrates (O. Cordin unpublished).

Future studies could provide much mechanistic insight by identifying the interaction surfaces common amongst the Brr2 C-terminal domains and interacting helicases. Protein-protein cross-linking studies as well as co-crystal structures of

protein complexes would advance our understanding of how physical interactions can contribute to coordinating the catalytic activities of the spliceosome.

7.3 RNA interactions place Brr2 at the centre of the spliceosome

In vivo cross-linking experiments indicated the N-terminal helicase cassette of Brr2 as the part of the protein that establishes RNA interactions (section 4.6). Furthermore, they confirmed that Brr2 is the factor required for U4/U6 dissociation. Brr2 cross-linking sites in the U4 and U6 snRNAs suggest a step-wise unwinding mechanism of the U4/U6 duplex, involving ATP-dependent, Brr2-mediated disruption of U4/U6 stem 1, followed by opening of stem 2. The latter seems to be initiated by a conformational switch in the protein-RNA network that stabilises the base-pairing of U4/U6 stem 2 (section 5.10.2). The processes involved in spliceosome activation appear to be highly conserved and are paralleled in the activation sequence identified in the minor spliceosome [12].

I identified novel interactions between Brr2 and the U5 loop 1 (section 5.5). Genetic interactions underscored the functional importance of this interaction. The phenotypic analyses of *brr2* and U5 loop1 mutants revealed an accumulation of first step intermediate, indicating an involvement of Brr2 in the second step of splicing (sections 5.6-5.7). Together with cross-linking interactions between Brr2 and intron containing transcripts near the 3' ss (section 5.8) these observations suggest a possible function for Brr2 in 3' exon positioning (section 5.10.2). Notably, the cross-linking patterns of Brr2 and Prp8 show a partial overlap. In yeast, Prp8 cross-links to the 5' exon and 5' ss, but it also cross-links to the 3' exon up to position +13 downstream of the 3' ss [13, 14]. Furthermore, Prp8 makes extensive contact to the U5 snRNA, including nt 97 in loop 1 [15]. These interactions place Prp8 at the centre of the spliceosome, and consequently place Brr2 close to it. But what does the similar RNA interaction pattern of Brr2 and Prp8 imply?

The mechanism by which Prp8 and Snu114 regulate Brr2 remains unknown. Could the tightly associated Snu114 and Prp8 regulate or mediate access of Brr2 to its RNA substrates? Hypothetically, together with Snu114, Prp8 might act as a gatekeeper allowing Brr2 to access the RNA substrate in order to promote conformational rearrangements mediated by Brr2 ATPase activity. Conformational rearrangements in Snu114 might provide part of the mechanism [16-18]. Intriguingly, the C-terminal domains of the elongation factor G-like structure of Snu114 are thought to facilitate extensive conformational rearrangements upon GTP hydrolysis [10] and are likely essential to the suggested regulatory capacity of Snu114, which mimics those of classical G-proteins [9]. Thus, it might be interesting to address if and how Prp8 and Snu114 could regulate access of Brr2 (its N-terminal helicase cassette) to RNA in particular during the catalytic and post-catalytic stages of splicing.

The identified Brr2-RNA interactions gave no clear evidence for the proposed function of Brr2 in U2/U6 dissociation during spliceosome disassembly [9]. Potentially, these interactions are too short-lived to allow detection by the employed cross-linking approach. As a suggested regulator of Brr2 activity, *prp8* alleles should also affect Brr2-mediated conformational rearrangements. Interestingly, so far Prp8 has not been implicated in the regulation of spliceosome disassembly. Much remains to be learned about the contribution of Brr2 to disassembly of the post catalytic spliceosomal complex. Extending cross-linking studies to other factors involved in disassembly might help to gain a better understanding of the succession of conformational rearrangements that are required to disassemble the spliceosome and how Brr2 contributes to them.

7.4 Does Brr2 affect splicing fidelity?

Apart from catalysing conformational rearrangements in the protein-RNA network of the spliceosome, RNA-helicases have been shown to be crucial

contributors to the fidelity of the splicing reaction (reviewed in [19]). Mutations in the ATPase domains of RNA helicases are thought to slow the rate of exit from one conformation into the following. Kinetic competition between the forward reaction (productive progression of splicing) and the rejection reaction (discard of the substrate) serves as the basis for the control of fidelity by helicase-mediated ATP hydrolysis, also known as the kinetic proofreading hypothesis [20-22].

An outstanding question is whether Brr2, has a proofreading function(s) in splicing. Firstly, the rate of ATP-hydrolysis by Brr2 determines the rate of U4/U6 dissociation during spliceosome activation. Therefore, it could allow control of the correct formation of U2/U6 as well as 5′ ss/U6 interactions, which are crucial to ensure accurate 5′ ss cleavage (section 5.10.1, [23, 24]). Secondly, its interactions with the U5 loop 1 and 3′ ss region suggest an involvement of Brr2 in 3′ ss positioning and exon alignment (sections 5.5-5.9). Whether this process involves ATP hydrolysis by Brr2 remains to be determined. Interestingly, the Brr2 mutant allele *rss1-1* showed a reduced rate of second step catalysis (section 5.6), which could potentially influence the fidelity of 3′ ss selection. Thirdly, the observation that mutations in the C-terminal helicase cassette of Brr2 influence the activity of the whole protein suggests that the C-terminal domains govern the activity of the catalytically competent N-terminal cassette. Hence, it is tempting to speculate that mutations in the C-terminal domains might indirectly affect the fidelity of the above mentioned events by reducing the normal rate of Brr2 ATP hydrolysis. Finally, changes in spliceosomal factors that influence the association of ATPases with the spliceosome were suggested to result in altered fidelity (e.g. the effect of Isy1 on Prp16, section 3.7)[25]. Likewise, if mutations in the C-terminal helicase cassette of Brr2 affect the association and ATPase activities of other RNA helicases (see above, sections 3.3.3, 3.10), these mutations might affect the kinetics and with that the fidelity of the reactions catalysed by interacting helicases. Therefore, future work should address whether Brr2 itself (via its N-terminal helicase cassette) elicits proofreading

functions and whether it can promote or reduce the fidelity of other proofreading factors (via its C-terminal helicase cassette).

In all, the advances made by recent structural and biochemical analyses, in combination with the genetic and cross-linking studies presented here, have broadened our understanding of Brr2's architecture and provided mechanistic relevance to its domain organisation (Fig. 7.1). With continued efforts, increasingly sophisticated structural analyses and targeted biochemical and genetic approaches, a fuller understanding of the overall structure and functions of this unusual RNA helicase will emerge.

7.5 References

1. Pena, V., Mozaffari Jovin, S., Fabrizio, P., Orlowski, J., Bujnicki, J.M., Lührmann, R. and Wahl, M.C. (2009) Common Design Principles in the Spliceosomal RNA Helicase Brr2 and in the Hel308 DNA Helicase. Molecular Cell. **35**, 454-466.

2. Zhang, L., Xu, T., Maeder, C., Bud, L.-O., Shanks, J., Nix, J., Guthrie, C., Pleiss, J.A. and Zhao, R. (2009) Structural evidence for consecutive Hel308-like modules in the spliceosomal ATPase Brr2. Nature Structural & Molecular Biology. **16**, 731-739.

3. Hahn, D. and Beggs, J.D. (2010) Brr2p RNA helicase with a split personality: Insights into structure and function. Biochemical Society Transactions. **38**, 1105-1109.

4. van Nues, R. and Beggs, J.D. (2001) Functional Contacts With a Range of Splicing Proteins Suggest a Central Role for Brr2p in the Dynamic Control of the Order of Events in Spliceosomes of *Saccharomyces cerevisiae*. Genetics. **157**, 1457-1467.

5. Liu, S., Rauhut, R., Vornlocher, H.-P. and Lührmann, R. (2006) The network of protein-protein interactions within the human U4/U6.U5 tri-snRNP. RNA. **12**, 1418-1430.

6. Kuhn, A. and Brow, D.A. (2000) Suppressors of a Cold-Sensitive Mutation in Yeast U4 RNA Define Five Domains in the Splicing Factor Prp8 That influence Splicosome Activation. Genetics. **155**, 1667-1682.

7. Kuhn, A.N., Reichl, E.M. and Brow, D.A. (2002) Distinct domains of splicing factor Prp8 mediate different aspects of spliceosome activation. PNAS. **99**(14), 9145-9149.

8. Kuhn, A.N., Li, Z.R. and Brow, D.A. (1999) Splicing factor Prp8 governs U4/U6 RNA unwinding during activation of the spliceosome. Molecular Cell. **3**(1), 65-75.

9. Small, E.C., Leggett, S.R., Winans, A.A. and Staley, J.P. (2006) The EF-G-like GTPase Snu114p Regulates Spliceosome Dynamics Mediated by Brr2p, a DExD/H Box ATPase. Molecular Cell. **23**, 389-399.

10. Brenner, T.J. and Guthrie, C. (2005) Genetic Analysis Reveals a Role for the C Terminus of the Saccharomyces cerevisiae GTPase Snu114 During Splicosome Activation. Genetics. **170**, 1063-1080.

11. Maeder, C., Kutach, A.K. and Guthrie, C. (2008) ATP-dependent unwinding of U4/U6 snRNAs by the Brr2 helicase requires the C terminus of Prp8. Nature Structural & Molecular Biology. **16**(1), 42-48.

12. Frilander, M.J. and Steitz, J.A. (2001) Dynamic Exchanges of RNA interactions Leading to Catalytic Core Formation in the U12-dependent Spliceosome. Molecular Cell. **7**, 217-226.

13. Teigelkamp, S., Newman, A.J. and Beggs, J.D. (1995) Extensive interactions of PRP8 protein with the 5' and 3' splice sites during splicing suggest a role in stabilization of exon alignment by U5 snRNA. EMBO. **14**, 2602-2612.

14. Teigelkamp, S., Whittaker, E. and Beggs, J.D. (1995) Interaction of the yeast splicing factor PRP8 with substrate RNA during both steps of splicing. Nucleic Acids Research. **23**, 320-326.

15. Dix, I., Russell, C.S., O'Keefe, R.T., Newman, A.J. and Beggs, J.D. (1998) Protein-RNA interactions in the U5 snRNP of Saccharomyces cerevisiae. RNA. **4**, 1239-1250.

16. Bartels, C., Urlaub, H., Luhrmann, R. and Fabrizio, P. (2003) Mutagenesis suggests several roles of Snu114p in pre- mRNA splicing. Journal of Biological Chemistry. **278**(30), 28324-28334.

17. Bartels, C., Klatt, C., Luhrmann, R. and Fabrizio, P. (2002) The ribosomal translocase homologue Snu114p is involved in unwinding U4/U6 RNA during activation of the spliceosome. Embo Reports. **3**(9), 875-880.

18. Novak Frazer, L., Lovell, S. and O'Keefe, R.T. (2009) Analysis of Synthetic Lethality Reveals Genetic Interactions Between the GTPase Snu114p and snRNAs in the Catalytic Core of the *Saccharomyces cerevisiae* Spliceosome. Genetics. **183**, 497-515.

19. Egecioglu, D.E. and Chanfreau, G. (2011) Proofreading and spellchecking: A two-tier strategy for pre-mRNA splicing quality control. RNA. **17**, 383-389.

20. Query, C.C. and Konarska, M.M. (2006) Splicing Fidelity revisited. Nature Structural & Molecular Biology. **13**(6), 472-474.

21. Hopfield, J.J. (1974) Kinetic Proofreading: A new Mechanism for Reducing Errors in Biosynthetic Processes Requiring High Specificity. PNAS. **71**(10), 4135-4139.

22. Burgess, S.M. and Guthrie, C. (1993) A Mechanism to Enhance mRNA Splicing Fidelity: The RNA-Dependent ATPase Prp16 Governs Usage of a Discard Pathway for Aberrant Lariat Intermediates. Cell. **73**, 1377-1391.

23. Xu, D.M., Nouraini, S., Field, D., Tang, S.J. and Friesen, J.D. (1996) An RNA-dependent ATPase associated with U2/U6 snRNAs in pre-mRNA splicing. Nature. **381**, 709-713.

24. Xu, D.M., Field, D., Tang, S.J., Moris, A. and Bobechko, B.P. (1998) Synthetic lethality of yeast slt mutations with U2 small nuclear RNA mutations suggests functional interactions between U2 and U5 snRNPs that are important for both steps of pre-mRNA splicing Molecular and Cellular Biology. **18**, 2055-2066.

25. Villa, T. and Guthrie, C. (2005) The Isy1p component of the NineTeen Complex interacts with the ATPase Prp16p to regulate the fidelity of pre-mRNA splicing. Genes & Development. **19**(16), 1894-1904.

Appendix

Supplementary material on CD